Rijksuniversiteit Groningen

Exposure to natural radioactivity in the Netherlands: the impact of building materials

Proefschrift

ter verkrijging van het doctoraat in de
Wiskunde en Natuurwetenschappen
aan de Rijksuniversiteit Groningen
op gezag van de
Rector Magnificus, dr. F. Zwarts,
in het openbaar te verdedigen op
vrijdag 25 juni 2010
om 13.15 uur

door

Peter de Jong

geboren op 20 december 1953
te Delft

Promotor:	Prof. dr. R.J. de Meijer
Copromotor:	Dr. E.R. van der Graaf
Beoordelingscommissie:	Prof. dr. H.A.J. Meijer
	Prof. dr. W.F. Passchier
	Prof. dr. H. Wilschut

Aim of this thesis

This thesis focuses on the levels of radioactivity and ionizing radiation from building materials. It describes the development and validation of measurement techniques and calculation methods, identifies the contribution of the main stony building materials and investigates the possibilities to reduce the resulting indoor exposures. These exposures have their origin in radionuclides from the elements uranium (^{235}U, ^{238}U), thorium (^{232}Th) and potassium (^{40}K). These so-called primordial radionuclides were formed 4.55 billion years ago in one or more supernova events leading to our solar system. The half-lives of ^{235}U, ^{238}U, ^{232}Th and ^{40}K, i.e. the time required for the disintegration of one-half of the radioactive atoms, are 0.704, 4.47, 14.1 and 1.28 billion years, respectively, long enough to leave significant amounts in current materials.

For many years the exposures from natural sources were excluded from regulation or control. At the end of the 1970's, however, results from foreign surveys became available, which showed that indoor exposures sometimes exceed the dose limits of radiological workers. For the Dutch population the annually induced number of fatal cancers due to exposure to indoor radiation is estimated to be of the order of one thousand (Van Bruggen *et al*., 2004).

Contents

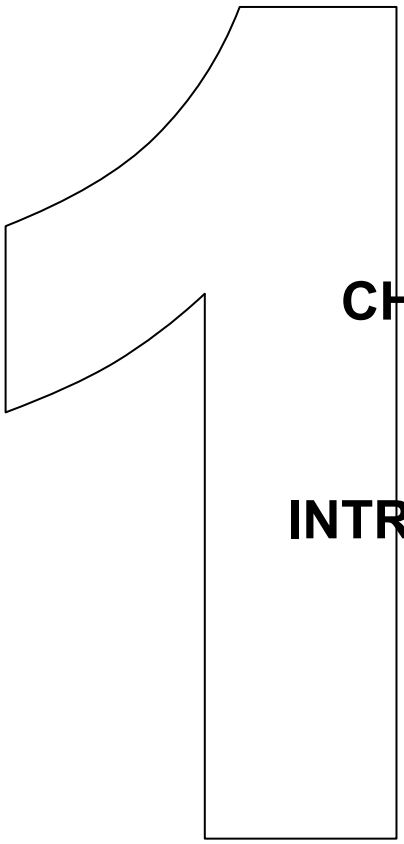

CHAPTER 1

INTRODUCTION

In the first part of this thesis the latest insights and developments concerning indoor radiation exposure are incorporated and this chapter reflects the current state of knowledge on indoor radiation exposure in the Netherlands. The sections of this chapter deal with the following subjects:

- *Primordial radionuclides*; in this section some background information is provided on the primordial radionuclides, their decay schemes and the various decay products. The main gamma-emitting radionuclides are identified, responsible for the part of the indoor exposures that is generally denoted as external exposure.
- *Radon*; this section focuses on one element from the decay series, i.e. the noble gas radon. This gas is responsible for the other part of the indoor exposure. The three processes are described how radon is released from building materials and soil into the indoor atmosphere.
- *Exposure*; based on the activity concentrations in building materials and indoor air, the radiation exposure due to gamma radiation and the short-lived decay products of the main radon isotopes, ^{222}Rn and ^{220}Rn, are described.
- *Dosimetry*; section in which the effects of ionizing radiation, the dosimetric quantities to quantify these effects and the conversion factors for evaluating the exposures are discussed.
- *Epidemiological data*; presents the results of epidemiological studies on the lifetime mortality risks of ionizing radiation in general and ^{222}Rn especially, based on either dosimetric or exposure-related quantities.
- *Research on natural radiation in the Netherlands*; this section provides an overview of research on natural radiation in the Netherlands as emerged from the various national research programmes and additional investigations.
- *Radon policy in the Netherlands*; shows the development of the policy on indoor exposures with time, with an outlook on coming European regulations. Most studies presented in chapter 2 to 4 of this thesis were part of one of the national research programmes and had a direct relation with prevailing or future policy in this field. This and the previous section are inserted to put these studies in the proper context.
- *National levels and estimated consequences*; summarizes the results of national surveys and gives a best estimate of the number of fatalities based on the previous sections.

This chapter 1 concludes with an outline of this thesis.

1.1 Primordial radionuclides

Uranium was isolated by Martin Heinrich Klaproth in 1789 from the mineral pitchblende. At that time uranium was not considered as particularly dangerous and was used for colouring pottery and glass. In 1896 Henri Becquerel observed that uranium was emitting invisible rays that fogged a photographic plate as if it was exposed to daylight (Emsley, 2003). In honour of his discovery of radioactivity, the unit for radioactivity is given the name becquerel (Bq), corresponding to one disintegration per second. Natural uranium mainly contains ^{238}U (99.27%), which is the parent of a decay series schematically presented in Figure 1.1. As shown in this figure each member of this series is unstable and decays by either alpha or beta emission until stable ^{206}Pb has been formed. Besides ^{238}U, natural uranium contains 0.73% ^{235}U. This isotope is also the parent of a decay series ending at ^{207}Pb.

Thorium was extracted by Jöns Jakob Berzelius in 1829 from a mineral that nowadays is known as thorite ($ThSiO_4$). Thorium oxide has found wide application in e.g. gas mantles which, when heated, emit a bright white light. In 1898 the radioactivity of thorium was demonstrated by Gerhard Schmidt and confirmed later that year by Marie Curie (Emsley, 2003). Like ^{235}U and ^{238}U, ^{232}Th heads a decay chain, but ends at another stable isotope of lead (^{208}Pb). The principal decay scheme is shown in Figure 1.2 along with the type of decay.

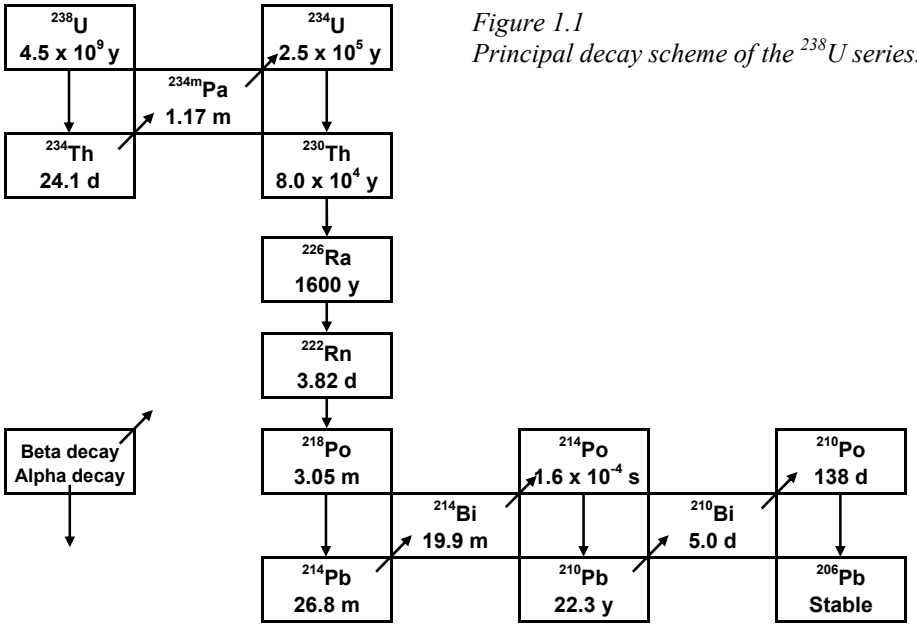

Figure 1.1
Principal decay scheme of the ^{238}U series.

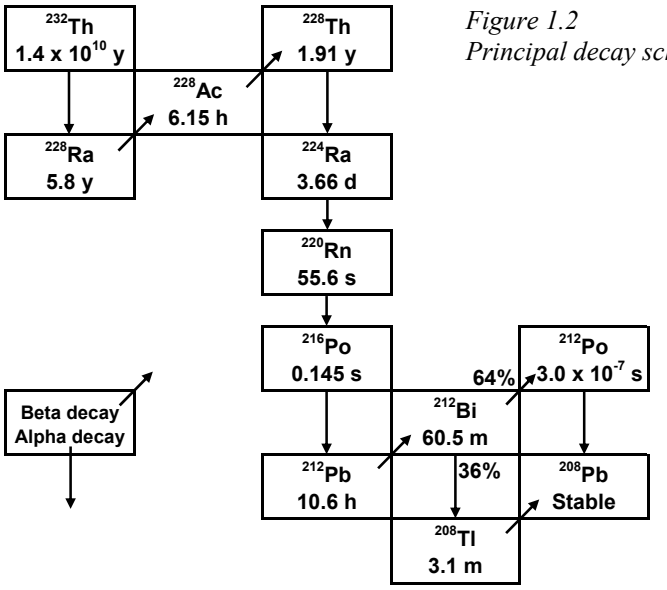

Figure 1.2
Principal decay scheme of the ^{232}Th series.

In most materials the parent nuclides ^{235}U, ^{238}U and ^{232}Th are nearly in a state of secular equilibrium with their decay products, meaning that the activities of all radionuclides within a series are equal. In case a building material (or a major constituent) is a residue of chemical processing, for instance gypsum from phosphate production units, certain radionuclides can be specifically enriched or depleted. The secular equilibrium is then violated and the initially single decay series will be split up in several smaller sub-series headed by longer-lived radionuclides.

As indicated in Figures 1.1 and 1.2 some members of the series decay by beta emission. After emission of a beta particle, the nucleus may still be slightly unstable and the excess energy is released by one or more gamma rays. The main gamma-emitting radionuclides in soil and building materials are compiled in Table 1.1, together with the energy of their major gamma rays. Besides radionuclides from the decay series of ^{238}U and ^{232}Th, also ^{40}K contributes to the indoor exposure due to gamma radiation. It is an isotope of the element potassium. Potassium was discovered by Humphry Davy in 1807 and named so after the material from which he isolated it: potash. Natural potassium comprises three isotopes, ^{39}K, ^{40}K and ^{41}K of which only ^{40}K is radioactive. Its abundance in nature is limited to 0.012% and it decays to stable ^{40}Ar (11.2%) and ^{40}Ca (88.8%).

Table 1.1
The main, natural gamma-emitting nuclides in soil and building materials and the energy (keV) of their major gamma rays.

^{238}U series		**^{232}Th series**	
^{234}Th	63, 93	^{228}Ac	338, 911, 969
^{234m}Pa	765, 1001	^{212}Pb	239, 300
^{226}Ra	186	^{212}Bi	40, 727, 1620
^{214}Pb	242, 295, 352	^{208}Tl	511, 583, 860, 2614
^{214}Bi	609, 1120, 1764	**Others**	
^{210}Pb	47	^{40}K	1461

1.2 Radon

1.2.1 General

Radon isotopes are found in all three natural decay series: ^{219}Rn in the ^{235}U series, ^{220}Rn in the ^{232}Th series and ^{222}Rn and ^{218}Rn in the ^{238}U series. The half-lives of these isotopes are 3.96 s, 55.6 s, 3.824 d and 35 ms, respectively. In many publications, e.g. the *CRC Handbook of Chemistry and Physics* (Lide and Haynes, 2010), the discovery of the element radon is attributed to Friedrich Ernst Dorn. However, recent publications suggest that the credit for the discovery should go to Ernest Rutherford and his young colleague Frederick Soddy, who studied the radioactive gas emanating from thorium (Emsley, 2003; Marshall and Marshall, 2003). As early as 1902 they believed that they were dealing with a new element from the helium-argon family. In 1908 William Ramsay and Robert Whytlaw Gray isolated enough radon to complete the characterization, noting that it was the heaviest gas known. Although Rutherford preferred the name emanation, Ramsay gave it the name niton, after *nitens*, the Latin word for shining, which is what it appears to do in the dark when cooled below its freezing point (-71ºC). In 1923 the International Committee on Chemical Elements proposed the current name radon.

Since radon is a gas, it can exhale from soil or building materials and accumulate in the living spaces of the dwelling. In the release of radon three steps can be distinguished: the first is the escape of radon from the mineral grain into the pore space, known as emanation, the second is the subsequent diffusive or advective transport of radon from the site of generation through the microstructure to the surface of a soil or the exterior of a building block. The latter process, the release of radon from the surface, is named exhalation. These three steps will be treated separately in the next sections.

1.2.2 Emanation

The escape of radon from the mineral grain mainly takes place through the recoil energy it obtains upon decay of a radium atom. In most minerals the recoil distance is in the range 20-70 nm (Tanner, 1980). Therefore only those radon atoms that are formed near the surface of the grain, will be able to leave it. Since the recoil distance in water is much smaller than in air (100 nm versus 60 μm), the presence of water in the pores increases the probability that a recoiled radon atom is stopped in the pore space instead of crossing the pore and being embedded in an adjacent grain surface. The fraction of the radon atoms that are released into the pore space of the matrix is called the emanation factor or emanating power, generally being inversely proportional to the grain size.

1.2.3 Diffusion

The radon atoms in the air-filled pore space are transported by diffusion – and in soil or extreme porous building materials also by advection – until they decay or exhale from the surface of soil and building materials. In building materials the diffusion is often described as a one-dimensional process, i.e. directed to the living space and its opposite site, following Fick's Law. If the middle of a construction element is taken as x=0, the diffusion along the x-axis is governed by the equation

$$\frac{\partial C(x)}{\partial t} = D\,\frac{\partial^2 C(x)}{\partial x^2} - \lambda\, C(x) + f\,, \qquad (1.1)$$

where

$C(x)$ the radon activity concentration in the air-filled pore space (Bq m^{-3});
t time (s);
D pore diffusion coefficient (m^2 s^{-1});
λ decay constant of radon (s^{-1}), the quotient of ln (2) and the half-life; and
f production rate of radon per unit of interstitial space (Bq m^{-3} s^{-1}).

For a steady-state situation eq. (1.1) yields the following, general solution:

$$C(x) = A\cosh(x/l) + B \quad \text{with} \quad l = \sqrt{D/\lambda}\,, \qquad (1.2)$$

in which A and B are constants and l is the so-called diffusion length. The diffusion length is the characteristic distance travelled by the radon atoms during one half-life. Taking the second derivative of $C(x)$ and combining it with eq. (1.1) for a steady-state situation provides the constant B. The constant A follows from the boundary condition that the radon concentration outside the construction element can be neglected, i.e. $C(L) = C(-L) =$

0 with L half of the thickness of the construction element. The radon concentration in the pore space can then be rewritten as:

$$C(x) = \frac{f}{\lambda}\left(1 - \frac{\cosh(x/l)}{\cosh(L/l)}\right). \tag{1.3}$$

In Figure 1.3 a 3D-plot is given of the interstitial radon concentration as a function of the diffusion length and position in a construction element of thickness 20 cm. For small diffusion lengths, the radon concentration reaches its maximum value for most parts in the element, with a sharp decrease near the edges. For increasing values of l, a smoother picture is obtained and the maximum radon concentration decreases rapidly. These features can be understood from the fact that at low values of l, compared to the thickness of the material, radon hardly diffuses and builds up in the material. At higher l-values radon rapidly moves out of the material, with as a consequence that the build-up will be lower.

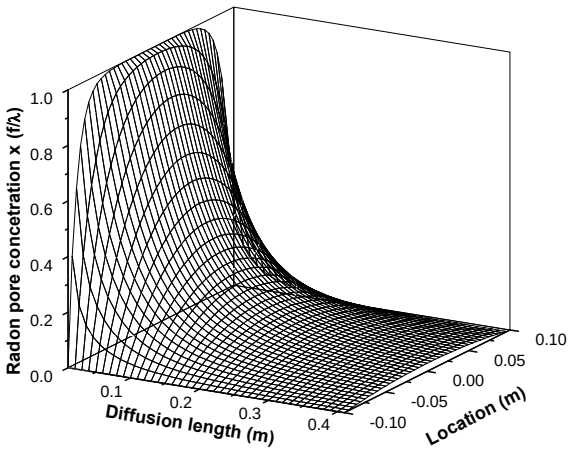

Figure 1.3
A 3D-plot of the radon pore concentration, according to eq. (1.3) as a function of the diffusion length and the position in a construction element of thickness 20 cm.

1.2.4 Exhalation

The area exhalation rate E_a (unit: Bq m^{-2} s^{-1}) of the construction element is defined as

$$E_a = -\varepsilon\, D \left.\frac{dC(x)}{dx}\right|_{x=L}, \tag{1.4}$$

with ε the porosity of the construction element (dimensionless). Combination of the eqs. (1.3) and (1.4) results in the following expression for E_a:

$$E_a = \varepsilon\, f\, l\, \tanh(L/l). \tag{1.5}$$

The production rate of radon per unit of interstitial space, f, can be written as:

$$f = \frac{\lambda\, a_1\, \eta\, \rho}{\varepsilon} \quad . \tag{1.6}$$

The parameters in this equation are a_1, the radium activity concentration (Bq kg^{-1}); η, the emanation factor (dimensionless); and ρ, the material density (kg m^{-3}). Substitution of f into eq. (1.5) results in the following expression for E_a:

$$E_a = \lambda\, a_1\, \eta\, \rho\, l\, \tanh\left(L/l\right). \tag{1.7}$$

For most building materials as gypsum, aerated concrete, sand-lime and clay bricks the diffusion length l of ^{222}Rn is over 40 cm (Keller *et al*., 2001), as a result of which the hyperbolic term in eq. (1.7) approaches the value of its argument for most commonly used construction elements. Eq. (1.7) then reduces to

$$E_a = \lambda\, a_1\, \eta\, \rho\, L\,. \tag{1.8}$$

In this situation the area exhalation rate does no longer depend on the diffusion coefficient and almost all emanated radon atoms reach the exterior of the wall in question. In the case the diffusion length is much smaller than half of the thickness of the wall, the hyperbolic term in eq. (1.7) almost equals unity, resulting in a simplified expression:

$$E_a = \lambda\, a_1\, \eta\, \rho\, l\,. \tag{1.9}$$

This exhalation rate is governed by the diffusion length, l, for a situation in which ^{222}Rn exhales from tight materials such as heavy concrete's. The expression also holds for the exhalation of the other radon isotopes because their short half-lives correspond to short diffusion lengths (see eq. (1.2)) and hence the condition for the hyperbolic term to approach unity is fulfilled.

Moisture not only plays an important role in the emanation of radon, as indicated above, but is also a key parameter in the subsequent transport to the atmosphere. Once radon has entered the pore space, a fraction of it will adsorb to the solid surfaces of the pores. This adsorption decreases rapidly as the pore water content increases, becoming insignificant at pore saturation fractions of 0.01 (Van der Pal, 2003). A second effect of the presence of water in the pores is the partitioning of radon between the liquid and the gas phase. This partitioning is governed by the so-called Ostwald coefficient, defined as the ratio of the radon concentrations (on volume basis) in e.g. water and in air. At room temperature this coefficient for water equals 0.26. Consequently, the radon concentration in the air-filled fraction of the pores increases as the pore saturation fraction rises. Moreover, moisture influences the effective diffusion coefficient; this coefficient gradually

decreases as a function of the pore-water content. At high water content more and more pores will be blocked and the diffusion will then drop significantly. The overall effect of moisture on the exhalation rate of building materials has been studied by Cozmuta (2001) and Cozmuta *et al*. (2003). In Figure 1.4 this is illustrated for a sample of ordinary concrete, showing low exhalation rates for the dry and fully saturated sample, with a maximum at pore-saturation fractions of 0.7-0.8. It clearly demonstrates the necessity to condition the test specimen in relation to humidity prior to the exhalation measurement. Mathematical equations on the multiphase transport of radon have been published for soil (Rogers and Nielson, 1991), sand (Van der Spoel, 1998) and concrete (Cozmuta, 2001).

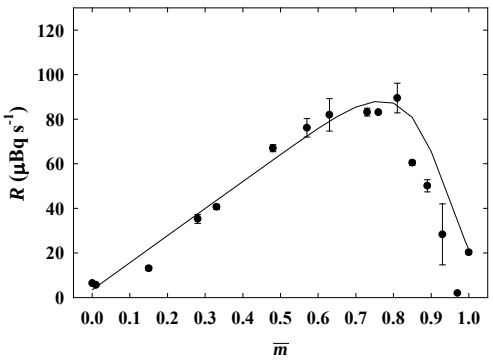

Figure 1.4
The ^{222}Rn exhalation rate, R, of a concrete cube as a function of the mean pore saturation fraction, m. The line indicates the results from model calculation (from Cozmuta, 2001).

1.3 Exposure

1.3.1 Gamma radiation

Gamma radiation is strongly penetrating: when emitted within the construction material, the material itself absorbs only a part of the radiation, leaving the rest to reach the living environments. The resulting absorbed dose in air depends on the activity concentrations of the primordial radionuclides in the various construction elements and is expressed in the unit gray (Gy): the amount of energy deposited in 1 kg of material, in the present case 1 kg of air (J kg^{-1}). Koblinger (1978) made the first Monte Carlo code to calculate the absorbed dose rate due to the presence of gamma-emitting radionuclides in building materials. The dose rate (Gy h^{-1}) follows from

$$\dot{D}_{Air} = \sum_i \sum_j \left(k_j a_j\right)_i , \qquad (1.10)$$

in which i is the index for the various construction elements in the dwelling and j for the considered primordial radionuclides; k_j is the specific absorbed dose rate, defined as the absorbed dose rate in air due to an activity concentration of the construction material of 1

Bq kg^{-1} of the parent in secular equilibrium with its decay products (Gy h^{-1} per Bq kg^{-1}); and a_j the activity concentration of the primordial radionuclide *j* of construction element *i* (Bq kg^{-1}). The specific absorbed dose rate is calculated by Monte Carlo codes or codes that make use of gamma-ray attenuation and build-up factors. The value of this specific absorbed dose rate depends amongst others on the thickness, density, and dimensions of the various construction elements. Since the absorbed dose rate is assumed to be constant through the year, the external radiation exposure of an individual is simply estimated by taking the occupancy factor into account.

1.3.2 Radon

In dwellings the concentrations of ^{218}Rn and ^{219}Rn are too low to play a significant role. The exposure to radon therefore mainly arises from the isotopes ^{222}Rn and ^{220}Rn. As indicated in the Figures 1.1 and 1.2 ^{222}Rn has four short-lived decay products, i.e. ^{218}Po, ^{214}Pb, ^{214}Bi and ^{214}Po and ^{220}Rn five: ^{216}Po, ^{212}Pb, ^{212}Bi, ^{208}Tl and ^{212}Po. Since these short-lived decay products are formed as ions, they will adhere almost immediately to water or other polarized molecules present in the air. This ultra-fine sized fraction of the radon progeny is known as the unattached fraction. Most of these particles will attach rapidly to ambient aerosols and this much larger sized fraction is called the attached fraction. The concentration of the decay products in air is a dynamic balance between on the one hand formation and on the other hand removal by decay, deposition to room surfaces and/or ventilation. On inhalation the short-lived decay products, whether attached or unattached, may deposit along the walls of the airways and thus provide a radiation exposure of the lungs. The corresponding dose is dominated by the alpha-emitting radionuclides, i.e. the polonium isotopes and ^{212}Bi.

For the assessment of the radiation dose due to inhalation of the various daughter products some special quantities are introduced. The potential alpha energy (PAE) is defined as the total alpha energy emitted during the decay of a daughter atom to ^{210}Pb or ^{208}Pb for ^{222}Rn en ^{220}Rn, respectively. In Table 1.2 the PAE is given for each of the daughter nuclides, expressed per atom and per unit activity. In the third column of this table the energy of the emitted alpha particle(s) is given, the next column shows the PAE per atom. The nuclides ^{214}Pb and ^{214}Bi decay by beta emission and therefore their PAE follows from the alpha energy of the decay of ^{214}Po. For ^{218}Po, the precursor of ^{214}Pb and ^{214}Bi, the alpha energy of ^{214}Po adds to the alpha energy released in its own decay. For the short-lived ^{220}Rn progeny a comparable calculation applies, but branching in the decay scheme (see Figure 1.2) and emission probabilities have to be taken into account. Dividing the obtained values by the respective decay constants results in the PAE per Bq (column 5). The last column shows the relative contribution of each of the short-lived progeny.

Table 1.2
Potential alpha energy (PAE) per atom and per unit activity for ^{222}Rn and ^{220}Rn short-lived progeny (1 MeV=1.602 x 10^{-13} J).

Nuclide	Half-life	Alpha energy (MeV)	PAE per atom (10^{-12} J)	PAE per Bq (10^{-9} J Bq^{-1})	Relative contribution
^{218}Po	3.05 m	6.00	2.19	0.58	0.105
^{214}Pb	26.8 m	--	1.23	2.86	0.515
^{214}Bi	19.9 m	--	1.23	2.12	0.380
^{214}Po	164 µs	7.69	1.23	$3x10^{-7}$	$5x10^{-8}$
^{222}Rn at equilibrium (total)				5.56	1.000
^{216}Po	0.145 s	6.78	2.33	$5x10^{-4}$	$7x10^{-6}$
^{212}Pb	10.6 h	--	1.24	68	0.913
^{212}Bi	60.5 m	6.05, 6.09[a]	1.24	6.5	0.087
^{212}Po	299 ns	8.78	1.41	$6x10^{-10}$	$8x10^{-12}$
^{208}Tl	3.05 m	--	0.00	0	0.000
^{220}Rn at equilibrium (total)				75	1.000

[a] Emission probability 0.25 and 0.10, respectively.

The potential alpha energy concentration (PAEC) of any mixture of ^{222}Rn or ^{220}Rn progeny in air is normally expressed in the so-called equilibrium equivalent radon concentration, C_{eq}:

$$C_{eq}^{222} = 0.105\, C_1 + 0.515\, C_2 + 0.380\, C_3 . \quad (1.11a)$$

$$C_{eq}^{220} = 0.913\, C_4 + 0.087\, C_5 . \quad (1.11b)$$

In these equations C_{eq}^{222} is the equilibrium equivalent ^{222}Rn concentration (Bq m^{-3}); C_1, C_2 and C_3 are the activity concentrations of ^{218}Po, ^{214}Pb and ^{214}Bi (Bq m^{-3}), respectively; C_{eq}^{220} is the equilibrium equivalent ^{220}Rn concentration and C_4 and C_5 are the activity concentrations of ^{212}Pb and ^{212}Bi. The constants are the relative contributions of each decay product to the total PAE from the decay of a unit radon gas, as presented in the last column of Table 1.2. In most cases the activity concentrations C_1 to C_3, the short-lived ^{222}Rn daughter nuclides, are not directly measured, but estimated on assumptions made on concentration ratios. Therefore an equilibrium factor is introduced as the ratio between C_{eq}^{222} and the ^{222}Rn gas concentration (C_{gas}^{222}). In formula:

$$F^{222} = C_{eq}^{222} \big/ C_{gas}^{222} . \quad (1.12)$$

In this way a measured ^{222}Rn gas concentration can be linked directly to an equilibrium equivalent concentration. For ^{220}Rn it is not possible to use the gas concentration for dose evaluations, since the ^{220}Rn concentration, due to its short half-life, strongly depends on

the distance to the source. The equilibrium equivalent ^{220}Rn concentration therefore should be based on the measured or modelled activity concentrations of ^{212}Pb and ^{212}Bi in the living space. Because of their relatively long half-lives, the concentrations of these daughter products are nearly homogeneously distributed.

The exposure P of an individual is calculated from the time integral of the equilibrium equivalent radon concentration according to:

$$P = \int_0^T C_{eq}(t)\, dt\,, \tag{1.13}$$

with T the time period of the exposure and $C_{eq}(t)$ the equilibrium equivalent radon concentration at time t. The exposure P is expressed in Bq h m^{-3} or in WLM (Working Level Month), the historical unit for specifying occupational exposures. 1 WL was originally defined as the concentration of potential alpha energy associated with the ^{222}Rn progeny in equilibrium with 100 pCi per litre of air. Nowadays the WL is taken as the potential alpha energy concentration of 1.300x10^{8} MeV m^{-3}, equivalent to 2.08x10^{-5} J m^{-3}. The length of the exposure is normalized at a working period of one month, defined as 170 hours. Together with the conversion that the PAE per Bq of ^{222}Rn and ^{220}Rn at equilibrium equals 5.56x10^{-9} J and 75x10^{-9} J, respectively (Table 1.2), the following relationships can be deduced:

1 Bq h m^{-3} ^{222}Rn at equilibrium $\equiv$ 5.56x10^{-9} J h m^{-3} = 1.57x10^{-6} WLM; (1.14a)
1 Bq h m^{-3} ^{220}Rn at equilibrium $\equiv$ 75x10^{-9} J h m^{-3} = 2.1x10^{-5} WLM. (1.14b)

From these relationships it can be concluded that the exposure per equilibrium equivalent radon concentration is 13 times higher for ^{220}Rn than for ^{222}Rn. In section 1.8 the dose consequences in the Netherlands will be evaluated.

1.4 Dosimetry

The interaction of ionizing radiation with biological material results in ionizations and excitations of molecules and atoms, which may cause molecular changes in the DNA in the cell nucleus. The induced damage includes single- and double-strand breaks in the DNA sugar-phosphate backbone and a variety of modifications in DNA bases. Although the cells possess very efficient mechanisms for signalling and repairing the induced DNA damage, there is a small chance for unrepaired or misrepaired double-strand breaks, thought to be a principal lesions that may lead to modification of healthy cells into malignant ones. Both frequency and complexity of the damage depend on the linear energy transfer (LET) of the radiation, the radiation energy lost per unit of path in the material. As

indicated in the previous paragraph inhabitants are exposed to alpha and gamma radiation, examples of high-LET and low-LET radiation, respectively. High-LET radiation will produce more complex, closely spaced damage, which will be less repairable and more likely to result in chromosomal abnormalities and gene mutations.

Besides various DNA repair pathways, the cellular response to DNA damage also includes arrest at one of several cell-cycle checkpoints and onset of apoptosis, i.e. the active biochemical process of programmed cell death. These two processes prevent the propagation of damaged cells and thus offer an additional protection of an individual against tumour formation. Recent summaries of the biological and epidemiological information on radiation-related cancer risk are given by ICRP and the National Research Council's Committee on the Biological Effects of Ionizing Radiation, BEIR VII (ICRP, 2005; NAS, 2006).

The induction of a radiation-induced cancer is taken to be probabilistic in nature, with no threshold, and in a way that is proportional to the radiation dose. This is known as the linear, non-threshold theory (LNT). Given the uncertainties at low doses, it seems to be unlikely that epidemiological studies will establish the presence or absence of a threshold. However, there is no strong evidence that there is a radiation dose below which all induced DNA damage is repaired with absolute certainty. The National Academy of Science (NAS, 1999) posed that at the typical low radon concentrations in homes most bronchial epithelial cells will never be traversed by an alpha particle and only rarely by more than one per human life span. Doubling the exposure will therefore double the number of cells struck, and so doubles the chances to develop a cancer, yielding a linear dose-response relationship. This conclusion ignores the so-called *bystander effect* that irradiated cells transmit damage signals to neighbouring, non-irradiated cells (for instance Brenner and Sachs, 2002). Multiple biological effects are described for these bystander cells, including the induction of mutations and chromosomal aberrations. However, also beneficial effects have been postulated. Other open questions are whether bystander effects occur *in vivo* and at low doses.

Furthermore, several studies have reported a hormetic dip in the low dose range, for instance by Thompson and colleagues (2008), suggesting a beneficial, protecting effect at low exposures. The effect is contrary to many other studies and also the underlying mechanism is not clear. Both bystander effect and hormesis suggest that the shape of the dose-response curve is non-linear, yielding a lower or greater mortality risk per unit exposure. On the basis of the current literature NAS (2006) and ICRP (2007) judged that the knowledge of these phenomena is insufficient to be incorporated in a meaningful way into the modelling of epidemiological data. The LNT-model is considered as the most appropriate at this time. Studies in biological material indicate an effect of dose rate. We come back to that topic in section 1.5.

The fundamental dosimetric quantity is the absorbed dose, the energy imparted per unit mass. In the low dose range it is assumed that the absorbed dose averaged over a specific organ or tissue can be correlated with the probability of the effect. In the 1990 recommendations of the ICRP (ICRP, 1991) the protection quantity equivalent dose H_T is introduced, defined as

$$H_T = \sum_R w_R D_{T,R} \,, \tag{1.15}$$

where w_R is the radiation weighting factor for radiation R and $D_{T,R}$ the average absorbed dose of organ or tissue T, due to radiation of type R. The sum includes all types of radiation. The SI unit for equivalent dose is J kg^{-1}, given the special name sievert (Sv). The radiation-weighting factor allows for the differences in the effect of various radiations in causing stochastic effects. The effective dose E is defined as the weighted sum of tissue equivalent doses:

$$E = \sum_T w_T H_T \text{ with } \sum_T w_T = 1 \,. \tag{1.16}$$

In these formulae w_T is the tissue-weighting factor for tissue T, representing the relative contribution of that tissue to the total health detriment resulting from uniform irradiation of the body. The effective dose is also expressed in the unit sievert.

The introduction of the quantities dose equivalent and effective dose has enabled the summation of doses from total or partial exposure from external radiations of various types and from intakes of radionuclides. For the indoor exposure to gamma radiation and alpha particles, radiation-weighting factors of 1 and 20 prevail. For the lungs a tissue-weighting factor of 0.12 is recommended (ICRP, 1991). In recently revised recommendations of the ICRP (ICRP, 2007) the above-mentioned values have remained unchanged.

To convert the absorbed dose rate in air due to exposure to gamma radiation into an effective dose, various coefficients are available which depend on radiation geometry and gamma-ray energy. Considering an isotropic irradiation at an average energy of 800 keV, a conversion coefficient of 0.7 Sv Gy^{-1} can be adopted from ICRP publication 74 (ICRP, 1996). Also cosmic radiation will contribute to the absorbed dose rate indoors. The construction materials of the dwelling will partly shield this component. Observed shielding factors range from close to unity for wooden houses up to 0.3 for lower storeys of substantial concrete buildings (Miller and Beck, 1984). Julius and Van Dongen (1985a) have determined an average value of 0.6 for the Dutch situation, based on a contribution of the cosmic rays to the indoor absorbed dose of 24%. Since mostly muons are involved, a conversion coefficient for the cosmic component of unity is appropriate (UNSCEAR,

2000); application of the mentioned 24% as a weighting factor, a weighted overall conversion coefficient for residential absorbed doses in air is obtained of 0.77 Sv Gy^{-1}.

Also the exposure due to the short-lived ^{222}Rn and ^{220}Rn progeny can be expressed in terms of effective dose. In the Basic Safety Standards (EC, 1996), which form the basis for the national legislation on radiation in each of the European Member States, it is stated that for members of the public the conversion from ^{222}Rn exposure to effective dose amounts 1.1 Sv per J h m^{-3}. This factor is adopted from ICRP publication 65 (ICRP, 1993) and was derived by a direct comparison of the detriment associated with a unit effective dose and a unit ^{222}Rn exposure. Given the aforementioned relationship (eq. 1.14a), this corresponds to 6 nSv (Bq h m^{-3})$^{-1}$. This conversion factor, however, seems to be rather low. The improved dosimetric model of the respiratory tract as published in ICRP publication 66 (ICRP, 1994), predicts for ^{222}Rn a three times higher dose conversion factor (Vanmarcke, 1994). Furthermore, in an evaluation of the available data on the absorbed dose to the basal cells of the bronchial epithelium, UNSCEAR (2000) comes to a central estimate of a conversion factor of about 15 nSv (Bq h m^{-3})$^{-1}$. On this basis it can be expected that the official, legal conversion factor will be adjusted upwards in the coming years. Recently the ICRP (2009) published a statement that it indeed intends to publish dose coefficients that result in an increase of around a factor of two of the effective dose per unit exposure.

Anticipating this increase UNSCEAR (2000) applies a conversion coefficient of 9 nSv (Bq h m^{-3})$^{-1}$. For evaluating the exposures due to ^{220}Rn UNSCEAR (2000) has adopted a value of 40 nSv (Bq h m^{-3})$^{-1}$. Based on the evaluation of the principal dosimetric assessments of lung dose from deposited ^{222}Rn and ^{220}Rn decay products, a continued use of these conversion factors is advised in the UNSCEAR 2006 report (UNSCEAR, 2008).

The uptake of ^{222}Rn and ^{220}Rn in blood with distribution throughout the body following inhalation makes up an additional exposure for inhabitants. However, the contribution to the effective dose is small and this pathway is mentioned here only for completeness. The dose coefficients are 0.17 and 0.11 nSv (Bq h m^{-3})$^{-1}$ for ^{222}Rn and ^{220}Rn, respectively (UNSCEAR, 2000).

1.5 Epidemiological data

1.5.1 Gamma radiation

The main source of information on cancer risk of low-LET radiation is the so-called Life Span Study (LSS) on the survivors of the atomic bomb explosions in Hiroshima and Nagasaki. The LSS cohort has some unique features, distinguishing it from many other studies as a large size (87,000 persons), not selected because of disease or occupation,

includes both sexes and all ages and is characterized by a long follow-up period (1950-2000) and high quality mortality and cancer incidence data. Since the distance to the hypocenter is the primary determinant of the radiation dose, the study is probably less subject to confounding factors. In 2004 a new dosimetry system is implemented. This change has resulted in a systematic increase of about 10% in the gamma-ray dose estimates in both cities. An anticipated large increase of the neutron component in Hiroshima for low-dose survivors did not materialize (Preston *et al*., 2004). Figure 1.5 shows the relative risk of solid cancer for Japanese atomic bomb survivors.

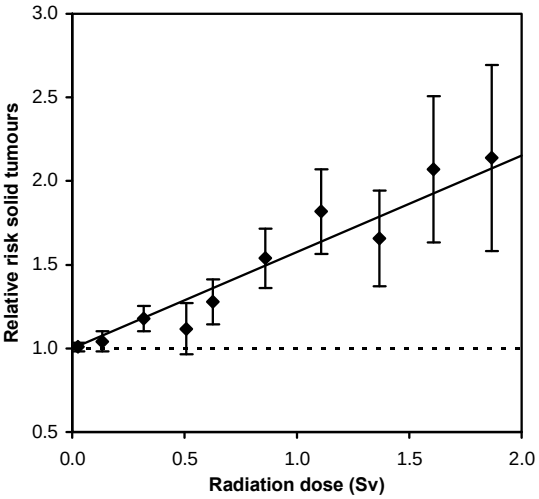

Figure 1.5
Relative risk of solid cancer incidence for Japanese atomic bomb survivors. The relative risk is the rate of solid cancer in the exposed population divided by the rate in an unexposed population. A relative risk of 1, represented by the dotted line, indicates that there is no attributed risk. The straight line indicates a linear fit for the data between 0 to 1.5 Sv. The error bars represent the 95% confidence intervals (after NAS, 2006).

The LSS cohort also has some limitations; all subjects are exposed during wartime and, to be included in the study, had to survive the initial effects of the bombing. This selection might have biased the findings (NAS, 2006). In addition, the subjects are exposed to an acute dose at high dose rates. For application to low dose, low dose rate, continuous exposures, acute exposure data are divided by a dose and dose-rate effectiveness factor (DDREF) to allow for the effect of DNA repair. The BEIR VII Committee indicated that DDREF values are in the range 1.1–2.3, with 1.5 as central number (NAS, 2006). ICRP (2007) retains a summary value of 2.

In Table 1.3 a compilation is given of estimated number of cancer deaths by gender as published by BEIR VII. These results are accompanied by 95% confidence intervals that reflect the most important uncertainty sources, namely (a) statistical variation, (b) uncertainty in the DDREF and (c) uncertainty related to transporting risks from the Japanese A-bomb survivors to the U.S. population. Averaged over both sexes BEIR VII comes to a mortality risk for the whole population of 5.7 per cent per Sv (Table 1.3). ICRP estimates this risk at 4.0 and 4.9 per cent per Sv based on incidence and mortality data,

respectively (ICRP, 2009). In this thesis an averaged and rounded risk factor of 5 per cent per Sv is applied. The 95% confidence interval is taken as 2.5 to 10 per cent per Sv.

Table 1.3
Lifetime attributable mortality risk and 95% confidence intervals for all solid cancers and leukaemia for the U.S. population. Risk expressed in 10^{-2} per Sv whole body dose (after NAS, 2006).

	Males		Females	
	Average	**Range**	**Average**	**Range**
Solid tumours	4.1	2.0 – 8.3	6.1	3.0 – 12
Leukaemia	0.7	0.2 – 2.2	0.5	0.1 – 1.9

Numerous epidemiologic studies have been carried out following the Chernobyl power station accident on April 26, 1986. The explosion resulted in the contamination of a large area, leading in exposures due to external radiation, inhalation, and consumption of contaminated foods. Extensive overviews on this subject have been prepared by the World Health Organization and the aforementioned BEIR VII Committee (WHO, 2006; NAS, 2006). Epidemiological studies of residents of contaminated areas so far have not revealed any strong evidence for an increased mortality in the general population. Among the 61,000 Russian emergency workers about 5000 deaths were recorded during the period 1991-1998, from which 2.3% (95% confidence limits 1.4% to 3.2%) can be attributed to radiation-induced solid neoplasms. For leukaemia the percentage is estimated at 0.3% of fatalities (WHO, 2006). These values are lower than presented in Table 1.3; however, one should bear in mind that the follow-up period is limited to 1998. As the recognized latency period for many solid tumours is about 10 years or more, radiation-associated mortality increases can be expected in the decades to come.

1.5.2 Radon

Inhalation of short-lived decay products of radon may result in their deposition in the lungs. There these products will irradiate the cells lining the airways, thus enhancing the risk of lung cancer. The occurrence of a high mortality rate among miners goes back to the early 16th century. At that time extensive mining of silver took place in the Schneeberg region in Germany and an unusually high mortality from lung disease was observed among the younger miners. A German physician, Agricola (1494-1555), was employed in Joachimstal as a municipal medical officer; he thought that it was caused by the inhalation of dust. In his book *Von der Bergsucht oder Bergkranckheiten drey Bücher*[1] Paracelsus

[1] On lung and other miners' diseases (published after his death in 1567)

(1493-1541), reports on the disease at the same time and suggested it resulted from breathing metallic gases that were deposited in the lungs (Swedjemark, 2004). In the 17th and 18th century the mining in this area was intensified and with that the frequency of this lung disease increased. The disease was later identified as lung cancer. In the 1920s more precise radon measurements were carried out in the Schneeberg mines, but it took to around 1940 before it was generally accepted that the inhalation of ^{222}Rn was as a plausible cause for the high lung cancer frequency among the miners. The causative role of the decay products of ^{222}Rn was postulated another 10 years later by Bale (1951). A comprehensive review on the history of the radon problem is given by Jacobi (1993).

In ICRP publication 65 (ICRP, 1993) the mortality probability coefficient for ^{222}Rn was taken to be 0.08 per J h m^{-3} (2.8×10^{-4} per WLM). It was based on the analysis of data from six epidemiological studies of underground uranium miners and one on iron miners. Since this publication, updated and expanded epidemiological miner data have become available. In 1999 the National Academy of Science published the report of the 6th Committee on Biological Effects of Ionizing Radiations (BEIR VI). In this review the results of 11 miner cohorts have been incorporated, involving a total of 68,000 workers and 2,700 deaths from lung cancer (NAS, 1999). The EPA document (EPA, 2003) is based primarily on the BEIR VI report, with some adjustments and extensions. Among these are numerical estimates of the risk per unit exposure and the number of years of life lost per cancer death. Table 1.4 addresses the estimates by gender and smoking category. For a stationary U.S. population the average risk is calculated at 5.4×10^{-4} per WLM.

Table 1.4
Estimates of risk per WLM by gender and smoking category, fraction of ^{222}Rn-attributable lung cancer deaths and years of life lost per ^{222}Rn-induced lung cancer death for U.S. population (from EPA, 2003).

Gender	Smoking category	Risk per WLM	^{222}Rn-related fraction[a]	Years of life lost	
				Average	Median
Total		5.4×10^{-4}	0.134	17.2	16.4
Male	Ever smokers	10.6×10^{-4}	0.129	16.1	14.9
	Never smokers	1.7×10^{-4}	0.279		
Female	Ever smokers	8.5×10^{-4}	0.116	18.6	17.6
	Never smokers	1.6×10^{-4}	0.252		

[a] ^{222}Rn-related fraction of lung cancer deaths.

The data in the table indicate a clear synergistic effect of the two carcinogens, cigarette smoke and ^{222}Rn. Among the category 'Never smokers' there is no difference between the genders. The 25% larger risk per WLM among the male smokers in comparison to the female smokers has to be attributed to a heavier smoking habit by males. The 90% confidence interval of the average risk factor is estimated at (2–12)x10^{-4} per WLM (EPA, 2003). Several sources contribute to this uncertainty such as limitations in the underground miner data (i.e. cause of death, errors in exposure rates and duration, confounding factors). Furthermore uncertainties arise from an extrapolation from mines to homes. Exposure conditions in homes differ substantially from those in mines, amongst others with respect to breathing rates, size distribution of aerosol particles, number of particles, the level of the unattached fraction and the age at exposure. Such effects may result in a higher or a lower residential lung dose per WLM. To account for these effects a factor K is introduced that is defined as the ratio of the dose per WLM exposure in homes relative to mines. In BEIR VI it was estimated that the effects on average approximately counterbalance and the factor K was taken to be 1.

In data from miner studies a so-called inverse exposure-rate effect is observed, i.e. for equal total exposure, relative risks are greater for exposures at low exposure rate and longer duration than those occurring at high rates and short duration. (Hornung and Meinhardt, 1987; Darby and Doll, 1990; Lubin *et al*., 1995). The estimates derived from miner cohorts may not accurately reflect the risk at low exposures and low exposure rates as experienced in homes. Lubin *et al*. (1997) made an analysis of miners that were exposed to levels either under 50 WLM or 100 WLM, exposures at which the inverse exposure-rate effect is minimal. The analysis showed an estimated ^{222}Rn-attributable risk for lung cancer of 10% to 14% in U.S. population, compatible with the suggested risk based on models from unrestricted miner data by EPA (Table 1.4). UNSCEAR (2008) reviewed results of 9 miner cohorts in her 2006-report. The excess relative risk (ERR) per unit ^{222}Rn concentration is estimated at 0.12 per 100 Bq m^{-3}, with a 95%-confidence interval of 0.04 to 0.2.

Besides epidemiological studies of mining cohorts, more and more data become available on residential exposure and lung cancer. An extensive study has been carried out by Cohen (1995), who found a negative correlation between the average ^{222}Rn concentration and the local lung cancer rate in 1600 U.S. counties. This study is a so-called ecologic study, a type that has been criticized widely. Ecologic studies analyse exposure, outcome and other variables at a group-level instead of an individual-level. The loss of information caused by this aggregation can lead to a severe bias. In the case of the study by Cohen a possible confounding with smoking has been suggested (NAS, 1999; Puskin, 2003).

Case-control studies among inhabitants overcome many of the limitations in ecologic studies. To date more than 20 case-control studies have been completed (see overview by

Al-Zoughool and Krewski, 2009) but in general these have not been large enough to reliably assess the risk associated with low ^{222}Rn levels in comparison to those in mines. However, by clustering these studies greater statistical power can be achieved. Darby *et al.* (2004) reported a pooled analysis of a European collaborative study comprising 13 case-control studies. This study includes 7,148 cases of lung cancer and 14,208 controls. Before corrections for random uncertainties in measuring ^{222}Rn concentrations a risk of lung cancer is reported to be increased by 8.4% per 100 Bq m^{-3} ^{222}Rn. Figure 1.6 shows the relation between the relative risk of lung cancer and residential ^{222}Rn concentration.

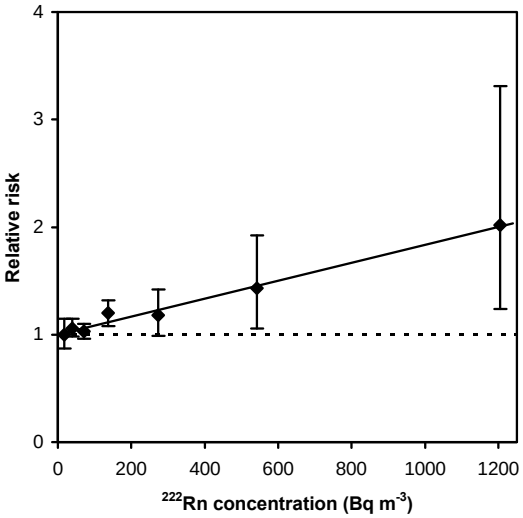

Figure 1.6

Relative risk of lung cancer according to the residential ^{222}Rn concentration. The relative risk is the rate of lung cancer in the exposed population divided by the rate in an unexposed population. A relative risk of 1, represented by the dotted line, indicates that there is no attributed risk. The straight line is the best fit of the data. The error bars represent the 95% confidence intervals (after Darby et al., 2004).

In Table 1.5 the results of this and some recent other studies on pooled data are presented. These studies indicate a significant association between exposure to residential ^{222}Rn and the risk of lung cancer; the central estimate of the excess relative risks (ERR) of these studies coincide very well, with a range from 0.08 to 0.13 per 100 Bq m^{-3} ^{222}Rn. This range increases from 0.09 to 0.32 when the analysis was restricted to people who had lived in at most two residences during the last 30 years. Using the inverse of the variance in the relative risk values as a weighting factor, UNSCEAR (2008) has reported combined relative risks of 0.09 and 0.11 per 100 Bq m^{-3} for the primarily and restricted analysis, respectively. These data compare remarkable well with the results of the pooled epidemiological studies of miners.

A number of ^{222}Rn measurements made in the same house but in different years may show considerable random variability. This could lead to misclassification and, as a result, to large confidence intervals. The best way to extract the relation between risk and measured ^{222}Rn concentration is to make use of individual long-term average concentration values. Darby *et al*. (2004) made a correction for random uncertainties in the assessment of

^{222}Rn, whereupon the dose-response relationship remained linear but nearly doubled in strength to an ERR of 0.16 (95% confidence interval 0.05 – 0.31). Although the correction requires a number of assumptions, it is considered at this time as an appropriate estimate of the lifetime risk from ^{222}Rn in homes.

For lung cancer risk following exposure to ^{220}Rn no epidemiological data are available. Unlike ^{222}Rn, it is therefore not possible to extract mortality risks directly from epidemiological studies. For evaluating the consequences of the exposure to ^{220}Rn a dosimetric approach is followed, instead. In section 1.8 this approach is specified further.

Table 1.5
Excess relative risk (ERR) of lung cancer and 95% confidence intervals at 100 Bq m^{-3} ^{222}Rn as found in pooled residential case-control studies.

Reference	Pooled data	ERR	ERR[a]
Lubin (2003)	2 Chinese studies	0.13 (0.01 – 0.36)	0.32 (0.08 – 0.88)
Darby *et al*. (2004)	13 European studies	0.08 (0.03 – 0.16)	0.09 (0.03 – 0.18)
Krewski *et al*. (2005)	7 N-American studies	0.11 (0.00 – 0.28)	0.18 (0.02 – 0.43)
UNSCEAR (2008)	Combined	0.09 (0.04 – 0.15)	0.11 (0.05 – 0.19)

[a] Restricted analysis to those who had lived in at most two residences.

1.6 Research on natural radiation in the Netherlands

1.6.1 SAWORA programme

Triggered by results of foreign studies the Dutch government started in 1982 the national research programme SAWORA (*Stralingsaspecten van Woonhygiëne en verwante Radio-ecologische problemen*[2]). In this initial programme the situation in the Netherlands was investigated with respect to the natural background radiation. This included surveys on the ^{222}Rn level and external dose rates in Dutch dwelling (De Meijer *et al*., 1986; Julius and Van Dongen, 1985b), and the activity concentrations of soils and building materials (Ackers, 1985; Ackers *et al*., 1985; Bannink *et al*., 1986). The results of these and other studies are summarized by Hogeweg (1986b) and PEO (1986). The general picture that emerged from these early studies was that the situation in the Netherlands was more favourable than in most other European countries with low average indoor ^{222}Rn levels and neither radon-prone areas nor soils, nor building materials with exceptionally high activity concentrations.

[2] Radiation aspects of domestic hygiene and related radio-ecological problems.

1.6.2 RENA programme

The next research program was given the acronym RENA (1987-1990: *Reguleerbare vormen van natuurlijke achtergrondstraling*[3]) and focussed on sources of natural origin, that are more or less controllable by human actions. The aim of this program was to describe these sources in more detail and to identify their distribution and exposure. The sources were grouped into (a) emission from the non-nuclear industry; (b) housing in relation to infiltration of ^{222}Rn from soil; (c) housing in relation to building materials; and (d) food consumption. Most of the findings of this programme are laid down in reports that are released in the so-called *Stralenbeschermingsreeks* of the Ministry of VROM. In the framework of this programme new and improved methods are developed for the determination of low ^{222}Rn concentrations in air. The time-dependent infiltration of ^{222}Rn into dwellings is investigated in detail in a test dwelling in Roden. For this house, ^{222}Rn concentrations were measured for several years and the air permeability's of the ground floor and the building envelope were determined from pressurisation measurements. These data were used to estimate the average ^{222}Rn source terms of crawl space and living room. For the crawl space, infiltration of ^{222}Rn originating from the soil beneath the dwelling is the dominant pathway, which transport is influenced by the groundwater level, pressure difference and soil moisture. In the living room ^{222}Rn originates from the building materials and the crawl space. Mass balance considerations identified an additional source (De Meijer, 1992).

Also in part c. of the programme concerning the building materials, new methods were developed to quantify the building materials-related exhalation rate and emanation factor of ^{222}Rn. These methods have been used to complete the picture of building materials available on the Dutch market concerning these quantities and to investigate the reducing action of coatings. Coatings commonly used in the Netherlands for decoration of walls and ceilings, however, were found to be ineffective (Van Dijk and De Jong, 1989). Furthermore a study was completed after the radiological consequences of the re-use of industrial by-products into building materials. Among these by-products were fly ash, blast furnace slag, recycled aggregates, and various gypsum residues. Especially the processing of gypsum from phosphoric acid production has been identified as dose increasing (Winder *et al*., 1990).

The overall conclusions from the RENA-programme were that residence in dwellings comprises the largest contribution to the radiation exposure of the Dutch population. The use of building materials with advantageous radiological properties, ventilation of the crawl space and reduction of the air leak of the ground floor are considered as most cost-

[3] Controllable forms of natural background radiation.

effective countermeasures. A summary of the results achieved in this programme is published by NOVEM (1992).

1.6.3 STRATEGO programme

Although the RENA-programme significantly contributed to the understanding of the radon problem and to policymaking, it also raised some new questions that needed an answer. Therefore a follow-up programme was started (STRATEGO: *Straling ten aanzien van de gebouwde omgeving*[4]), in which framework the effectiveness of increase of crawl space ventilation and reduction of the air leak of the ground floor have been investigated in detail. A large-scale study based on measurement in 175 dwellings revealed an average crawlspace ^{222}Rn concentration of 43 Bq m^{-3} (Schaap, 1996), much lower than the anticipated 300 Bq m^{-3} that formed the basis of the model calculations by Van der Ham *et al*. (1991). Introduction of both countermeasures, therefore, resulted in only slightly lower ^{222}Rn concentrations in the living rooms of these dwellings, not significantly different from the original ones.

Based on the assumption that in the Netherlands the soil under and beneath the house was the main source of the indoor ^{222}Rn concentration, two studies in large laboratory facilities are performed, i.e. a radon vessel to study the transport in sand (Van der Spoel, 1998) and a laboratory dwelling for the evaluation of ^{222}Rn transport from crawl space to living spaces (De Jong and Van Dijk, 1995; 2005). In the first study it was shown that ^{222}Rn transport and exhalation from dry sand could be fairly well described on the basis of independently measured characteristics of the sand. When the sand is wetted, however, the situation is more complex; the difference between measurements and model results is such that the conclusion is drawn that the model not adequately covers all processes and/or that the studied sand column was not homogeneous. The experiments in the laboratory dwelling showed that the ratios of the ^{222}Rn concentrations in living area and crawl space as a function of the air leakage of the floor and the pressure difference across the floor follow a transport model within just a few per cent. The construction was used to test some countermeasures to reduce infiltration of ^{222}Rn into a living space. Three options were simulated:

(a) Thin-film membrane spread over the ground within the crawl space;
(b) Thin-film membrane applied underneath the concrete floor; and
(c) As option (b), but with a small fan fitted in the membrane.

---

[4] Radiation in relation to buildings.

Relative to the otherwise identical situation without a membrane, the effectiveness of the options (a) and (c) was 25% and >95%, respectively, and found to be independent of the air leakage of the floor. This is not the case for option (b); for this situation the effectiveness ranged from 20% to 90%.

In the STRATEGO-programme also attention has been paid to the release of ^{222}Rn from building materials; below these studies are shortly summarized:

- One anticipates a shortage in river gravel in near future and would like to replace coarse aggregates with broken stony materials. The natural radioactivity concentrations and the release of ^{222}Rn of these materials have been investigated. Tested were sandstone and various limestones from Belgium, granite from UK and Norway, and German basalt. Compared to an apartment building constructed from concrete with Meuse gravel, the annual dose to an inhabitant would be about 70% larger in case sandstone and basalt was used. Replacement by limestone on the contrary, results in a lower exposure up to 60% (Hol *et al*., 1991).
- A pilot study was carried out on the possibilities to reduce ^{222}Rn releases by concrete samples. Type and amount of cement, addition of fly ash and some alternatives for gravel were varied (Van Hulst *et al*., 1993). More details are given in section 4.2.
- KEMA published a model to convert measured activity concentrations and ^{222}Rn exhalation rates of construction materials to an indoor radiation dose (Roelofs and Wiegers, 1995). Starting points for this model are a fixed geometry and ventilation rate of the model room. Based on the prevailing market share of various common stony building materials and their average radiological parameter values, the total external dose rate due to building materials sums to 0.7 mSv per year.
- A national survey was conducted by NRG, in cooperation with KVI on the radioactivity concentration and exhalation rate of building materials, available on the Dutch market (De Jong *et al*., 2001). This study is described in detail in section 3.1 of this dissertation.

A more detailed overview of the STRATEGO programme is given by Lembrechts (2002).

1.7 Radon policy in the Netherlands

In the Dutch environmental policy an individual risk approach is taken as an instrument for setting limits and priorities (VROM, 1989; 1990a). For radon this has been effectuated subsequently in *het Beleidstandpunt Radon*[5] (VROM, 1994), for the most part based on the results of research programmes and summarized in a criteria document on radon (Vaas *et*

[5] Policy Position on Radon.

al., 1993). In this policy plan the following objectives are considered to be feasible: (a) adjustment of the common building practice to reduce the ^{222}Rn concentration in newly build houses to an average of 20 Bq m^{-3}; (b) in the long-term mitigation in existing dwellings to arrive also at an average ^{222}Rn concentration of 20 Bq m^{-3}; and (c) no increase of the dose contribution from building materials. A further elaboration of these requirements was foreseen in the next years in which the modelled efficiencies could be verified by actual measurements.

These measurements showed that the basis of this policy plan was incorrect, i.e. the most important ^{222}Rn source is not the crawl space but the construction materials. In June 1997, the deputy minister Tommel of VROM, presented an adapted plan on ^{222}Rn to the Dutch Lower House (Tommel, 1997). Starting point was to conserve the relative favourable situation on radiation exposure in Dutch buildings. In analogy with an energy performance standard a radiation performance standard (SPN) was proposed as an instrument, to be embedded in the Dutch Building Directive (Bouwbesluit; DB (1991)). It was thought that it would already stimulate attention for radiation in the design phase. In the preparation of such a standard, Schaap *et al*. (1998) have carried out a preliminary investigation, in which several recommendations were proposed, including a ventilation module and a way to assess the indoor radiation dose. Most of these recommendations have been incorporated in the present SPN (NEN, 2002).

In the same period the action program Health and Environment was started with the aim to improve the decision-making process of environmental problems with known or expected health effects. And since indoor radiation exposure was recognized as an ongoing question, it was selected as one of the subjects for such an assessment. The report covers aspects as the scale of the problem, the severity of health effects, necessity, possibilities and effectiveness of countermeasures and an analysis of costs and benefits (Van Bruggen *et al*., 2004). In the note *Nuchter omgaan met risico's: beslissen met gevoel voor onzekerheden*[6] (VROM, 2004) it is concluded that former objectives to stop the ongoing increase of the indoor ^{222}Rn concentration levels with time, are still valid.

The building industry, however, has indicated more than once to have major objections against the introduction of an SPN. Arguments are an increasing number and complexity of rules and fear for cost increase. The industry has taken on commitments, laid down in a covenant with the Government, in which amongst others it is agreed on that (a) the exhalation rate and radioactivity concentrations of building material will not increase; (b) a control program will run to check this; and (c) a research program is started, looking at the possibilities to reduce indoor radiation doses due to building materials (Van Geel, 2004).

---

[6] Facing risks realistically: make decisions with a sense for uncertainties.

The covenant expires in 2015. Thereafter the focus will be on the European approach. Although published in 1989 the Construction Product Directive (EC, 1988) is given a new impulse. In this Directive it is stated that (annex I):

> *"The construction work must be designed and built in such a way that it will not be a threat to the hygiene or health of the occupants or neighbours, in particular as a result of any of … (i) the presence of dangerous particles or gases in the air or (ii) the emission of dangerous radiation…."*

In this Directive no specification is given of the concept "radiation", nor does it suggest any methods or limits to be applied. Analogously a reformulation of the Basic Safety Standards (EC, 1996) is currently in process, a Council Directive that forms the basis of the national legislation on radiation in all European Member States. The Commission published some considerations on this revision (EC, 2009) for both ^{222}Rn levels and building materials. The Commission proposes that Member States shall establish national reference concentrations for ^{222}Rn not exceeding (as an annual average):

- 200 Bq m^{-3} for new buildings;
- 400 Bq m^{-3} for existing buildings;
- 400 Bq m^{-3} for buildings with a high occupancy of the public[7]; and
- 1000 Bq m^{-3} for existing workplaces and other public buildings.

The first two reference levels correspond to those from a recommendation on indoor exposure to ^{222}Rn (EC, 1990). The policy adjustment therefore does not change the levels but promotes them from recommendation to regulation.

By introducing requirements for building materials the Commission pursues further harmonization of regulatory approaches by the various Member States. The proposal (EC, 2009) involves measurement of the activity concentrations of the three primordial radionuclides from which an index is calculated according to the formula (EC, 1999b; Markkanen, 2001):

$$I = a_1/300 + a_2/200 + a_3/3000\,. \qquad (1.17)$$

In this formula a_1, a_2 en a_3 represent the activity concentrations of ^{226}Ra, ^{232}Th and ^{40}K in Bq kg^{-1}. Since the constants in this formula are expressed in mSv a^{-1} per Bq kg^{-1}, the dimension of index I is mSv a^{-1}. The relation between activity concentration index and calculated resulting annual external radiation dose is given in Table 1.6. Reference values depend both on the way a material is applied in a construction (i.e. bulk or surface) and a dose criterion. In the guidance RP 112 (EC, 1999b) it is noted that this criterion should be

[7] For instance nursery rooms, schools and prisons.

based on a dose in the range 0.3 – 1 mSv a^{-1}. On the one hand building materials should be exempted from all restrictions if the dose due to gamma radiation is less than 0.3 mSv a^{-1}, but on the other hand doses larger than 1 mSv a^{-1} should be accepted only in some very exceptional cases. In the current considerations (EC, 2009) the 1 mSv per year level is proposed as dose criterion. If the activity concentration index exceeds the value of 1 (bulk material) or 6 (surface materials) the authority should consider control measures.

Table 1.6
Relation between activity concentration index, dose criterion and use of the material (EC, 1999b).

Use of building material	**Dose criterion**	
	0.3 mSv a^{-1}	**1 mSv a^{-1}**
Materials used in bulk amounts, e.g. concrete	$I \leq 0.5$	$I \leq 1$
Surface and other materials with limited use[a]	$I \leq 2$	$I \leq 6$

[a] e.g. tiles, boards, …

The method described above is a very simple one and easy to apply. The ^{222}Rn emission of building materials is not taken into account in calculating the dose to inhabitants. It is argued that when the annual gamma dose is limited to 1 mSv, the ^{226}Ra activity concentration in materials is limited to levels which are unlikely to cause indoor ^{222}Rn levels exceeding the design level of 200 Bq m^{-3} as established in the Commission's recommendation (EC, 1990). Such indoor levels, however, are uncommon in the Netherlands; large-scale introduction of building materials with an activity concentration index of 1 will therefore certainly increase the average radiation burden to inhabitants, by that thwarting the current Dutch standstill policy. On the other hand correction factors on for example thickness and density of a material and the presence of doors and windows are omitted in eq. (1.17), leading to a considerable overestimation of building material-induced external dose rates. According to data presented by De Jong and Van Dijk (2008b; section 3.4) this amounts to 40% for an average Dutch situation. Another point of criticism is the total absence of ^{220}Rn in the control of the radiation dose due to building materials. Limiting the external dose rate according to eq. (1.17) for a surface material as plaster to $I \leq 6$, is no guarantee for sufficiently low exhalation rates of ^{220}Rn.

1.8 National levels and estimated consequences

In this section the results are summarized of national surveys and a best estimate is given of the number of fatalities due to (a) exposure to external radiation; (b) inhalation of short-lived ^{222}Rn progeny; and (c) inhalation of short-lived ^{220}Rn progeny. These three components are discussed separately.

1.8.1 External radiation

Absorbed dose rates in Dutch dwellings due to gamma and cosmic radiation have been deduced from four national surveys. The first survey comprised 400 living rooms and was carried out with a high-pressure ionization chamber; the others surveys determined the absorbed dose rate by thermoluminescence dosimetry in 400, 1000 and 300 dwellings, respectively. Table 1.7 presents an overview of these studies.

Table 1.7
Absorbed dose rates in air in Dutch living rooms.

Parameter (unit)		**Ionization chamber[a]**	**TLD[be]**	**TLD[c]**	**TLD[de]**
Mean	(nGy/h)	83	84	90	85
Median	(nGy/h)	82	82	88	84
SD	(nGy/h)	12	13	n.a.	10
n		399	401	1005	298
Minimum	(nGy/h)	52	61	n.a.	60
Maximum	(nGy/h)	117	166	n.a.	128

[a] Source: Julius en Van Dongen (1985b); conversion 1 R = 8.76 mGy (ICRU, 1992).
[b] LiF(Mg,Ti); Source: Julius en Van Dongen (1985b).
[c] CaF_2(Dy); Source: De Meijer *et al*. (1986); conversion 1 R = 8.76 mGy (ICRU, 1992).
[d] LiF(Mg,Ti); Source: De Jong and Van Dijk (2009).
[e] Conversion coefficient 1.19 Sv Gy^{-1} (800 keV) (ICRU, 1998).

As shown in this table, the results of various studies agree very well. Furthermore it shows that the mean and median values are almost the same, consistent with near-Gaussian distributions. The average value is about 85 nGy h^{-1} with an estimated standard deviation of 10 to 13 nGy h^{-1}. Absorbed dose rates in bedrooms are reported at a mean and standard deviation of 83 ± 10 nGy h^{-1} (n=295 observations), which is not significantly deviating from those in living rooms (De Jong and Van Dijk, 2009). A similar finding is reported by De Jong and Van Dijk (2001) for a small housing estate. If the time spent indoors is taken as 7000 h per year (80% of the total time) and using a conversion factor of 0.77 Sv Gy^{-1} (paragraph 1.4), an annual effective dose of 0.46 mSv can be calculated due to external radiation. The building material-induced portion that contributes to the resulting effective dose is estimated by De Jong and Van Dijk (2008b) at 0.25 mSv a^{-1}.

1.8.2 Short-lived ^{222}Rn progeny

In the Netherlands data on three surveys on indoor ^{222}Rn are available. The first survey covered about 1000 dwellings constructed in the period up to 1983 (Put *et al*., 1985; De Meijer *et al*., 1986). The second one was conducted in 1995-1996 and provides additional information on 1500 dwellings built in the period 1985-1993 (Stoop *et al*., 1998). From these studies it emerges that the ^{222}Rn concentration in the living room gradually increases with the date of construction. In dwellings constructed before 1970 the average concentration in the living room is around 20 Bq m^{-3} and increases to 25 Bq m^{-3} for dwellings build in the period 1970-1980. For houses built after 1980 the living room concentration increased by another 5 Bq m^{-3} to an averaged value of about 30 Bq m^{-3}, with a range of 5 to 400 Bq m^{-3}. The air-tightness of Dutch dwellings has increased gradually since 1970 (Cornelissen and De Gids, 1997) to reduce energy consumption. The associated lower ventilation rate is thought to be the main cause for this shift to higher indoor ^{222}Rn levels with time. Through the years also a gradual change in the building materials has occurred, a factor identified as an additional cause for the increase of the ^{222}Rn level (Lembrechts *et al*., 2001). Recent results show that during the last two decades no increase of the indoor ^{222}Rn concentration with the year of construction could be demonstrated anymore (Blaauboer *et al*., 2007).

As reported by Stoop *et al*. (1998) about 70% of the ^{222}Rn concentration originates from the construction materials of the dwelling. The remaining ^{222}Rn comes in almost equal parts from outside air and from the crawl space. Averaged over the entire housing stock the indoor ^{222}Rn concentration is 23 Bq m^{-3}. In bedrooms the ^{222}Rn level is in general 10-30% lower (Put *et al*., 1985; Stoop *et al*., 1998; De Jong and Van Dijk, 2001). So far, the situation in the Netherlands offered a clear, unambiguous picture. The third national survey, however, changed that image. In that survey, covering 1000 newly-built houses in the period 1994-2003, considerably lower ^{222}Rn levels are found; in living rooms and bedrooms an annually averaged concentration is measured of about 13 to 14 Bq m^{-3} (Blaauboer *et al*., 2007), more than a factor of two lower than expected on the basis of the earlier surveys. The most likely explanation for this finding is that the previous applied measuring devices erroneously included a part of the available ^{220}Rn, leading to systematically higher results. Recent studies confirm this lack of specificity for these devices (Vargas en Ortega, 2007).

Additionally, the results of the last survey are in agreement with results of the ^{222}Rn exhalation rates of Dutch building materials. For calculation of the ^{222}Rn source term in the living room two methods can be followed:

- The source term is determined from the difference between the ^{222}Rn efflux and influx of living rooms, or

– From the ^{222}Rn exhalation rates of the various building materials in combination with averaged results of the occurrence of these building materials in Dutch livings.

In the first method the calculation is based on the results on average ^{222}Rn levels and air flows presented by Bader *et al*. (2009), the second on the ^{222}Rn exhalation rates and housing data from De Jong *et al*. (2006) and De Jong and Van Dijk (2008b). According to De With and De Jong (2009) these two methods result in average ^{222}Rn source terms for the living room of 138 mBq s^{-1} and 133 mBq s^{-1}, respectively. Since these values are in close agreement, this supports the idea that the results of the third ^{222}Rn survey reflect the situation in the Netherlands closer than the former data.

Based on the average indoor concentrations in living rooms and bedrooms as found in the last survey, an annual effective dose due to inhalation of short-lived ^{222}Rn decay products can be calculated as follows:

– To convert the ^{222}Rn concentration into an equilibrium equivalent concentration (EEC) a typical equilibrium factor of 0.4 is adopted (Hopke *et al*., 1996; UNSCEAR, 2000);
– To convert the EEC into an effective dose rate a conversion factor of 9 nSv h^{-1} per Bq m^{-3} is applied (paragraph 1.4);
– The time spent indoors is taken as 7000 h per year (80% of the total time). The inhabitant is assumed to be in the living room for 61% of that time and 39% in the bedroom (ICRP, 1994).

In this way the annual effective dose due to ^{222}Rn progeny is calculated to be 0.34 mSv.

1.8.3 Short-lived ^{220}Rn progeny

Triggered by the results of the third survey ^{220}Rn, the radon isotope from the ^{232}Th series, is put on the agenda of future programmes on the natural radiation environment. So far Hogeweg (1986a) published the only Dutch data on ^{220}Rn; in that study an EEC is reported of 0.4 ± 0.2 Bq m^{-3}, but included only a limited number of 6 dwellings. De With and De Jong (2009) have applied a Computational Fluid Dynamics (CFD) calculation model to estimate the three-dimensional distribution of ^{220}Rn and its short-lived decay products in an average living room. The calculations include attachment to aerosol particles, deposition to room surfaces, decay and ventilation. Due to its short half-life the building materials are the only source of ^{220}Rn in a dwelling. Since no ^{220}Rn exhalation measurements are available in the Netherlands, the source term for ^{220}Rn in the living room is estimated from eq. (1.9) by assuming that (a) the ^{220}Rn emanation factor is the same as for

^{222}Rn and (b) the ratio between the diffusion lengths of ^{222}Rn and ^{220}Rn can be described as:

$$l_{222}/l_{220} = \sqrt{\lambda_{220}/\lambda_{222}} = 77\,, \qquad (1.18)$$

with l the diffusion length (m) and λ the decay constant (s^{-1}). This equation follows from eq. (1.2). Given the distribution of the various building materials in an average Dutch living room, the ^{220}Rn source term is estimated to be 14 Bq s^{-1} (De With and De Jong, 2009), two orders of magnitude larger than for ^{222}Rn. Based on this source term the ^{220}Rn concentration is calculated to decrease gradually from almost 15 Bq m^{-3} close to the walls to 3 Bq m^{-3} in the centre of a room, with an average value of 9 Bq m^{-3}. Due to the relatively long half-lives of the ^{220}Rn decay products ^{212}Pb en ^{212}Bi, the indoor concentrations of these radionuclides are nearly uniformly distributed throughout the room; according to eq. (1.11b) the EEC is calculated as 0.33 Bq m^{-3}.

The annual indoor effective dose due to inhalation of short-lived decay products of ^{220}Rn is determined in the same way as described above for ^{222}Rn, except that a conversion factor is applied of 40 nSv (Bq h m^{-3})$^{-1}$ as mentioned in paragraph 1.4. This results in a contribution to the annual effective dose of about 0.09 mSv (Table 1.8).

Table 1.8
Average indoor effective dose per component and per room. To reflect the occupancy pattern a weight of 61% is assumed for the living room and 39% for the bedroom (ICRP, 1994). Time spent indoors is taken as 7000 h per year.

Component	**Room**[a]	**EEC (Bq m^{-3})**	**Dose rate (nGy h^{-1})**	**Eff. dose (mSv a^{-1})**	**Fraction**[b] **(%)**
External radiation	LR	--	85	0.28	55
	BR	--	83	0.18	55
^{222}Rn daughter nuclides	LR	5.4	--	0.21	70
	BR	5.2	--	0.13	70
^{220}Rn daughter nuclides	LR	0.33	--	0.06[c]	100
	BR	0.30	--	0.03[c]	100
^{222}Rn + ^{220}Rn gas	LR/BR	--	--	0.02	80
Sum				0.90	65

[a] LR: living room; BR: bedroom.
[b] Building material related percentage of the annual effective dose.
[c] No coatings (paint, plaster, …) assumed.

Some additional remarks should be placed at the deduction of this value:

- It is assumed that building materials are not covered with a decoration, as a paint coating. The traditionally applied coatings in the Netherlands have no effect on the ^{222}Rn exhalation rates (De Jong en Van Dijk, 1994). However, since the diffusion length of ^{220}Rn is much shorter than for ^{222}Rn (eq. (1.18)), such coatings may reduce the release of ^{220}Rn;
- The presence of a plaster is not considered either. In an earlier study it was shown that some plasters, available on the Dutch market, contain gypsum from phosphate production, resulting in ^{228}Ra levels up to 250 Bq kg^{-1} (De Jong *et al*., 1998). This strongly affects the ^{220}Rn source term and with that the indoor effective dose. Back-of-the-envelop calculations suggest a raise of the ^{220}Rn source term by a factor of 25 for a 1 cm thick coat of such a plaster, resulting in an additional effective dose of the order of 2 mSv a^{-1}.

As indicated at the end of section 1.4, an uptake of inhaled ^{222}Rn and ^{220}Rn in blood and a subsequent distribution throughout the body results in a small contribution to the effective dose. Based on average concentrations and conversion factors listed in section 1.4, this contribution is calculated[8] to be 0.02 mSv a^{-1}. Table 1.8 presents an overview of the average indoor effective dose per component. The total dose is estimated at 0.9 mSv, of which 65% is due to construction materials. These data are based on the present, incomplete information; future investigations have to confirm the assumptions made.

1.8.4 Number of fatalities

The number of fatalities in the Netherlands can be estimated from the results presented in the previous sections. The number due to external radiation, including the cosmic and terrestrial components is based on the computed annual effective dose as listed in Table 1.8. The number of fatalities follows from the product of this value, the mortality risk as given in section 1.5 and the number of inhabitants in the Netherlands of 16.5 million (CBS, 2009) and amounts to almost 400 individuals per year. According to the European pooled residential case-control studies 16% of the cases of lung cancer per exposure to 100 Bq m^{-3} can be attributed to ^{222}Rn. The number of individuals in the Netherlands that died from lung cancer in 2008 is reported at 9918 (CBS, 2009). Combination of these figures with an average indoor ^{222}Rn concentration of 13-14 Bq m^{-3} as found in the last survey, leads to a best guess of the number of fatalities of around 200, with a range of 50 to 400. These values differ considerably from the central estimate of 800 (range of 100 to 1200) per year

[8] Calculation: [13 Bq m^{-3} x 0.17 nSv (Bq h m^{-3})$^{-1}$ + 9 Bq m^{-3} x 0.11 nSv (Bq h m^{-3})$^{-1}$] x 7000 h a^{-1}.

as published by the Health Council of the Netherlands (Gezondheidsraad, 2000). The main reasons for this are (a) the correction of the actual ^{222}Rn concentration by a factor of 2; and (b) the use of a lower risk factor based on residential exposures instead of on mining cohorts.

There are no epidemiological data available for lung cancer risk following exposure to ^{220}Rn (thoron) daughter nuclides. Therefore it is assumed that the number of fatalities due to inhalation of the progeny of ^{220}Rn and ^{222}Rn is in the proportion of their effective doses from Table 1.8. When no additional coating of construction elements is assumed, a number of ^{220}Rn-induced lung cancer deaths of about 60 per annum is obtained. In Table 1.9 these results have been summarized and yield a total value of 650 fatalities per year with a range of 250 to 1300 individuals.

Table 1.9
Overview of the estimated mortality rate in the Netherlands attributed to natural radioactivity in Dutch dwellings.

Component	**Number of fatalities per annum**	**95% confidence limits**
External radiation	375	188 – 751
^{222}Rn daughter nuclides	211	66 – 409
^{220}Rn daughter nuclides	56[a]	18 – 109
Sum	642	272 – 1269
Sum (rounded values)	650	250 – 1300

[a] No coatings (paint, plaster, …) assumed.

1.9 This thesis

The situation with regard to the exposure to natural radiation in Dutch dwellings differs in a number of aspects from that in most other countries. In the Netherlands building materials are thought to be responsible for about 55% of the external radiation burden and 70% of that due to ^{222}Rn and thereby play a more prominent role than the soil beneath a dwelling. As a consequence, building materials have always received relatively much attention in various research programmes in the Netherlands. This thesis contains a selection of studies in this field, conducted over the last twenty years. Most of these studies were commissioned by the Dutch government and therefore had a direct relation with actual or future radon policy. The studies are classified into the themes:

- Methods (chapter 2)
- Concentrations and exposures (chapter 3), and
- Radon-transport mechanisms and mitigation (chapter 4)

These chapters contain sections that are essentially copies of articles that for the majority are published in peer-reviewed journals.

In section 2.1 a method is described for the determination of the ^{222}Rn exhalation rate of building materials, arising from the experiences in the SAWORA research programme for a more precise measuring method. The described method was entered into the standard NEN 5699 (NEN, 2001b) as the main procedure. In section 2.2 the performances and equivalence of three measuring methods, all following this standard method, are worked out. In section 2.3 a model is presented to calculate the external dose rate in dwellings due to the presence of primordial radionuclides in building materials.

The above-mentioned standard on ^{222}Rn exhalation is applied to a representative set of Dutch building materials (section 3.1). Section 3.2 focuses on the Dutch situation with respect to the activity concentrations in gypsum plasters and mortars. In section 3.3 ^{222}Rn concentrations, absorbed dose rates and annual exposures are presented as determined for a small housing estate. In the next section the calculation model to assess the indoor absorbed dose rate in a dwelling as pointed out in section 2.3 was applied to a representative set of Dutch dwellings and the dose distribution was determined using a Monte Carlo technique.

One of the objectives in the RENA research programme was to examine the effects of various countermeasures to reduce the exposure in dwellings. In section 4.1 the results are presented of a study on the retaining action of various surface coatings to reduce the ^{222}Rn release from construction materials. The last two sections deal with the exhalation from concrete samples, mixed according to various recipes to gain a better insight in the underlying mechanisms.

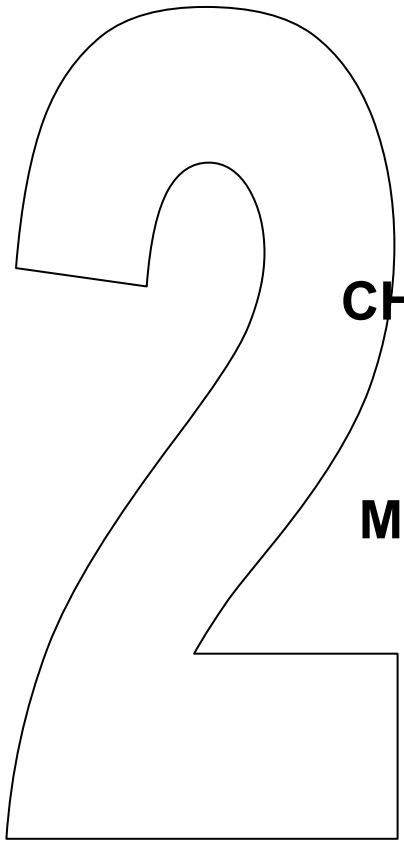

CHAPTER 2

METHODS

2.1

Determining the ^{222}Rn exhalation rate by liquid scintillation counting[9]

2.1.1 Introduction

Various methods for determining the ^{222}Rn exhalation rate have been developed. Most of these can be roughly divided into two types. In the first type, the sample is enclosed in a can and the ^{222}Rn concentration in the free gas volume is determined after a given time. The exhalation rate is subsequently calculated (Mustonen, 1984; Poffijn *et al*., 1984; Stranden *et al*., 1984). This method has the disadvantage that, as the ^{222}Rn concentration in the can increases, the exhalation rate decreases due to a lower concentration gradient between pore and ambient air. In practice, the ambient air will be practically free from ^{222}Rn, resulting in a "free exhalation rate". According to Jonassen (1983), the difference between the free exhalation rate and the rate determined using the accumulation method mentioned above could be as large as about 15%. Samuelsson (1987) suggested that the difference might even reach 100%. The method can be improved by monitoring ^{222}Rn build-up in the can with time, the free exhalation rate calculated from the resulting curve by determining the ^{222}Rn increase at zero time (Jonassen, 1983; Folkerts *et al*., 1984; Ulbak *et al*., 1984). Samuelsson (1987), however, states that the exhalation rate is already influenced at the moment the can is closed. The deviation with respect to the free exhalation rate is less than 5% only when, as suggested by Poffijn *et al*. (1984), the ratio between the free gas volume and the sample volume exceeds a factor of 10 (Samuelsson, 1987).

In the second method, the surface of the sample is partly covered with a collection container (Eichholz *et al*., 1980; Folkerts *et al*., 1984; Ackers *et al*., 1985). The free exhalation rate is determined from the continuously measured ^{222}Rn concentration in the collection container as described above. A disadvantage is that it is not always easy to make airtight the joining of the cover to building material.

In this chapter, we introduce a third method for determining the exhalation rate, using a continuously ventilated sample container. ^{222}Rn production is quantified by liquid scintillation counting. The advantages of this method are that it determines the free exhalation rate and that the influence of external factors, such as vapour pressure, on the exhalation rate can be easily studied. We will examine the accuracy, repeatability and the reproducibility of the method.

---

[9] This chapter is based on a paper published in Health Physics 61:501-509 (1991), entitled *Determining the ^{222}Rn exhalation rate of building materials using liquid scintillation counting*. Authors: W. van Dijk and P. de Jong.

2.1.2 Materials and methods

Samples

Test walls were prepared with an area of about 45 x 45 cm^2. Wall thicknesses varied from 7 cm (gypsum samples) to 10 cm (concrete samples). Table 2.1 shows the concrete samples studied. After preparation, the concrete test walls were allowed to cure for over 18 months. Prior to exhalation measurements, the walls were conditioned with respect to humidity for 3-8 weeks, depending on the material.

Table 2.1
Composition of concrete mixtures; thickness 10 cm.

Type of cement	Composition (%)				Density
	Cement	Gravel	Sand	Water	(kg m^{-3})
Portland cement	14	48	33	5	2360
Blast furnace slag cement	14	48	33	5	2360
Portland cement with fly ash	14	48	33	5	2330
Portland cement	17	34[a]	42	7	1900
Blast furnace cement with fly ash	14[b]	24	58	4	2300

[a] Fly ash pellets.
[b] Includes 2% fly ash.

Procedure

The test wall to be examined was placed in a 36-L container. A constant flow of ^{222}Rn-free nitrogen gas of known humidity was passed from the moment of closing the sample container. The relative humidity of the nitrogen flow was regulated within the full range of 0 to 100% by means of a controlled mixing of dry and water-saturated nitrogen gas (see Figure 2.1). Resulting humidity was verified using a hygrometer placed in the sample container. After a given time (normally within 3 h after starting the experiment), when the

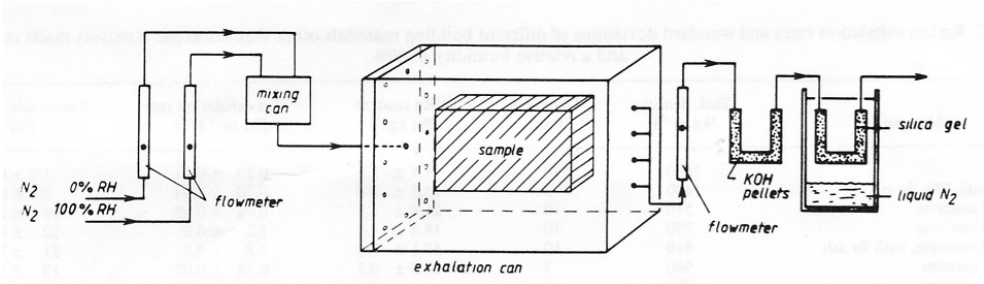

Figure 2.1
Measuring arrangement

^{222}Rn concentration within the container had reached a steady-state concentration, the outflow was led through two U-shaped tubes for 10-30 min. The first tube contained KOH tablets (20 g) to dry the gas flow. The second one, which contained 4 g of silica gel (size distribution 1-3 mm, Fluka Chemie AG), was cooled over liquid nitrogen to trap the ^{222}Rn. After absorption, the tube with silica gel was warmed in ice water for 5 min, after which the content was poured through a funnel into a counting vial containing 20 mL of a toluene-based scintillation liquid (Packard Instruments). During this procedure, no loss of ^{222}Rn was observed (Darrall *et al*., 1973).

Determination

Secular equilibrium in the counting vial is attained after about 3 h. However, as described by Darrall *et al*. (1973) and confirmed by our own observations, it takes about 16 h before the equilibrium of ^{222}Rn and its daughters between the silica gel and the scintillation cocktail is reached. After desorption, a spectrum was recorded using a liquid scintillation spectrometer (Model Tricarb CA2000, Packard Instruments). The count rate was determined from the optimal window settings of 110-600 keV. The background count rate under these counting conditions is 0.15 cps, using a counting vial that contains the same amount of scintillation cocktail and silica gel as applied for the samples.

The counting efficiency is approximately 2.8 cps Bq^{-1}, calculated from standard curves by linear interpolation. All standard curves were linear ($r > 0.99$), with a minimum of five calibration points. To measure the standard curve, calibrated ^{226}Ra solutions (Amersham) were prepared, from which ^{222}Rn was purged with nitrogen gas and trapped as described in the previous section. The calibration is described in more detail elsewhere (Darrall *et al*., 1973).

All ^{222}Rn activities were corrected for radioactive decay and normalized to the middle of the absorption period. A systematic error of at most 0.5% was introduced by not considering the mean residence time of the ^{222}Rn in the sample container. The area exhalation rate was calculated by dividing the corrected sample activities by the exhalation area of the test wall and the applied absorption period.

Standard conditions

Unless it is specified, the exhalation rates were determined under the following conditions: flow rate nitrogen: 600 mL min^{-1}; relative humidity: 50%; temperature: 20 ± 1°C; waiting time before sampling: 2 to 3 h; absorption time: 10-30 min; counting time: 60 min. All samples were analysed in triplicate.

2.1.3 Results

Influence of analysing parameters

The influence of some variables relating to the method is examined in more detail. The influence of the flow rate variation of purge gas is shown in Figure 2.2. At flow rates exceeding 800 mL min^{-1}, the activity diminished due to a shorter residence time of purged ^{222}Rn gas in the cold trap resulting in a decreased trapping efficiency. No significant activity regression was found for flow rates less than 800 mL min^{-1} (Student's *t*-test, $p > 0.10$). All flow rates were therefore kept below 800 mL min^{-1}.

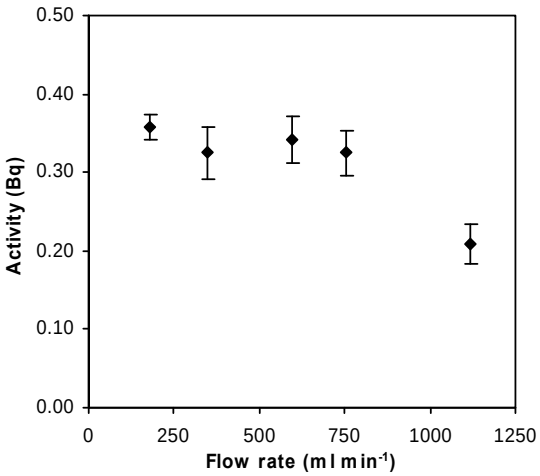

Figure 2.2
^{222}Rn activity measured as a function of nitrogen flow rate. The error bars indicate 1 SD.

Application of longer absorption periods would be preferable in cases where the exhalation rates are low. Figure 2.3 shows the measured ^{222}Rn activity as a function of the absorption

Figure 2.3
^{222}Rn activity measured as a function of the absorption time. The regression line was found to be $y = -0.017 + 0.029x$ ($r = 0.99$).

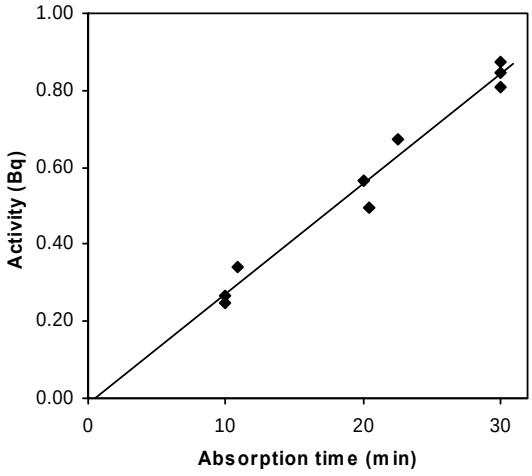

time for a phosphogypsum block; it appears that the absorbed activity increases linearly with the absorption time up to at least 30 min.

Influence of external factors

The proposed method offers the opportunity to examine the influence of external factors on the exhalation rate. We studied the exhalation rate in relation to water vapour pressure for a phosphogypsum and a concrete block. The two test walls were placed in conditioned rooms at various water vapour pressures for several weeks. In order not to disturb the balance between the humidity of the block and ambient air during the measurements, the nitrogen flow had the same humidity as the air in the conditioned room. Results are given in Figures 2.4 and 2.5 for the phosphogypsum and concrete sample, respectively. The two materials show opposite effects with increasing air humidity; whereas the exhalation increases for phosphogypsum, a decrease is found for the concrete sample.

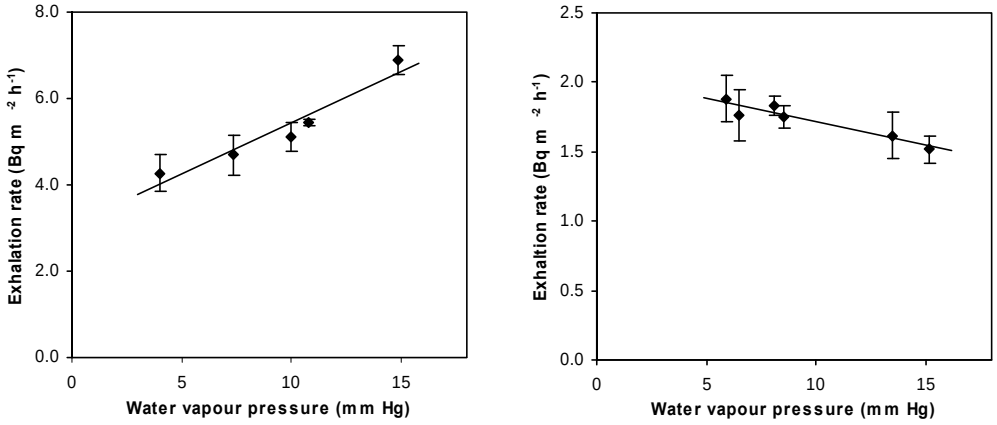

Figure 2.4 and 2.5
^{222}Rn exhalation rate of a gypsum wall (left) and of a concrete wall (right) as a function of the vapour pressure. The error bars indicate 1 SD.

Accuracy, repeatability and reproducibility

The best way to assess the accuracy of the described method is a direct comparison with an alternative method. The first four samples from Table 2.1 were also analysed using a technique described by Ackers *et al*. (1985). In this technique a container was placed air-tight against the sample and the increase of ^{222}Rn with time was measured using a zinc sulphide detector. Table 2.2 compares the reported area exhalation rates with those found by the present method. The Student's t-test showed that there was no significant difference between the two series of results ($p > 0.10$). The table also shows that the precision of the

proposed method is about a factor of two better than the technique used by Ackers *et al*., the results of which, however, were not obtained under controlled conditions with respect to the water vapour pressure.

Table 2.2
Comparison of exhalation rates obtained by the proposed method (LSC) and an alternative method (ZnS) of four samples of concrete.

Sample no.	Exhalation rate ± SD (Bq m^{-2} h^{-1})		LSC/ZnS
	LSC[a]	ZnS[b]	
1	2.2 ± 0.3	2.5 ± 0.5	0.88
2	3.7 ± 0.3	3.4 ± 0.7	1.09
3	2.4 ± 0.1	1.6 ± 0.5	1.50
4	2.0 ± 0.2	2.7 ± 0.5	0.74
Average ± SD			1.1 ± 0.3

[a] n = 3 determinations.
[b] Ackers *et al*. (1985).

The repeatability of the method has been calculated from replicate measurements on each sample at two fixed levels. At the higher level (16 Bq m^{-2} h^{-1}), the average coefficient of variation, as found for 42 triplicate determinations of a phosphogypsum product, amounts to a value of 5.2%. At the lower level of 5 Bq m^{-2} h^{-1}, the coefficient was 5.5%. The latter result was obtained from one phosphogypsum test wall followed for almost 14 years and analysed according to the standard conditions given in section 2.1.2. The results are presented in Figure 2.6. As a measure of the reproducibility, one can take the coefficient of variation between the various measuring days, which results in a coefficient of 4.7% (n=23 days). If this figure is compared with the variation coefficient of 5.5% within the series, no significant difference can be demonstrated (F-test, $p > 0.10$); it can be concluded that the results show no trend in time.

The detection limit of the method, calculated according to Currie (1968) under the standard conditions, was determined as 11 mBq; thus, for an exhalation area of 0.4 m^2 and an absorption time of 10 min, the minimum detectable area exhalation rate is 0.2 Bq m^{-2} h^{-1}. This low limit of detection is due to the high counting efficiency of about 2.8 cps Bq^{-1}, which is a factor of 1.6 higher than the value published by Darrall *et al*. (1973). The reason for this difference was not investigated further.

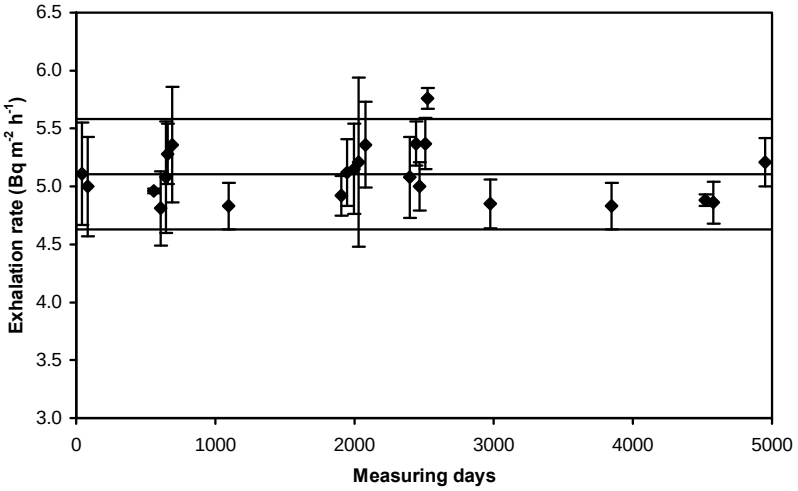

Figure 2.6
^{222}Rn exhalation rate of one and the same sample of phosphogypsum during a nearly 14-y examination period (temperature 20ºC and relative humidity 50%). The error bars indicate 1 SD. The upper and lower straight lines cover the 95% confidence interval. The average exhalation rate of the gypsum sample ± 1 SD over the examination period is 5.1 ± 0.2 Bq (m^2 h)$^{-1}$ with n=23 observations.

2.1.4 Discussion and conclusions

We tested a new method for determining the free ^{222}Rn area exhalation rate of building materials using a continuously ventilated sample container. In comparison with methods that use a hermetically closed system, this method results in lower ^{222}Rn concentrations in the free air volume of the container. As a consequence, the back diffusion will be less. The question arises whether or not the free air concentration is close enough to zero to meet the definition of the free exhalation rate. According to the equations for a leaking can, as derived by Samuelsson (1987), this is indeed the case, resulting in a deviation with respect to the free exhalation rate of less than 0.1%.

Another advantage of our method is that external parameters that may influence the area exhalation rate can be easily studied. We examined the extent to which the area exhalation rate is dependent on the ventilation rate. From the data given in Figure 2.2, it was deduced that the exhalation rate was not influenced by the ventilation rate over a range of 0.5 - 2.1 h^{-1}. Experiments in a test structure in the framework of the Dutch Radiation Program SAWORA (Hogeweg, 1986a) likewise showed no relation between exhalation rate and ventilation rate.

Initially, dry nitrogen was used to purge the ^{222}Rn gas from the container. During ongoing experiments on a gypsum sample, it was shown that the area exhalation rate decreased proportionally with time. Since the only plausible explanation was that the nitrogen stream dried the test wall during the experiment, this phenomenon was examined in more detail. Through a simple modification of the testing equipment, we were able to measure the area exhalation rate at various water vapour pressures. This was done for two different building materials: gypsum and concrete. The gypsum wall showed an increase in the area exhalation rate as the vapour pressure increased (Figure 2.4), whereas the concrete slab showed the opposite (Figure 2.5). An increase in exhalation rate as a function of the percentage of moisture of the material has been reported by others for concrete and shale (Stranden *et al*., 1984), soil (Stranden *et al*., 1984; Fleischer, 1987), uranium mill tailings (Strong and Levins, 1982), and coal ash (Barton and Ziemer, 1986). The presence of water in the internal pores may diminish the recoil energy of the emanating ^{222}Rn atoms, making a larger percentage available for diffusion into the surrounding air. Furthermore, a water film in the pores will hinder the adsorption of ^{222}Rn gas onto internal surfaces, also leading to higher exhalation rates (Stranden *et al*., 1984; Gan *et al*., 1986). When the pores are completely saturated with water, however, the exhalation rate will decrease due to the lower diffusion coefficient of ^{222}Rn in water in comparison to that in air (Stranden *et al*., 1984; Barton and Ziemer 1986; Fleischer 1987). Which effect will dominate at what moisture content varies from one material to another.

Although in this study the water vapour pressure was a parameter rather than the moisture content, similar arguments apply, since water adsorption and capillary condensation in the material are reported to occur even at low vapour pressures (Tammes and Vos, 1980). Within the range studied, the effect of capillary condensation is more pronounced in concrete than in gypsum, due to its smaller pore sizes. This may be the reason why we found an opposite relation between exhalation rate and water vapour pressure for this material. Since Auxier *et al*. (1974) showed a similar relation in concrete to ours, it would be interesting to determine whether or not the pore size distribution plays a definite role.

From the results it can be concluded that the proposed liquid scintillation method is an accurate and, above all, reproducible technique for determining the free ^{222}Rn exhalation rate, having a coefficient of variation of about 5% over a period of almost 14 years at the 5 Bq m^{-2} h^{-1} level. The low limit of detection offers the possibility to determine the exhalation rates of most building materials and to study the effects of mitigation measures. The water vapour pressure clearly influences the ^{222}Rn exhalation rate; the test specimen should therefore be conditioned prior to the exhalation measurements.

2.2

Interlaboratory comparison of radon exhalation rates[10]

2.2.1 Introduction

The average ^{222}Rn concentration in the Netherlands is one of the lowest in Europe (UNSCEAR, 2000). To preserve this relatively advantageous situation, at the time of this study regulations were in preparation to limit the natural radiation burden to inhabitants of newly built houses due to building materials (NEN, 2002). As part of this, the methodology to assess the ^{222}Rn exhalation rate has been specified in the Dutch standard NEN 5699 (NEN, 2001b). This standard requires the use of a purge-and-trap method as described in section 2.1. In this method the sample is enclosed in a container from which the exhaled ^{222}Rn is continuously purged with nitrogen gas with a RH of 50% (20 °C). The ventilation rate of the sample container has to fulfil the following relationship:

$$\frac{V_S}{V} \cdot \frac{\lambda_{Rn}}{\lambda_{Rn} + \lambda_V} < 0.1, \qquad (2.1)$$

where V_S is the volume of a test sample in the container (m^3); V is the volume of the container (m^3); λ_{Rn} is the decay constant of ^{222}Rn and λ_V the ventilation rate (both s^{-1}). This requirement guarantees that the ^{222}Rn concentration near a sample is sufficiently low to avoid problems of back diffusion and to ensure that the free ^{222}Rn exhalation rate is determined.

In this section the performances and equivalence of three measuring methods are reported, all following the standard method but deviating within the freedom of choice offered by the protocol.

2.2.2 Methods and materials

Test samples

To test the intralaboratory repeatability, ten concrete cubes, dimensions 15x15x15 cm^3, were prepared according to the national standard procedure (NEN, 1999). The composition of the fresh concrete paste was: (a) Portland cement 315 kg m^{-3} (CEM I 32.5 R), (b) aggregates 1200 kg m^{-3} (river gravel), (c) sand 740 kg m^{-3} and (d) water 165 kg m^{-3}. One

[10] This chapter is based on a paper published in Health Physics 88:59-64 (2005), entitled *Inter-laboratory comparison of three methods for the determination of the radon exhalation rate of building materials.* Authors: P. de Jong, W. van Dijk, W. de Vries, E. R. van der Graaf and L.M.M. Roelofs.

day after pouring, the samples were demoulded and thereafter left immerged in water for 28 d for further curing. The interlaboratory comparison was carried out for six samples: (a) two of the fore-mentioned concrete cubes, (b) three phosphogypsum blocks from test productions and (c) one commercially available (natural) gypsum block. The gypsum blocks, thickness 7 cm, were sawn to a size of 20x25 cm^2. Furthermore some additional test samples of brick, limestone and aerated concrete from industrial productions were analysed, to investigate the correlation between the applied methods. These samples were obtained from several manufacturers and reflect typical samples from the national market.

Prior to the exhalation measurements, all test samples were conditioned at 20 °C in an environment at 50% relative humidity (RH) until equilibrium was established in the moisture content of the sample. According to the standard procedure (NEN, 2001b) such equilibrium is reached when the decline in weight is less than 0.07% per week. The conditioning period lasts for three months at most. To prevent the samples to change in humidity during transport from one laboratory to another, they were thoroughly packed in plastic and reconditioned if necessary.

Methods

The standard prescribes that the free volume of the set up should be refreshed at least five times thereafter it is assumed that the ^{222}Rn concentration within the sample container has reached a steady-state value. The nitrogen stream from the sample container is directed through a device to trap the ^{222}Rn gas. The trapping efficiency has to be verified using an identical second trapping device, placed in series. Relative to the first device, the activity in the second one should be less than 1% (NEN, 2001b).

The calibration procedure requires that during five time periods of increasing length the ^{222}Rn is purged from a calibrated ^{226}Ra source and trapped. From the counting results of these standardized amounts of ^{222}Rn gas a calibration curve is prepared, which is used to calculate the exhalation rate of the building material samples by interpolation. The dimensions of the exhalation container, the applied trapping agent, trapping temperature, the duration of the trapping and the analytical method to determine the trapped ^{222}Rn activity are not specified. In the interlaboratory comparison an assessment is made of the results of three methods (denoted as method A, B and C) that are all three consistent with the Dutch standard.

A detailed description of method A is given in section 2.1. Method B has been published by Cozmuta *et al*. (2003). In short: after being pre-dried with silica gel and freeze-dried via a second vial cooled with liquid nitrogen, the nitrogen flow is passed through a vial that contains 17 g of activated charcoal. During the adsorption (typically for 5-24 h) the charcoal is kept at –190 °C with liquid nitrogen. After the adsorption the charcoal is transferred to a standard counting geometry and analysed by γ-ray spectrometry

using an HPGe detector, placed in a low-background environment. The adsorbed ^{222}Rn is related to the total count rate in the energy range between 52 and 680 keV.

Method C also utilises activated charcoal to trap the ^{222}Rn. In contrast with method B the trapping takes place at 18°C and has a typical duration of 10 days. The amount of charcoal is about 400 g. Next the charcoal is thoroughly homogenised and analysed for 16 h by gamma-ray spectrometry using an HPGe detector. The ^{222}Rn activity in the charcoal was calculated from the lines at 352 and 609 keV originating from the decay of the ^{222}Rn daughter nuclides ^{214}Pb and ^{214}Bi, respectively. This method was applied in an investigation on the influence of ageing on the exhalation rate. For more details see Roelofs and Scholten (1994).

In Table 2.3 the main characteristics of the applied methods are summarized.

Table 2.3
Main differences between the applied methods.

Item	Method A	Method B	Method C
Volume sample container (dm^3)	30	80	17
Trapping agent	Silica gel	Charcoal	Charcoal
Amount of trapping agent (g)	4-5	17	400
Trapping temperature (°C)	-190	-190	18
Trapping time	10-30 min	5-25 h	10 days
Method of analysis	LSC	Total gamma	Gamma-ray spectr.
Counting time per sample (h)	1	3-16	16

Regression

For linear regression fits to bivariate data in most cases the method of ordinary least squares (OLS) is applied for calculating the slope and intercept coefficients and their uncertainties. The regression line of the dependent variable Y against the independent variable X i.e. OLS(Y|X), is the line in which the sum of the squares of the Y residuals is minimised. This method is only applicable if the X variable is free or almost free from uncertainty. The regression in this section, however, is used to test the coherence between the results of the methods under consideration and therefore the Y as well as the X data are affected by uncertainties. Several methods that treat the variables symmetrically have been described. In an overview Isobe *et al*. (1990) discuss them and give formulae for calculating the coefficients. In this section we used the method known as bisector OLS in which the best line is the line that bisects the OLS(Y|X) and the inverse OLS(X|Y) lines.

2.2.3 Results

The intralaboratory repeatability and reproducibility are determined for method A and are based on the results of the ten concrete cubes prepared from one batch. For the whole series the ^{222}Rn exhalation rate is 7.1 µBq kg^{-1} s^{-1} on average, with a standard deviation of 0.3 µBq kg^{-1} s^{-1} (4.3%) for n=10 samples. The results are shown in Figure 2.7. The horizontal solid lines in this figure indicate the 95% confidence interval. According to Dixon's test no outliers could be identified at the significance level of 0.05. Since the concrete cubes were analysed on different days the standard deviation of 4.3% provides a good estimate of the intralaboratory reproducibility.

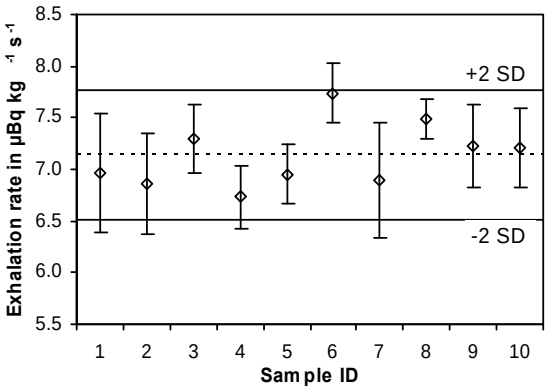

Figure 2.7
^{222}Rn exhalation rate of 10 identical concrete cubes, according to method A. The solid lines enclose the 95% confidence interval; the dashed line represents the averaged result.

The vertical error bars in Figure 2.7 indicate the standard deviations of the triplicate analysis of each of the ten concrete cubes. Since the three counting samples per specimen were prepared within an hour, the standard deviations of these triplicates show the repeatability of method A. The standard deviations of the ten triplicates varied between 2.6% and 8.2%, with an average of 5.4%. For a single determination the repeatability of method A can therefore be considered to be 5.4%. For a standard triplicate analysis the repeatability will be √3 lower, resulting in 3.1%.

In the interlaboratory exercise six samples with ascending exhalation rates were measured by the three participating laboratories A, B and C in succession. Thereafter the samples were returned to laboratory A. Four samples were remeasured to check for any changes in exhalation rate due to transport, handling or time-effect. Table 2.4 shows the results. No significant difference is present between the two results of laboratory A for any of the four samples (Student's t-test, p<0.05). The average results of the three laboratories were calculated from the first three results in Table 2.4, using the respective inverse variances as weighting factors. The ratio of the individual results relative to the weighted average is also shown in Table 2.4.

Table 2.4
Results of the interlaboratory exercise. The exhalation rate is given as the mean ± the combined standard uncertainty u_C (see text) in $\mu Bq\ s^{-1}$. The ratio r relative to the average result of the three methods is reported between brackets. The weighted average is calculated using the inverse of the variances as weighting factors. The variation fraction of the weighting average is given between squared brackets.

Sample	Method A(1st) mean ± u_C (r)	Method B mean ± u_C (r)	Method C mean ± u_C (r)	Method A(2nd) mean ± u_C (r)	Weighted average mean ± sd [sd%]
Gypsum A	4.1 ± 0.7 (1.7)	1.6 ± 0.9 (0.7)	2.1 ± 0.4 (0.8)	2.1 ± 0.9 (0.8)	2.5 ± 1.1 [44%]
Concrete I	56 ± 4 (1.12)	50 ± 3 (1.00)	49 ± 2 (0.97)	n.d.[a]	50 ± 3 [6.2%]
Concrete II	60 ± 4 (1.07)	52 ± 3 (0.92)	58 ± 2 (1.02)	n.d.[a]	57 ± 3 [6.1%]
Gypsum B	127 ± 8 (1.02)	132 ± 7 (1.07)	120 ± 4 (0.97)	134 ± 8 (1.08)	124 ± 6 [5.0%]
Gypsum C	410 ± 30 (0.94)	440 ± 20 (1.02)	439 ± 12 (1.01)	440 ± 30 (1.00)	436 ± 13 [2.9%]
Gypsum D	450 ± 30 (1.05)	480 ± 20 (1.13)	405 ± 12 (0.96)	470 ± 30 (1.11)	420 ± 40 [8.4%]
Average[b]	(1.04)	(1.03)	(0.98)	(1.06)	[5.6%]

[a] Not determined.
[b] Sample coded Gypsum A not included.

Especially when the ^{222}Rn release rate is close to the limit of detection, as in the case of the sample coded Gypsum A (natural gypsum), a relative broad range in the ratio from 0.7 to 1.7 is found. If this sample is left out, the ratio varies between 0.92 and 1.13.

The variation coefficient of the weighted average when the fore-mentioned gypsum sample is omitted, amounts to about 6% on average. This value is regarded as a good estimator of the interlaboratories' reproducibility. Taking the variation coefficient into account none of the results differs significantly from the corresponding weighted average (p<0.05). The combined standard uncertainties, u_c, presented in Table 2.4 are calculated according to the instructions in the national standard (NEN, 2001b). These standard uncertainties combine the uncertainties in (a) the calibration factor, (b) the quantification of the trapped activity and (c) the activity or production rate of the radium standard. Table 2.5 compares the uncertainty budgets of the three methods at an investigation level of 50 μBq s^{-1}. The uncertainty of the various components for method A, B and C are combined according to an ISO-guideline (ISO, 1995) to values of 6, 5 and 3%, respectively.

Table 2.5
Main sources of uncertainty of the three methods in % at the 50 μBq s^{-1} level.

Source	Method A	Method B	Method C
Calibration factor	5.6	2.5	1.5
Counting uncertainty trapped activity	2.7	1.5	1.1
Radium standard	1.2	4.0	2.0
Combined standard uncertainty (rounded)	6	5	3

The observations from the interlaboratory exercise are graphically presented in Figures 2.8 and 2.9. Also the results of some additional measurements of commercial available building materials are incorporated in these figures. The results obtained by method C are plotted against the results of method A in Figure 2.8 and against method B in Figure 2.9. The drawn line in these figures indicate the line of identity Y=X.

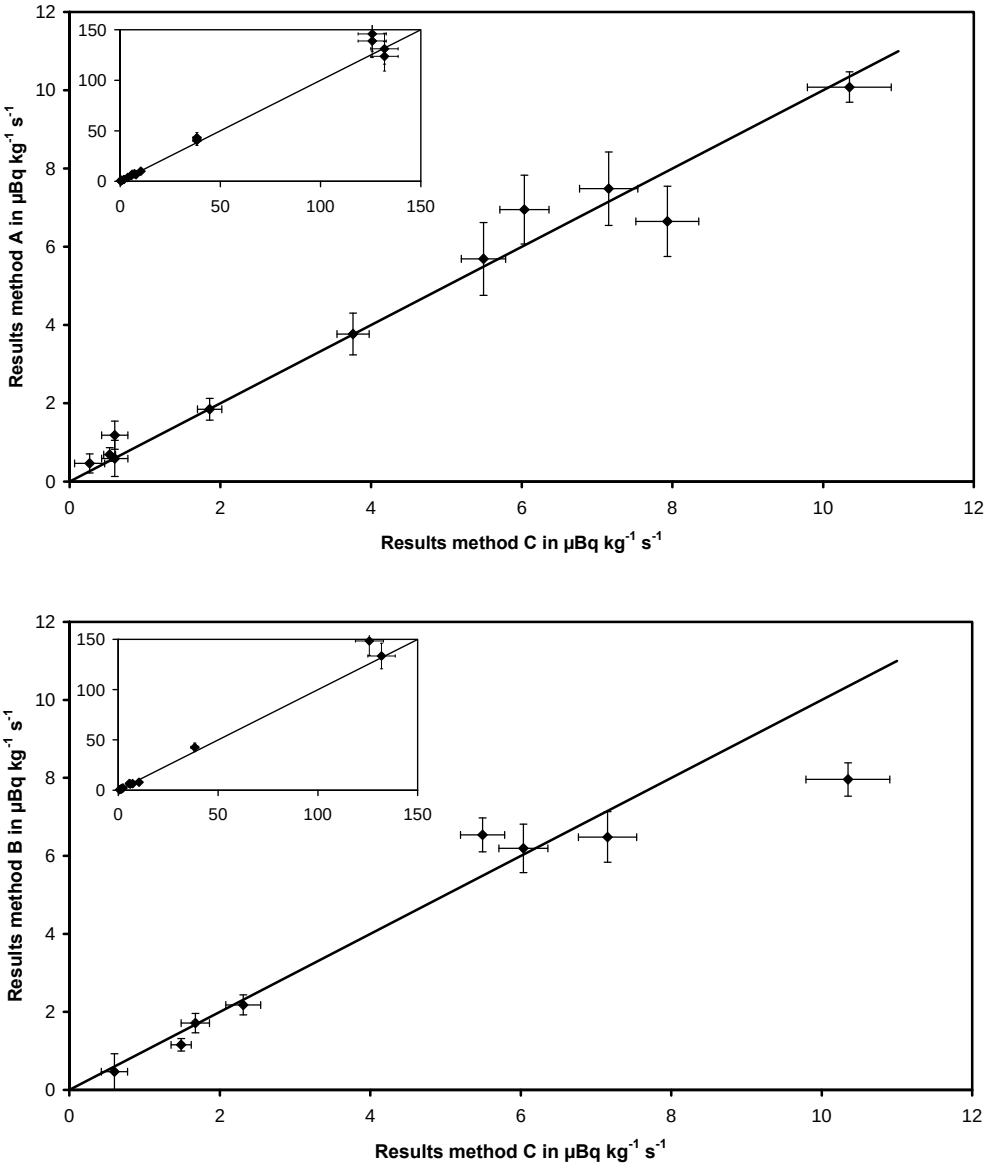

Figures 2.8 and 2.9

Results of method A (top) and method B (bottom) plotted against the results of method C. The insets show the results up to 150 µBq kg^{-1} s^{-1}. The lines Y=X are drawn for reference purposes. The error bars indicate the combined standard uncertainty u_C in the data points.

As indicated in the experimental section bisector linear regression analysis is used to fit the data. The results of this regression analysis are summarized in Table 2.6.

Table 2.6
Mean ± SD of the linear regression coefficients a_0 (intercept) and a_1 (slope) as obtained by bisector linear regression analysis. The Pearson's correlation coefficient R is given in the fourth column and the number of observations in the last.

Tested correlation	a_0	a_1	R	n
Method A versus C	-0.0 ± 0.4	1.05 ± 0.04[b]	0.995	17
Method B versus C	-0.7 ± 0.6[a]	1.10 ± 0.06[b]	0.996	11
Method A versus B	0.9 ± 0.4[a]	0.95 ± 0.01[b]	1.000	12

[a] Significantly different from 0.0 (Student's t-test, $p<0.05$)
[b] Significantly different from 1.00 (Student's t-test, $p<0.05$)

The slope coefficient a_1 is in all cases close to unity, indicating that the three methods essentially yield identical results. Nevertheless small and statistically significant differences between the methods can be demonstrated and on average the results follow the sequence B > A > C. The maximum deviation occurs between method B and C and amounts to 10%. Only in the case of method A versus C the regression line pass through the origin, taking the uncertainties into account. For the other combinations the regression coefficient a_0, the intercept, differs significantly from zero (Student's t-test, $p<0.05$), indicating there is some bias or a not quite linear calibration curve.

2.2.4 Discussion

In this study we examined the validity of a standard method for the determination of the ^{222}Rn exhalation rate of building material. The standard method requires the use of a continuously ventilated sample container, as described in section 2.1. Compared to methods that make use of a closed can system, this method has the advantage that the so-called free exhalation rate is determined and back diffusion of ^{222}Rn into the test sample can be neglected. An example of the effect of back diffusion is reported by Kovler and colleagues (2004). Using a hermetic can the exhalation rate was deduced from the time-integrated ^{222}Rn concentration using both an electret and a charcoal method. The electret method resulted in a 25% lower exhalation rate. This is due to adsorption of the exhaled ^{222}Rn by the charcoal that results in a lower ^{222}Rn concentration and minimises back diffusion.

As the RH of test samples and purge gas is standardised to a value of 50% (NEN, 2001b), the test results allow a good comparison between various studies. Another

advantage of the standard method is that the influence of for instance the water content of the test samples on the exhalation rate can easily be studied under steady-state conditions by an adaptation of the RH of the purge gas (section 2.1; Cozmuta *et al*., 2003). In this study three performance characteristics of the standard method are determined: (a) the repeatability and (b) the intralaboratory reproducibility, both measures for the precision of the method and (c) the interlaboratory reproducibility as a measure of the agreement between the results generated by different laboratories. The repeatability of method A appears to be 3.1%, which differs only slightly from the 2.7% mentioned in Table 2.5 due to counting statistics. The reproducibility of method A was found to be 4.3%, which is close to data reported in the sections 2.1 and 4.2.

Linear regression analysis revealed that on average method B gives higher and method C the lowest values. The difference between these two methods is about 10%. The responses of method C, A and B are in the proportion of 0.95:1.00:1.05 from which a variation coefficient can be calculated of 5%. From the results of the interlaboratory exercise (Table 2.4) a similar value (5.6%) was deduced.

Thus far only limited attention has been paid to the validation of methods for the determination of the ^{222}Rn exhalation rate. Hutter and Knutson (1998) have reported a variation coefficient of 37% in a laboratory exercise on exhalation measurements from a ^{226}Ra-spiked concrete slab. Petropoulos *et al*. (2001) have published the results of an intercomparison exercise among twenty participants from thirteen countries. The comparison consisted of a concrete slab that was generally analysed by closed can techniques. The coefficient of variation in that study was in the range of 10-15%. In the present study this coefficient is a factor of two to three lower, indicating the importance of a well-documented standard method.

2.2.5 Conclusion

In this study we examined the validity of a standard method for the determination of the ^{222}Rn exhalation rate of building material. Within the scope of the method it is allowed, within specified limits, to choose among others the trapping agent and analytical method, leaving some room to the laboratories own preference and specific expertise. The results show that a very good degree of accuracy in the determination of the ^{222}Rn exhalation rate can be attained, provided the methods' key items as sample conditioning, ^{222}Rn sampling and the calibration procedure are precisely embodied in the standard.

2.3

Modelling of the indoor gamma radiation dose[11]

2.3.1 Introduction

The first Monte Carlo code to calculate exposure rates due to ^{226}Ra, ^{232}Th and ^{40}K in building materials was presented by Koblinger (1978). Since then many alternative methods have been published, either based on Monte Carlo codes or on codes that make use of gamma-ray attenuation and build-up factors (Stranden, 1979; Mustonen, 1984; Mirza *et al*., 1991; Ahmad *et al*., 1998; Máduar and Hiromoto, 2004; Ademola and Farai, 2005; De Jong *et al*., 2006). The standard geometry as defined by Koblinger (1978), in which all construction elements consist of 20 cm thick concrete, is still in use for comparison reasons. The specific absorbed dose rates in air for that geometry is defined as the absorbed dose rate in air due to a activity concentration of the construction material of 1 Bq kg^{-1} of the parent and any daughters.

With multi-purpose codes as MCNP (Briesmeister, 2000), the resulting absorbed dose rate in a room can be calculated satisfactorily for each individual geometry and any combination of materials and thickness of the construction elements. However, application of such calculation methods is quite laborious, especially when the study covers a large number of dwellings. An alternative for these Monte Carlo codes is to base the calculation on the above-mentioned specific absorbed dose rates and make corrections for alternative situations. In this section this approach is worked out in more detail and several correction factors for parameters as the thickness, density and dimensions of the construction materials, the effect of ^{222}Rn exhalation and the contribution from adjacent rooms, are quantified. Combination of the correction factors with the specific absorbed dose rates offers a quick reference for the building material induced absorbed dose rate in a dwelling. The proposed method is applied to three Dutch reference dwellings and the results are compared with those obtained with MCNP to verify the accuracy.

2.3.2 Mathematical model

The calculations in this section are carried out using three general-purpose transport codes: MCNP, version 4C (Briesmeister, 2000), MARMER, version 2.00 (Kloosterman, 1990; NEA, 2004), and MicroShield, version 5.05 (Grove, 1999). The physical data on yield and

[11] This chapter is based on a paper published in Health Physics 94:33-42 (2008), entitled *Modelling gamma radiation dose in dwellings due to building materials*. Authors P. de Jong and W. van Dijk.

gamma-ray energies were either extracted from the Oak Ridge National Laboratory database (MCNP) or derived from the codes' own libraries (MARMER, MicroShield). For the MCNP calculations a point detector is assumed with conversion coefficients to relate fluence to kerma, according to ICRU report 47 (ICRU, 1992). For the Microshield code, absorbed dose rates are calculated separately for each floor and wall and then are summed to obtain the result for an entire room. Data on the chemical composition of concrete are taken from a publication of Hubbell and Seltzer (1995). The density of concrete was fixed at a value of 2350 kg m^{-3}, unless otherwise stated.

The standard geometry as defined by Koblinger (1978) is taken as starting point for our calculation model. This geometry has as (inner) dimensions of 5 x 4 m^2 and 2.8 m in height, with each of the six construction elements (i.e. floor, walls and ceiling) made of 20 cm thick concrete and no doors or windows are present. For this set-up the above-mentioned specific absorbed dose rates (unit: nGy h^{-1} per Bq kg^{-1}) are determined. These data relate to the centre of the standard geometry for concrete as construction material, a 20 cm thickness of each of the six construction elements, decay series that are assumed to be in secular equilibrium and a room without internal partition walls. In this section correction factors are deduced for alternative situations. The absorbed dose rate in air in a particular dwelling is than calculated according to:

$$\dot{D} = \left\{ \sum_{i=1}^{6} \left[F_{dose} \cdot F_1 \cdot F_2 \cdot F_3 \cdot \cdots \cdot F_n \right]_i \right\} F_{zoning} \cdot F_{adjac}, \qquad (2.2)$$

in which i is the index for a construction element in that dwelling, F_1 to F_n are the subsequent correction factors for construction element i, F_{zoning} is a correction factor which takes internal zoning of the construction into account, and F_{adjac} is the contribution from adjacent floors and dwellings. F_{dose} is the so-called dose factor in which the specific absorbed dose rates are incorporated. The specific absorbed dose rates and this factor will be discussed first and the various correction factors will be described in the next paragraphs.

Specific absorbed dose rates

Specific absorbed dose rate were calculated for the centre of the standard room, using the three computer codes. As shown in Table 2.7, the results of these codes yield comparable results with deviations of no more than 6%. Several authors have also calculated this quantity for the same geometry. If one compares these results with those of the present study, differences ranging from –20% to +40% can be noticed, depending on the study and the respective primordial radionuclide (see Table 2.7). Besides methodological differences, additional sources of variation may be the applied physical data, concrete composition and

density. Based on literature data and our own calculations, the average specific absorbed dose rates in air are taken as 0.90, 1.10 and 0.080 nGy h^{-1} per Bq kg^{-1} for the ^{238}U series, the ^{232}Th series and ^{40}K, respectively.

In the considered energy range Compton scattering dominates the interaction of photons and matter. The cross section per unit of mass is almost independent on the atomic number Z. Therefore, for materials other than concrete, the same specific absorbed dose rate values can be applied.

Table 2.7
Results from this study and literature values on the specific absorbed dose rate in air at the centre of a 4 x 5 x 2.8 m^3 room made of concrete with a thickness of 20 cm for all building elements. Where appropriate a conversion of 1 R=8.76 mGy has been applied (ICRU, 1992).

Specific absorbed dose rate (nGy h^{-1} per Bq kg^{-1})			**Method/reference**
^{238}U series	**^{232}Th series**	**^{40}K**	
0.85	1.18	0.076	MCNP[a]
0.91	1.11	0.076	MARMER
0.81	1.15	0.072	MicroShield
0.86 ± 0.05	1.15 ± 0.03	0.075 ± 0.002	Mean ± SD
0.93	1.03	0.078	Koblinger (1978)
0.92	1.11	0.078	Stranden (1979)
0.93	1.10	0.081	Mustonen (1984)
1.21	1.29	0.10	Mirza *et al*. (1991)
0.95	1.21	0.081	Ahmad *et al*. (1998)[b]
0.70	0.92	0.072	Máduar and Hiromoto (2004)
0.92	1.24	0.084	Ademola and Farai (2005)
0.94 ± 0.15	1.13 ± 0.13	0.082 ± 0.009	Mean ± SD
0.90	1.10	0.080	Averaged over all data[c]

[a] Personal Communication. J.Th.M. Jansen; Technical University Delft, Radiation, Radionuclides & Reactors department; Delft, The Netherlands. January 2005.
[b] Floor thickness 50 cm.
[c] Rounded values; these are used in the calculation of the dose factors.

Dose factor

The activity concentrations of the construction materials are the primary factors determining the absorbed dose rate in air. These activity concentrations are combined with the aforementioned specific absorbed dose rates according to:

$$F_{dose,i} = k_1 a_{1,i} + k_2 a_{2,i} + k_3 a_{3,i} . \qquad (2.3)$$

In this formula $F_{dose,i}$ is the dose factor of construction element i; $a_{1,i}$, $a_{2,i}$ and $a_{3,i}$ refer to the activity concentrations of construction element i in Bq kg^{-1} as derived by gamma-ray spectrometry for ^{226}Ra, ^{228}Ra and ^{40}K, respectively; k_1, k_2 and k_3 are the corresponding specific absorbed dose rates of the standard geometry in nGy h^{-1} per Bq kg^{-1}.

In this equation secular equilibrium in both decay series is assumed and thus the effect of radon exhalation is ignored. The emanation process and the subsequent diffusion of the emanated radon isotopes to the exterior of the building blocks determine the validity of this equilibrium assumption. As the half-life of ^{220}Rn, the radon isotope in the ^{232}Th series, is very short (56 s), only a thin layer near the surface of the construction element is involved. Therefore for this isotope the effect of exhalation can be neglected. ^{222}Rn atoms, however, show a much larger diffusion length. Due to the exhalation process, the ^{222}Rn daughter profile in a construction element can therefore seriously deviate from unity. And since the absorbed dose rate in a room due to the ^{238}U series mainly originates from ^{214}Pb and ^{214}Bi, both short-lived daughters of ^{222}Rn, the effect of non-equilibrium is taken as an additional parameter.

Effect of ^{222}Rn exhalation

If the x-axis in a construction element is directed towards the living space and the centre of that element is taken as x=0, the ^{222}Rn concentration in the pore space of the material of that element $C(x)$ (in Bq m^{-3}) can be represented by the following equation (eq. (1.3)):

$$C(x) = \frac{f}{\lambda}\left(1 - \frac{\cosh(x/l)}{\cosh(L/l)}\right), \qquad (2.4)$$

in which f is the production rate of ^{222}Rn per unit of volume of interstitial space (Bq m^{-3} s^{-1}); λ is the decay constant of ^{222}Rn (2.1 x 10^{-6} s^{-1}); l is the diffusion length (m); and L half of the thickness of the construction element (m). According to eq. (1.6) the production rate f can be expressed as:

$$f = \frac{\lambda\, a_1\, \eta\, \rho}{\varepsilon}\ , \qquad (2.5)$$

with a_1, the ^{226}Ra activity concentration (Bq kg^{-1}); η is the emanation factor (dimensionless); ρ is the density in kg m^{-3}; and ε the porosity of the material. In eq. (2.4) $C_{Rn}(x)$ is expressed as Bq per m^3 pore volume. To convert this quantity into Bq per kg building material, a correction factor ε/ρ is implemented such that, according to eq. (2.5), the first term in eq. (2.4) changes from f/λ into the product of a_1 and η. The total ^{222}Rn activity concentration in the construction element, $a_{Rn}(x)$, consists of ^{222}Rn in the pore space (eq. (2.4)) and that in the solid part of the material, i.e. the non-emanated ^{222}Rn:

$$a_{Rn}(x) = a_1\eta\left(1-\frac{\cosh(x/l)}{\cosh(L/l)}\right)+a_1(1-\eta). \qquad (2.6)$$

Under steady-state conditions eq. (2.6) also applies to the profile of each of the short-lived ^{222}Rn daughters.

According to eq. (1.7) the area exhalation rate (Bq m^{-2} s^{-1}) can be expressed as:

$$E_a = \lambda\, a_1\, \eta\, \rho\, l\, \tanh(L/l). \qquad (2.7)$$

Furthermore a ^{222}Rn release factor F_{Rn} is introduced, defined as the ratio between the released amount of ^{222}Rn and the amount produced within a construction element per unit of time. The released amount of ^{222}Rn can be derived from eq. (2.7); the total amount produced in a material is the product of λ and a_1. This results in the following expression for F_{Rn}:

$$F_{Rn} = \frac{E_a}{\rho L}\;\frac{1}{\lambda a_1} = \eta\;\frac{l}{L}\tanh(L/l). \qquad (2.8)$$

When eq. (2.6) is combined with eq. (2.8), the following expression for the activity concentration of each ^{222}Rn decay product $a_{Rn\text{-}d}$ relative to that of its parent is obtained:

$$\frac{a_{Rn-d}(x)}{a_1} = 1 - F_{Rn}\frac{L}{l}\;\frac{\cosh(x/l)}{\sinh(L/l)}. \qquad (2.9)$$

Due to self-absorption, the contribution to the resulting specific absorbed dose rate inside the room will depend on the position x in the construction. This effect can be accounted for by the exponential attenuation factor with the exception that the absorber thickness in the present situation is given by L-x, because of the shift of the origin to the centre of the construction element. The effect of the ^{222}Rn exhalation on the dose rate can then be quantified by:

$$F_{equil} = \frac{1}{N}\cdot\int_{-L}^{+L}\frac{a_{Rn-d}(x)}{a_1}\cdot e^{-\mu(L-x)}dx \text{ with } N = \int_{-L}^{+L} e^{-\mu(L-x)}dx \qquad (2.10)$$

The second integral N in this equation is introduced to fulfil the condition that the transmission factor summed over the construction is numerically equal to unity. The variable μ represents the linear attenuation coefficient (m^{-1}). Eq. (2.10) is solved analytically, resulting in an extensive formula. The solution is plotted as a function of the ^{222}Rn release factor F_{Rn} and the diffusion length in Figure 2.10. The outcome shows an almost flat plane, independent of the diffusion length. The correction factor F_{equil} is well correlated

with (1-F_{Rn}). The effect of exhalation of a construction element i can therefore simply be included in the model calculations by correcting the ^{226}Ra activity concentration. Eq. (2.3) is so converted into:

$$F_{dose,i} = k_1 a_{1,i}(1 - F_{Rn,i}) + k_2 a_{2,i} + k_3 a_{3,i} \,. \qquad (2.11)$$

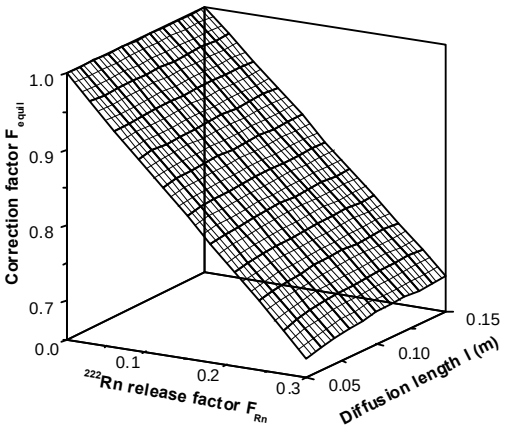

Figure 2.10
3D-plot of the specific absorbed dose rate in air in non-equilibrium situations, according to eq. (2.10). The specific absorbed dose rate is taken relatively to the results obtained for a ^{238}U series that is fully in equilibrium. The construction thickness is fixed at 20 cm.

The ^{226}Ra, ^{228}Ra and ^{40}K activity concentrations of the predominant construction materials concrete, sand-lime brick, gypsum, clay brick and aerated concrete, including the ^{222}Rn release factors are determined in a national survey and reported in section 3.1. From these results the dose factor is calculated according to eq. (2.11) for each sample; in Table 2.8 the results are summarized per class of building material as means and standard deviations (SD). As shown, the dose factor of the various building materials can differ sub-

Table 2.8
Measured ^{222}Rn release factor from section 3.1, dose factor F_{dose} corrected for ^{222}Rn exhalation according to eq. (2.11) and the ratio between the corrected and not corrected dose factors.

Material	**F_{Rn}[a] (-)**	**F_{dose}[b] (nGy h^{-1})**	**Ratio[c] (-)**
Concrete	0.14 ± 0.06	51 ± 11	0.95
Sand-lime brick	0.10 ± 0.03	36 ± 11	0.98
Gypsum	0.13 ± 0.05	9 ± 4	0.91
Clay brick	0.00 ± 0.01	120 ± 8	1.00
Aerated concrete	0.13 ± 0.04	31 ± 6	0.96

[a] Mean ^{222}Rn release factor. [b] Mean ± SD of the corrected dose factor.
[c] Ratio of corrected and uncorrected dose factor.

stantially, in this study to a factor of 13, but also that even within the same class the variation coefficient can rise up to 45%. In the same table the ratio between the corrected and uncorrected dose factor is given. The reduction of the absorbed dose rate due to exhalation of ^{222}Rn gas is most pronounced for gypsum with a value of 9% on average.

Dose location

Measurements of the absorbed dose rate in air, for instance with a high-pressure ionization chamber, are usually performed at a standard height of 1 m above the floor. This height can be considered as a typical reference point for the dose to an inhabitant staying in a room. To verify whether the position is of major importance, the specific absorbed dose rates were assessed for various places at 1 m above the floor. For that purpose the floor of the standard geometry is divided into 20 equal parts measuring 1 by 1 m^2; the dose points are taken at the crossings of the grid lines, at least 1 m from the walls. Given the floor dimensions of the standard room of 4 by 5 m, 12 positions were evaluated at 1 m above the floor. The results of these dose points are expressed relative to that in the centre of the standard geometry (at 1.40 m). When all construction elements are assumed to consist of 20 cm concrete, MARMER calculations showed mean values of 1.024, 1.016 and 1.017 for the ^{238}U series, ^{232}Th series and ^{40}K, respectively. Since these data are almost identical, they are taken together, resulting in an average and SD of 1.019 ± 0.009 for 12 x 3 observations. The low variation coefficient within this series (0.9%) points to the equivalence of the various positions in the room.

A much larger variation coefficient of almost 10% is obtained when the calculations are repeated for a standard room with one of the long walls replaced by a wall considered to be free of natural radioactivity. In that situation the decline of the relative specific absorbed dose rate in the room is highly asymmetric. For this series of calculations the result is 0.99 ± 0.09 (mean ± SD, n=36). As in the former case the obtained mean ratio, however, is close to unity, which indicates that the centre position still can be considered as representative for the dose to an inhabitant sitting randomly anywhere in the room. Therefore, in the following the effects on the specific absorbed dose rates are evaluated for the centre position only.

Thickness and density of construction elements

The thicker and denser a construction element, the more activity is present in a construction and therefore these parameters play an important role in determining the value of the absorbed dose rate. Both variables are combined to the surface density, the product of thickness and density. Using the MARMER code, this parameter is varied by changing the density from 500 to 3000 kg m^{-3} at a fixed wall thickness of 20 cm, corresponding to surface densities of 100 to 600 kg m^{-2}. Additional (MicroShield) calculations are

performed at a fixed density of 2350 kg m^{-3} (concrete), varying the construction thickness from 0 to 30 cm (surface densities 0 to 705 kg m^{-2}). The relation between the specific absorbed dose rates, relative to that in the standard geometry and the surface density, is presented in Figure 2.11. The specific absorbed dose rate increases with increasing thickness, but due to self-absorption the effect diminishes at the higher ranges. As can be concluded from this figure, it makes no difference whether the surface density is varied by thickness or by density. The best line is obtained by regression analysis resulting in the following expression:

$$F_{constr,i} = 4.48x10^{-3} m_i - 7.16x10^{-6} m_i^{\,2} + 5.33x10^{-9} m_i^{\,3} - 1.51x10^{-12} m_i^{\,4}$$
$$\text{with } m_i = \rho_i \cdot d_i \,. \qquad (2.12)$$

In these equations $F_{constr,i}$ is the correction factor as a function of the surface density m_i of construction element i in kg m^{-2}, i.e. the product of the density ρ_i (kg m^{-3}) and the thickness d_i (m) of construction element i. This factor is defined as unity for a surface density of 470 kg m^{-2} i.e. 20 cm of concrete with a density of 2350 kg m^{-3}.

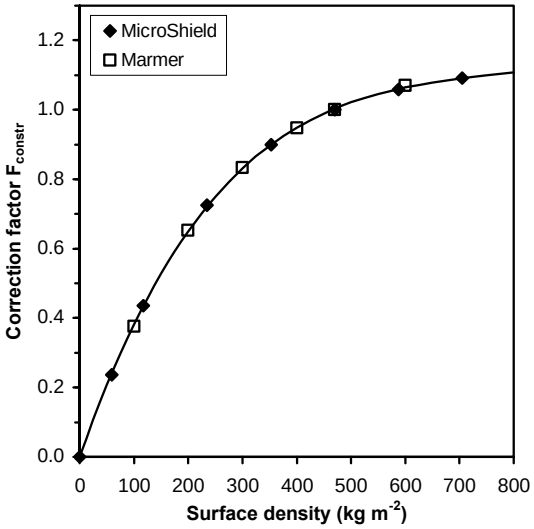

Figure 2.11
The influence of thickness and density on the specific absorbed dose rate in air. The x-axis is expressed as surface density, the product of density and thickness. The specific absorbed dose rate is expressed relative to the results obtained for the standard room (470 kg m^{-2}). The error bars due to differences in outcomes for the ^{238}U and ^{232}Th series or ^{40}K are within the size of the symbols. Calculations are performed either using the computer code Microshield (thickness) or MARMER (density).

Dimensions of body constructions

The influence of geometry other than the standard one is evaluated by MARMER calculations. Both height and floor area are varied, while the construction thickness is kept at 20 cm concrete, with no doors or windows. Table 2.9 specifies some of the examined geometries, together with their results. All results are taken relatively to that of the standard Koblinger geometry. From this table the following conclusions can be drawn:

Table 2.9
The influence of some room dimensions on the specific absorbed dose rate in air. For both natural decay series and ^{40}K the contribution from each construction element is expressed relative to that in the centre of the standard geometry. The last column in the table reports the relative area taken by the construction element in each geometry. Calculations are performed with the MARMER code. Each construction element is kept at 20 cm concrete.

Dimensions (cm) (volume)	**Construction element**	**Relative specific absorbed dose rate**				**Relative area**
		^{238}U series	**^{232}Th series**	**^{40}K**	**Average**	
500x400x280	all elements	1.000[a]	1.000[a]	1.000[a]	1.000 ± 0.000[a]	1.000[a]
(56 m^3)	floor/ceiling	0.266	0.266	0.267	0.266 ± 0.002[b]	0.221
	long walls	0.140	0.140	0.140	0.140 ± 0.002[b]	0.155
	short walls	0.095	0.094	0.094	0.094 ± 0.001[b]	0.124
800x400x280	all elements	1.012	1.013	1.019	1.015 ± 0.004	1.000[a]
(90 m^3)	floor/ceiling	0.296	0.297	0.298	0.297 ± 0.001	0.244
	long walls	0.166	0.166	0.167	0.166 ± 0.001	0.171
	short walls	0.043	0.044	0.044	0.044 ± 0.001	0.085
800x400x250	all elements	1.022	1.016	1.019	1.019 ± 0.006	1.000[a]
(80 m^3)	floor/ceiling	0.319	0.317	0.319	0.318 ± 0.002	0.258
	long walls	0.153	0.152	0.151	0.152 ± 0.001	0.161
	short walls	0.040	0.039	0.039	0.039 ± 0.001	0.081
1000x800x250	all elements	1.025	1.030	1.039	1.031 ± 0.008	1.000[a]
(200 m^3)	floor/ceiling	0.396	0.399	0.403	0.399 ± 0.004	0.320
	long walls	0.072	0.071	0.071	0.071 ± 0.001	0.100
	short walls	0.045	0.045	0.045	0.045 ± 0.002	0.080

[a] Defined as 1.000. Average ± SD for the two considered series and ^{40}K.
[b] Corresponding values found by MicroShield are 0.260, 0.145 and 0.094.

(a) the SD of the relative contributions, averaged over the considered radionuclides, is limited to 1% at most; (b) for the largest volume considered in this study, 200 m^3, an increase of only a factor of 1.03 compared to the standard geometry is found; and (c) the relative contribution of each of the construction elements changes with the dimensions. In Figure 2.12 this last variable is plotted against the relative area of the construction element in question, resulting in an S-shaped curve. The regression coefficients are obtained by linear regression using the method of least squares:

$$F_{dimens,i} = -0.135\ A_i^{rel} + 9.40\left(A_i^{rel}\right)^2 - 15.9\left(A_i^{rel}\right)^3, \qquad (2.13)$$

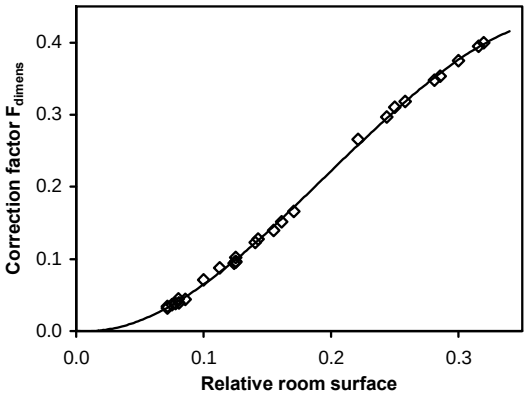

Figure 2.12
Relation between the specific absorbed dose rate in air induced by a construction element and its relative area. The specific absorbed dose rate is expressed relative to the results obtained for the standard construction. The error bars due to differences in outcomes for the ^{238}U and ^{232}Th series or ^{40}K are within the size of the symbols.

with $F_{dimens,i}$ the relative dose contribution of a construction element i and A_i^{rel} the relative area taken by that construction element (both dimensionless). Note that in this equation the room volume is indirectly taken into account.

Outer leaf

In the Netherlands it is common practice that the exterior walls of the dwelling consist of two elements with a cavity in between. The outer leaf is usually made of brickwork, found to have relatively high activity concentrations (see Table 3.2), with as a consequence that its contribution to the indoor dose rate cannot be neglected *a priori*. The calculation is similar to that for the other construction elements with the exception that attenuation by the inner leaf is taken into account. The attenuation factor F_{leaf} is determined as a function of the surface density of the inner leaf using the MicroShield code. The best fit is:

$$F_{leaf} = 1 - 3.14x10^{-3} m_{leaf} + 3.48x10^{-6} m_{leaf}^2 - 1.30x10^{-9} m_{leaf}^3 \quad (2.14)$$

with m_{leaf} the surface density of the *inner* leaf (kg m^{-2}). The three natural radionuclides behave in a similar way and there is no need to treat these separately. The maximum standard deviation in the correction factor is calculated at 0.03.

Doors and windows

Doors and windows themselves will not contribute to the absorbed dose rate. The areas of the various construction elements are corrected according to:

$$F_{do/wi,i} = \frac{A_i - A_{wi/do,i}}{A_i} = 1 - A_{wi/do,i}^{rel}, \quad (2.15)$$

in which A_i is the area of construction element i (m^2) and $A_{wi/do,i}$ the area of doors and windows in that construction element (m^2).

Internal partition walls

The present model assumes a beam-shaped body construction with a rectangular floor area. Presence of internal partition walls in such a construction needs a further correction. In general the zoning of the body construction is achieved by lightweight materials. In the Netherlands gypsum blocks and panels are predominantly used for this purpose. Since this material is characterised by low activity concentrations (Table 3.2), these non-bearing inner walls will hardly contribute, if at all, to the absorbed dose rate. However, these walls may attenuate the contribution from other construction elements; according to eq. (2.14) the attenuation is about 25% for 10-cm gypsum blocks.

The overall attenuation, as to what portion each construction element is shielded, depends on the local layout. Without more detailed information only a rough estimate can be made. If one is interested in the absorbed dose rate in one of the rooms, the total mass of the non-bearing inner walls belonging to that room is thought to be spread among the total room area, including floor and ceiling. This results in a hypothetical shielding of all construction elements with a surface density of:

$$m'_{inner} = m_{inner} A^{rel}_{inner} . \qquad (2.16)$$

m_{inner} is the surface density of the non-bearing inner walls (kg m^{-2}) and A^{rel}_{inner} the relative area of these walls in the specified room (dimensionless). The correction factor F_{zoning} is found by entering the value of m'_{inner} into eq. (2.14).

Adjacent floors and dwellings

The denser and thicker the construction elements of the dwelling, the higher the absorbed dose rate due to the building materials will be, but also the smaller the dose contribution from adjacent floors and dwellings. This effect is assessed for a configuration consisting of three times three standard units as illustrated in Figure 2.13. Each of the walls, ceilings, and floors has a thickness of 20 cm and the density was varied from 500 to 3000 kg m^{-3} (100 to 600 kg m^{-2}). For each construction element the contribution to the absorbed dose rate in the centre of unit A is calculated using the MARMER code. A part of the results, for a surface density of 100 kg m^{-2}, are plotted in Figure 2.13. It shows the combined effects of attenuation by partition elements and expansion of the distance between source and dose point.

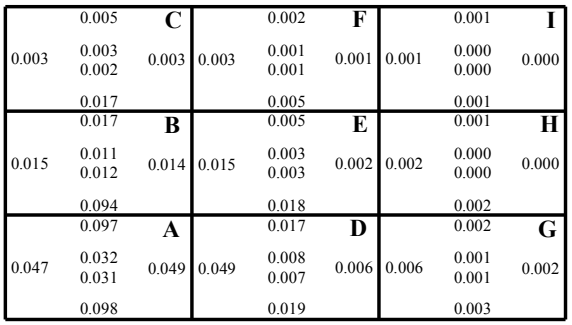

Figure 2.13
Contribution of the various walls, floors and ceilings to the specific absorbed dose rate in air at the centre of room A. The values are expressed in nGy h^{-1}. All construction elements are assumed to contain 1 Bq kg^{-1} ^{238}U in secular equilibrium with their decay products and have a surface density of 100 kg m^{-2}. The values given in the centre of each room represent the induced dose rate of the front and back (short) walls. The inner dimensions of each unit are 5 x 4 x 2.8 m^3.

From the results estimates are made for the extra dose rate contribution from the building materials applied in adjacent floors and/or dwellings, depending on the type of house. Considering a two-floor detached house, that contribution is derived from the results obtained for the walls and ceiling of unit B (see Figure 2.13). For a three-floor coupled house the results for the units B-F are taken, including mutual walls and floors/ceilings only once. The same procedure is followed for a three-floor end house (contribution from units B-I), a three-floor row house (contribution from B, C and 2x D-I) and a multi-storey apartment building (2x B, C, D, G and 4x E, F, H, I). The calculation results are summarized in Figure 2.14 and show the correction factor as a function of the surface density of the partition walls/floors and the type of house. When no contribution arises from adjacent parts, the correction factor is defined as unity. The lower the surface density of the partition walls/floors the higher this contribution will be.

The data points in Figure 2.14 are fitted using the method of least squares; the resulting regression coefficients per type of house are given in Table 2.10. In the model calculations the surface densities of the floor, walls and ceiling are assumed to be the same. In practice, however, some differences may arise between these construction elements. Therefore for the calculation of the contribution of adjacent rooms the surface density can be averaged over that of the ceiling and the supporting inner walls.

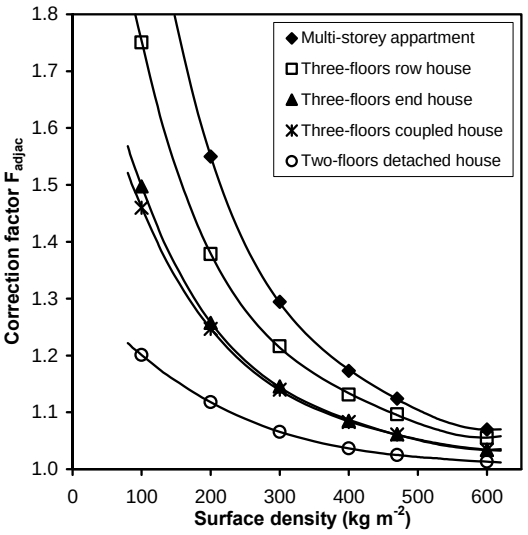

Figure 2.14
Contribution from adjacent rooms expressed as a correction factor for the calculated absorbed dose rate in air for the room in question as a function of the surface density of the construction elements and type of house. Identical units are assumed. The error bars due to differences in outcomes for the ^{238}U and ^{232}Th series or ^{40}K are within the size of the symbols.

Table 2.10
Overview of the regression coefficients with respect to the calculation of the correction factor F_{adjac} for various types of houses to calculate the contribution to the absorbed dose rate from building materials present in adjacent rooms. The x-coordinate is the average surface density of ceiling and supporting inner walls.

Type of house	a_0	a_1	a_2	a_3	a_4
Two-floors detached	1.32	-1.45×10^{-3}	2.43×10^{-6}	-1.51×10^{-9}	1.09×10^{-13}
Three-floors coupled	1.85	-5.09×10^{-3}	1.35×10^{-5}	-1.74×10^{-8}	8.80×10^{-12}
Three-floors end	1.96	-6.17×10^{-3}	1.77×10^{-5}	-2.47×10^{-8}	1.34×10^{-11}
Three-floors row	2.51	-1.02×10^{-2}	3.10×10^{-5}	-4.49×10^{-8}	2.50×10^{-11}
Multi-storey apartment	3.30	-1.57×10^{-2}	4.66×10^{-5}	-6.57×10^{-8}	3.56×10^{-11}

2.3.3 Comparison with MCNP calculations

The best way to prove the validity of a new calculation method is to apply it to a set of dwellings and compare the results with measured values. A prerequisite thereby is that for each dwelling the activity concentrations of all construction materials are well known. And since terrestrial and cosmic radiation partly contribute to the absorbed dose rate, also the indoor level of these exterior sources have to be known for each individual dwelling. Such a complete and detailed data set, however, is not available.

We therefore followed another approach and made a comparison of the results of the present model with those obtained by an alternative code. The choice was made for the Monte Carlo code MCNP, well bench marked and not involved in the set-up of the present model (Briesmeister, 2000; Gualdrini and Ferrari, 2004). Calculations are conducted for

three Dutch standard dwellings, i.e. a row house, a coupled house and an apartment building, the plans of which are given in Figure 2.15 (SenterNovem, 2006; slightly modified dimensions). The floors and ceilings are assumed to be constructed of concrete, the outer walls of brickwork, the inner leaf and bearing inner walls of sand-lime brick and the non-bearing walls of gypsum. The applied thicknesses are 20, 10, 10, 24 and 10 cm, respectively. The activity concentrations and densities of these materials are assumed to be equal to the average values reported in Table 3.1 and 3.2, respectively; the ^{226}Ra activity concentration was not corrected for exhalation. The chemical composition for concrete is extracted from a publication of Hubbell and Seltzer (1995), that for the other materials from Roelofs and Wiegers (1995).

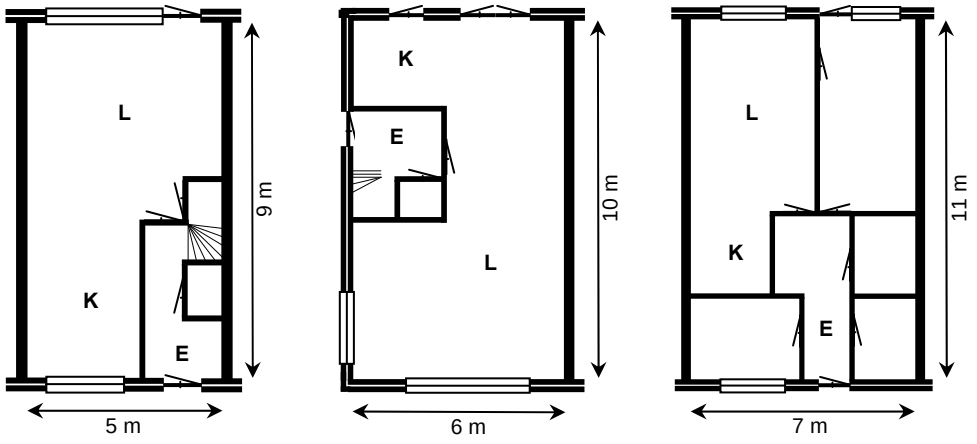

Figure 2.15
Plans of three reference dwellings: from left to right row house, coupled house and gallery apartment, with L: living room; K: kitchen; and E: Entrance. See text for dose points and considered situations.

Per dwelling three separate calculations are made: (1) the body construction without doors, windows and inner non-bearing walls; (2) as (1) but with outer doors and windows; and (3) as (2) provided with inner walls and doors. For situation 1 the centre of the body construction is taken as the dose point. For the proposed method the absorbed dose rate in air is calculated according eq. (2.2), including the correction factors as specified in eqs. (2.11) to (2.14). For situation 2 also the correction factor for the presence of doors and windows, presented in eq. (2.15), is applied. For situation 3 the absorbed dose rate is determined in the centre of the living room. The outcome is equal to that of situation 2 but corrected for shielding according to the eqs. (2.16) and (2.14). MCNP calculations are carried out for

exactly the same configurations and dose points as indicated above. As a consistency test also the calculations results with the MARMER code are incorporated.

Table 2.11 shows the calculation results of the specified methods. The differences between the proposed model and the MARMER results range from –1% to +5% with a value of about 1% when averaged over all considered situations. The corresponding results of the MCNP code are 0 to 7% with an average of 4%.

Table 2.11
Results of the calculated absorbed dose rates in air in three Dutch reference dwellings as computed with the proposed model, MARMER and with MCNP. For each dwelling three situations are considered: (1) body construction without doors and windows, (2) as (1) with outer doors an windows and (3) as (2) with inner walls and doors. In this comparison the contribution from adjacent rooms is not taken into account.

Reference dwelling		**Proposed model**	**MARMER**		**MCNP**	
		(nGy h^{-1})	**(nGy h^{-1})**	**(%)[a]**	**(nGy h^{-1})**	**(%)[a]**
Standard constr.	(1)	53.9	53.9	0.0	53.7	0.4
Row house	(1)	51.4	50.9	1.1	49.1	4.6
	(2)	49.6	48.6	2.1	47.2	4.9
	(3)	47.8	47.4	0.9	45.6	4.7
Coupled house	(1)	54.3	54.2	0.2	51.9	4.4
	(2)	51.6	50.7	1.6	49.3	4.5
	(3)	50.1	47.7	4.7	46.6	6.9
Apartment building	(1)	52.2	52.5	-0.5	50.6	3.1
	(2)	50.9	51.1	-0.4	49.0	3.8
	(3)	47.3	47.7	-0.9	45.5	3.9
Average				0.9		4.1

[a] Difference with the proposed model.

2.3.4 Discussion and conclusions

Model calculations on the absorbed dose rate in dwellings due to building materials date from the end of the 1970's. Since then several multi-purpose codes and other calculation tools have become available that facilitate and improve the calculation. In this section we applied either the computer code MARMER or MicroShield to study the various parameters. Both codes essentially yield the same results. This is for instance demonstrated in Table 2.9; MicroShield calculates a relative contribution of the construction elements in the standard geometry at 0.260, 0.145 and 0.094, while the corresponding values found by MARMER are 0.266, 0.140 and 0.095, respectively. Another example is found in Figure

2.11 on the relation between the relative dose rate and the surface density; also in this case the data of both codes are in good agreement.

With the aid of both codes it is verified to what extend a number of parameters affect the building material induced absorbed dose rate in a dwelling. The first parameter investigated was the position of the reference dose point. The centre of the room is demonstrated to be an adequate basis for the dose assessment to an inhabitant; the calculated specific absorbed dose rates for this position deviate not more than a few percent from the average value calculated from 12 other dose points spread over the room. This is in accordance with Koblinger (1978) who also found no significant differences between various positions in the room. In the same study it was shown that the results on the absorbed dose rates are essentially the same for the materials silicon oxide, concrete and gypsum. Our own calculations (not presented) confirmed that the chemical composition of the regular building material has no significant effect on the specific absorbed dose rate, provided that the densities remain the same. The specific absorbed dose rates determined for concrete are therefore also valid for other building materials.

Several publications describe the influence on the construction thickness and density separately (Koblinger, 1978; Stranden, 1979; Risica *et al*., 2001; Máduar and Hiromoto, 2004). In the present section these parameters are combined to the surface density, which allows a material-independent approach that facilitates the calculations. The calculations are performed for the ^{238}U series, ^{232}Th series and ^{40}K, separately. However, when these results are taken relative to those obtained for the standard geometry, as performed in Figure 2.11, the differences between the three derived ratios appear to be negligible. The nuclide-independence is also demonstrated for other variables as the room dimensions (Table 2.9, Figure 2.12), the transmission by the inner leaf and the contribution from adjacent constructions (Figure 2.14). This phenomenon rules out the need to treat the considered primordial radionuclides separately.

The influence of the dimensions of the construction was investigated by several researchers. Risica *et al*. (2001) have found a gradual increase in dose rate when the volume of the construction is enlarged. Relative to the dose rate in the standard geometry the effect ranges from –3% for a 10 m^3 room to 6% for large rooms up to 280 m^3. A variation of about 5% is reported by Màduar and Hiromoto (2004) for a range in room volumes from 20 to 110 m^3. For the dimensions tested in this section (from 56 up to 200 m^3) a somewhat lower increase of about 3% is noted (Table 2.9). In this study the influence of the size of the construction element is investigated in more detail. As shown in Figure 2.12 there is a S-shaped relation between the relative contribution of each construction element and its relative area in the room. Large areas contribute more than would be expected on the basis of their relative area, whereas the opposite holds for small construction elements. The turning point, at which both variables have actually the same numerical values, lies at

0.165 according to eq. (2.13). A similar value would be obtained for a cubically shaped room with equivalent materials, in which each construction element accounts for 1/6 of the total area and also for 1/6 of the absorbed dose rate. This correction factor plays an important role when the activity concentration, thickness and density of the various construction elements differ widely.

The contribution due to building materials applied in adjacent rooms depends on both the type of construction and the surface density of the partition elements. For constructions with 20 cm concrete partition elements this value ranges from 2% for a detached house to 12% for a multi-storey apartment. Also Koblinger (1978) has performed some calculations for a multi-storey apartment (unit size 5.6 x 3.1 x 2.5 m^3) for which a correction factor of 1.16 was reported. The walls and floors of that construction consist of 14 cm and 20 cm concrete, respectively, with a density of 2500 kg m^{-3}; this implies an average surface density of 425 kg m^{-2}. Based on this value the same correction factor of 1.16 can be deduced from our results (Table 2.10, 'Multi-storey apartment').

In previous modelling exercises the ^{222}Rn exhalation so far is ignored, although suggested to be of major importance for some types of building material (Stranden, 1979; Mustonen, 1984). From a theoretical treatise of the ^{222}Rn exhalation a simple relation is deduced between the ^{222}Rn release rate and the contribution to the absorbed dose rate in a room. For brickwork ^{222}Rn exhalation has no effect on the induced dose rate (Table 2.8) while for gypsum products this can lead to a correction of –9% on average. The effect on the average (computed) gamma-ray dose rate in the Netherlands is estimated at -4%.

The results of our model have been compared with those of the multi-purpose code MCNP in three reference dwellings. The differences between the two methods are 4% on average. In view of the variation coefficients of 9 to 14% in the reported specific absorbed dose rates (Table 2.7), this value can be considered as acceptable. On the other hand, the evaluation of the indoor absorbed dose rates with our model takes considerably less time. This makes our method especially suited for an evaluation of dose assessments for large clusters of dwellings in existing residential sections or evaluations of dose consequences due to new construction trends and/or building materials. The calculation involves various correction factors that encompass most practical situations. The consequences of each of these factors will be investigated in a sensitivity analysis, reported in section 3.4. In that section also the results are incorporated of a study after application of our model to a representative set of Dutch dwellings.

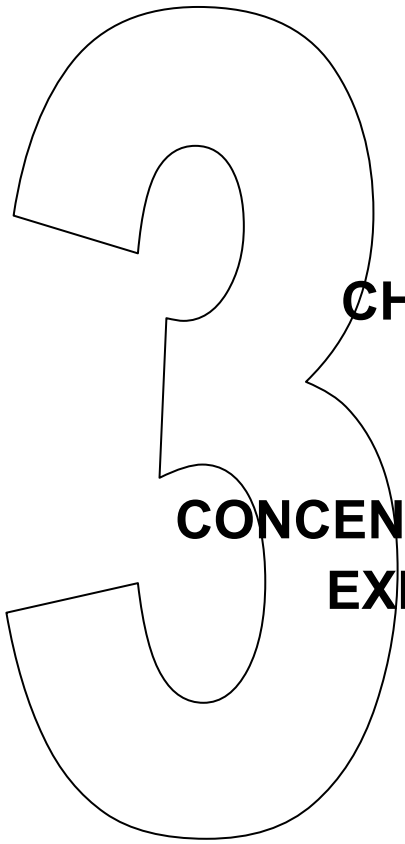

CHAPTER 3

CONCENTRATIONS AND EXPOSURES

3.1

Natural radioactivity and radon exhalation rate of building materials[12]

3.1.1 Introduction

A boundary condition to assess the exposure of the Dutch population due to natural radioactivity in building materials is to determine their ^{222}Rn exhalation rates and radioactivity concentrations. Therefore the test samples should constitute a representative reflection of building materials used in the construction of dwellings. The samples were selected in close consultation with various relevant parties and cover about 95% of the national market and included gypsum products, aerated concrete, sand-lime and clay bricks, mortars and concrete. Within each class of materials several samples were taken; the number was dependent on the expected radiological variation based on earlier investigations. Special attention has been paid to the quality assurance of the applied analytical methods.

3.1.2 Materials and methods

Test samples

The gypsum specimens were either from natural origin or from flue gas desulphurization installations. The products included gypsum boards and building blocks of various thickness, density and manufacturer. The boards were cut to small plates, dimensions 30x30 cm^2, the blocks were sawn dry into test samples not exceeding 40x50 cm^2. The thickness of the samples ranged from 1 to 10 cm. Blocks of aerated concrete of two densities were sampled at seven production locations. Sand-lime bricks are produced at eleven factories in the Netherlands and each of them was sampled twice. The production time between the two batches was at least one week. Also in the category of the fired clay bricks the difference between the two clutches are realized by different dates of production. The bricks are oven fresh or taken from stock of the pile field. Seven brickyards were sampled, all using another type of clay. The other products consisted of porous inner wall bricks manufactured with or without fly ash.

In the Netherlands so far mortars were not extensively examined for their radiometric properties. Each mortar sample consisted of 48 small beams (dimensions 4x4x16 cm^3), a geometry equal to that as used in the general quality control of mortars. After mixing the

[12] This chapter is based on a paper published in Health Physics 91:200-210 (2006), entitled *National survey on the natural radioactivity and ^{222}Rn exhalation rate of building materials in the Netherlands*. Authors: P. de Jong, W. van Dijk, E.R. van der Graaf and T.J.H. de Groot.

mortars with water, the beams were prepared and stored for seven days at a relative humidity (RH) of over 95% and thereafter for 21 days at a RH of 65%. The sampled material varied in strength, binder and manufacturer. The exhalation rate per sample is determined from 40 beams in total. The remaining beams were used for the determination of the activity concentrations. The concrete applied in the construction of dwellings includes a wide variety of recipes with respect to type of cement (Portland, Portland/fly ash, blast furnace), amount of cement (260-380 kg m^{-3}), class of strength (32.5-52.5 MPa), water/binder ratio (0.40-0.65) and type of gravel (river gravel, concrete granulate, lime stone and combinations). Twenty-eight mixtures were collected from pre-cast production and ready mix plants. From each mixture five cubes, dimensions 15x15x15 cm^3, were prepared according to a national standard (NEN, 1999). Four cubes served the determination of the exhalation rate, one the activity concentration. Table 3.1 presents some characteristics of the test specimens.

Table 3.1
Number of test specimens, density (mean, range) and range in sample thickness of the evaluated construction materials.

Building material	**n**[a]	**Density (kg m^{-3})**		**Thickness (cm)**
		mean	**range**	**range**
Gypsum	10	900	700 – 1200	1.0 – 10.0
Aerated concrete	14	580	390 – 820	9.9 – 15.0
Sand-lime bricks	22	1820	1720 – 1910	10.0 – 10.4
Clay bricks (I)	16	1670	1370 – 2000	9.5 – 10.3
Clay bricks (II)	5	1370	1350 – 1390	10
Mortar	6	1830	1740 – 1890	4
Concrete	28	2350	2250 – 2460	15

[a] Number of test specimens.

Quality control

The determination of the activity concentrations and ^{222}Rn exhalation rates are performed by a combination of laboratories. For the determination of the natural radioactivity levels three laboratories are involved, for the ^{222}Rn exhalation rate two. The samples were divided equally and arbitrarily over the participating laboratories. For quality control purposes about 10% of the samples is also analysed by a second laboratory according to the same standard procedures. Within the material classes the control samples were chosen arbitrarily.

Sample treatment

Prior to the gamma-ray measurements, the samples are broken to pieces with a size smaller than 0.2 cm. Two of the participating laboratories have dried the broken material until a constant weight was reached. According to the standard method (NEN, 2001a) it is also allowed to do a separate determination of the dry weight and correct the analytical results afterwards. The third laboratory followed that route.

The test samples for the ^{222}Rn exhalation rate measurements were conditioned at a temperature of 20 ± 2 °C and a relative humidity of 50 ± 5%. According to the applied standard method (NEN, 2001b) the conditioning was continued till the decrease in moisture content of the material is less than 0.07% measured over a period of seven days. Furthermore, the standard method requires the samples to be analysed within four months after preparation.

Natural radioactivity concentrations

As stated above the natural radioactivity concentrations of the specimens are determined according to a standard method published as NEN 5697 (NEN, 2001a). According to this method the density-dependent photo-peak efficiencies are determined for the gamma-ray energies 352 keV (^{214}Pb, parent ^{226}Ra), 583 keV (^{208}Tl, parent ^{228}Th), 911 keV (^{228}Ac, parent ^{228}Ra) and 1461 keV (^{40}K). Four calibration standards are assembled with increasing densities. The materials used were stearic acid, starch, gypsum and quartz sand, homogeneously mixed with certified amounts of ^{238}U and ^{232}Th, in equilibrium with their daughter nuclides, and ^{40}K. The standards are placed into Marinelli beakers with a volume of about 1 litre, weighed, and closed radon-tight. To obtain secular equilibrium, a waiting time of at least three weeks was taken into account before counting the samples. All samples were counted using a HPGe detector in a low-background facility. The samples of broken building material were analysed in an identical way as the calibration standards with respect to geometry, waiting time and radon-tightness of the beaker. The photo-peak efficiencies of the samples were deduced from the efficiency curves of the standard samples by interpolation. The results are expressed per unit of dry weight.

The standard method includes a test for the determination of the tightness of the sealed Marinelli beaker. In this test about 500 Bq or more of ^{222}Rn gas is injected into an almost closed beaker using a gas syringe, where after the beaker is sealed in the usual way. The beaker is counted for at least ten successive time periods of 4 h. From the time-dependence of the count rate at the 609 keV photon peak of ^{214}Bi, the leakage rate is calculated. This factor should satisfy the following inequality:

$$\lambda_L + 2s_A < 0.1\,\lambda_{Rn}, \tag{3.1}$$

in which λ_L is the ^{222}Rn leakage rate, s_A the standard deviation of this factor as determined by the method of least squares and λ_{Rn} the decay constant of ^{222}Rn (2.1×10^{-6} s^{-1}). In case the beaker leaks at its maximum allowed rate of 0.1 λ_{Rn}, the ^{222}Rn concentration in the beaker will deviate from its equilibrium concentration by a factor of $1/(1 + 0.1) = 0.91$ or 9%. If the assumed emanation factor of the building materials is less than 50%, the potential underestimate in the ^{226}Ra activity concentration of the sample will be smaller than 50 % of that 9% or no more than about 5%.

Prior to publication, the standard method was tested in an interlaboratory exercise. The results of that study are published elsewhere (Blaauw *et al*., 2000; 2001). The three laboratories contributing to this survey also participated in this intercomparison and the results obtained by these laboratories were consistent within their uncertainties.

^{222}Rn exhalation rate

The ^{222}Rn exhalation rate is determined according to the standard method NEN 5699 (NEN, 2001b). Descriptions of the methods applied by laboratory A and B can be found in section 2.2. The results are expressed as mass and area exhalation rates by normalizing the amount of ^{222}Rn per kg material (at 50% RH) or per m^2, respectively. To calculate the area exhalation rate, a one-dimensional exhalation is assumed, as is the case in practice, taking the area normally facing the room and its opposite side as exhaling surfaces. For the mortars it is assumed that the joint of the brick-work is 1 cm and the bricks itself have the dimensions of 5x20x10 cm^3.

Radon release factor

The ^{222}Rn release factor of a sample, F_{Rn}, is defined as the ratio between the amount of ^{222}Rn gas released to the environment and the amount that is generated within the material. In formula:

$$F_{Rn} = \frac{E}{\lambda_{Rn}\, a_1}\ 100\%, \qquad (3.2)$$

where E is the ^{222}Rn exhalation rate in Bq (kg s)$^{-1}$, λ_{Rn} is the decay constant of ^{222}Rn (2.1×10^{-6} s^{-1}) and a_1 is the activity concentration of ^{226}Ra (Bq kg^{-1}). This factor is calculated for each of the test samples. Per class of material the average and standard deviation of F_{Rn} are derived from these values.

External dose factor

To facilitate a comparison of the dose rate consequences between various samples, the activity concentrations per sample are combined to a quantity to which in this dissertation we will refer to as dose factor F_{dose} (nGy h^{-1}). This factor is calculated according to eq. (2.3).

Statistics

The data points were fitted according to a method known as bisector ordinary least squares (OLS) as described by Isobe *et al*. (1990). In this method the Y and X variables are treated symmetrically and the best line is the line that bisects the OLS(Y|X) and the inverse OLS(X|Y) lines.

Mathematical room model

In a survey on ^{222}Rn concentrations in Dutch dwellings also an inventory was made of the various building materials applied for construction (Stoop *et al*., 1998). From these data an overview is prepared to construct a virtual average living room consisting of all main stony materials with their representative area percentages, based on information from 1336 dwellings. Combining these data with the averaged results on dose factor, as reported in this section, an estimate of the resulting external dose rate in a living room due to building materials is obtained. The calculation is based on the following equation:

$$\dot{D} = \sum_i A_{rel,i} F_{dose,i} F_{constr,i}, \qquad (3.3)$$

in which $\dot{D}$ is the absorbed dose rate in air in the centre of the living room in nGy h^{-1}; i is the material index; $A_{rel,i}$ the relative area taken by material I; and $F_{dose,i}$ the average dose factor of material i. Since the dose factor refers to a construction thickness of 20 cm and a density of 2350 kg m^{-3} (see section 2.3), a correction factor $F_{constr,i}$ is introduced in eq. (3.3) for alternative values. The relation of $F_{constr,i}$ with the surface density (the product of thickness and density expressed as kg m^{-2}), is given in Figure 2.11.

3.1.3 Results

The results of the activity concentrations of ^{226}Ra, ^{228}Ra, ^{228}Th and ^{40}K are presented in Table 3.2. For all materials the ^{228}Ra and ^{228}Th activity concentrations are equal, indicating the secular equilibrium in the ^{232}Th series. In some gypsum samples, however, small but significant differences in the levels of these radionuclides are recorded. The lowest activity concentrations are found in the construction materials made of gypsum, followed by aerated concrete, sand-lime bricks and mortar. Highest levels are obtained for fired clay

Table 3.2
Mean ± standard deviation and range of the mass activity concentrations, ^{222}Rn exhalation rate, radon release factor and dose factor of the investigated materials.

Building material (no. of observations)	Activity concentration				Rn exhalation rate		Rn release factor	Dose factor
	^{226}Ra (Bq kg^{-1})	^{228}Ra (Bq kg^{-1})	^{228}Th (Bq kg^{-1})	^{40}K (Bq kg^{-1})	(μBq kg^{-1} s^{-1})	(μBq m^{-2} s^{-1})[a]	(%)	(nGy h^{-1})
Gypsum (10)	8 ± 4	1.7 ± 1.7	1.3 ± 1.2	10 ± 5	1.7 ± 0.5	40 ± 30	13 ± 5	10 ± 4
	3 – 14	0.6 – 6.4	0.4 – 4.5	3 – 17	1.1 – 2.7	6 – 75	5 – 17	5 – 15
Aerated concrete (14)	11 ± 3	8 ± 3	8 ± 2	170 ± 30	2.8 ± 1.2	100 ± 50	13 ± 4	32 ± 6
	6 – 16	5 – 12	5 – 12	120 – 210	1.5 – 6.1	50 – 200	7 – 19	22 – 41
Sand-lime bricks (22)	10 ± 4	9 ± 3	9 ± 3	230 ± 80	2.1 ± 0.9	190 ± 90	10 ± 3	37 ± 12
	4 – 17	4 – 14	3 – 13	70 – 360	0.7 – 3.8	60 – 360	6 – 15	14 – 58
Clay bricks-I (16)	39 ± 5	42 ± 4	41 ± 4	500 ± 100	0.3 ± 0.3	20 ± 20	0.3 ± 0.4	121 ± 8
	27 – 45	36 – 50	36 – 50	300 – 630	<0.03 – 1.0	<2 – 73	<0.03 – 1.3	110 – 132
Clay bricks-II (5)	74 ± 2	86 ± 2	82 ± 2	720 ± 30	0.3 ± 0.2	20 ± 11	0.2 ± 0.1	218 ± 5
	71 – 75	83 – 88	79 – 84	690 – 750	<0.1 – 0.4	<7 – 31	<0.07 – 0.3	213 – 224
Mortar (6)	12 ± 4	9 ± 3	9 ± 3	150 ± 30	7 ± 4	130 ± 70[b]	26 ± 6	33 ± 8
	7 – 18	6 – 14	5 – 13	100 – 190	3 – 13	70 – 250[b]	20 – 34	21 – 45
Concrete (28)	24 ± 8	18 ± 6	18 ± 6	160 ± 30	7 ± 3	1200 ± 400	14 ± 6	53 ± 12
	11 – 36	7 – 32	6 – 31	120 – 230	1 – 11	310 – 1950	6 – 26	32 – 81

[a] Calculated according to assumptions given in the Materials and methods section.
[b] Per m^2 brick-work; per m^2 mortar the values are approximately a factor of 4.8 larger.

bricks. In this class of material a subset can be distinguished (clay bricks II, see Table 3.2) that comprises porous inner wall bricks to which fly ash was added. These bricks have a two times higher radioactivity concentrations than the normal clay bricks. Table 3.2 also contains the results of the ^{222}Rn exhalation rates normalized per kg material as well as per m^2 exhaling area. The highest exhalation rates are found in the materials mortars and concrete, intermediate levels in gypsum, aerated concrete and sand-lime brick. Clay bricks have the lowest exhalation rates. For some clay brick samples the rates were lower than the detection limit. In calculating the mean and standard deviation the level of these samples is considered to be identical to the lower limit. Figure 3.1 presents the individual results for the exhalation rate.

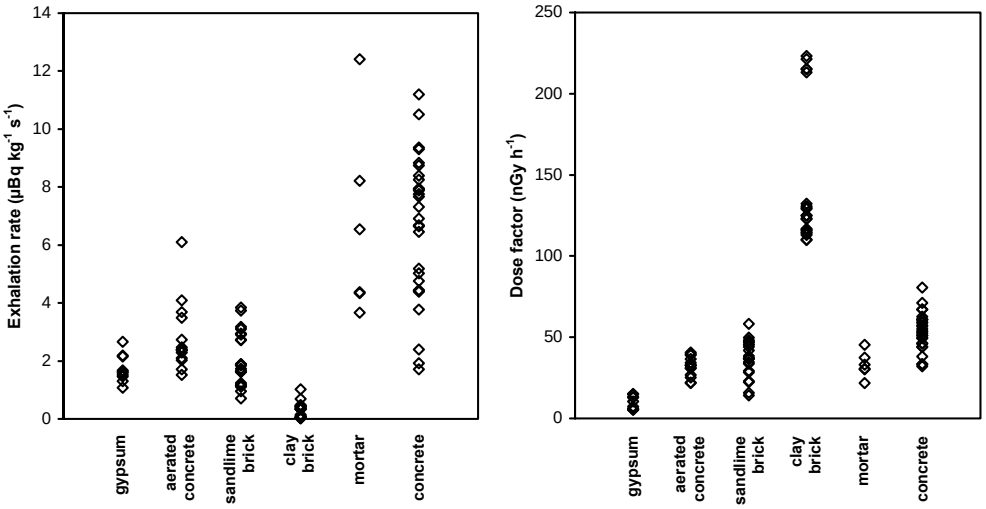

Figure 3.1 and 3.2
Results of the ^{222}Rn exhalation rate per unit of mass (left) and the dose factor (right) for six classes of building material.

As indicated in the *Materials and methods* section two factors are calculated from the measuring results: a so-called ^{222}Rn release factor and a dose factor. The ^{222}Rn release factor is calculated for each sample according to eq. (3.2); from the results the mean and standard deviation are calculated per class of material (see Table 3.2). Over all building material classes this factor shows a range from less then 0.03% to 34%. Very low values are met in clay bricks: even in case of enhanced levels up to 75 Bq ^{226}Ra per kg as found in inner wall bricks spiked with fly ash (clay bricks-II, Table 3.2), only 0.3% of the ^{222}Rn actually exhales. The highest release factors are found among the mortar and concrete samples.

The second factor in this study calculated from the measuring results is the dose factor, introduced to combine the measured activity concentrations to one dose value. In Table 3.2 the results are summarized as means and ranges per class of building material. Figure 3.2 presents the dose factors of the individual samples.

About 10% of the sampled material is also analysed by another laboratory. In Figure 3.3 the results are shown of the duplicate analysis of the activity concentrations, combined to the dose factor. For two laboratories seven paired observations were available. Using the method of least squares, the best fit can be represented by the equation $Y = (0.0 \pm 0.3) + (1.035 \pm 0.007)X$, having a correlation coefficient R of 1.000 (n=7). The slope is statistically significant different from the value 1 (Student's *t*-test, $p < 0.05$), which indicates that the two laboratories deviate systematically by 3 to 4%.

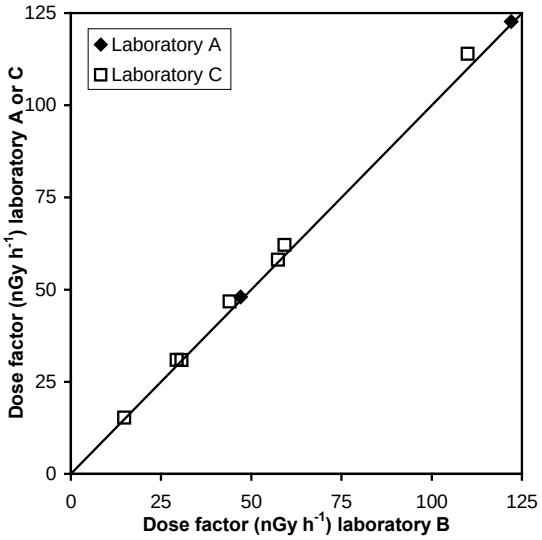

Figure 3.3
Results of the duplicate control analyses concerning the activity concentrations, expressed as the dose factor. The solid line indicates the line Y=X.

3.1.4 Discussion

In the present survey, standard methods are applied for the determination of the natural radioactivity concentrations and ^{222}Rn exhalation rate. The performance characteristics of both methods have been ascertained in intra- and interlaboratory validations (Blaauw *et al*., 2000; 2001; section 2.2). The conclusion of these exercises was that both methods were well embodied and yield results of sufficient precision and accuracy. The agreement between the laboratories dealing with the determination of the activity concentrations is reported to be within 8%; that of the exhalation rate measurements within 6%. Our control analyses confirm this. Only a slight systematic difference of 3 to 4% could be demon-

strated for the determination of the dose factor (Figure 3.3). The results of the duplicate exhalation rate measurements are incorporated in the above-mentioned study on the validation of this method and found to be around 5%.

The natural radioactivity concentrations found in this study have a comparable range as reported in earlier studies on Dutch products (Ackers *et al*., 1985; Vaas *et al*., 1993; Bosmans, 1996). A European-wide literature survey (EC, 1999a) showed for most construction materials much larger ranges. The data presented in this study are in general at the low side of that range. ^{222}Rn exhalation rates of Dutch building materials are also reported in some earlier studies. Table 3.3 presents an overview of some of the studies on concrete. These show ranges that are comparable with the outcomes of the present study.

Table 3.3
Reported ^{222}Rn exhalation rates of concrete in earlier studies.

Reference	**Geometry specimen (cm^3)**	**Reported range ($\mu Bq\ kg^{-1}\ s^{-1}$)**
This study	Cubes 15 x 15 x 15	1 – 11
Roelofs and Scholten (1994)	Cube 15 x 15 x15	1 – 13
Calculated from section 2.1	Slab 50 x 45 x 10	3 – 9
Calculated from section 4.2	Slab 50 x 45 x 10	5 – 15

For clay bricks also some reference data are available. However, the earlier test specimen consisted of small test walls of laid, cemented bricks. The ^{222}Rn exhalation rate of these test walls arises to a large extend, as turned out from this study, from the mortar instead of from the brick itself. The relative contribution of the mortar amongst others depends on the dimensions of the bricks and the brickwork bond. Assuming brick dimensions of 5x20x10 cm^3 and a joint of 1 cm, the ratio of the exhaling areas between mortar and bricks amounts 0.26. Based on the average results of the present study the most likely ^{222}Rn contribution from the mortar is almost one order of magnitude higher than from the clay bricks itself. Comparison of the results from earlier studies with the measurements of the present survey is therefore not appropriate.

From the measuring results a ^{222}Rn release factor is calculated which normalizes the liberated amount of ^{222}Rn gas per Bq of the parent ^{226}Ra. It indicates to what extent ^{222}Rn can escape from the material and therefore depends amongst others on the pore structure of the tested specimen. It is reported that the release factor of concrete is related with the water/binder ratio, amount and type of binder, the compressive strength, and the water content (Cozmuta *et al*., 2003; section 4.2). The relation between ^{222}Rn exhalation and porosity is described in more detail in section 4.3.

As reported by Koblinger (1978) and confirmed by own observations, the dimensions of the room hardly affect the dose rate at the centre. Therefore the dose factor provides a good indication of the resulting external dose rate due to the various construction materials. These results are applied to a room model in which the various walls and floors have a similar composition of that of an average Dutch living room. The second column of Table 3.4 gives an overview of the fraction of each of the materials as averaged over 1336 Dutch living rooms. In the Netherlands it is nowadays-common practice that all floors and ceilings are made of concrete, not only in multi-storey apartments, but also in types as detached and row houses. Therefore this material dominates in all dwellings. The third column presents the thickness of the materials as applied in practice. Since the dose factor is valid for a 20 cm wall thickness and a density of 2350 kg m^{-3} (470 kg m^{-2}), a correction is incorporated according to eq. (2.12). The absorbed dose rate in the centre of the model room is calculated according to eq. (3.3). The results per class of material are shown in Table 3.4, column 5, with a summed value of 43 nGy h^{-1}.

Table 3.4
Overview of input values and results of the applied mathematical room model. The relative area taken by the various building materials is deduced from an inventory of 1336 Dutch dwellings. The absorbed dose rate in air is calculated according to eq. (3.3). For an explanation of the correction factor see text.

Building material	**Relative area (-)**	**Thickness (cm)**	**Correction factor (-)**	**Absorbed dose rate (nGy h^{-1})**
Concrete	0.63	20	1.00	34.0
Sand-lime brick	0.16	10/24[a]	0.72[a]	4.2
Gypsum	0.11	5	0.19	0.2
Clay bricks (I)	0.02	10	0.57	1.6
Aerated concrete	0.01	10	0.24	0.1
Others/combinations	0.04			1.5[b]
Unknown	0.03			1.3[b]
Outer leaf[c]	0.19	10	0.57	7.6[d]
Total excl. outer leaf	1.00			43
Total incl. outer leaf				50

[a] For supporting walls a thicker construction is applied. Correction factor is based on a ratio of 70 to 30 as met in practice.
[b] Average composition assumed.
[c] Homes in the Netherlands usually have cavity walls. The outer leaf of these walls usually is made of clay bricks.
[d] Includes the attenuation by the inner leaf (applied transmission 0.58, see text).

In this value the contribution from the outer leaf of the cavity wall is not included. In general, the outer leaf is made of clay bricks and its contribution is calculated in the same way as outlined above, with the distinction that attenuation by the inner leaf is taken into consideration. Based on an average composition of the inner leaf, a transmission of 0.58 is assumed. Including the outer leaf the absorbed dose rate in the living room due to building materials is calculated at 50 nGy h^{-1}, which is lower than found in a measuring campaign for 400 dwellings as reported by Julius and Van Dongen (1985a). In that study an absorbed dose rate excluding cosmic rays is reported of 65 nGy h^{-1}, 30% higher than found in the present study. However, two components are not taken into consideration here, viz. the contribution due to (a) terrestrial radiation and (b) the gamma radiation from adjacent rooms. The terrestrial component is reported to amount to 13% (± 4%) of the indoor level (Julius and Van Dongen, 1985a). The increment due to adjacent rooms is investigated in more detail by Koblinger (1978, 1984). Depending on the thickness of the construction this contribution ranges from almost no effect for 30-cm concrete walls to up to 40% for thin walls. For a typical Dutch wall/floor thickness of 20 cm concrete, the increase is estimated at about 10%. Combining these two components, this effects in an extra dose rate of 15 nGy h^{-1}. It therefore can be concluded that our calculations are consistent with the measurements of Julius and Van Dongen.

More detailed calculations of the building material-induced absorbed dose rate are presented in section 3.4. These calculations are based on our model described in section 2.3. Besides a correction for density and thickness, also other corrections are implemented as the effects of ^{222}Rn exhalation, dimensions and internal partition walls.

In contrast to the results of the activity concentrations, the laboratory results on the exhalation rate are not always easy to extend to the housing situation. Some problems may arise. The first to mention is that the exhalation of the test specimen takes place from all sides, while in practice the ^{222}Rn transport is mainly one-dimensional, i.e. directed towards the room and its opposite side, which may lead to an overestimation of the measured mass and area exhalation rates. Berkvens and co-workers (1988) have introduced a formalism to calculate the one-dimensional exhalation rate from the experimentally determined results, based on the dimensions of the test specimen and their ^{222}Rn diffusion length. Therefore, they defined an equivalent sample geometry with a reduced thickness to compensate for the ^{222}Rn diffusion to the planes other than the front and backside. With the x-axis directed towards the room, the shortest mean distance is given by (Berkvens *et al*., 1988):

$$\frac{L'_x}{2} = \frac{L_x}{2} - \frac{1}{6}\left(\frac{L_x^2}{L_y} + \frac{L_x^2}{L_z} - \frac{1}{2}\frac{L_x^3}{L_y L_z} \right). \qquad (3.4)$$

In this expression L_x, L_y and L_z represent half of the sample thickness in the x-, y- and z-direction. Subsequently the exhalation rate from a wall in practice is calculated from the measured exhalation rate according to:

$$\frac{E_m^{(1)}}{E_m^{(3)}} = \frac{E_a^{(1)}}{E_a^{(3)}} = \frac{L'_x}{L_x} \frac{\tanh(L_x / l)}{\tanh(L'_x / l)}, \tag{3.5}$$

with $E_m^{(1)}$ and $E_a^{(1)}$ the one-dimensional mass and area exhalation rates; $E_m^{(3)}$ and $E_a^{(3)}$ the corresponding experimentally determined values; and l the ^{222}Rn diffusion length. If eqs. (3.4) and (3.5) are applied to the present samples of gypsum, aerated concrete, sand-lime and clay bricks, with diffusion lengths over 40 cm (Keller *et al*., 2001), the correction factor is found to be very close to one, i.e. almost all emanated ^{222}Rn atoms do exhale from the sample. This is probably also the case for the relatively porous mortars in this study. For heavy concrete, however, literature data on diffusion lengths range from about 5 to 20 cm (Rogers *et al*., 1994). For the low side of this range this results in a serious discrepancy between the one- and three-dimensional rates. The corresponding correction factors are calculated at 0.71 to 0.97, respectively.

For the analysed concrete samples another aspect is of importance, namely the thickness. Preferably the thickness of the test samples is the same as that met in practice. In this study this coarse is followed for most building materials. Concrete products, however, are used for several construction elements and with that the applied thickness varies. The standard procedure therefore prescribes the dimensions of the concrete test specimen exactly as 15 cm cubes to allow a correct comparison between various mixtures. A disadvantage of this approach is that, apart from the one- and three-dimensional discussion, the laboratory results may not be representative. For construction elements with a thickness different from 15 cm a correction can be made on the release rates. For the mass exhalation rate this expression resembles that given in eq. (3.5):

$$\frac{E_m^{(1)}(L_x)}{E_m^{(1)}(0.075)} = \frac{0.075}{L_x} \frac{\tanh(L_x / l)}{\tanh(0.075 / l)}. \tag{3.6}$$

In this equation $E_m^{(1)}(L_x)$ and $E_m^{(1)}(0.075)$ are the corrected one-dimensional mass exhalation rates for a construction of which half of the thickness is L_x and 0.075 m, respectively.

In Figure 3.4 the effects of one- versus three-dimensional and the thickness are combined and plotted against the diffusion length of concrete. The correction factor is defined as the ratio between the one-dimensional mass exhalation and the measured mass exhalation rate. In all cases the determined mass exhalation rate overestimates the real release, especially the smaller the diffusion length and the thicker the considered wall. For a 10 cm wall the difference limits to, on average, a few percent. This explains the agreement between the results on the test cubes and that of earlier measurements on 10 cm thick slabs, as reported in Table 3.3.

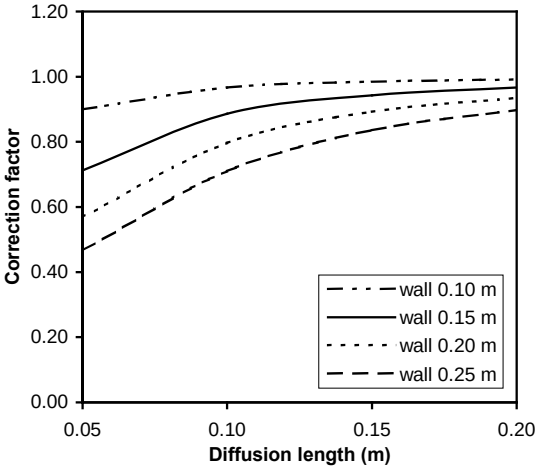

Figure 3.4
Correction factor for concrete to compensate for the three-dimensional exhalation from test samples and their 15 cm-thickness as a function of the ^{222}Rn diffusion length. The relation is given for a wall thickness ranging from 10 to 25 cm concrete. A correction factor equal to 1.00 indicates that the measured mass exhalation rate complies with that of a real wall.

3.1.5 Conclusions

In this survey the radiological properties of the common stony building materials have been mapped using two standard methods. Both the method on the determination of the activity concentrations as well as the method on the ^{222}Rn exhalation rate fully answers the expectations. The systematic deviations between the various laboratories, determined in this study, remain limited to 5% on average. In view of the large spread in results from sample to sample, even within a same class of material, the inaccuracy introduced by the analysis is acceptable. Since concrete is widely used for the construction of Dutch houses, knowledge of the diffusion lengths of this material is indispensable to estimate the total ^{222}Rn production rate due to building materials.

3.2

^{226}Ra, ^{228}Ra and ^{228}Th concentrations in gypsum plasters and mortars[13]

3.2.1 Introduction

The most important primordial radionuclides are ^{40}K, ^{238}U and ^{232}Th, all having half-lives in excess of several billions of years. ^{238}U and ^{232}Th head natural decay series of 14 and 11 significant radionuclides, respectively, also contributing to natural radiation exposure. The occurrence of these nuclides in building material will enhance the indoor ^{222}Rn and ^{220}Rn concentrations and thus the internal radiation dose due to inhalation of their short-lived decay products. In addition, the primordial radionuclides contribute to the external radiation dose of inhabitants.

The activity concentration of the primordial radionuclides per unit of mass in building materials varies considerably, depending on both the nature and the origin of the compounds. In the Netherlands, average ^{226}Ra and ^{232}Th activity concentrations in construction materials such as sand-lime brick, concrete and clay brick are about 10, 20 and 40 Bq kg^{-1}, respectively (Ackers *et al*., 1985; Vaas *et al*., 1993; see also section 3.1). The activity concentration of natural gypsum is about 10 Bq kg^{-1} ^{226}Ra and ^{232}Th or less (Ingersoll, 1983; Ackers *et al*., 1985; Keller and Schmier, 1988). However, in building products based on phosphogypsum, a by-product of the processing of phosphate fertilisers, levels equal to or in excess of 400 Bq ^{226}Ra per kg are reported (Van Dijk and De Jong, 1991; Othman and Mahrouka, 1994; O'Brien *et al*., 1995; Rutherford *et al*., 1995). Thus far only limited attention has been paid to the natural radionuclides in gypsum plasters and mortars (Malanca *et al*., 1993; Van Deynse *et al*., 1997). In the present study, the activity concentrations of ^{226}Ra, ^{228}Ra and ^{228}Th have been determined for almost all ready mixed plasters and mortars available on the Dutch market. The consequences for doses to both inhabitants and plaster-workers are discussed.

[13] This chapter is based on a presentation at the second International Symposium on Naturally Occurring Radioactive Materials (NORM II), November 10-13, 1998, Krefeld, Germany and incorporated in the proceedings, pp 58-61, entitled *^{226}Ra and ^{228}Ra concentrations in gypsum plasters and mortars used in the Netherlands*. Authors: P. de Jong, W. van Dijk and H.P. Burger.

3.2.2 Materials and methods

Test samples

The professional plasters and flooring mortars are obtained from several suppliers of building materials from various parts of the Netherlands. The non-professional products are purchased at some local shops. All samples are obtained in their original packing. The sampled materials cover the market for ready mixed plasters in the Netherlands almost completely. For comparison purposes some plaster materials are also ordered in Germany.

Gamma-ray analysis

About 600-1000 grams of each material are weighed into polyethylene bottles and encapsulated. After a waiting time of at least three weeks to establish radioactive equilibrium within the decay series, the samples are counted during 50,000 s using a Ge detector (EG&G). The recorded spectra are analysed using the Genie-PC software (Canberra) for peak areas and uncertainties. The ^{226}Ra content was *not* based on the 186 keV peak area of ^{226}Ra itself because this area is interfered by that of ^{235}U. Furthermore the abundance of this photon energy is limited (3.3%), which would result in a relative high limit of detection for ^{226}Ra. Instead, the ^{226}Ra concentration is determined as the average of the equilibrium concentrations of ^{214}Pb and ^{214}Bi, likewise the ^{228}Th activity is calculated from ^{212}Pb and ^{212}Bi. The ^{228}Ra activity is equated with that of ^{228}Ac.

Using a ^{60}Co point source, the counting efficiency is determined at several points above the detector as a function of the distance to the end cap and the central vertical axis. From these data an efficiency curve is prepared. Numerical integration of this curve over the volume taken by the test sample results in a response factor in terms of counts per disintegration. From the relative efficiency curve of the detector, the counting efficiency of each detected gamma-ray peak is determined. Together with the energy-dependent absorption coefficients, extracted from a transmission measurement of the sample, a correction is made for self-absorption. The method is described in more detail by Noguchi *et al*. (1981). The reported standard deviations relate to the uncertainty introduced by the counting statistics and the calculation of the counting efficiency.

Comparison

The results of the routine described above (method I) are compared with the results of two alternative methods (Blaauw *et al*., 2001). In the first the density-dependent photo-peak efficiencies at the gamma-ray energies 352 keV (^{214}Pb), 911 keV (^{228}Ac), 583 keV (^{208}Tl) and 1461 keV (^{40}K), are deduced from the efficiency curves of four standard samples with certified amounts of ^{238}U, ^{232}Th and ^{40}K. Both standards and samples were analysed in the same Marinelli-beaker geometry. This method, in this chapter referred to as method II, is

described in more detail in NEN (2001a). Details on the second reference method are also published elsewhere (Blaauw *et al*., 2001). In this method a 15 cm cubic sample is rotated continuously during measurement in front of a side looking HPGe detector. The detector response for the above peak energies is deduced from the efficiency curve of a ^{152}Eu point source, positioned at where the test cube has its centre. An additional ^{152}Eu transmission measurement was performed to obtain absorption coefficients for the matrix material, from which the energy-dependent counting efficiencies for the sample geometry are computed. This method is referred to as method III. The comparison is done with one batch of concrete, from which three sub samples are prepared; each method has analysed the same three sub samples.

3.2.3 Results

The results of the comparison are presented in Table 3.5. The deviations between the various methods are limited as can be concluded from the values for r, the ratio of the result relative to that of the average of the three methods. On average the value of r amounts to 0.99, 1.02 and 1.00 for method I, II and III, respectively.

Table 3.5
Mean, standard deviation (SD) and standard error of the mean (SEM) of a sample of concrete analysed by three different methods for n=3 observations; r is the ratio of the result relative to that of the average of the three methods. See text for description of the applied methods. The results of method II and III are taken from Blaauw et al. (2001).

Nuclide	Method	Average ± SD (Bq kg^{-1})	SEM (%)	r (-)
^{226}Ra	I	21.7 ± 2.6	7.0	0.98
	II	22.8 ± 1.4	3.6	1.03
	III	21.7 ± 0.7	1.9	0.98
^{228}Th	I	14.4 ± 1.0	3.9	1.02
	II	13.5 ± 0.7	3.2	0.95
	III	14.6 ± 0.2	0.8	1.03
^{228}Ra	I	12.9 ± 2.2	9.9	0.93
	II	14.9 ± 0.9	3.6	1.08
	III	13.6 ± 0.2	0.9	0.99
^{40}K	I	151 ± 6	2.3	1.01
	II	150 ± 8	3.1	1.00
	III	149 ± 3	1.2	0.99

The results of the professional products are shown in Table 3.6. The alphabetical codes A-E indicate the five manufacturers, the successive numbers the various products. Some of these products were sampled again 12 months later, to investigate possible changes in composition over time. These results are not included. In general, the differences between the two series are less than 10%. In addition to gypsum for stuccowork, some calcium sulphate mortars, which are used as a screed, are incorporated in this study. The results for these samples, coded F1 and G1, indicate low radium levels, similar to those in natural gypsum.

Table 3.6
Mean and standard deviation of the activity concentrations of professional gypsum plasters in Bq kg^{-1}; the samples are obtained in the Netherlands.

Sample code	Description	^{226}Ra	^{228}Ra	^{228}Th
A1	Single-coat gypsum plaster	239 ± 4	237 ± 8	239 ± 13
A2	Plaster for floated surface	121 ± 3	111 ± 4	111 ± 7
A3	Plaster for mechanical application	6.7 ± 0.7	0.6 ± 0.6	1.6 ± 0.5
A4	Gypsum plaster	242 ± 4	228 ± 6	206 ± 11
A5	Bonding and finish plaster	234 ± 15	199 ± 13	163 ± 9
A6	Plaster for floated surface	121 ± 3	97 ± 4	107 ± 6
A7	Joint filler	< 3	< 3	< 2
A8	Bond plaster for floated surface	131 ± 3	132 ± 4	124 ± 7
A9	Gypsum bonding plaster	221 ± 4	217 ± 6	210 ± 10
A10	Joint filler	7.1 ± 0.6	1.6 ± 0.9	2.3 ± 0.8
B1	Gypsum plaster	12.9 ± 1.4	< 7	3.9 ± 1.0
B2	Moulding gypsum	10.1 ± 2.1	1.9 ± 0.6	2.1 ± 0.4
B3	Bonding and finish plaster	4.9 ± 1.0	< 5	< 3
B4	Plaster for mechanical application	11.2 ± 1.2	3.9 ± 1.8	< 4
C1	Moulding gypsum	3.1 ± 0.6	3.2 ± 0.9	2.3 ± 0.3
D1	Bonding plaster	224 ± 4	238 ± 6	243 ± 10
D2	Plaster for floated surface	121 ± 3	107 ± 6	108 ± 6
D3	Plaster for mechanical application	5.3 ± 1.1	< 6	< 4
E1	Plaster for mechanical application	2.8 ± 1.2	< 5	< 3
E2	Plaster for mechanical application	2.5 ± 1.0	< 6	3.2 ± 1.0
E3	Plaster for mechanical application	< 3	< 5	2.5 ± 0.8
F1	Calcium sulphate screed	4.9 ± 0.8	< 5	1.6 ± 0.9
G1	Calcium sulphate screed	4.6 ± 1.2	< 5	< 3

Three products (viz. A1, A3 and A9) were also obtained from Germany. The results are presented in Table 3.7. The samples with the codes A1(G) and A9(G) show low radium levels, contrary to the ‘same’ products available in the Netherlands (Table 3.6). The A3-coded samples show similar (low) levels. Some products are also available in retail

packages, meant for skilful do-it-yourself enthusiasts. The results of the gamma-ray analysis of these latter samples are shown in Table 3.8. If these are compared with the similar products for professional use (Table 3.6), then striking differences are observed for the samples coded A4, A8 and A9.

Table 3.7
Mean and standard deviation of the activity concentrations of professional gypsum plasters in Bq kg^{-1}; the samples are obtained in Germany.

Sample code	Description	^{226}Ra	^{228}Ra	^{228}Th
A1 (G)	Single coat gypsum plaster	2.8 ± 1.0	< 6	< 4
A3 (G)	Plaster for mechanical application	5.3 ± 0.8	< 6	< 3
A9 (G)	Gypsum bonding plaster	9.5 ± 1.0	< 8	< 4

Table 3.8
Mean and standard deviation of the activity concentrations of non-professional gypsum plasters in Bq kg^{-1}; the samples are obtained in the Netherlands.

Sample code	Description	^{226}Ra	^{228}Ra	^{228}Th
A4 (S)	Gypsum plaster	6.5 ± 1.1	< 6	1.5 ± 1.0
A8 (S)	Bond plaster for floated surface	9.2 ± 1.2	< 6	3.0 ± 0.9
A9 (S)	Gypsum bonding plaster	5.0 ± 0.9	< 8	3.1 ± 1.1
A10 (S)	Joint filler	4.0 ± 0.9	< 6	< 3
A11 (S)	Repair product (holes and cracks)	11.1 ± 1.0	< 8	1.5 ± 1.0

3.2.4 Discussion

For the determination of the natural radioactivity several methods are in use. In this chapter three of them have been compared. No differences could be observed between these methods, taking the uncertainties of the determinations into account. With one of these methods the natural activity concentrations in gypsum products are recorded. Based upon the results reported in the Tables 3.6 to 3.8, the materials can be subdivided into three categories:

- Gypsum products of low activity (i.e. around 10 Bq kg^{-1} or less per identified primordial radionuclide);
- Products having intermediate levels of 100-150 Bq kg^{-1} for each of these nuclides;
- Products with high activity concentrations ranging from 200 up to 250 Bq kg^{-1} for each of the nuclides.

Also, in earlier studies the rather broad range in activity concentrations has been mentioned (Ackers *et al*., 1985; Van Deynse *et al*., 1997). An activity concentration around 10 Bq kg^{-1} or less corresponds to those found in natural gypsum. The activity concentrations found in the other categories points to the use of phosphogypsum. Some of the materials contain almost pure gypsum, while others are mixed with large amounts of sand to create a certain surface effect. This might explain the levels in the intermediate category. It is remarkable that some corresponding products obtained in Germany have strongly different radioactivity levels. Also some of the retail products differ from the professional materials. It is clear that the manufacturer in question has at least two production lines, one using phosphosgypsum as base material, the other natural gypsum. The higher activity concentrations may have consequences for two distinct classes of individuals, namely inhabitants and stucco-workers. These will be discussed separately.

The indoor ^{222}Rn concentration in the Netherlands is low in comparison to other European countries (UNSCEAR, 2000). The building materials are identified as the major source (Stoop *et al*., 1998; Bader *et al*., 2009). Application of plasters with a 20-25 higher activity concentration than products based on natural gypsum will therefore increase the ^{222}Rn-source term in homes. However, in view of the thin layers of plasters in practice (i.e. 1-10 mm) compared to the total building mass of a house, it is unlikely that this material will seriously affect either the indoor ^{222}Rn concentration or the gamma dose rate (O'Brien *et al*., 1995; O'Brien, 1997).

Until now, only limited attention has been paid to the radon isotope from the thorium series, ^{220}Rn. Because of its short half-life of 55 s, it was thought that only building materials and infiltration of outside air accounted for indoor ^{220}Rn. However, Li *et al*. (1992) have shown that in certain houses, soil can be the predominant source. Since in the Netherlands most ^{222}Rn originates from the building materials, it is assumed that this applies to ^{220}Rn, too. As the diffusion length of ^{220}Rn in gypsum is in the order of 10 mm, only the surface layer of these materials is involved, which for most inner walls and ceilings mean the gypsum plaster decoration. Therefore, application of plaster layers high in ^{228}Ra and ^{228}Th may play an important role with regard to the indoor ^{220}Rn level.

The dose consequences are, however, hard to evaluate due to a lack of sufficient measurement data. The only data on ^{220}Rn in the Netherlands are reported by Hogeweg (1986a). In that study an equilibrium equivalent concentration (EEC) is reported of 0.4 Bq m^{-3}. Combining this figure with the current dose coefficient of 40 nSv per Bq h m^{-3} (UNSCEAR, 2000) and assuming an occupancy factor of 80%, the annual effective dose in the Netherlands due to ^{220}Rn is calculated at about 0.1 mSv. Whether plasters high in ^{228}Ra and ^{228}Th can seriously cause an elevation of this level, taking the retarding action of coatings and wallpaper into account, has to be verified in future research.

For flooring and stucco-workers the main source of exposure is the inhalation of dust particles during mixing and processing. Besides the radionuclide contents of the material, the individual working practice plays a prominent part in the resulting radiation exposure. To investigate whether radiological precautions may be required, some dose assessments have been made. The applied assumptions are (a) continuous exposure conditions according to ICRP (1994); (b) no respiratory protection; (c) activity concentrations at the maximum reported level of 250 Bq kg^{-1} of all radionuclides in both series; and (d) an activity median aerodynamic diameter (AMAD) of 5 μm. Further assumptions are:

- Per radionuclide the most restrictive EU dose coefficient is applied (EC, 1996), in general associated with a slow lung clearance;
- A maximum allowed time-weighted average airborne respirable dust concentration of 5 mg m^{-3} (SZW, 1997);
- A working time of 8 h per day, 5 days a week during 45 weeks per year.

Given these assumptions, a maximal effective dose of about 200 μSv per year can be derived, suggesting that the radiation exposure of stucco-workers remains in all cases well below the prevailing dose limit of 1 mSv per year (EC, 1996). In an additional study the dust exposure of 25 stucco-workers has been determined in practice with personal air samplers. The results show an arrhythmic mean of the respirable fraction of 12.5 mg per working day, with a range of 1 to 40 mg per day (De Jong *et al*., 1998b). This broad range points to the large differences in the individual working practice. The radiation dose in that study is calculated at an average of about 45 μSv per year with a maximum value of 100 μSv per year.

3.3

The radiation dose in a small new housing estate[14]

3.3.1 Introduction

As outlined in numerous studies, ^{222}Rn concentrations depend on the type of rock or soil underlying the dwelling and several housing characteristics, like type of house, floor type, year of construction, the building materials applied and the type of foundation (Buchli and Burkart, 1989; Gunby *et al*, 1993; Verger *et al*., 1994; Keller *et al*., 1996; Lévesque *et al*., 1997). Furthermore, seasonal variations in indoor ^{222}Rn levels are well documented (Majborn, 1992; Arvela, 1995; Pinel *et al*., 1995). Statistical analysis of collected ^{222}Rn data has revealed a highly significant influence for a number of these and some other factors. However, all in all they account for only 28% or less of the total variability between dwellings (Gunby *et al*, 1993; Verger *et al*., 1994; Lévesque *et al*., 1997).

In the present survey we examined whether the design of the dwellings might be an additional factor. Therefore, a survey was done in a new housing estate, where nine different designs had been realised. Since all dwellings were built over the same period of time and all have the same underlying soil, the number of variables affecting the ^{222}Rn concentration is more restricted than in other studies. Also, the absorbed dose rate in air was recorded to estimate the total annual indoor effective dose.

3.3.2 Materials and methods

Housing estate

The housing estate, with a total surface area of about 150 x 400 m^2, is located in Alphen a/d Rijn, a small town in the western part of the Netherlands. The objective of this pilot project was to show that it is possible to construct houses in such a way that the environmental aspects are improved. Nine architects worked along the three main lines of the Dutch National Environmental Policy Plan, i.e. reduction of energy consumption, integral chain control and quality improvement. Table 3.9 summarizes the main features of each design A to I.

---

[14] This chapter is based on a presentation at the International Symposium on Radon in the Living Environment, 19-23 April, 1999, Athens, Greece and incorporated in the proceedings, pp 911-919, entitled *Factors affecting the radiation dose to inhabitants in a small new housing-esate in the Netherlands*. Authors: P. de Jong and W. van Dijk. Results are published in The Science of the Total Environment 272: 141-142 (2001).

Table 3.9
Some characteristics of the different designs.

ID	Ground floor	Other floors	Walls	
			Supporting	**Non-supporting**
A	concrete	concrete	sand-lime brick	gypsum block
B	concrete	wood/gypsum board	wood/gypsum board	wood/gypsum board
C	aer. concrete[a]	aerated concrete	sand-lime brick	glass
D	concrete	wood/gypsum board	wood/gypsum board	wood/gypsum board
E	concrete	wood/gypsum board	sand-lime brick	gypsum block
F	concrete	concrete	sand-lime brick	wood/gypsum board
G	concrete	concrete	sand-lime brick	gypsum block
H	concrete	concrete	sand-lime brick	gypsum block
I	clay brick	wood	sand-lime brick	wood/gypsum board

[a] Aerated concrete.

All homes are of the single-family type, provided with a crawl space. Only design C has a basement, half-below ground, instead. Some general measures were taken to reduce the ^{222}Rn concentration in the dwellings. The most important of these were:

(a) improved ventilation of the crawl space by means of at least two gratings in fore and back front;
(b) air-tight construction of the trapdoor to the crawl space; and
(c) application of a gypsum screed on the ground floor, to reduce the air ingress from the crawl space.

Determination of the absorbed dose rate in air

The dose rate was determined by thermoluminescence (TL) dosimetry. Each dosemeter contained four selected TL detectors (3x3x0.9 mm^3) of lithium fluoride (TLD-100, Harshaw), with individually determined response factors. The dosemeters were placed in three dwellings of each design in the crawl space, the living room and a first-floor bedroom. The standard height in the crawl space was 30 cm above the soil. In the living room the dosemeters were located as centrally as possible. In most cases they were attached to the dining table at about 80 cm above the floor. In the bedrooms the height ranged between about 1.5–2.5 m. For the outdoor measurements the dosemeters were placed in a (well-ventilated) nesting cage at 100 cm above the soil surface. The exposure time was 384–389 days. The results were corrected for a period of one year.

During this period 23 comparable reference dosemeters were stored in a low background facility in the laboratory. At ten moments, distributed equally over the exposure period, each time two of these dosemeters were exposed once to gamma radiation from a ^{60}Co source to 2.50 mSv. The remaining three dosemeters were not irradiated and served as controls in the evaluation.

All dosemeters, including the calibration and control dosemeters, were evaluated on the same day using a hot gas reader (Van Dijk and Julius, 1993). From the results a calibration factor was derived of 1.30 ± 0.08 counts per μGy (n=10). As indicated above, the results of each location (dosemeter) were made up of four independent results. Based on the 80 evaluated dose meters, the average variation fraction was 2.4%, with a range of 0.8–6.0%.

Radon measurements

The time-weighted average ^{222}Rn concentration was determined in the same rooms and during the same period as indicated above for the TL dosemeters. For the measurements passive track-etched detectors were used of the type described by Urban and Piesch (1981). These devices contain a polycarbonate track etch foil (Makrofol). Except for the living room, the ^{222}Rn dosemeters were positioned in the same place as the TL dose meters. In general, the ^{222}Rn cup in the living room was placed in or on a cupboard, as far as possible from the wall.

After exposure the foils were pre-etched and electrochemically etched according to the method described by Urban and Piesch (1981). The accuracy of the results was deduced from ten duplicate measurements (annual average ^{222}Rn concentration 2 to 60 Bq m^{-3}) and was found to be 16% on average, with a range from 0 to 30%. The ^{222}Rn analysis was performed by KVI (Groningen, the Netherlands).

Soil analysis

Soil samples were taken from six different locations. Three of these (locations 1-3) are situated in the housing estate proper. At each location two samples were taken, i.e. from the surface (A-samples) and at ground water level (B-samples). The other three locations (locations 4-6) are outside the housing estate and represent the original soil. From these locations only the surface layer was sampled. One litre of sample material was analysed according to method I described in section 3.2.

Dose calculations

From the ^{222}Rn concentrations and absorbed dose rates in air, the resulting annual effective dose was calculated. The living room and bedroom averages were combined using a weight of 0.39 for the bedroom value and 0.61 for the living area, to reflect the occupancy pattern of a housewife (ICRP, 1994). The time spent indoors is taken as 7000 h per year, an occupancy factor of 80%. In the assessment of the indoor radiation burden due to ^{222}Rn, furthermore an equilibrium factor of 0.4 and a dose coefficient of 9 nSv (Bq h m^{-3})$^{-1}$ were retained (UNSCEAR, 2000). As a conversion coefficient from absorbed gamma dose in air to effective dose, a value of 0.7 Sv Gy^{-1} was adopted (UNSCEAR, 1993).

Table 3.10
Absorbed dose rates in air in nGy h^{-1} for crawl space, living room and bedroom per design (mean ± SD, n=3 dwellings).

Design	Crawl space	Living room	Bedroom
A	70 ± 1	59 ± 2	67 ± 3
B	80 ± 1	68 ± 7	73 ± 10
C	78 ± 2 [a]	75 ± 4	66 ± 3
D	76 ± 1	58 ± 1	57 ± 2
E	85± 4	81 ± 8	82 ± 6
F	78 ± 4	68 ± 3	65 ± 4
G	72 ± 3	62 ± 3	74 ± 5
H	71 ± 1	69 ± 4	73 ± 3
I	90 ± 1	73 ± 2	76 ± 5
All	77 ± 7	68 ± 9	70 ± 9

[a] Basement, half below ground.

3.3.3 Results

The average results per design pertaining to the TL dosemeters are compiled in Table 3.10. The average absorbed dose rates for the living room and the bedroom range from about 60 to 80 nGy h^{-1}. Slightly higher values are found in the crawl spaces (range 70–90 nGy h^{-1}). For the outdoor absorbed dose rate a value was found of 68 ± 4 nGy h^{-1} (mean ± SD, n=3 locations), which is the same as the values for living room and bedroom averaged over all houses (see Table 3.10). Table 3.11 shows the results of the collected ^{222}Rn data.

Table 3.11
Annual average ^{222}Rn concentrations in Bq m^{-3} for crawl space, living room and bedroom per design (mean ± SD, n=3 dwellings).

Design	Crawl space	Living room	Bedroom
A	28 ± 5	17 ± 9	11 ± 6
B	17 ± 6	4.0 ± 1.5	3 ± 3
C	44 ± 16 [a]	23 ± 10	12 ± 2
D	57 ± 2	8 ± 4	2.2 ± 0.8
E	7 ± 3	49 ± 9	25 ± 15
F	19 ± 3	14 ± 5	14 ± 3
G	17 ± 1	16 ± 14	10 ± 3
H	11 ± 2	14 ± 14	12 ± 6
I	8 ± 2	10.6 ± 1.8	20 ± 12
All	21 ± 16	17 ± 15	11 ± 9

[a] Basement, half below ground.

Depending on the design, the average ^{222}Rn concentrations in the living rooms range from 4 to 50 Bq m^{-3}, with a mean value of 17 Bq m^{-3}. The concentrations at the low end of this range are close to the outdoor level of 3.3 ± 0.6 Bq m^{-3} (mean ± SD, n=6 locations). In general, the ^{222}Rn concentrations in the (first-floor) bedroom were lower than in the living room. In this study a ratio between the two rooms was found of about 0.7 on average. This value is somewhat lower than found in the 1995 national survey on newly built dwellings of 0.9 (Stoop *et al*., 1998).

Figure 3.5 shows the results of the calculated indoor effective dose to inhabitants due to inhalation of short-lived ^{222}Rn progeny and the indoor gamma radiation levels. The annual effective dose ranges from 0.4 to 1.4 mSv, depending on the design. In most designs the internal and external radiation exposure are of equal magnitude; on average the ^{222}Rn induced component accounts for about 53% of the total radiation burden.

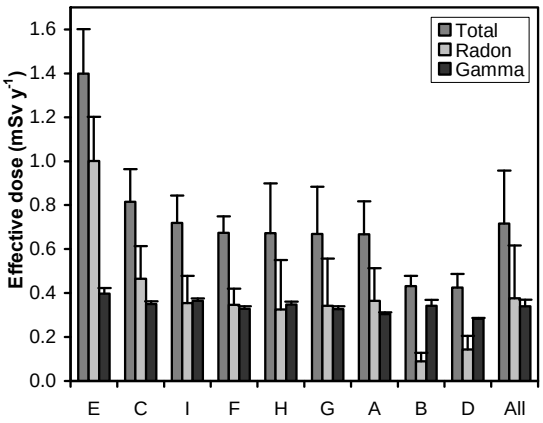

Figure 3.5
Calculated indoor effective dose per design.

The low crawl space levels are in agreement with the low ^{226}Ra concentrations of the stabilizing sand layer. As determined by gamma-ray spectrometry, the level ranges from 5 to 10 Bq per kg, which is about a factor of three lower than the original clayey soil (Table 3.12). Both levels are typical for the soils in question (Köster *et al*., 1988). In design D a higher crawl space level (57 ± 2 Bq m^{-3}, n=3 houses, Table 3.11) was established, which appeared to be caused by stopped ventilation gratings in the crawl spaces of all three dwellings.

Table 3.12
Specific activities of soil samples in Bq per kg dry weight (mean ± SD).

Loc.[a]	code	Depth (cm)	Soil	^{226}Ra	^{232}Th	^{40}K
1	1A	10-20	sand	7.0 ± 0.8	11.2 ± 0.8	320 ± 10
	1B	100-110	sand	5.1 ± 0.7	8.6 ± 0.8	291 ± 8
2	2A	10-25	sand	7.3 ± 0.8	10.5 ± 0.8	295 ± 9
	2B	105-115	sand	9.5 ± 0.8	11.7 ± 0.8	294 ± 9
3	3A	10-25	sand	9.6 ± 0.8	12.0 ± 0.8	350 ± 10
	3B	90	sand	11.1 ± 0.9	11.7 ± 0.9	390 ± 10
4	4A	10-20	clay	32 ± 2	38 ± 2	480 ± 20
5	5A	10-20	clay	25 ± 2	29 ± 3	350 ± 20
6	6A	10-20	clay	13 ± 2	27 ± 3	320 ± 20

[a] Locations 1 to 3 within and 4 to 6 outside the building estate.

3.3.4 Discussion

As indicated in the previous section the ^{222}Rn crawl space concentrations in this housing estate are low, even to Dutch standards. The 1995 national survey on ^{222}Rn in 1500 dwellings built in the period 1985 - 1993, revealed an average value for this space of 70 Bq per m^3 (Stoop *et al*., 1998). The replacement of about 1 m of the original soil by sand of a low specific ^{226}Ra activity, in combination with a relatively high ground water level, is undoubtedly an important reason for this finding. Moreover, to reduce the crawl space concentration, extra ventilation gratings have been applied in the outer walls of all dwellings (see chapter 3.3.2). The net area of these gratings correlated well with the crawl space concentration ($r = -0.85$, $p<0.01$).

In the national survey the crawl space concentration is reported to be significantly correlated with the ^{222}Rn level in the living room (Stoop *et al*., 1998). In the present study, however, no such correlation could be demonstrated. The highest crawl space concentration is found in design D, while the ^{222}Rn concentrations in the living areas were actually among to the lowest in this study. Also, the opposite was encountered: in design E the crawl space concentration was close to the outdoor concentration, but the ^{222}Rn levels in the living room and the bedroom were the highest in this survey. The most likely explanation is that in the present housing estate special measures have been taken to reduce the ingress of air from the crawl space and with that the influence on the indoor ^{222}Rn concentrations in the living areas.

Since the building materials are the major source of ^{222}Rn in this study, some relation is expected between the indoor ^{222}Rn level and the gamma dose rate. The correlation coefficients were 0.52 and 0.58 for the living room and bedroom, respectively ($p<0.01$). A similar relation was reported by Leung *et al*. (1998) in high-rise buildings, where the

building materials were likewise the predominant source of ^{222}Rn. In considering the effects of building material, the type of material together with the surface area occupied per dwelling were incorporated into a statistical analysis. However, no apparent correlation with either the ^{222}Rn concentration or the absorbed dose rate could be demonstrated.

The annual indoor effective dose varies in this study from 0.4 to 1.4 mSv a^{-1}, depending on the design. The lowest doses are encountered in lightweight constructions based on a timber frame construction with an airtight concrete ground floor, with the remaining floors made of timber and with flue gas desulphurization gypsum inner walls (i.e. designs B and D). Also, designs constructed according to a corresponding 'conventional' building style (concrete floors, cavity walls made of clay brick and sand-lime brick) show almost equal average ^{222}Rn levels and absorbed dose rates in both living room and bedroom (i.e. designs A, G, H and F). The design with the highest radiation burden (design E) is characterised by a higher-than-average surface-to-volume ratio, together with the use of phosphogypsum.

Finally, a statistical analysis is performed to discriminate between the occupants' and the design-related impact on the annual effective dose. This is done by an analysis of variance. In doing so, the variance *within* the designs is considered as a measure for the occupants' behaviour. The variance *between* the designs was significantly higher at the level $p<0.01$. These results indicate that – at least in this housing estate – the design has a more pronounced influence on the radiation burden than the inhabitants' behaviour. A similar conclusion can be drawn from the study performed by Lomas and Green (1994), who found that it did not seem to matter much that a dwelling had changed hands.

3.3.5 Conclusion

This survey has shown that the design is an important factor in relation to the annual effective dose and that it has a more apparent influence than the habits and preferences of its occupants. It also shows that it is possible to construct houses in such a way that the radiation burden resembles outdoor levels.

3.4

Calculation of the indoor gamma dose rate distribution[15]

3.4.1 Introduction

In many countries national measuring campaigns are organized to determine the indoor absorbed dose rate in air (UNSCEAR, 2000). In general, these campaigns are performed either using electronic devices or by a passive measuring technique, i.e. thermoluminescence dosimetry. As described in section 1.8 both techniques are applied in the Netherlands, which have resulted in a range from 50–170 nGy h^{-1} with about 83 nGy h^{-1} as a central estimate. The major part originates from the construction materials of the dwelling, with smaller contributions from cosmic and terrestrial radiation. In section 2.3 a model is described that is based on the absorbed dose rates in a standard construction as defined by Koblinger (1978). To allow for alternative geometries and/or construction materials, various correction factors were derived and expressed as polynomials of relevant housing and building material parameters

In this section the model is applied to a representative set of Dutch dwellings to determine the distribution of the building material induced absorbed dose rate. For that purpose a Monte Carlo method (Cox and Harris, 2006) is used that folds the distributions of the various building materials with those of the activity concentrations reported in section 3.1. This method has the advantage above the classical approach for the propagation of uncertainties that the experimentally observed distributions of the inputs of the model can be used. The method is valid for any distribution and not only for (almost) symmetrical ones. It also copes with dependency of input quantities. The output is the probability distribution of the absorbed dose rate from which the mean, standard deviation and confidence intervals can easily be obtained. Besides, direct insight is gained on the shape of the resulting distribution. The results were compared with those found in measuring campaigns on the indoor dose rate. Since in these campaigns the absorbed dose rates are determined in living rooms only, also the model calculations have been restricted to this room. The model calculation involves various correction factors that together cover most practical situations. To verify the consequences of each of these factors a sensitivity analysis is incorporated.

[15] This chapter is based on a paper published in Radiation Protection Dosimetry 132: 381-389 (2008), entitled *Calculation of the indoor gamma dose rate distribution due to building materials in the Netherlands*. Authors: P. de Jong and J.W.E. van Dijk.

3.4.2 Materials and methods

Building material data

Based on the results of a survey on the activity concentrations of the most commonly used stony building materials in the Netherlands (section 3.1), the so-called dose factor F_{dose} was calculated for each analysed sample according to:

$$F_{dose} = k_1 a_1 (1 - F_{Rn}) + k_2 a_2 + k_3 a_3 . \qquad (3.7)$$

In this formula k_1, k_2 en k_3 are the specific absorbed dose rates in nGy h^{-1} per Bq kg^{-1} for the ^{238}U series, ^{232}Th series and ^{40}K, respectively; and a_1, a_2 and a_3 the corresponding activity concentrations in Bq kg^{-1}. F_{Rn} is defined as the ratio between the released amount of ^{222}Rn and the amount produced within the building material per unit of time (see eq. 3.2). As mentioned in section 2.3 for k_1 to k_3 the values 0.90, 1.10 and 0.080 nGy h^{-1} per Bq kg^{-1} have been applied, the rounded means from literature data and own calculations (see Table 2.7). For each analysed sample in section 3.1 these values were combined with their activity concentrations and their ^{222}Rn release factor F_{Rn}. Table 2.8 summarizes the resulting dose factors F_{dose} to be used in this section. Besides the specific data on F_{dose} also the density of each sample is used as an input for the model calculations. A compilation of these data is given in Table 3.1.

Housing data

Stoop and colleagues (1998) have made an inventory of the building materials applied in Dutch living rooms. From the available questionnaires 70 were left out due to the absence of one or more data. From the remaining 1336 dwellings the relative area taken by the main stony building materials was determined. In Table 3.13 the data are summarized per construction element and per type of material. The summed relative area amounts to 90%; the remaining 10% is taken by doors and windows.

The composition of the construction was deduced from the living room data by assuming that the area taken by the non-bearing inner walls can be neglected. In the Netherlands lightweight materials as gypsum blocks or boards are predominantly used for this purpose (Table 3.13). As shown in Table 2.8 this material is characterized by a low dose factor and will hardly contribute to the absorbed dose rate. In section 3.1 the contribution of the gypsum non-bearing inner walls to the overall absorbed dose rate is estimated to be as low as 0.4%. Omitting the contribution from these walls therefore will have no serious consequences.

Table 3.13
Relative areas of Dutch living rooms by class of building material and by construction element, together with the typical thickness in practice of each construction element (in m).

Material class	Floor	Ceiling	Outer walls		Inner walls		Sum[a]
			Outer leaf	Inner leaf	Bearing	Non-bearing	
Concrete	0.23	0.21	0.01	0.03	0.09	0.00	0.57
Sand-lime brick	-	-	0.01	0.09	0.04	0.01	0.13
Gypsum	-	-	-	0.01	-	0.10	0.11
Clay bricks	-	-	0.15	0.01	0.01	-	0.01
Aerated concrete	-	-	-	-	-	0.01	0.01
Others/ combinations	0.00	0.01	0.01	0.01	0.00	0.01	0.03
Unknown	-	-	-	0.01	0.01	0.00	0.03
Not applicable	-	0.00	-	0.00	0.00	0.00	0.00
Sum	0.23	0.22	0.17	0.17	0.16	0.13	0.90[b]
SD	0.02	0.04	0.06	0.06	0.06	0.06	0.02
Thickness (m)	0.20	0.20	0.10	0.10	0.24	0.10	

[a] Sum excluding outer leaf.
[b] Remaining 10% taken by doors and windows.

Application of our dose model

In this section we will apply our model, described in section 2.3, to a selection of living rooms. In that section correction factors were deduced for situations that deviate from the original Koblinger-geometry. The building material related absorbed dose rate in air in a specific living room is computed according to:

$$\dot{D} = \left\{ \sum_{i=1}^{6} \left[F_{dose} \cdot F_{constr} \cdot F_{dimens} \cdot F_{leave} \cdot F_{do/wi} \right]_i \right\} F_{zoning} \cdot F_{adjac} \quad (3.8)$$

in which i is the index of a construction element of the considered storey of the dwelling (floor, ceiling and each of the four walls) and F_{dose} the above-mentioned dose factor as defined in eq. (3.7). Other correction factors are:

- F_{constr} : accounts for thickness and density of a construction element;
- F_{dimens} : takes the dimensions of a construction elements into consideration;
- F_{leaf} : accounts for the gamma-ray attenuation by the inner leaf;
- $F_{do/wi}$: compensates for the presence of doors and windows;
- F_{zoning} : estimate for shielding by the non-bearing inner walls;
- F_{adjac} : correction factor for a contribution of other storeys and/or adjacent houses.

For details we refer to section 2.3. An example of a calculation is given in an Appendix to this section.

Assessing the dose rate distribution

To obtain the distribution in dose rate according to the model of eq. (3.8), the convolution integral of the distributions of the various input quantities of this model must be evaluated. The convolution integral is calculated using Monte Carlo integration following the recommendations in supplement 1 to the GUM, the Guide to the Expression of Uncertainty in Measurement (JCGM, 2008). The calculation essentially consists of M repetitions, e.g. $M=10^5$, of the following steps:

(a) Using a uniform random generator select one of the 1336 dwellings. This defines all (relative) areas and type of materials used, together with the areas taken by doors and windows per construction element and a code for the type of house (i.e. detached house, end house, ...);
(b) From each material randomly select a sample and use the measured properties for dose factor and density;
(c) Determine the various correction factors;
(d) Calculate the dose rate in the living room of the *j*-th sampled dwelling.

From the distribution of these dose rates, the parameters mean, standard deviation (SD), median and first and third quartile are easily obtained (JCGM, 2008).

Sensitivity analysis

The calculation of the absorbed dose rate in a dwelling involves a combination of correction factors that together cover most practical situations. To ascertain the influence of each factor a sensitivity analysis is done. In the first place the median values of each correction factor are determined per construction element, using the above given input data and Monte Carlo method. Secondly, the separate effect of each correction factor on the median absorbed dose rate is verified. The results are compared with the median absorbed dose rate that is obtained if none of the aforementioned corrections are applied. Also in this case the same input data and Monte Carlo method were used. The analysis is based on median values, since this parameter is less sensitive for outliers. However, a comparable ranking is obtained when the means are taken for the evaluation instead

.

Table 3.14
Some characteristics of the indoor dose rate in Dutch living rooms as found by the proposed model and a measuring campaign in nGy h^{-1}.

Parameter	This study		Ionization chamber[b]
	Without correction[a]	With correction[a]	
Mean ± SD	51 ± 6	79 ± 10	83 ± 12
Median	51	79	82
25/75 percentile	48 / 55	72 / 85	74 / 91
Range	19 – 81	38 – 120	52 – 117
Number of houses	1336	1336	399

[a] With and without correction for cosmic and terrestrial radiation.
[b] Calculated from measuring data in Julius and Van Dongen (1985b).

3.4.3 Results

When the results are taken from 10^5 repeated calculations, an average and median value of the building material-induced absorbed dose rate in the living rooms is obtained as 51.4 and 51.5 nGy h^{-1}, respectively. Since these values are very similar, it indicates that the distribution is near Gaussian. In Table 3.14 some other statistical indicators are given; the probability density function and the cumulative distribution are drawn in Figure 3.6.

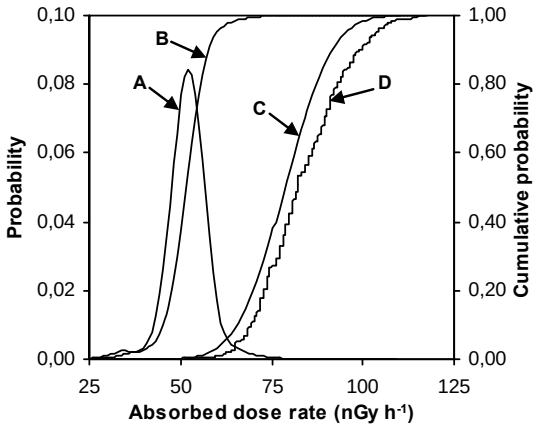

Figure 3.6
Probability density function (A) and cumulative distributions (B to D) of the absorbed dose rate in air in Dutch living rooms: (A,B) building material induced contribution as modelled; (C) as corrected for terrestrial and cosmic radiations and (D) measured by a high pressure ionization chamber.

Table 3.15 shows the correction factors as computed by the Monte Carlo code. In this table the dose correction factor, F_{dose}, and the area correction factor, F_{dimens}, are normalized to make their results better comparable with the other correction factors; now for all factors a value of 1 indicates that the factor has no influence, and has a larger effect the more it deviates from 1.

Table 3.15
Median values and mean absolute deviation of the various correction factors by construction element as met in the calculation of the building materials induced dose rate distribution.

Correction factor	Floor	Ceiling	Outer walls		Bearing inner walls
			Outer leaves	Inner leaves	
F_{dose}/F_{dose}' [a]	0.93 ± 0.03	0.93 ± 0.03	1.00 ± 0.00	0.98 ± 0.01	0.97 ± 0.03
F_{constr}	1.00 ± 0.01	1.00 ± 0.01	0.56 ± 0.07	0.62 ± 0.03	1.04 ± 0.02
F_{dimens}/A_i^{rel}	1.24 ± 0.01	1.24 ± 0.02	0.74 ± 0.09	0.74 ± 0.09	0.74 ± 0.15
F_{leaf}	1.00 ± 0.00	1.00 ± 0.00	0.52 ± 0.02	1.00 ± 0.00	1.00 ± 0.00
$F_{do/wi}$	1.00 ± 0.00	1.00 ± 0.00	0.69 ± 0.08	0.69 ± 0.08	1.00 ± 0.00
F_{zoning}	0.96 ± 0.02				
F_{adjac}	1.07 ± 0.05				

[a] Ratio of F_{dose} with and without correction for ^{222}Rn exhalation.

The overall significance of each correction factor cannot be deduced from Table 3.15, since the area size and the activity concentrations of the construction elements are contributory. In Table 3.16 the results are given for the situation that each correction factor is tested separately. F_{constr}, the correction factor for density and thickness of construction elements is found to be most significant, while the correction for ^{222}Rn exhalation has the lowest effect.

Table 3.16
Ranking of the correction factors according to their effect on the median absorbed dose rate, when tested individually. The situation that no corrections are applied is taken as reference.

Included correction	Parameter involved	Median (nGy/h)	Difference (%)
No corrections	None	86	0
^{222}Rn exhalation	F_{dose}	83	-3
Attenuation inner walls	F_{zoning}	82	-5
Area size	F_{dimens}	79	-8
Adjacent rooms	F_{adjac}	93	+9
Attenuation inner leaf	F_{leaf}	71	-18
Doors and windows	$F_{do/wi}$	69	-20
Density and thickness	F_{constr}	67	-22
All corrections	All	51	-41

3.4.4 Discussion

Based on the information on the occurrence of building materials in 1336 living rooms and the analytical results of 90 samples of building material, the distribution of the absorbed dose rates in Dutch livings due to building materials is assessed. For that purpose a Monte Carlo method is used. One of the advantages of this method is that the experimentally observed distributions of the inputs of the model are used and that other pitfalls such as dependency of inputs are avoided. The result is a near-Gaussian distribution with an average value of 51 nGy h^{-1} and a standard deviation of 6 nGy h^{-1}. To calculate the resulting effective dose to an inhabitant, it is necessary to have knowledge of the absorbed dose rates in other rooms, especially those in bedrooms. However, the absorbed dose rates in bedrooms in the Netherlands are reported to be essentially the same as those in living rooms (section 3.3); the building material-induced effective dose to an inhabitant can therefore be based on the data from the living rooms. For the conversion from absorbed dose to effective dose a value of 0.7 Sv Gy^{-1} is adopted from UNSCEAR (2000). If the time spent indoors is taken as 7000 h per year (80% of total), the annual effective dose due to building materials comes to 0.25 ± 0.03 mSv.

For the comparison of the model results with measured data, several nationwide surveys are available as reviewed in Table 1.7. The difference between the mean values of the ionization chamber data and the modelling is 32 nGy h^{-1} (Table 3.14). The reason for this difference is that the modelled values relate to the applied building materials only, while the measured data also include a contribution from the outdoor components, i.e. cosmic and terrestrial radiation. Besides assessing the dose rate with the aid of an ionization chamber, Julius and Van Dongen (1985b) additionally used a gamma-ray spectrometer to discriminate between both components. From these results the average contribution of both outdoor components together in the Netherlands is calculated at 28 nGy h^{-1}. In calculating this value, several indoor and outdoor measuring data have to be combined that are not independent from each other. The propagation of the successive uncertainties therefore has to take the various covariances into consideration. These, however, are not known. An estimate of the standard deviation comes to 8 nGy h^{-1}.

In Figure 3.6 and Table 3.14 the modelled results of the building material-induced absorbed dose rate are corrected for the outdoor components. The difference between the corrected model values and the results of the measuring campaigns is about -5%. This percentage is close to that found in an earlier study (-4%) in which the outcomes of the present model on three different types of reference dwellings were compared with those of the Monte Carlo code MCNP (see section 2.3).

In the model various correction factors are applied to correct for situations that deviate from the standard Koblinger-geometry with respect to:
(a) the effect of ^{222}Rn exhalation;
(b) the surface densities of the construction elements;
(c) size of the construction;
(d) the presence of inner leaves, doors, windows, and internal partition walls; and
(e) the contribution from adjacent floors and dwellings.

In Table 3.15 an overview is given of the magnitude of each factor per construction element as emerged from the determination of the absorbed dose distribution in this study. Even within a same correction factor the values may vary widely from one construction element to another. Reasons for this are the differences in the release of ^{222}Rn (F_{dose}), density and/or thickness (F_{constr}), relative area of the construction element in question (F_{dimens}) or whether the correction factor is applicable to the construction element or not (F_{leaf}, $F_{do/wi}$). Also the uncertainty in the median result within a correction factor fluctuates from construction element to construction element. The mean absolute deviation (MAD) of for instance F_{constr} is 0.01 for floor and ceiling, while a value of 0.07 is obtained for the outer leaf. This reflects the (in)homogeneity of the surface density of the respective construction elements within the housing data set.

The overall effect of each correction factor is closely connected to the relative area and the activity concentrations of the successive construction elements. The role of each correction factor was therefore examined individually in a separate Monte Carlo analysis. As shown in Table 3.16 correction for density and thickness, the presence of doors and windows and attenuation by the inner leaf are identified as the main inputs of the model, given the considered (Dutch) housing stock. If the sum of the separated effects of these three corrections is taken, a value is obtained that is larger than for the situation that all corrections together are included. This indicates the interrelation of the correction factors.

Correction of the construction elements for density and thickness is widely applied, amongst others by Koblinger (1978), Stranden (1979) and Mustonen (1984) and is sometimes combined with a correction for the presence of doors and windows (Ahmad *et al*., 1998; Ademola and Farai, 2005) or the dimensions of the room (Risica *et al*., 2001; Máduar and Hiromoto, 2004). For a discussion of the various correction factor findings is referred to section 2.3. Although application of correction factors is common practice in this field, a working party of the Article 31 group of experts omitted this in their suggested model on the regulatory control of building materials with regard to the natural radioactivity concentrations (EC, 1999b). The reason for this is probably to keep the calculation as simple as possible, but has the drawback of a severe overestimation of the building

material induced dose rates; according to the data presented in Table 3.16 this amounts to 40 percent for an average Dutch situation.

3.4.5 Conclusions

Between the model calculations and the results found in measuring campaigns only marginal differences are noted of not more than 5%. The present study shows that this model is well suited for the evaluation of large clusters of dwellings. The specific absorbed dose rate in a room is mostly influenced by the thickness and density of the various construction elements, a correction that is generally employed. Less established correction factors that nevertheless also have a high impact are the correction for doors and windows and the attenuation by the inner leaf.

Appendix

As an example Figure 3.7 shows a plan of the first floor of a standard Dutch row house for which a detailed calculation of the absorbed dose rate in the living room is presented. Table 3.17 outlines the assumed material and density of each first-floor construction element, its area and the area taken by doors and windows in that element. In Table 3.18 the various correction factors are computed using the polynomial coefficients from section 2.3, based on the input data from Table 3.17. Per construction element the product is taken of the correction factors and the obtained absorbed dose rates are summed according to eq. (3.8). Thus for the first floor, without internal partition walls, an absorbed dose rate is obtained of 47.7 nGy h^{-1}.

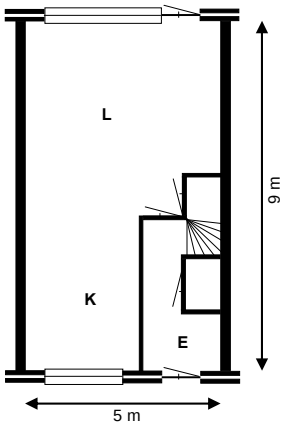

Figure 3.7
Plan of the first floor of the modelled three-floors row house, with entrance (E) and living room (L), which includes an open kitchen (K). The bedrooms are at the second floor and the third floor is the attic. The height is 2.5 m per floor.

In this example, the calculation is focussed on the dose rate in the living room. Therefore, a correction for the attenuation by the non-bearing inner walls at the first floor is taken into account. The total area of these walls in the living room is 18 m^2 (Table 3.17) at a total area of the living room of 141 m^2. The surface density of the hypothetical wall that shields the total area of the living room, including floor and ceiling is then according to eq. (2.16): 0.1 m x 900 kg m^{-3} x 18/141 = 11.5 kg m^{-2}, on the basis of which the value for F_{zoning} can be established as 0.96.

For computing F_{adjac}, the correction factor for the contribution from the other floors of the house and that of adjacent houses, the average of the surface densities of the ceiling and bearing walls are taken as input variable, i.e. (475+444)/2 = 460 kg m^{-2}. For a row house this results in a correction factor of 1.13. Multiplication of the previous result with these two last correction factors gives 51.8 nGy h^{-1} for the material induced absorbed dose rate in the living room.

Table 3.17
Assumed material and areas of the construction given in Figure 3.7.

Construction element	**Material**	**Density** (kg m^{-3})	**Thickness** (m)	**Area**[a] (m^2)	**Relative area** (--)	**Area do/wi** (m^2)
Floor	Concrete	2375	0.20	45.0	0.28	0.0
Ceiling	Concrete	2375	0.20	45.0	0.28	0.0
Outer leaf front	Brick	1750	0.10	12.5	0.08	4.8
Inner leaf front	Sand-lime	1850	0.10	12.5	0.08	4.8
Outer leaf back	Brick	1750	0.10	12.5	0.08	5.0
Inner leaf back	Sand-lime	1850	0.10	12.5	0.08	5.0
Bearing inner wall left	Sand-lime	1850	0.24	22.5	0.14	0.0
Bearing inner wall right	Sand-lime	1850	0.24	22.5	0.14	0.0
Sum[b]				160	1.00	9.8
Non-bearing walls[c]	Gypsum	900	0.10	18.0		

[a] Including doors and windows.
[b] Excluding outer cavity walls.
[c] Living room only. Total area living room 141 m^2.

Table 3.18
Calculated correction factors and absorbed dose rates for the living room in the row house given in Figure 3.7. In this example F_{dose} is taken equal to the mean values reported in Table 2.8.

Construction element	**Surface density (kg m^{-2})**	**F_{dose} (nGy h^{-1})**	**F_{constr} (--)**	**F_{dimens} (--)**	**F_{leaf} (--)**	**$F_{do/wi}$ (--)**	**Dose rate (nGy h^{-1})**
Floor	475	51	1.01	0.35	1.00	1.00	18.1
Ceiling	475	51	1.01	0.35	1.00	1.00	18.1
Outer leaf front	175	120	0.59	0.04	0.53	0.62	0.9
Inner leaf front	185	36	0.62	0.04	1.00	0.62	0.5
Outer leaf back	175	120	0.59	0.04	0.53	0.60	0.9
Inner leaf back	185	36	0.62	0.04	1.00	0.60	0.5
Bearing wall left	444	36	0.99	0.12	1.00	1.00	4.4
Bearing wall right	444	36	0.99	0.12	1.00	1.00	4.4
Sum				1.03[a]			47.7
F_{zoning}	11.5						x 0.96
F_{adjac} (row house)	460						x 1.13
Total							51.8

[a] Excluding outer cavity walls.

CHAPTER 4

RADON-TRANSPORT MECHANISMS AND MITIGATION

4.1

Effect of surface coatings on radon exhalation[16]

4.1.1 Introduction

Radon-reduction measures can be classified into various categories, depending their point of action:

a. Reduction of the sources
   Examples of this category are the preferential use of construction materials known to have low exhalation rates or replacement of the original soil by materials low in ^{226}Ra. This method is only practical for new constructions or drastic renovations.
b. Application of barriers
   Barriers will prevent or reduce the ingress of ^{222}Rn into a dwelling. Increasing the groundwater level and sealing of the groundfloor will reduce the transport of ^{222}Rn from crawl space into living compartments of a dwelling.
c. Reduction of indoor ^{222}Rn concentration
   Enhanced ventilation can keep the actual ^{222}Rn concentrations sufficiently low, but has as drawback a rise in energy consumption.
d. Reduction of the inhalation dose
   Given a ^{222}Rn concentration a reduction of the inhalation dose can be obtained by air cleaning devices. However, the obtained dose reduction leaves a lot to be desired.

Research on radon-mitigation measures therefore has focussed on methods belonging to the second category. Sealing of the indoor building surfaces seems to be an attractive method to reduce the ^{222}Rn exhalation rate and with that the ^{222}Rn concentration in dwellings due to construction materials. Several studies have been performed on the suitability of synthetic foils (Pohl-Rühling *et al*., 1980; Jha *et al*., 1982; Hafez and Somogyi, 1986; Daoud and Renken, 2001; Jiránek and Hůlka, 2001), plasters (Abu-Jarad and Fremlin, 1983; Morawska, 1983), caulking compounds (Fleischer, 1992) and surface coatings (Auxier *et al*., 1974; Abu-Jarad and Fremlin, 1983; Morawska, 1983) as barriers to ^{222}Rn gas diffusion. In this section the number of paint systems was extended and the effect on the free exhalation rate when the surface of the test walls was coated on all sides was tested. From the results the retaining action was calculated for the situation in which the coating would be applied to only one side of the wall.

---

[16] This chapter is based on a presentation at the international workshop on Indoor Radon Remedial Action, held in Rimini, Italy, 27 June to 2 July 1993 and paper published in Radiation Protection Dosimetry 56:179-183 (1994), entitled *Reduction of the radon entry rate from building materials by industrial surface coatings*. Authors P. de Jong and W. van Dijk.

4.1.2 Materials and methods

Selection of paint systems

Several acrylate dispersion paints commonly used for decoration of walls and ceilings have been tested. They were selected on the basis of their share in the market in the Netherlands. Most of them belong to the so-called do-it-yourself sector, but some professional paints were included as well. The experiments showed that the coatings chosen were not successful in retaining ^{222}Rn. Therefore, a second set was composed of coatings of lower vapour permeability. This set includes paints, which are not normally applied indoors. All paints were obtained from a wholesale business or kindly provided by the manufacturer. The paints of set 2 are listed in Table 4.l.

Table 4.1
Reduction factors of the various types of surface coatings (set 2).

Application	Type	μ value	No of layers	R [a]
Concrete paint	Acryl resin	10,000	2	0.95
Concrete paint	Silicates	1,000	3	0.98
Wood/concrete paint	Alkyd resin	20,000	2	1.04
			3	0.98
			4	1.09
Construction paint	Chlorinated rubber	50,000	2	1.09
Construction paint	Chlorinated rubber	100,000	2	0.77
			4	0.57
Construction paint	Polyurethane	30,000	2	0.31
Construction paint	Coal-tar/epoxy resin	100,000	2	0.67
Building paint	Epoxy resin	50,000	2	0.70
			4	0.24
Building paint	Polyurethane	30,000	2	0.37
			4	0.25
Façade paint	Acrylate dispersion	3,000	2	0.53

[a] Reduction factor by a double-sided coating (measured values).

Preparation of test walls

The first set of paints was applied to small (phosphogypsum) test walls (size 0.45 x 0.45 x 0.07 m^3), originating from a commercial test production batch. The second set of paints was applied to commercially available concrete blocks (size about 0.5 x 0.45 x 0.1 m^3). In successive steps, the test walls were coated on all (six) sides by a professional painter, according to the directions for use of the manufacturer. Special attention was given to the distribution of the paint near the edges. Prior to the exhalation measurements the test walls

were conditioned with respect to temperature and relative humidity (20°C, 50% RH) during at least four weeks.

Determination of the ^{222}Rn exhalation rate

The free exhalation rate of each individual test sample was determined before and after application of the ^{222}Rn sealant, using a purge and trap method described in section 2.1. Each test wall is analysed in triplicate under standard conditions (20°C, 50% RH).

Calculation of the reduction factor

The retaining action of the sealants is expressed by a reduction factor R, which is defined as the quotient of the area exhalation rate of the coated test wall and its original value. Based on the mean variation coefficient of the analytical method (see section 2.1) a significant reductive effect is obtained if $R \leq 0.85$ ($p < 0.01$, Student t-test).

Modelling

In common practice the coating is applied to the side that faces the living area only. Due to a diminished build-up of ^{222}Rn gas within the material, the area exhalation on the painted side will be lower than in the case where both sides of the wall are provided with a surface coating. This effect is examined in more detail by model calculations.

Three situations are considered: a bare wall (A), the same wall provided with a coating on both sides (B) and a single-sided coated wall (C). Figure 4.1A schematically shows the ^{222}Rn concentration profile of the original wall assuming that the ^{222}Rn concentration of the air outside at both sides of the wall is negligibly low. If this wall is provided with a surface coating on both sides, the ^{222}Rn concentration profile will change depending on the retaining effect of the coating in question. Profile I (Figure 4.1B) applies when the coating is totally ineffective (compare Figure 4.1A), profile II when the exhalation rate is partly diminished and profile III when a totally impervious barrier is used. If the decoration is limited to one side of the wall only (Figure 4.IC), a fraction of the ^{222}Rn gas formed in the material can escape via the unpainted side. As a consequence, the plane of symmetry shifts from the central point to the painted front (drawn for profile II in Figure 4.IC). The profiles I, II and III refer to the same retention as indicated above. If the point of the profiles at which the concentration is maximal is taken as $x = 0$, the diffusion along the x-axis follows Fick's Law and can be described by the differential equation given in eq. (1.1). For a steady-state situation the solution of this equation can be expressed as:

$$C(x) = A \cosh(x / l) + \frac{f}{\lambda} \quad . \tag{4.1}$$

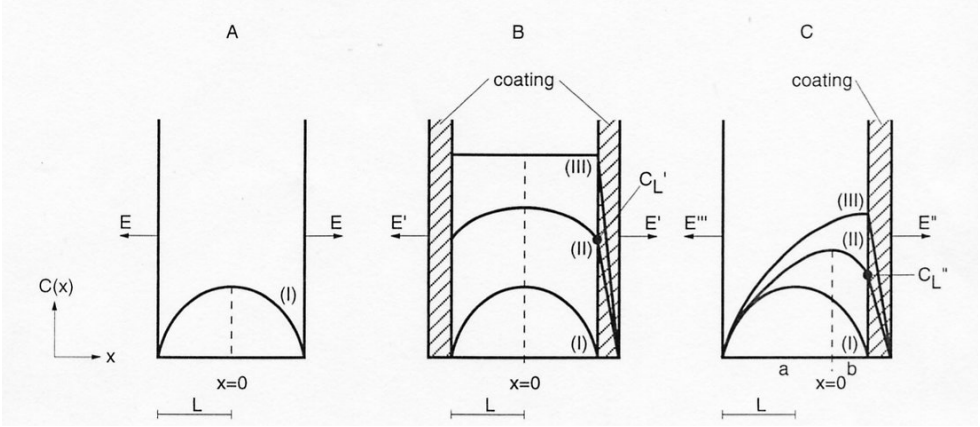

Figure 4.1
Schematic picture of the ^{222}Rn concentration profiles of a bare wall (A), the same wall provided with a coating on both sides (B) and coated on one side (C). The profiles I, II and III refer to an open, ineffective coating, an intermediate acting coating and a totally impervious coating, respectively.

In this equation $C(x)$ is the ^{222}Rn concentration in the interstitial space of the material (Bq m^{-3}); A is a constant (Bq m^{-3}); l is the diffusion length (m); f is the production rate of ^{222}Rn per unit of volume of interstitial space (Bq m^{-3} s^{-1}); and λ is the decay constant of ^{222}Rn (s^{-1}). From the boundary conditions, the constant A can be determined; for the three situations under consideration these conditions are (see also Figure 4.l):

- situation A: $C(L) = 0$
- situation B: $C(L) = C_L'$
- situation C: $C(b) = C_L''$

which results for each situation in a value for A. Substitution of these boundary conditions in eq. (4.1), the ^{222}Rn concentration in the interstitial spaces can be written as:

A: $$C(x) = \frac{f}{\lambda} - \frac{f}{\lambda}\frac{\cosh(x/l)}{\cosh(L/l)}; \qquad (4.2)$$

B: $$C(x) = \frac{f}{\lambda} - \left(\frac{f}{\lambda} - C_L'\right)\frac{\cosh(x/l)}{\cosh(L/l)}; \qquad (4.3)$$

C: $$C(x) = \frac{f}{\lambda} - \left(\frac{f}{\lambda} - C_L''\right)\frac{\cosh(x/l)}{\cosh(b/l)}. \qquad (4.4)$$

The ^{222}Rn exhalation rate per unit area is defined in eq. (1.4) as:

$$E = -\varepsilon\, D \left.\frac{d(C(x)}{dx}\right|_{x=L} . \qquad (4.5)$$

In this equation E is the ^{222}Rn flux from the wall (Bq m^{-2} s^{-1}); ε is the porosity of the wall (dimensionless); and D is the pore diffusion coefficient (m^2 s^{-1}). If eq. (4.5) is solved for each of the ^{222}Rn profiles given in eqs. (4.2) to (4.4), for each considered situation A to C an exhalation rate is obtained. Dividing the obtained expressions for the exhalation rate for situation B and C by that of situation A, the following ratios are found:

$$\frac{E'}{E} = \left(\frac{f}{\lambda} - C'_L\right) \Big/ \frac{f}{\lambda} \quad \text{and} \qquad (4.6)$$

$$\frac{E''}{E} = \left(\frac{f}{\lambda} - C''_L\right) \Big/ \frac{f}{\lambda} \quad \frac{tgh(b/l)}{tgh(L/l)}, \qquad (4.7)$$

with E the exhalation rate of the bare wall (situation A); E' the exhalation rate of the wall coated on both sides (situation B); and E'' the exhalation rate of the wall coated on one side (situation C, coated side).

According to Hart and Levins (1986) the ^{222}Rn concentration $C(x)$ in the coating can be described by the formula:

$$C(x) = \beta \sinh\left[(L + \delta - x)/l_1\right] \; for \; L \le x \le L + \delta \,, \qquad (4.8)$$

where β is a constant; L is half of the thickness of the wall; δ is the thickness of the coating; and l_1 is the diffusion length of ^{222}Rn in the coating material. An estimate derived from permeability's of some plastic membranes (Jha and al., 1982; Hafez and Somogyi, 1986) gives an average diffusion length of about 700 μm. As the thickness of the applied coating layers were less than 500 μm, sinh [$(L + \delta - x)/ l_1$] approaches ($L + \delta - x$)/ l_1, within 10%, which implies a near linear concentration gradient across the coating. This being the case, the ^{222}Rn fluxes E' and E'' transmitted by the coating are assumed to be proportional to the ^{222}Rn concentration at the interface between wall and coating. As equations:

$$\frac{E'/E}{C'_L} = \frac{E''/E}{C''_L} . \qquad (4.9)$$

The variable C''_L is calculated from an additional boundary condition for eq. (4.4); for this equation applies that $C(-a) = 0$ (see Figure 4.1), leading to the following expression:

$$C_L'' = \frac{f}{\lambda}\left(1 - \frac{\cosh(b/l)}{\cosh(a/l)}\right) \tag{4.10}$$

Furthermore applies:

$$a + b = 2L \tag{4.11}$$

The above set of equations is solved mathematically with half of the thickness of the wall (L) and the diffusion length (l) as variables. Figure 4.2 and 4.3 show the relations of the exhalation rates of a wall coated at one side and the same wall coated on both sides for two wall thicknesses and a number of diffusion lengths. The results will be discussed in the next paragraph.

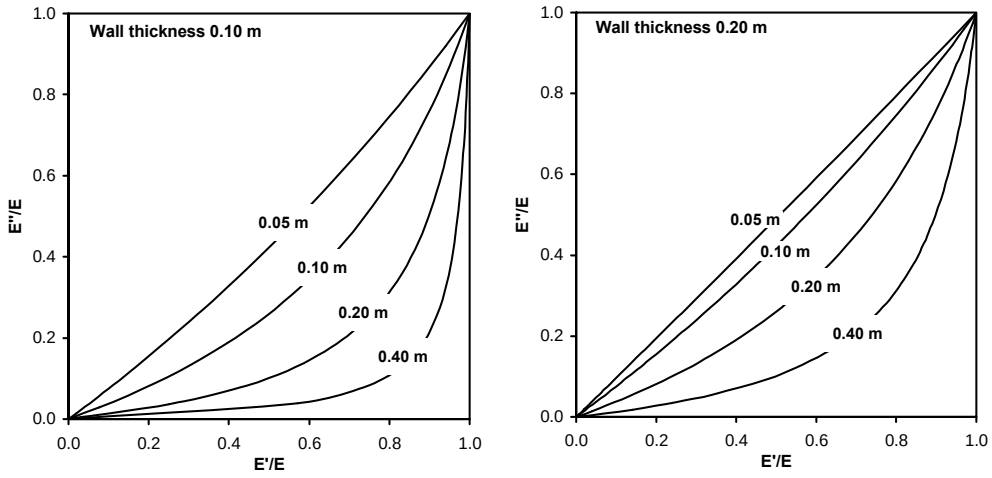

Figure 4.2 and 4.3
The ratio of the exhalation rates of a double sided coated wall and a bare wall (E'/E) as a function of the ratio of the exhalation rates of a single-sided coated wall and a bare wall (E''/E) for a diffusion length, 1, equal to 0.05, 0.10, 0.20 m and 0.40 m, respectively. The left figure shows the results for a wall thickness of 0.10 m (L=0.05 m), the right figure for a thickness of 0.20 m (L=0.10 m).

4.1.3 Results and discussion

In this study the first set of coatings consisted of 13 different acrylate dispersion paints, normally applied for decoration purposes in homes. No reduction in the exhalation rate could be demonstrated in any of the investigated sealants. The results pertaining to the second set of coatings are compiled in Table 4.l. The measured reduction factors ranged from l (no effect) to values of up to 0.25. The highest reduction is obtained for

polyurethane-based coatings. As indicated above, the coatings from set 2 were selected for their vapour permeability. A measure for this parameter is the so-called μ-value: the higher the μ value, the lower the vapour permeability. As can be concluded from Table 4.l, there is no relation between this parameter and the ^{222}Rn retaining effects of the coatings. The μ-value for the dispersion paints from set l ranged from 500-5000.

Studies by others indicated an inherent advantage for epoxy paints over various alternatives. Reported reduction factors for coatings applied single-sided or all-sided ranged from 0.07-0.5 (Auxier *et al*., 1974; Eichholz *et al*., 1980; Abu-Jarad and Fremlin, 1983). A reduction close to 100% was reported by Culot *et al*. (1978) for thick layers up to 4 mm. In our study the two polyurethane coatings tested were superior to the two epoxy paints. Application of two layers of paint to all sides of the test wall resulted in reduction factors of 0.3-0.4 and 0.7 for polyurethane and epoxy-based coatings, respectively.

Model calculations indicate that if the coatings had been applied to one side of the construction only, the reduction might have been higher due to the diminished build-up of ^{222}Rn gas within the material. As shown in the Figures 4.2 and 4.3 this effect depends on both the ^{222}Rn diffusion length of the building element and its thickness; the lower the diffusion length and the thicker the construction, the more the exhalation rates from the bare and coated side will resemble. The largest effect, therefore, can be expected if the coating is applied to one side of a wall made of sand-lime, gypsum, aerated concrete or clay brick for which diffusion lengths are reported of 40 cm or more (Keller *et al*., 2001). Assuming a thickness of 10 cm, this would result in a reduction factor of less than 0.05 if two layers of the tested polyurethane or epoxy paints had been applied (Figure 4.2). It is obvious that the ^{222}Rn exhalation rate from the unpainted area will, however, be increased, as has already been observed by Abu-Jarad and Fremlin (1983). From the model approximation it is calculated that for a totally impervious coating the area exhalation rate of the unpainted side will increase by a factor 1.97 (L = 0.05 m; l = 0.40 m), which is slightly lower than 2 due to the enlarged mean path length of the emanated ^{222}Rn atoms.

For concrete lower diffusion lengths are reported, ranging from 6 cm for heavy concretes to 30 cm for lightweight species (Kovler *et al*., 2004). The thickness of concrete construction elements in residences varies from about 10 cm (inner leaf) to 20-25 cm for floors, ceilings and dwelling-separating walls. If a typical diffusion length of 10 cm is adopted, it can be concluded from Figure 4.2 that for a 10 cm-thick construction element the reduction factor for a polyurethane coating reduces from 0.3 to 0.1. For concrete construction elements with a thickness of 20 cm or more, the effect of the ^{222}Rn release in the situation in which the coating is applied to only one side is negligible (Figure 4.3).

In the Netherlands acrylate dispersion paints are the most commonly applied paints for decoration of walls and ceilings, such as ceiling relief paints, rawl-facer paints, wall paints and cement paints. As found in this study, no reducing effect of these paints on the ^{222}Rn entry rate can be expected in practice. Nevertheless, some other sealants have proved to be much more effective and this technique provides a relatively inexpensive method for controlling the ^{222}Rn emissions from walls and floors in existing homes. However, it should be borne in mind that any cracks that may develop later in the paint lead to leaks that negate a large portion of its sealing effectiveness (Morawska, 1983; Moeller and Fujimoto, 1984).

4.2

Exhalation rate and the role of concrete composition and production[17]

4.2.1 Introduction

^{222}Rn in the home is the main source of exposure to ionizing radiation. ^{222}Rn concentrations vary considerably and depend mainly on the influx from soil and building materials. In the Dutch Building Decree (DB, 1991) the pressure-driven airflow from crawl space into the dwelling is limited to 2 x 10^{-5} m^3 $(m^2\ s)^{-1}$. Together with the relatively low crawl space concentrations in the Netherlands this results in a more prominent role for the building materials as a ^{222}Rn source. Among the building materials, concrete generally accounts for the highest contribution to indoor ^{222}Rn (Folkerts *et al*., 1984; Poffijn *et al*., 1984; Vaas *et al*., 1993). The large number of variables of this material can be altered over fairly wide ranges. Some of these variables are related to the manner of production, others to the composition of the concrete products. Both classes of variables are known to affect the capillary pores, the residue of the water-filled spaces in the fresh paste. These capillary pores form an extensive, interconnected network of voids, responsible for the permeability of the concrete and the exchange of water and gases (Reinhardt, 1985).

The coherence of structural changes in concrete and the ^{222}Rn emanation process, however, is presently not fully understood and so far only limited attention has been given to this subject. Some authors studied the influence of raising the water-cement ratio, known to provide an increase of the capillary pore volume (Reinhardt, 1985). Progressive hydration and carbonation are also known to affect the microstructure and hence the pore volume of concrete over time. Some studies established an effect of the ageing on the ^{222}Rn exhalation rate (Roelofs and Scholten, 1994; Yu *et al*., 1995); however, no relation with the physical characteristics of the mortar structure was determined.

In this section the ^{222}Rn exhalation rate was determined as a function of the amount and type of cement, the water-cement ratio, curing time, type of aggregates, and compressive strength. And since earlier studies (Stranden *et al*., 1984; section 2.1) showed that the moisture content of the concrete samples strongly influences the exhalation rate, the evaporation rate during conditioning was determined as an additional variable. The results are interpreted in view of the capillary pore volume and pore size of the concrete samples.

---

[17] This chapter is based on a presentation at the International Symposium on the Natural Radiation Environment (NRE VI), June 5-9, 1995, Montreal, Canada and published in Environment International 22(Suppl.1):S287-S293 (1996), entitled *The effect of the composition and production process of concrete on the ^{222}Rn exhalation rate*. Authors: P. de Jong, W. van Dijk, J.G.A. van Hulst and R.J.J. van Heijningen.

4.2.2 Methods and materials

Composition, preparation, and conditioning of test samples

In the first set of samples, three types of cement (blast furnace, Portland, and Portland/fly ash cement) are applied in amounts of 280 kg/m^3, 315 kg/m^3, and 350 kg/m^3 each. The water-cement ratio was 0.53, a normal value for the in situ production of concrete walls and floors. The prefab industry frequently uses mixtures which are lower in water-cement ratio (0.40). To allow a comparison between in situ and prefabricated concretes, some additional mixtures using Portland and Portland/fly ash cement are prepared.

In the next set of samples, two production parameters are varied because of their supposed influence on the exhalation rate, namely the water-cement ratio and the curing time the samples are kept in plastic foil. In most cases, river gravel of Dutch origin (Panheel) is used. Since the supply of this material is expected to become more problematic in near future, alternative aggregates are incorporated into this study. They are limestone (origin Meuse valley, Belgium), granulates derived from recycled masonry (35%) and concrete (65%) (Dutch origin), and sea gravel (Humber, England).

The concrete mixtures are prepared in an amount of about 150 kg according to the compositions listed in Table 4.2. All ingredients are obtained from local manufacturers or importers. After intensive mixing of the ingredients, the concrete is poured into plywood moulds, sized 45 x 50 x 10 cm^3, and condensed using a 40 mm vibrating needle. After 1 d, the samples were demoulded and allowed to cure for 2 months in indoor conditions (18-25°C, RH 45-55%). After demoulding, some samples (indicated in Table 4.2) were kept in plastic foil for 3 and 28 d, respectively. At the end of the 2-month period, all samples were transferred to a conditioning room, set to 20°C and 50% RH. During a conditioning period of 6 months, the weight of the samples was repeatedly determined to follow the loss of water. Together with the above-mentioned concrete slabs, test cubes sized 15 × 15 × 15 cm^3 were prepared for determination of the compressive strength and the density.

Determination of the ^{222}Rn exhalation rate

The free exhalation rate of each individual sample was measured according to the method presented in section 2.1. During the study, the correct operation of the absorption and counting equipment was checked using a phosphogypsum laboratory standard test block.

Determination of the radioactivity concentration

After the determination of the exhalation rate, about 10 kg of each sample is crushed to a particle size of less than 0.5 cm. One litre of this material is enclosed in an airtight bottle for at least three weeks and analysed by gamma-ray spectrometry according to method I described in section 3.2.

Table 4.2
Composition of the concrete mixtures (rounded figures).

Sample code	Cement[a] (kg m^{-3})	Aggregates (kg m^{-3})	Sand (kg m^{-3})	Water (kg m^{-3})	Days in plastic
1	280 (BF)	1250 (river gravel)	700	150	0
2	315 (BF)	1200 (river gravel)	670	170	0
3	350 (BF)	1150 (river gravel)	650	190	0
4	280 (P)	1260 (river gravel)	710	150	0
5	315 (P)	1210 (river gravel)	680	170	0
6	350 (P)	1160 (river gravel)	650	190	0
7	280 (PF)	1250 (river gravel)	700	150	0
8	315 (PF)	1200 (river gravel)	670	170	0
9	350 (PF)	1140 (river gravel)	640	190	0
10	280 (P)	1320 (river gravel)	740	110	0
11	280 (PF)	1310 (river gravel)	740	110	0
12	315 (BF)	1270 (river gravel)	710	130	3
13	315 (BF)	1200 (river gravel)	670	170	3
14	315 (BF)	1130 (river gravel)	640	200	3
15	315 (BF)	1200 (river gravel)	670	170	28
16	315 (BF)	1280 (limestone)	670	170	3
17	315 (BF)	990 (granulates)	670	170	3
18	315 (BF)	1200 (sea gravel)	670	170	3

[a] BF: Blast furnace cement, type A
P: Portland cement, type B
PF: Portland/fly ash cement, type A

Other determinations

The density and compressive strength were determined 28 d after preparation. The emanating power was calculated from the measuring results according to the following approximation (Van Dijk and De Jong, 1991):

$$\eta = \frac{E}{0.5\, L\, \rho\, \lambda\, a_1}\ x\, 100\%, \qquad (4.12)$$

where E is the free area exhalation rate (Bq m^{-2} h^{-1}); L the thickness of the test wall (0.1 m); ρ the density (kg m^{-3}); λ the decay constant of ^{222}Rn (h^{-1}); and a_1 the ^{226}Ra content of the material (Bq kg^{-1}).

4.2.3 Results

The influence of the drying process on the area exhalation rate was followed for one sample, the sample coded 2. The results (Table 4.3) showed no significant trend over time (Spearman rank test, $p > 0.05$ two sided). On the basis of this observation, the other

concrete samples were analysed for the exhalation rate starting on day 190 and ending on day 217 after preparation. The results are presented in Table 4.4 as the average value and standard deviation of three determinations. The determined exhalation rates vary between 2 and 6 Bq $(m^2\ h)^{-1}$ and are in the normal range (Ingersoll, 1983; UNSCEAR, 1988). As indicated above, the sample coded 2 was analysed on several days. For correct comparison with the other results, the exhalation rate of this sample was taken as the mean value of the last two measuring days from Table 4.3.

Curing time (d)	**Exhalation rate ($Bq/m^2\ h$)[a]**
88	3.7 ± 0.2
134	4.2 ± 0.3
157	4.0 ± 0.3
190	3.6 ± 0.2
217	3.8 ± 0.3
Average ± SD	3.9 ± 0.3

[a] Mean ± SD (n = 3 determinations)

Table 4.3
^{222}Rn exhalation rates of sample 2 as function of the curing time.

During the study, a phosphogypsum laboratory standard test block was analysed on four different days and showed an average exhalation rate of 5.2 ± 0.2 Bq $m^{-2}\ h^{-1}$ (n=4 days). This is in good agreement with earlier observations, using the same test sample (i.e. 5.1 ± 0.2 Bq $m^{-2}\ h^{-1}$ (n=17 days, spread over a period of 7 y). Obviously, the analytical procedure does not demonstrate any significant trend over time.

Table 4.4 also includes the results of the ^{226}Ra analysis, the compressive strength, and the calculated emanating power. The ^{226}Ra concentrations are in the same range as reported earlier (Ackers *et al*., 1985; section 2.1) and the compressive strengths also show expected values. Only sample 3 has a relatively low value. In general, the results of the emanating power are at higher levels as reported by UNSCEAR (1988). This will be discussed in the next section. The density of the samples varied only slightly, ranging from 2320 kg/m^3 to 2430 kg/m^3, so this parameter was not included. The only exception was sample 17, with a density of 2160 kg/m^3 due to the low density of the granulates.

Table 4.4
Results of measurements.

Sample code and short description		Compressive Strength (MPa)	Loss of water[a] ($g\ kg^{-1}$)	Exhalation rate ($Bq\ m^{-2}\ h^{-1}$)	Eman. power (%)	^{226}Ra content ($Bq\ kg^{-1}$)
Amount/type of cement						
1	280 Blast furnace	39.3 ± 1.3	6.9	3.9 ± 0.4	22 ± 3	20 ± 2
2	315 Blast furnace	44.6 ± 0.8	7.2	3.7 ± 0.2	20 ± 2	21 ± 2
3	350 Blast furnace	25.1 ± 0.8	12.2	6.3 ± 0.4	37 ± 4	20 ± 2
4	280 Portland	49.4 ± 1.1	7.3	3.9 ± 0.3	45 ± 7	10 ± 2
5	315 Portland	49.3 ± 1.0	7.8	4.5 ± 0.3	58 ± 9	9 ± 2
6	350 Portland	44.7 ± 0.2	9.0	4.6 ± 0.2	48 ± 6	11 ± 2
7	280 Portland fly ash	41.2 ± 2.0	7.6	4.2 ± 0.3	41 ± 6	12 ± 2
8	315 Portland fly ash	43.6 ± 1.5	8.8	4.7 ± 0.2	46 ± 6	11 ± 2
9	350 Portland fly ash	41.0 ± 1.0	9.4	5.4 ± 0.4	51 ± 7	12 ± 2
Pre-fab concretes						
10	0.40 Portland	56.3 ± 2.7	6.9	3.5 ± 0.3	42 ± 7	9 ± 2
11	0.40 Portland fly ash	52.1 ± 2.0	5.7	3.9 ± 0.4	33 ± 5	13 ± 2
Water-cement ratio						
12	0.40 Blast furnace	46.4 ± 4.4	4.5	2.3 ± 0.1	10 ± 1	26 ± 2
13	0.53 Blast furnace	41.2 ± 1.3	6.6	3.3 ± 0.2	18 ± 1	21 ± 2
14	0.65 Blast furnace	25.7 ± 2.6	8.3	5.5 ± 0.3	24 ± 3	26 ± 2
Time in plastic						
2	0 days	44.6 ± 0.8	7.2	3.7 ± 0.2	20 ± 2	21 ± 2
13	3 days	41.2 ± 1.3	6.6	3.3 ± 0.2	18 ± 1	21 ± 2
15	28 days	42.8 ± 1.4	6.8	3.2 ± 0.2	17 ± 2	21 ± 2
Aggregates						
13	Meuse gravel	41.2 ± 1.3	6.6	3.3 ± 0.2	18 ± 1	21 ± 2
16	Limestone	49.7 ± 0.3	5.0	3.1 ± 0.2	9 ± 1	39 ± 2
17	Granulates	39.4 ± 3.1	11.2	4.8 ± 0.2	22 ± 2	26 ± 2
18	Sea-gravel	45.8 ± 2.4	7.6	3.2 ± 0.3	21 ± 3	17 ± 2

[a] Loss of water after six months curing.

In Figure 4.4 the results of the emanating power are plotted against the loss of water after the six months of conditioned curing at 20°C, 50% RH. Figure 4.5 and 4.6 graphically present the relations between the emanating power and both the water-cement ratio and compressive strength, respectively.

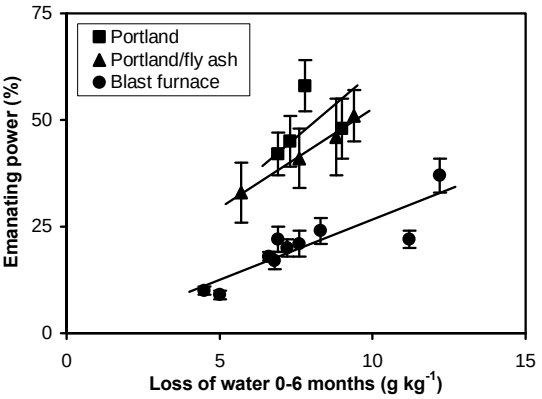

Figure 4.4
Emanating power as a function of the loss of water after six months of conditioning at 20°C, 50% RH. Line for blast furnace cement fitted using method of least squares. The correlation coefficient equals 0.89. Other lines drawn by eye.

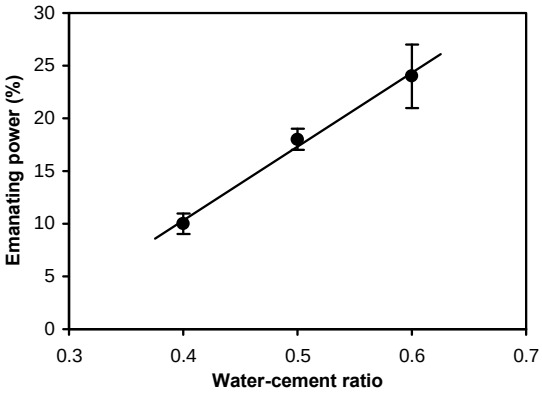

Figure 4.5
Emanating power as a function of water-cement ratio (blast furnace cemented samples only). Line fitted using method of least squares. The correlation coefficient equals 1.00).

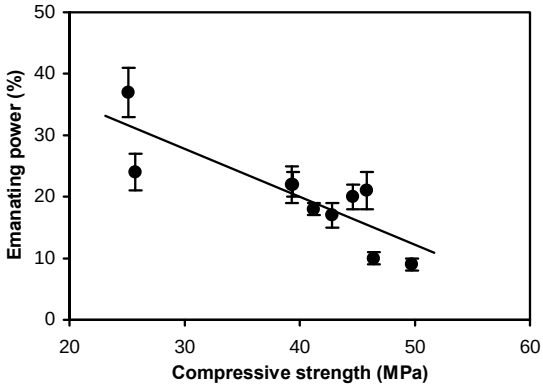

Figure 4.6
Emanating power as a function of compressive strength (samples prepared with blast furnace cement). Line fitted using method of least squares. The correlation coefficient equals 0.83.

4.2.4 Discussion

If the results of samples of similar composition (Table 4.5) are compared with the results of concrete samples of an earlier study (section 2.1), it strikes that (1) the ^{226}Ra concentrations agree well for all three samples; (2) the same applies for the area exhalation rate and emanating power of the blast furnace slag sample; and (3) the samples containing Portland or Portland/fly ash cement differ by about a factor of 2 in exhalation rate and emanating power.

Table 4.5
Comparison with earlier results.

Type of cement/reference	Exhalation rate ($Bq\ m^{-2}\ h^{-1}$)	Eman. power (%)	^{226}Ra ($Bq\ kg^{-1}$)
Blast furnace slag cement			
Section 2.1	3.7 ± 0.3	26 ± 3	16 ± 2
Sample 2 (this study)	3.7 ± 0.2	20 ± 2	21 ± 2
Portland cement			
Section 2.1	2.2 ± 0.3	26 ± 9	10 ± 1
Sample 5 (this study)	4.5 ± 0.3	58 ± 9	9 ± 2
Portland fly ash cement			
Section 2.1	2.4 ± 0.1	21 ± 2	13 ± 2
Sample 8 (this study)	4.7 ± 0.2	46 ± 6	11 ± 2

Although there are some differences in sample composition and curing conditions, this can hardly explain differences of this order of magnitude. Also, a bias introduced by the analytical procedure can be excluded since its reproducibility has been found to be better than 5% (see section 4.2.3). A plausible explanation for the observed differences is found in the age of the test samples at the time of measurement. The present samples were cured for only 6-7 months, while in the earlier study mentioned above, the samples were about 4 y of age. From the results presented by Roelofs and Scholten (1994), comparable ratios concerning the ^{222}Rn exhalation rates at different time intervals after preparation can be deduced for both blast furnace and Portland based concretes.

Figure 4.4 shows the results of the emanating power as a function of the loss of water after the six months of conditioned curing. For the concrete slabs prepared with blast furnace cement, a clear relation is present between both parameters. Although there were only four test samples for Portland and Portland/fly ash cement, the same picture holds for these types of cement. The coherence between the two parameters indicates that, with an increase of the evaporation rate, more internal emanating pore surface will become available, allowing more ^{222}Rn to escape from the interior of the walls. The effect of the cement type is clearly demonstrated. Given a certain loss of water, concretes fabricated

with blast furnace cement show the lowest emanating power. Since this type of cement has smaller capillary pores in comparison with concretes based on Portland cement (Reinhardt, 1985), it is assumed that this relates to the lower probability of an emanated ^{222}Rn atom to be stopped within the pore volume. The intermediate position of the concretes prepared using Portland/fly ash cement can be explained by the condensing, choking effect of fly ash, which results in reduced pore sizes, as reported by Neville (1978).

In the first set of samples (samples 1 - 9), the amount of cement is raised in successive steps from 280 kg/m^3 to 350 kg/m^3. Because the water-cement ratio was maintained at a value of 0.53 within this series, the amount of free water (water not used for the chemical binding process) is somewhat larger as more cement is applied. As a result, the capillary pore volume in the cement paste increases with higher levels of cement, and consequently the ^{222}Rn exhalation increases. Taking the error margins into account, the measuring data support the above hypothesis for all three types of cement (Table 4.4).

The water-cement ratio was varied from 0.40 - 0.65 in three slabs, using a fixed amount of blast furnace slag cement of 315 kg/m^3 (samples 12 - 14). Raising the water-cement ratio also provides an increase of the capillary pore volume (Reinhardt, 1985) and consequently of the liberated amount of ^{222}Rn. A linear relation is obtained when the emanating power is plotted against the water-cement ratio (see Figure 4.5), which is in agreement with results reported by Kunsch and Hartl (1989). Rogers *et al*. (1994) indicated that the pore diffusion coefficient also increases with the water-cement ratio. Since in this study, the test slabs had a limited thickness (diffusion distance 0.05 m at the most), the influence on the emanating power is negligible. However, in the case of thicker samples, this parameter has an additional retarding effect on the ^{222}Rn exhalation. Another indicator for the capillary pore volume of concrete samples is the compressive strength (Reinhardt, 1985). Figure 4.6 shows that the emanating power decreases linearly with the compressive strength, confirming that the coherence within the cement paste decreases in favour of the emanating internal surfaces. Note the agreement between the Figures 4.4 and 4.6.

Two additional mixtures, which are frequently used in the prefab industry, were prepared (codes 10 and 11). In general, these mixtures are low in water-cement ratio as well as in the amount of cement. As discussed above, this will limit the ^{222}Rn exhalation rate in two ways. The results in Table 4.4 show that these samples indeed have lower exhalation rates and emanating powers compared to samples 5 and 8, respectively.

Curing under plastic foils for three days is one of the procedures recommended in the Dutch Regulations for concrete construction (NEN, 1989). It results in a higher compressive strength in combination with a closer surface structure. From this point of view, reduced ^{222}Rn exhalation was expected and three samples of the same composition were kept in plastic for periods of 0, 3, and 28 d, respectively. Although there is a tendency of the exhalation rate to be lower with progressive curing (Table 4.4, samples 2, 13, 15), only

the decrease between 0 and 3 d is significant from zero (Student t, $p < 0.01$). A greater effect is expected at lower water-cement ratios.

The last series of observations concern the type of aggregates in the concrete samples. As indicated in section 4.2.2, some alternatives for river gravel were incorporated into this study to see whether or not comparable exhalation rates could be obtained. The results in Table 4.4 (samples 13, 16-18) show that replacement of river gravel by limestone or sea-gravel actually results in the same ^{222}Rn exhalation rate. However, the sample concreted with recycled masonry and concrete granulates (sample 17) shows an increased rate, probably due to its high porosity. Although this material is an attractive alternative from an environmental point of view (recycling), more research into its applicability in residential concrete is necessary.

4.2.5 Conclusion

The measured differences in both exhalation rate and emanating power can mainly be attributed to the capillary pore volume of the concreted mixtures. Higher ^{222}Rn releases are associated with larger water-cement ratios, larger amounts of cement and Portland cement as binder. The compressive strength seems be a good indicator for the anticipated ^{222}Rn releases.

4.3

Influence of the porosity on the ^{222}Rn exhalation rate[18]

4.3.1 Introduction

In the Netherlands building materials on average account for 70% of the indoor radon (^{222}Rn) concentration (Stoop *et al*., 1998). Concrete is found to be a major contributor, mainly due to its large market share. There are, however, various kinds of concrete compositions applied in the construction of houses. Changes in the concrete composition affect both the porosity and the ^{226}Ra activity concentration of the construction material and with that the release of ^{222}Rn. The ^{226}Ra activity concentration is proportional to the amount of ^{222}Rn gas produced within the material. The fraction of ^{222}Rn that is released into the living environment is defined by three separate steps: (1) the escape of ^{222}Rn atoms from the mineral matrix into the pore space, known as emanation; (2) the subsequent diffusion of these atoms from the site of generation through the air-filled pore system to the outer surface of the building material; and (3) the release of ^{222}Rn from the building material, called exhalation. In ^{222}Rn transport models, the diffusion in building parts is often described as a one-dimensional process, i.e. directed to the living space and its opposite site (Jonassen and McLaughlin, 1980; Berkvens *et al*., 1988; see also section 1.2). In such a situation the exhalation rate can be described by the following expression (De Jong and Van Dijk, 2008):

$$E = \lambda\, a\, \eta\, \frac{l}{L} \tanh\left(\frac{L}{l}\right) \quad with \quad l = \sqrt{\frac{D}{\lambda}}. \tag{4.13}$$

In this equation E is the ^{222}Rn exhalation rate in Bq (kg s)$^{-1}$ for a one-dimensional approach; λ is the decay constant of ^{222}Rn (s^{-1}); a is the activity concentration of ^{226}Ra (Bq kg^{-1}); η is the emanation factor, the fraction of the produced ^{222}Rn atoms that reaches the pores (dimensionless); l the diffusion length of ^{222}Rn (m); L half of the thickness of the considered building part (m); and D the pore diffusion coefficient (m^2 s^{-1}). The combination of the first three variables in eq. (4.13) refer to the emanation of the ^{222}Rn atoms (step 1), the others to the diffusive transport to the exterior of the building part (step 2). The porosity of a building material influences both the emanation coefficient and the pore diffusion coefficient and therefore affects both steps in the exhalation of ^{222}Rn.

---

[18] This chapter is based on a paper submitted for publication to Health Physics, entitled *Influence of the porosity on the ^{222}Rn exhalation rate from concrete*. Authors P. de Jong, W. van Dijk and M. de Rooij.

Various studies have investigated the parameters that influence the exhalation rates of concretes. It is found that the presence of water in the pores increases the probability that a recoiled ^{222}Rn atom is stopped in the pore structure instead of crossing the pore and being embedded in an adjacent grain. Also a water film in the pores will hinder the adsorption of ^{222}Rn to internal solid surfaces (Stranden *et al*., 1984). Furthermore, the diffusion coefficient of ^{222}Rn gradually decreases as a function of the pore water content. At high water content more and more pores are filled by water, thereby effectively blocking the transport of ^{222}Rn.

The pores in concrete can be divided into gel pores and capillary pores. Through a drying experiment on mortar Valckenborg *et al*. (2001) have demonstrated that the gel pores remain water-filled under normal practical conditions. For this reason, as described above, this fraction of the porosity does not play a significant role in the exhalation of ^{222}Rn. The other part of the concrete porosity is taken by the capillary pores, which really can dry out in practice. These pores are the remnants of the water-filled space in the fresh paste, which are responsible for the transport of water and gases. Raising the water-to-cement ratio (w/c ratio) in the fresh paste is known to increase the capillary pore volume. However, contradictory results have been published on the effect of this parameter on the ^{222}Rn exhalation rate, showing either no relation (Ulbak *et al*., 1984), an (almost) linear increase (Kunsch and Hartl, 1989; section 4.2) or both an increase and decrease, depending on the ratio (Kovler *et al*., 2005). In the present study the effect of changing the w/c ratio of the mixtures is verified.

Besides the w/c ratio other important variables that can influence the porosity of concrete are the amount of cement, amount and type of aggregate materials and the addition of other substances to the base mixture, such as fly ash and silica fume (mineral admixtures) or air entrainers (chemical admixtures). For example, partial substitution of Portland cement by other pozzolanic material reduces the porosity of both matrix and the aggregate-paste transition zone. A retarding effect on the ^{222}Rn exhalation rate is demonstrated among others for silica fume (Yu *et al*., 2000), metakaolin (Lau *et al*., 2003), fly ash (Stranden, 1983; Ulbak *et al*., 1984; Kovler *et al*., 2005; section 4.2) and ground blast furnace slag (section 4.2).

In this section the porosity of concrete test specimen was varied in five separate series consisting of a total of 23 mixtures by changing type and amount of cement, the amount of water at a fixed cement level, addition of an air entrainer and by variation of the amount of recycled aggregates. The aim of this study was to investigate the influence of the induced porosities on the exhalation rates of the mixtures per series and to find common parameters that describe the observed effects for the total set of test specimen.

4.3.2 Methods and materials

Test series and concrete mixtures

The 23 mixtures are subdivided into five series. Each series focussed on the variation of one parameter to obtain a range in concrete porosities within that series:

- In series one (I) the amount of Portland cement (CEM I 32,5R[‡]) is used as the key parameter to change the porosity of the mixtures. More cement is known to result in a denser, less porous concrete.
- In series two (II) the compositions of series I are repeated, but with a different type of cement. In this series the content of blast furnace slag cement (CEM III/B 42,5) in the mixture is varied. Concretes manufactured with this type of cement are noted for their lower porosity as compared with corresponding mixtures with Portland cement.
- In series three (III) the amount of water in the fresh paste is increased in successive steps at a fixed amount of Portland cement, thus varying the w/c ratio. Although not all the prepared mixtures are common practice in concrete manufacturing, these mixtures are included in this study to enlarge the porosity of the matrix.
- In series four (IV) a few mixtures have been made to look at the influence of air content. Hereto an air-entraining agent (type AEA 3, manufacturer Tillman B.V., The Netherlands) is added to the mixtures. Air entrainers stabilize small air bubbles, sized 0.01 to 1.0 mm (Aligizaki, 2006) that remain intact during compaction and hardening. Air entraining agents are applied in practice to improve the freeze-thaw characteristics and the workability of concrete.
- The last (V) series comprises of mixtures in which the volume of coarse aggregates (Meuse gravel) is replaced in successive steps (0, 20, 50, 80, 100% v/v) by recycled aggregates. The total volume of aggregates in this series is kept at a constant value. The recycled aggregates consist of 40% recycled masonry and 60% recycled concrete (density 2160 kg m^{-3}) and are more porous than the gravel aggregates (2650 kg m^{-3}). Before mixing in, the recycled aggregates are fully saturated with water. Therefore, increasing the amount of recycled aggregates results in the addition of more water. However, this extra water has no influence on the composition of the cement paste matrix and the w/c ratio of all mixtures in this series is 0.52.

To obtain the variation in the five series, 23 concrete mixtures have been prepared by KEMA (Arnhem, The Netherlands), specialized in the preparation of research-related test specimen. For all mixtures the same Portland cement is used with the exception of series II

[‡] Specification of the cements follows the system as given in the European standard NEN-EN 197-1 (NEN 2000).

(blast furnace slag cement). For mixtures high in cement content a superplasticizer (Cugla 80/20, manufacturer Cugla B.V., The Netherlands) is mixed in with the fresh paste. Addition of plasticizer has no influence on the porosity but is applied to enhance the workability of the concrete mixture in question. For all mixtures the same river sand and river gravel is taken. The particle size distribution of the applied sand is 2-4 mm (11%), 1-2 mm (15%), 0.5-1 mm (29%), 0.2-0.5 mm (32%) and 0.1-0.3 mm (13%); that of the gravel 16-24 mm (26%), 8-16 mm (48%) and 4-8 mm (26%). Details on the compositions of the mixtures are given in Table 4.6.

Table 4.6
Composition of the concrete mixtures in kg m^{-3}.

Sample ID	Cement		Water[a]	Gravel	Recycled granulates[b]	Sand	Admix-tures
	Portland	Blast furnace					
1	550		127	1131		692	8.8[c]
2	450		137	1171		718	4.5[c]
3	350		148	1212		742	1.8[c]
4	315		166	1202		737	
5	280		176	1205		739	
6	200		174	1249		767	
7		550	143	1085		665	8.8[c]
8		450	145	1142		700	5.3[c]
9		350	145	1201		736	2.5[c]
10		315	165	1193		730	
11		280	175	1194		732	
12		200	174	1243		760	
13	315		90	1321		809	5.0[c]
14	315		103	1299		798	4.7[c]
15	315		134	1252		767	1.6[c]
16	315		196	1151		705	
17	315		165	1202		736	0.94[d]
18	315		165	1201		735	1.9[d]
19	350		182	1157	0	709	
20	350		193	926	189	709	
21	350		210	578	472	709	
22	350		227	231	754	709	
23	350		238	0	943	709	

[a] Includes water in sand and recycled aggregates.
[b] 40% masonry and 60% concrete.
[c] Superplasticizer CUGLA 80/20.
[d] Air entrainer Tilman AEA3.

From each concrete mixture six cubes, sized 15x15x15 cm^3, have been prepared and, as outlined in the European standard NEN-EN 206-1 (NEN, 2001c) demolded after three days and placed under water for 25 days for subsequent curing. Next, from the six cubes, one cube is used for a standard 28-day compressive strength test. This test is incorporated in the study to verify the integrity of the manufactured test cubes. One other cube is used for the determination of the activity concentrations; the remaining four cubes are used first to determine the release of water and next the ^{222}Rn exhalation rate.

Water release and porosity

As mentioned in the introduction the presence of water in the pores strongly influences the ^{222}Rn exhalation rate. This clearly demonstrates the necessity to condition test specimen with respect to humidity prior to exhalation measurement (section 2.1). In this study the following conditioning has been used. Directly after the period under water, the four cubes for the determination of the ^{222}Rn exhalation rate are placed in a climate controlled test chamber at a temperature of 20 ± 2 °C and a relative humidity of 50 ± 5 %. The cubes are weighed together at regular intervals to follow the drying process with time. When the decline in moisture content is less than 0.07% (w/w) in 7 days, the cubes are considered to be in equilibrium with their environment and ready for analysis (NEN, 2001b).

Furthermore, the drying data of these cubes are used for the calculation of the porosity of the concrete mixtures. Per concrete mixture the data can be described with the following equation:

$$W(t) = W_{\text{inf}} - W_c \cdot \exp(-kt). \tag{4.14}$$

In this equation $W(t)$ is the released amount of water (in kg) of the four test cubes together as a function of the conditioning time; W_{inf} is the released amount of water at t=∞ (kg); W_{inf} - W_c the released amount of water at t=0 (kg); k is a rate constant (d^{-1}); and t is the conditioning time (d), taking the start of the conditioning as t=0. Using the method of least squares the parameters W_{inf}, W_c and k are calculated for each concrete mixture. The fitting procedure did not use the first 3 days of drying data as the specimen lost relatively large amounts of water during these days. Therefore eq. (4.14) provides an accurate fit starting at day 3. Fig. 4.7 shows the results of some mixtures together with the fitted correlations.

Since the cubes are fully saturated at the moment they are taken out of the water bath, the porosity of each mixture can be calculated from the total released amount of water, i.e. W_{inf} from eq. (4.14); subsequent division by the density of water results in the total volume of the pores. It has been shown that only the capillary pores dry out, while the smaller gel pores remain water-filled. The porosity calculated in this way (eq. (4.15)) therefore reflects that of the capillary pores:

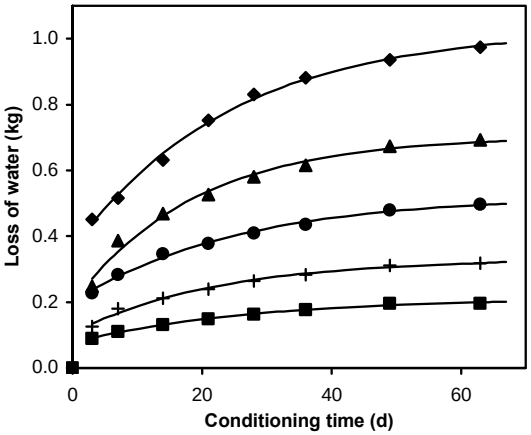

Figure 4.7
Loss of water of the mixtures as a function of the conditioning time. Each sample consists of four test cubes. The symbols indicate the measured values, the solid lines are the results according to eq. (4.14) for the samples coded 27, 20, 4, 19 and 2 from top to bottom.

$$\varepsilon_P = \frac{V_P}{V_T} = \frac{W_{\text{inf}}}{\rho_W V_T}. \tag{4.15}$$

In this equation ε_P represents the capillary porosity; V_P the volume of the capillary pores (m^3); V_T the total volume of the four test cubes (0.0135 m^3); and ρ_W the density of water (kg m^{-3}).

For the mixtures including an air entrainer (i.e. mixture coded 17 and 18 from series IV), this calculation results in too low values since the induced voids are largely air-filled all the time. Since the compositions of these mixtures are identical to that of mixture 4 (with the exception of the air entraining agent), the differences in densities have been used to determine the volume of the extra voids. The air bubbles porosity (ε_A) is calculated according to:

$$\varepsilon_A = \frac{V_A}{V_T} = \frac{M_{\text{inf},4} - M_{\text{inf},x}}{\rho_{\text{inf},4} V_T} = \frac{\rho_{\text{inf},4} - \rho_{\text{inf},x}}{\rho_{\text{inf},4}}, \tag{4.16}$$

with V_A the volume of the entrained air bubbles (m^3); V_T the total volume of the four test cubes (0.0135 m^3); $M_{\text{inf},4}$ and $\rho_{\text{inf},4}$ the mass of the four test cubes (kg) and density (kg m^{-3}) of mixture 4 at $t=\infty$, respectively; $M_{\text{inf,x}}$ and $\rho_{\text{inf,x}}$ are the same for mixture 17 or 18. The total porosity of mixture 17 and 18 is then equal to the sum of ε_P as calculated for mixture 4 according to eq. (4.15) and ε_A, calculated according to eq. (4.16).

Natural radioactivity concentrations

The natural radioactivity concentrations are determined by gamma-ray spectrometry according to the Dutch standard NEN 5697 (NEN, 2001a; section 3.1). The natural radioactivity levels of the base materials are determined in the same way as described above, except that these were not ground. The ^{226}Ra levels of these materials are presented in Table 4.7.

Table 4.7
^{226}Ra activity concentration of the base materials and standard deviation due to counting statistics in Bq kg^{-1}.

Component	Mean ± SD
Portland cement (CEM I 32.5R)	54 ± 2
Blast furnace slag cement (CEM III 42.5)	139 ± 2
Sand	5.4 ± 0.9
River gravel	2.4 ± 0.6
Recycled granulates	20.6 ± 1.2

Radon exhalation

The ^{222}Rn exhalation rate is determined according to the standard method NEN 5699 (NEN, 2001b; section 2.2).

Radon release factor

A side effect of the different compositions of the various concrete mixtures is that the ^{226}Ra activity concentrations vary considerably, which in itself can influence the ^{222}Rn exhalation rate. To compensate for this effect, the exhalation rates are normalized to the measured ^{226}Ra activity concentrations. Therefore a radon release factor is defined as the ratio between the amount of ^{222}Rn released per unit of time to the environment and that produced within the mixture by decay of ^{226}Ra,

$$F_{Rn} = \frac{E_m}{\lambda\ a} 100\,, \tag{4.17}$$

in which F_{Rn} is the ^{222}Rn release factor (%); E is the measured ^{222}Rn exhalation rate in Bq (kg s)$^{-1}$; λ is the decay constant of ^{222}Rn (s^{-1}); and a is the activity concentration of ^{226}Ra (Bq kg^{-1}). The release factor is calculated according to this equation, taking the ^{226}Ra radioactivity concentration as found by gamma-ray spectrometry for the broken concrete cube.

A disadvantage of eq. (4.17) is that it applies to the concrete mixture as a whole, ignoring the origin of ^{226}Ra. For a correct interpretation of the exhalation results it is therefore necessary to extend this equation to the component level; if the measured ^{222}Rn

exhalation rate is split up into a contribution of each of the components mentioned in Table 4.7, eq. (4.17) can be rewritten as:

$$F_{Rn} = \frac{100}{\lambda\ a} \sum_{i}^{n} E_{m,i} = \sum_{i}^{n} \left(\frac{a_i}{a}\ F_{Rn,i} \right). \tag{4.18}$$

In this equation the variables have the same meaning as in eq. (4.17) and in addition: n is the number of components from which the mixture is made up; $E_{,i}$ the ^{222}Rn exhalation rate in Bq (kg s)$^{-1}$ due to component i; a_i the activity concentration of ^{226}Ra of component i (Bq per kg concrete); and $F_{Rn,i}$ the ^{222}Rn release factor of component i (%). The ratio of a_i over a in the conditioned concrete mixtures is assumed to be the same as in the fresh paste and is calculated for each mixture from the values presented in Table 4.6 and 4.7

The release of ^{222}Rn from both sand and river gravel is thought to be negligible in comparison with that of the cements because of the much larger particle sizes of these aggregates. Furthermore most ^{226}Ra originates from the cements (Table 4.7). Kovler and co-workers (2005) also pointed to the crucial role of cement in the exhalation. If the ^{222}Rn release of sand and gravel in series I to IV is neglected, $F_{Rn,cement}$ follows directly from eq. (4.18). This release factor represents what part of the ^{226}Ra activity of the cement results in an actual release of ^{222}Rn. In the result section it will be demonstrated that the main role of cement also holds for the concrete mixtures with the recycled aggregates, i.e. the mixtures coded 20 to 23 from series V.

Radon emanation factor

In the introduction the ^{222}Rn emanation factor is put forward; it reflects the part of the produced ^{222}Rn that reaches the pores. This mixture-related factor is an important physical quantity in the line of events leading to the exhalation of ^{222}Rn from building materials. In this study the ^{222}Rn release factor is calculated from the measured exhalation rate. In this section we ascertain to what extend the release factor is equivalent to the emanation factor. For one-dimensional exhalation, the relation between the radon release factor and the emanation factor can be found by combining eq. (4.13) and eq. (4.17):

$$F_{Rn,1} = \eta\ \frac{l}{L} \tanh\left(L/l\right). \tag{4.19}$$

In this equation $F_{Rn,1}$ is the ^{222}Rn release factor for a one-dimensional approach (%); η is the emanation factor (%); l is the diffusion length of ^{222}Rn (m); and L is half of the thickness of the considered wall or floor (m). The average path length of a radon atom to reach the exterior of the construction part in this situation is $L/2$. The test cubes in this study, however, exhale from all sides and therefore will show higher exhalation rates. The

extent of the increase depends on the value of the diffusion length. The test cubes in this study with an edge of 2*L* can be considered to be made up of six identical pyramids with height *L* and their apex located in the centre of the cube. For such a pyramid the set of points having the same distance x to the base (i.e. the exterior of the cube), can be described as $4(L\text{-}x)^2$. The average distance that radon atoms have to bridge to reach the outside of the test cube can therefore be described as:

$$\bar{x} = \frac{1}{N}\int_0^L 4(L-x)^2 \cdot x\, dx \text{ and } N = \int_0^L 4(L-x)^2\, dx, \qquad (4.20)$$

in which *N* is a normalizing factor equal to the volume of the considered pyramid. Solving these equations leads to an average distance of *L*/4, twice as low as for a corresponding wall or floor with thickness 2*L*. Thus, provided that the parameter *L* is bisected (i.e. taken as 0.0375 m), the relation between the ^{222}Rn release factor, F_{Rn}, as calculated from the measuring results (eq. (4.17)) and the emanation factor can be described as in eq. (4.19).

As reported by Kovler and co-workers (2004) the literature data on the diffusion length range from about 0.06 m for heavy concretes to 0.30 m for lightweight species. In Fig. 4.8 the ratio between F_{Rn} and η for the test cubes is plotted against this range of diffusion lengths. From this figure it can be concluded that the ^{222}Rn release factor reflects the emanation factor very well with an underestimation of 10% at most. Therefore the differences in ^{222}Rn release factors as determined in this study have to be attributed to variations in the emanation factors of the concrete mixtures.

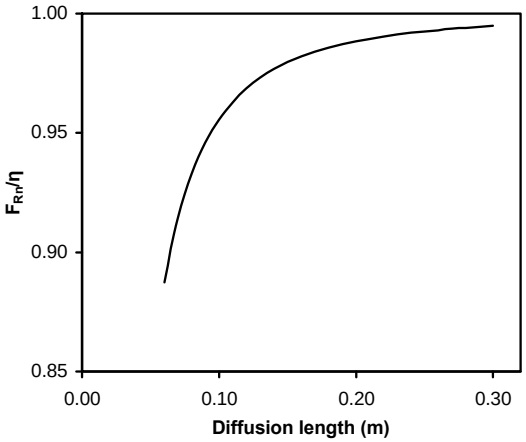

Figure 4.8
Equivalence of the ^{222}Rn release factor and emanation factor as a function of the diffusion length for the range 0.06 to 0.30 m.

4.3.3 Results and discussion

The results of the measurements and calculations are summarized in Table 4.8. The measured ^{222}Rn exhalation rates vary between 3.7 and 13 μBq (kg s)$^{-1}$, which is comparable with that in other (national) studies as summarized in Table 3.3. The uncertainties in the ^{222}Rn exhalation rates and the ^{226}Ra activity concentrations, averaged over all mixtures, are found to be about 4 and 5%, respectively. This results in an averaged uncertainty of 7% (range 5 to 11%) in the ^{222}Rn release factor.

The aim of this paper was to study the influence of the porosity on the exhalation rate. Therefore five series with a total of 23 mixtures were prepared to generate a wide range of porosities. For each series a key parameter was varied to induce the porosity. As shown in Table 4.8 the total porosities of the test specimen in this study range from less than 1% to 16%. As a check on the integrity of the manufactured test cubes, a standard compressive strength test has been incorporated in this study. It is known that the compressive strength has an inverse relationship with the porosity (e.g. Neville, 1995). Fig. 4.9 includes the expected exponential relation for the normal, standard concretes from series I to III. A linear relation is found for the mixtures that contain an air entraining agent (series IV) and the mixtures to which recycled aggregates are added (series V). The dashed line in this figure connects the data points of these series with that of the respective reference mixtures, i.e. the concrete mixtures 4 and 19, respectively. That distinct relations are found for the various combinations of series has to be attributed to the different ways to introduce the porosities. Since no irregularities are detected, the integrity of all concrete mixtures can be assumed.

In series I a range in porosities is obtained by varying the amount of Portland cement. Increasing the cement content leads to a denser, less porous concrete with a higher strength. All these effects are indeed found in Table 4.8. More cement also accounts for an increase of the ^{226}Ra activity concentration and proportional of the amount of ^{222}Rn gas produced within the test specimen. However, this increase is not accompanied by a similar trend in the measured ^{222}Rn exhalation rates, because the porosity reduces with increasing cement content. Repeating the experiments of series I with blast furnace slag cement (series II), shows results that are consistent with those from series I. Since the ^{226}Ra activity concentration of blast furnace slag cement is substantially higher (Table 4.7), this reflects the increased activity concentration in comparison to series I. Furthermore, mixtures cemented with blast furnace slag are known to have a much denser concrete structure, leading to lower porosities as compared to corresponding mixtures with Portland cement.

Table 4.8.
Results of measurements and calculations.

Concrete mixture and short description		Cement type[a]	W/C ratio[b]	^{222}Rn exh. rate[c] (μBq (kg s)$^{-1}$)	^{226}Ra[c] act. concentration (Bq kg^{-1})	Radon release factor[c] mixture (%)	Radon release factor[c] cement (%)	Moisture W_{inf} (kg)	Total porosity	Compressive strength (N mm^{-2})	Density[d] (kg m^{-3})
I. Amount of Portland cement											
1	550 kg m^{-3}	P	0.23	5.7 ± 0.6	13.9 ± 0.6	19.6 ± 2.1	23.9 ± 2.6	0.142	0.011	86.1	2469
2	450 kg m^{-3}	P	0.30	7.0 ± 0.3	11.5 ± 0.6	28.8 ± 2.0	36.7 ± 2.8	0.213	0.016	72.3	2441
3	350 kg m^{-3}	P	0.42	7.4 ± 0.2	9.7 ± 0.6	36.8 ± 2.5	50.2 ± 3.9	0.346	0.026	58.9	2425
4	315 kg m^{-3}	P	0.53	8.1 ± 0.3	7.7 ± 0.3	50.2 ± 2.8	70.5 ± 5.1	0.521	0.039	39.8	2384
5	280 kg m^{-3}	P	0.63	7.8 ± 0.0	7.5 ± 0.6	49.6 ± 3.9	72.2 ± 6.7	0.630	0.047	30.4	2357
6	200 kg m^{-3}	P	0.87	6.0 ± 0.2	5.4 ± 0.3	52.8 ± 3.2	87.8 ± 7.6	0.865	0.064	18.2	2333
II. Amount of blast furnace cement											
7	550 kg m^{-3}	B	0.26	3.7 ± 0.2	27.9 ± 1.6	6.3 ± 0.5	6.8 ± 0.6	0.128	0.009	82.2	2441
8	450 kg m^{-3}	B	0.32	4.4 ± 0.2	24.1 ± 1.1	8.8 ± 0.5	9.7 ± 0.6	0.164	0.012	69.7	2422
9	350 kg m^{-3}	B	0.41	5.3 ± 0.2	19.0 ± 0.8	13.3 ± 0.8	15.2 ± 0.9	0.245	0.018	59.2	2390
10	315 kg m^{-3}	B	0.52	5.7 ± 0.3	15.7 ± 0.6	17.2 ± 1.1	19.9 ± 1.3	0.350	0.026	44.3	2372
11	280 kg m^{-3}	B	0.63	6.4 ± 0.4	16.4 ± 0.8	18.4 ± 1.5	21.6 ± 1.8	0.417	0.031	36.1	2349
12	200 kg m^{-3}	B	0.87	6.9 ± 0.5	11.1 ± 0.5	29.6 ± 2.5	37.1 ± 3.3	0.611	0.045	21.3	2328
III. Amount of water											
13	90 kg m^{-3}	P	0.29	4.7 ± 0.1	9.0 ± 0.7	25.0 ± 2.1	36.0 ± 3.5	0.174	0.013	75.7	2460
14	103 kg m^{-3}	P	0.33	5.5 ± 0.4	9.9 ± 0.4	26.5 ± 2.3	38.0 ± 3.7	0.196	0.015	75.4	2466
15	134 kg m^{-3}	P	0.43	7.5 ± 0.1	9.2 ± 0.5	38.9 ± 2.0	55.3 ± 3.8	0.332	0.025	55.6	2423
4	166 kg m^{-3}	P	0.53	8.1 ± 0.3	7.7 ± 0.3	50.2 ± 2.8	70.5 ± 5.1	0.521	0.039	39.8	2384
16	196 kg m^{-3}	P	0.62	9.5 ± 0.3	9.7 ± 0.8	46.4 ± 4.3	64.4 ± 6.5	0.705	0.052	27.0	2328
IV. Amount of air entraining agent											
4	None	P	0.53	8.1 ± 0.3	7.7 ± 0.3	50.2 ± 2.8	70.5 ± 5.1	0.521	0.039	39.8	2384
17	0.94 kg m^{-3}	P	0.52	8.8 ± 0.2	10.9 ± 0.5	38.4 ± 1.9	53.9 ± 3.6	0.741	0.122[e]	21.1	2186
18	1.9 kg m^{-3}	P	0.52	7.8 ± 0.3	8.9 ± 0.3	42.0 ± 2.3	58.9 ± 4.1	0.782	0.163[f]	13.7	2088
V. Amount of gravel replacer											
19	0%	P	0.52	9.2 ± 0.4	10.5 ± 0.5	41.7 ± 2.6	56.3 ± 4.2	0.533	0.040	39.5	2369
20	20%	P	0.52	10.5 ± 0.4	12.7 ± 0.7	39.7 ± 2.6	60.6 ± 4.5	0.616	0.046	39.9	2324
21	50%	P	0.52	10.9 ± 0.1	13.6 ± 0.6	38.2 ± 1.8	68.5 ± 3.8	0.768	0.057	35.9	2277
22	80%	P	0.52	12.3 ± 0.7	18.6 ± 0.8	31.5 ± 2.3	64.8 ± 5.1	0.932	0.069	32.9	2211
23	100%	P	0.52	12.8 ± 0.3	23.6 ± 1.0	25.8 ± 1.3	57.6 ± 3.4	1.031	0.076	35.5	2161

[a] P=Portland cement; B=blast furnace slag cement.
[b] Water-to-cement ratio, excluding water to saturate recycled aggregate fraction.
[c] Mean ± 1SD.
[d] Density calculated for t=infinite.
[e] Of which 0.083 taken by air bubbles.
[f] Of which 0.124 taken by air bubbles.

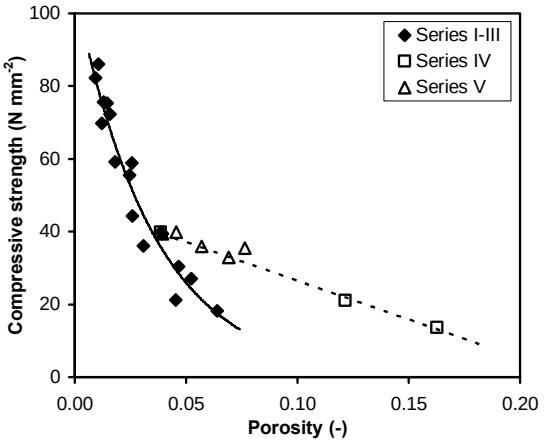

Figure 4.9
The compressive strength as a function of the porosity.

To compensate for the variation in ^{226}Ra activity concentration of the various mixtures, the measured ^{222}Rn exhalation rates are normalized to this activity concentration according to eq. (4.17) and expressed in the ^{222}Rn release factor of the mixture. When this factor is plotted against the porosity, Fig. 4.10 is obtained, showing distinct relations for the mixtures cemented with Portland and blast furnace slag. In series III also Portland cement is used, except that the range in porosities of the mixtures is realized by varying the amount of water at a fixed amount of cement. This leads to approximately identical ^{226}Ra activity concentrations, and less dense, more porous concrete specimen the more water is added, with increasing ^{222}Rn exhalation rates as a result (Table 4.8). As illustrated in Fig. 4.10 the results of this series comply well with that of series I. Evidently, there is no difference whether the porosity is changed either through the amount of water or through the amount of cement. As mentioned in the previous section the porosity in these three series reflects the volume of the capillary pores in the concrete mixtures.

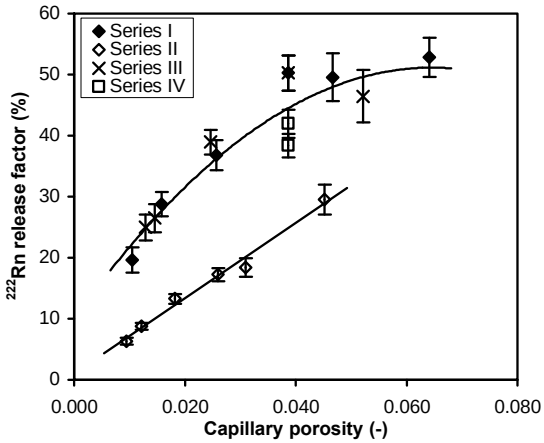

Figure 4.10
^{222}Rn release factor as a function of the porosity for the mixtures cemented with Portland (upper line) and blast furnace slag cement (bottom line). The error bars indicate ± 1 SD.

In series IV the total porosity is the largest of all series. This porosity has been created by the use of an air-entraining agent, keeping the rest of the compositions identical. Even though the mixture compositions are the same, the ^{226}Ra activity concentrations differ slightly, partly due to differences in sample density. The ^{222}Rn exhalation rates do not follow the expected trend from the first three series and the large porosities are not accompanied by high exhalation rates. However, when the ^{222}Rn release factor of these mixtures is plotted against the capillary porosity instead of the total porosity as is done in Fig. 4.10, these data points fit close to that of the other Portland-based series. This can be explained as follows. In the Materials and methods section it is demonstrated that the deduced ^{222}Rn release factors in this study are practically equal to the emanation factors, the portion of the ^{222}Rn atoms that reaches the pores. The escape of ^{222}Rn from the mineral matrix is mainly due to the recoil energy it obtains upon the decay of a ^{226}Ra atom. In most minerals the recoil distance is in the range 20 to 70 nm (Tanner, 1980). Thus, only those ^{222}Rn atoms that are formed near the surface of a pore wall will be able to leave it. In other words, not the pore volume but the internal pore area is indicative for the ^{222}Rn release factor. As demonstrated in the Appendix, addition of an air-entraining agent hardly adds to the internal pore area. This leaves a main role for the capillary pore area and makes that the results of mixtures 17 and 18 from series IV well fit into that of series I and III.

In series V the porosity was changed by replacing the dense river gravel in successive steps by more porous recycled aggregates (40% recycled masonry and 60% recycled concrete) without changing the composition of the matrix. As can be concluded from Table 4.8, the porosity goes up the more recycled aggregate is added and this is accompanied by a slight increase in the exhalation of ^{222}Rn gas; nevertheless the ^{222}Rn release factor decreases as a result of the 10 times higher ^{226}Ra activity concentration of the recycled aggregates in comparison with that of standard river gravel (Table 4.7). In Fig. 4.11 the exhalation rates of the mixtures 19-23 of series V are plotted against the recycled aggre-

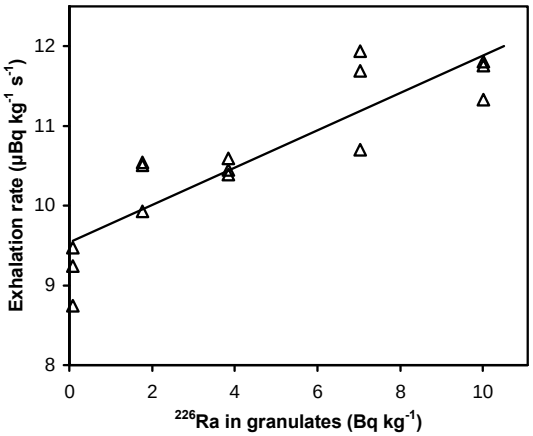

Figure 4.11
Triplicate results of the ^{222}Rn exhalation rate plotted against the activity concentration of ^{226}Ra present in the granulate fraction, expressed as Bq per kg concrete. The drawn line is the best fit as found by linear regression according to the method of least-squares. The correlation coefficient R is 0.89. The results of both quantities are normalized to the density of sample 19.

gate-related ^{226}Ra activity concentrations in these mixtures. The means and SD's of the linear regression coefficients c_0 and c_1 are found to be (9.6 ± 0.2) µBq (kg s)$^{-1}$ and (0.23 ± 0.03) x 10^{-6} s^{-1}, respectively (n=15). Assuming that the contribution of river gravel and sand to the ^{222}Rn exhalation is negligible, the ^{222}Rn release factor of the cement and recycled aggregate fraction can be calculated from these values in accordance with eq. (4.18). For the cement a release factor of (59 ± 2)% is inferred and (11 ± 2)% for the recycled aggregates. For the other concrete mixtures in this study cemented with Portland cement at a w/c ratio of 0.52, essentially the same cement-based release factor of (60 ± 7)% is found (n=4). If the ^{222}Rn release of the recycled aggregates is denied and entirely attributed to the cement, a cement-based release factor of (63 ± 5)% can be calculated (Table 4.8, n=4). Since this last figure is not significantly different from both others (Student's t-test, $p<0.05$), no corrections for the ^{222}Rn contribution from the recycled aggregate fraction were implemented.

Based on these results it can be concluded that the exhaled ^{222}Rn mainly originates from the applied cement, even in the case of series V where significant amounts of ^{226}Ra are introduced through the addition of recycled aggregates. The mixture-related ^{222}Rn release factor, as defined in eq. (4.17), appears not to be the adequate quantity to express the release of ^{222}Rn. This is illustrated in Table 4.8 in which for series V the increase in exhalation rate results in a decrease of the mixture-related ^{222}Rn release factor. Normalizing the exhalation rate of ^{222}Rn to the ^{226}Ra activity concentration introduced by the cements, leading to the cement-based release factor, overcomes this drawback.

In the continuation of the discussion two transitions are made: (a) the measured ^{222}Rn exhalation rates of all 23 mixtures are expressed in this cement-based ^{222}Rn release factor, and (b) since the capillary pore volume is governed by the w/c ratio, a switch to this parameter is made as well. Fig. 4.12 shows the cement-based release factor as a function of the w/c ratio for all five series. Although the ways to obtain the various porosities differ from series to series, the results coincide very well within each type of cement. For both types of cement applies that on raising the w/c ratio, the average size of the capillary pores will increase; as a result more internal pore area will become available and the more ^{222}Rn is able to emanate from the solid matrix into the pore system. If the curves are extrapolated, they appear not to cross the X-axis in the origin but at a w/c ratio of 0.08 and 0.12, respectively. Obviously, the w/c ratio has to exceed a certain threshold value before the induced pores are sufficiently interconnected to assure a transport of ^{222}Rn to the exterior of the test cubes.

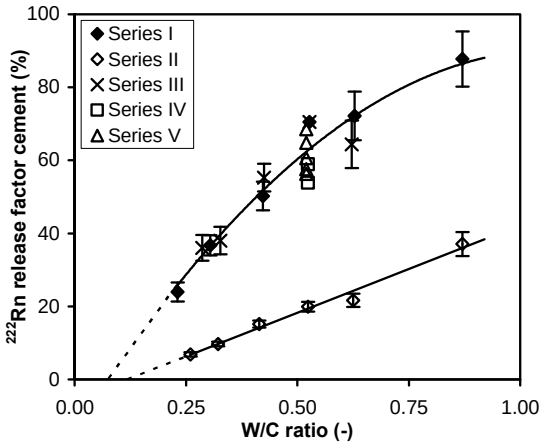

Figure 4.12.
Cement-based ^{222}Rn release factor as a function of the w/c ratio for the mixtures cemented with Portland (upper line) and blast furnace slag cement (bottom line). The error bars indicate ± 1 SD. The drawn lines are the best fits as found by regression according to the method of least-squares. The corresponding correlation coefficients are 0.95 and 0.99, respectively.

In prior research contradictory results of the effect of the w/c ratio on the exhalation rate have been published (Ulbak *et al*., 1984; Kunsch and Hartl, 1989; Kovler *et al*., 2005; section 4.2). Partly this is due whether the exhalation rate is normalized to the ^{226}Ra activity concentration or not. The present study shows a distinct increase with the w/c ratio, in agreement with the results reported earlier by Kunsch and Hartl (1989) and section 4.2.

In this study no attempt has been made to quantify the pore size distribution and internal pore area of the concrete mixtures, due to a lack of specialized equipment and experience to realize this. Besides, the determination of these parameters is not without discussion and a multitude of different test methods is in use, which sometimes shows considerably different results. Literature data, appropriate to the present study, are scarce; to our knowledge no pore area data in relation to the w/c ratios have been published for blast furnace slag mixtures. Mikhail and Selim (1966) have reported data on the internal pore area of Portland cement pastes. The data were obtained by gas adsorption measurements, using a number of adsorbates at various w/c ratios. The adsorbates included nitrogen gas, most commonly used in this technique. The advantages and limitations of the use of nitrogen have been summarized elsewhere (Aligizaki, 2006). From the nitrogen data of Mikhail and Selim the area/volume ratio of the pores is determined and a best fit is prepared as a function of the w/c ratio. Subsequently, based on the w/c ratio of each of the mixtures from series I and III, the corresponding area/volume ratio of the pores is calculated and multiplied by their porosity. Per concrete mixture this results in a specific pore area, expressed as m^2 pore area per m^3 of concrete specimen. Fig. 4.13 shows the results of this calculation together with the results on porosity found in this study. The latter variable shows a linear increment with the w/c ratio, while the pore area clearly deviates at higher ratios. This is due to the fact that raising the w/c ratio predominantly shifts the median diameter of the capillary pores to larger values. The drawn line in Fig.

4.13 represents the cement-based ^{222}Rn release factor and is copied from Fig. 4.12. The good correlation between the release factor and the pore area data supports the suggested role of the capillary pore area in the exhalation of ^{222}Rn.

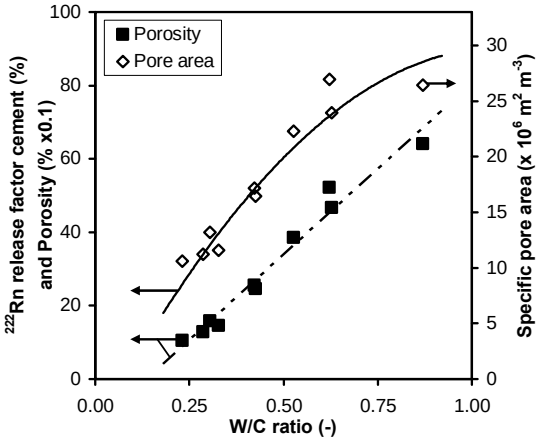

Figure 4.13
Cement-based ^{222}Rn release factor, porosity and specific pore area as a function of the w/c ratio for the mixtures from series I and III (Portland cement). The solid line indicates the cement-based ^{222}Rn release factor (left axis); the dashed line is the best fit of the porosity data indicated as filled squares (left axis); and the open diamonds represents the data points on specific pore area (right axis).

4.3.4 Conclusions

In this study five methods have been applied to create a range in concrete porosities by either varying the amount of Portland cement and blast furnace slag cement, the amount of water at a fixed amount of Portland cement, addition of an air entraining agent and replacing the river gravel in successive steps by recycled aggregates. In all mixtures the amount of cement is found to be the main contributor to the released amount of ^{222}Rn. Since changing the composition of the mixtures sharply influences the ^{226}Ra activity concentration of the mixtures, which in itself can affect the ^{222}Rn exhalation rate, the exhalation rate data are normalized to the ^{226}Ra activity concentration introduced by the cements into a quantity which in this paper is referred to as the cement-based ^{222}Rn release factor. Decreasing the amount of Portland or blast furnace slag cement in the mixtures results in a gradual increase of this release factor, as is the case when the amount of water of the fresh paste is raised at a fixed amount of cement. Mixtures cemented with blast furnace slag cement show lower cement-based release factors than corresponding mixtures with Portland cement. Addition of an air entraining agent or replacement of river gravel by recycled aggregates, although strongly influencing the porosity of the mixtures, has no significant effect on the above-mentioned release factor.

The porosity of the present set of concrete mixtures covers a range from 1 to 16%. From this study it can be concluded that, although the applied methods to attain the porosities in the concrete mixtures are widely different, the capillary porosity plays a dominant role in the release of ^{222}Rn, rather then the total porosity. Since the w/c ratio of

the fresh paste provides a good indication of the capillary porosity, it is demonstrated that in all cases this parameter is the guiding factor in the fabrication of concretes low in ^{222}Rn exhalation. There is no difference whether the w/c ratio is changed either through the amount of water or through the amount of cement. The lower the w/c ratio, the less capillary pore area will be available from which the ^{222}Rn can emanate from the mineral matrix into the pore system. The good correlation between the cement-based ^{222}Rn release factor and literature data on the internal capillary pore area support the results in this study.

Appendix

In the case of mixtures to which an air-entraining agent is added (series IV), the internal pore area includes that of the capillary pores and that of the entrained air bubbles. If the capillary pores are considered as cylinders with a fixed diameter d_P, the area/volume ratio of these pores equals $4/d_P$; for the spherical air entrained voids with diameter d_A this ratio is $6/d_A$. The ratio between the internal area of the spherical air voids and the capillary pores, K, can then be approximated by:

$$K = \frac{3}{2} \cdot \frac{\varepsilon_A}{\varepsilon_P} \cdot \frac{d_P}{d_A}; \qquad (4.21)$$

ε_A and ε_P in this equation refer to the porosity introduced by the air entrainer and that of the capillary pores, calculated according eq. (4.16) and eq. (4.15), respectively. For the capillary pores diameters are reported to range from about 10 nm to 10 μm (Gartner *et al.*, 2002) and for the spherical air voids from 0.01 to 1 mm (Aligizaki, 2006). If the log-average values are entered into eq. (4.21) together with the porosity data of the concrete mixture 17 and 18 from series IV, the ratio K is found to be less than 1%. Although this calculation approximates the actual situation only roughly, it demonstrates that the internal pore area introduced by the addition of an air-entraining agent is small in comparison to that of the capillary pore system. Therefore, addition of such an agent will have no influence on the internal pore area.

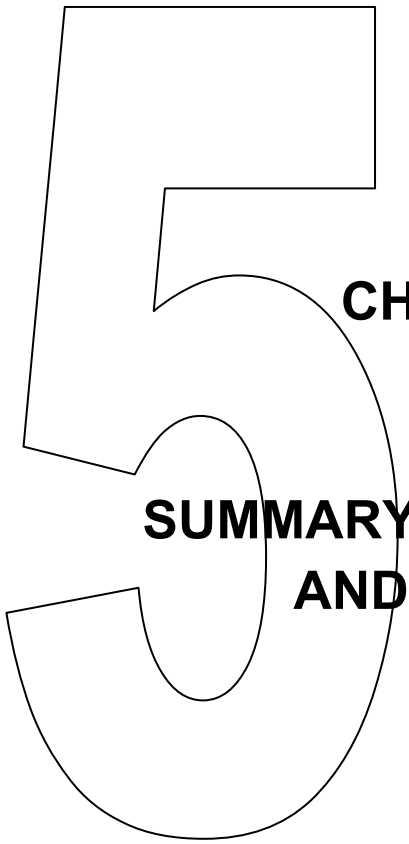

CHAPTER 5

SUMMARY, CONCLUSIONS AND OUTLOOK

5.1 Introduction

The progeny of ^{222}Rn is one of the most extensively investigated carcinogens. Epidemiological studies of ^{222}Rn-exposed underground miners have demonstrated clearly an excess risk of lung cancer at relatively high concentrations. Extrapolation from these studies to lower exposures has suggested that, next to smoking, residential ^{222}Rn is the second leading cause of lung cancer for the general population, provided that there is no threshold for cancer induction. However, breathing rates and smoking habits of miners are not representative for the general population and, moreover, the mine and home environments differ substantially, which made these risk projections uncertain.

Combined analysis of residential case-control studies dispelled these uncertainties and determined the increase lung cancer risk at about 16% per 100 Bq m^{-3} ^{222}Rn gas (Darby *et al*., 2004). If this is approximately correct, then about 2% of the cases of lung cancer in the Netherlands can be attributed to ^{222}Rn progeny, equivalent to 200 deaths per annum. Including the exposures due to ^{220}Rn progeny and external radiation, the total number of fatalities due to natural radiation in homes is estimated to be about 650 each year, with a 95% confidence interval of 250 to 1300.

The aim of this thesis was to determine the role of building materials as part of the natural radiation exposure in the Netherlands. For that, in chapter 2 methods for determination of the ^{222}Rn exhalation rate and absorbed dose rate in air from building materials have been introduced and validated. In chapter 3 these methods, together with one for the determination of the natural radioactivity concentrations are applied to a cross section of the building materials available at the Dutch market. An investigation of the indoor radiation exposure in a small housing estate is also part of this chapter. Chapter 4 includes studies after the possibilities to reduce the resulting exposure, i.e. the retarding effect of surface coatings and the effect of composition and production on the exhalation rate from samples of concrete.

In this chapter the highlights in the chapters 2 to 4 are put forward and discussed.

5.2 Methods

Chapter 2 of this dissertation describes the development of methods that were applied to map the situation in the Netherlands. The first method concerns the determination of ^{222}Rn exhalation rates of the most common stony building materials. It is a so-called purge-and-trap method in which a sample is enclosed in a container from which the ^{222}Rn is continuously purged by a constant flow of nitrogen gas and directed through a trapping agent. The trapped activity is quantified by liquid scintillation counting (LSC).

Three performance characteristics of the method have been assessed, i.e. (a) the repeatability; (b) the intralaboratory reproducibility; and (c) the interlaboratory reproduci-

bility. The values of these quantities range from 3 to 6% (section 2.2). These values should be considered in view of the large spread in exhalation rates from sample to sample, even within the same class of materials (Table 3.3); in that context uncertainties introduced by the measurements become insignificant compared to these inherent variations.

The limit of detection of the purge-and-trap method depends on (a) the analytical method to quantify the trapped activity; (b) the counting time; (c) the size of the analytical sample; and (d) the duration of the trapping period. Using LSC as analytical method and a counting time of 1 h, the standard conditions applied throughout this dissertation, the detection limit is calculated as 11 mBq ^{222}Rn, according to the method described by Currie (1968). For most building materials an absorption time of half an hour suffices; in special situations, for instance for bricks, longer absorption times may be necessary.

Although the method dates from the early 1990's, it is still state-of the-art; in 2001 the method was adopted as the primarily method in the Dutch standard NEN 5699 (NEN, 2001b). It has been used to verify the agreements in a covenant between the Dutch government and the Dutch building industry (De Wit and Nijland, 2009). The Working Group on radioactivity measurements of Technical Committee 85 (Nuclear Energy), Subcommittee 2 (Radiation Protection) of the International Organization for Standardization (ISO) has adopted a resolution to include the method into a new standard ISO 11665-9 (ISO/AFNOR, 2009). In view of the Construction Product Directive (EC, 1988), discussed in section 1.7, there is an urgent need for such a standard procedure.

In section 2.3 we present a method that allows the evaluation of gamma radiation doses in large groups of dwellings. The basis for these calculations is formed by a fixed set of specific absorbed dose rates, as determined for a standard geometry defined by Koblinger (1978). This quantity is defined as the absorbed dose rate in air due to an activity concentration of a construction material of 1 Bq kg^{-1} of the parent radionuclide in secular equilibrium with their daughters. Correction factors have been assessed that quantify the influence of various room and material related parameters on these specific absorbed dose rates. To verify the accuracy, our method is applied to three Dutch reference dwellings, i.e. a row house, a semi-detached house and an apartment building. The results of the model are compared with those found by MCNP (Briesmeister, 2000), a well-benchmarked multi-purpose Monte Carlo code. The differences are found to range from 3 to 7%, with an average of 4%. The advantage of our method over MCNP is that its computing time is much shorter, making it especially suited to evaluate large clusters of dwellings.

5.3 Concentration and exposures

In chapter 3 four studies have been presented on measured concentrations and exposure levels. The first study reports on a nation-wide survey, held in 2001, on the natural radioactivity concentrations and ^{222}Rn exhalation rates of the prevailing building materials in the Netherlands. The highest radionuclide concentrations were found in a porous inner wall brick to which fly ash was added. The second highest were clay bricks with average ^{226}Ra and ^{228}Ra levels around 40 Bq kg^{-1}. Concrete and mortar show the highest exhalation rates with a fairly broad range of 1 to 13 μBq kg^{-1} s^{-1}. Low natural radioactivity levels are associated with either natural gypsum or gypsum from flue gas desulphurization units, and low exhalation rates were found for clay bricks.

Natural radioactivity concentrations in the main building materials available on the Dutch market are in general on the low side of the range reported in a European-wide literature survey (EC, 1999a). As a consequence the absorbed dose rates in Dutch living rooms due to gamma radiation are also at the low side (UNSCEAR, 2000). The building material induced annual indoor effective dose is calculated at a mean and SD of 0.25 ± 0.03 mSv if 7000 h per year are spent indoors (section 3.4).

From the third national ^{222}Rn survey Bader and colleagues (2009) concluded that building materials contribute for about 70% to the indoor ^{222}Rn level in living rooms. This value is based on the difference between the ^{222}Rn efflux and influx of the living room. A similar value is obtained from the ^{222}Rn exhalation rates of the various building materials as determined in section 3.1 in combination with the average occurrence of these building materials in Dutch livings (De With and De Jong, 2009). In that study it is shown that almost 90% of the building material related ^{222}Rn originates from the concrete construction elements. From a control study carried out in 2008, it was concluded that the radiation dose due to this material has not changed with time (De Wit and Nijland, 2009).

In the second study a national survey is presented on natural radioactivity concentrations in gypsum plasters and mortars (section 3.2) and reflects the situation around 1995. The study encompassed materials from several manufacturers and included products for the non-professional sector. Three classes of material could be distinguished: class I materials of low activity concentrations, i.c. natural gypsum; class II products with intermediate levels (100-150 Bq kg^{-1} of both ^{226}Ra and ^{228}Ra); and class III products with levels up to 200-250 Bq kg^{-1} per radionuclide. The elevated levels of ^{226}Ra and ^{228}Ra as found in gypsum plasters will, in addition, lead to enhanced gamma dose rates and ^{222}Rn concentrations in homes. Nevertheless, in view of the thin layers of plasters compared to the total building mass of a dwelling, these increases will be negligible. A high ^{228}Ra-activity concentration in plaster will however result in an increase of the ^{220}Rn exhalation rate and hence to elevated indoor ^{220}Rn progeny levels and lung doses. A worst-case

estimate suggests an extra residential effective dose of around 2 mSv per annum (De With and De Jong, 2009).

The third study (section 3.3) deals with exposure to ^{222}Rn and external radiation of inhabitants in a new housing estate. In this estate 101 houses were built at about the same time, but according to nine designs. The effective dose to inhabitants ranged from 0.4 to 1.4 mSv per year, depending on the design. The houses at the low end of this range are characterized by a timber frame construction with an airtight concrete ground floor, with the remaining floors made of timber and with flue gas desulphurization gypsum inner walls; the radiation burden of the inhabitants resembles the outdoor situation. Designs constructed according to a 'conventional' building method (concrete floors, cavity walls made of brick and sand-lime brick), show similar ^{222}Rn concentrations and dose rates. One of the main findings of this study is that the design has a more pronounced influence on the radiation burden than habits and preferences of its occupants. A similar conclusion can be drawn from the results published by Lomas and Green (1994), who found no significant difference in ^{222}Rn concentration after new occupants moved into a dwelling.

The distribution of gamma dose rates due to building materials in the Netherlands is the topic of the fourth study (section 3.4). The model described in section 2.3 is applied to a representative set of dwellings of which the areas occupied by the various building material are well documented. Using a Monte Carlo method, building material and housing data are combined with activity concentrations and densities of 90 samples of building material, as emerged from section 3.1. By simulating 100,000 combinations, the distribution of the absorbed dose rate in Dutch livings is computed and found to be near Gaussian with an average and SD of 51 ± 6 nGy h^{-1}. After correction for the indoor contribution of cosmic and terrestrial radiation, their actual distribution corresponds to within 5% with measurements.

The last study is particularly relevant with respect to a recent publication of the European Commission on the revision of the Basic Safety Standards (EC, 2009). The proposal involves a limitation of the gamma dose rate induced by building materials, according to a simplified calculation model presented in section 1.7. In this EC-model no corrections factors are applied for the differences between dwellings, leading to a severe overestimation of the building materials induced dose rates. The model described in this dissertation takes almost the complete set of parameters into account. Although not all considered parameters are equally important, it clearly demonstrates the shortcomings of the European Commission's model and, to a lesser extent, that of the national model, known as the Stralingsprestatienorm (NEN, 2002).

5.4 Radon-transport mechanisms and mitigation

In the Netherlands building materials account for about 70% of the indoor ^{222}Rn concentration and hence various ways have been investigated to reduce their ^{222}Rn release rates. Knowledge of the underlying mechanisms is essential, because it may lead to new or additional reduction possibilities. The application of surface coatings to reduce ^{222}Rn exhalation rates in an existing situation has been verified by a number of investigators. The study in section 4.1 has evaluated the retaining effect of over 20 surface coatings commonly used in the Netherlands for decoration of walls and ceilings. These coatings were found to be ineffective. Reductions up to 75% can be achieved by industrial surface coatings based on epoxy resin and polyurethane, when applied to all sides of test walls. According to model calculations, the exhalation rates could be reduced by 95% if these coatings were applied to the inward facing surface of walls only. Lesions, however, can negate a large portion of the sealing effectiveness and the same applies for cracks that may develop over time in the paint layer due to ageing.

Concrete is found to be a major contributor to indoor ^{222}Rn. In the construction of houses various kinds of concretes mixtures are applied. In the sections 4.2 and 4.3 the influence of several parameters on the ^{222}Rn exhalation rate has been investigated. In section 4.2 the parameters related to composition and production processes on the ^{222}Rn exhalation rate of concretes were studied. Especially the water evaporation rate during conditioning was found to have a strong positive correlation with the calculated ^{222}Rn emanating power.

Within a series of 23 concrete mixtures, concrete compositions have been varied by changing the amount of cement, type of cement (Portland or blast furnace slag cement), water-to-cement ratio, use of an air entraining agent or the amount of recycled granulates. This resulted in a range of porosities from 1% to 16% (section 4.3). The ^{222}Rn exhalation rate is normalized to the ^{226}Ra level and expressed in the so-called ^{222}Rn release factor. Most ^{222}Rn originates from the cement and therefore a second ^{222}Rn release factor is based on the amount of ^{226}Ra in the cement fraction. Although the methods to attain the porosities in the concrete mixtures differ widely, this cement-related factor corresponds well with the capillary porosity of the mixtures. Since the water-to-cement ratio of the fresh paste is a good indicator of the capillary porosity, this is the guiding factor in the fabrication of concretes low in ^{222}Rn exhalation. The lower the water-to-cement ratio, the less capillary pore area will be available from which ^{222}Rn can emanate from the mineral matrix into the pore system. The good correlation between the cement-based ^{222}Rn release factor and literature data on the internal capillary pore area support the results of this study.

5.5 Final remarks and outlook

Building materials always have received special attention from the Dutch government, illustrated by the number of studies that were commissioned to develop a method to calculate and control building material-induced exposure of inhabitants (Ackers, 1990; Van Heijningen and Ackers, 1990; VROM, 1990b; Roelofs and Wiegers, 1995; NEN, 2002). According to the latest national ^{222}Rn survey, covering 1000 newly built houses in the period 1994-2003, the average ^{222}Rn concentration in the living room is 13-14 Bq m^{-3} (Blaauboer *et al*., 2007). As outlined in Table 5.1 the Netherlands has the lowest average ^{222}Rn level in the European Communities. The main four reasons are:

- a low ^{238}U contents of Dutch soils;
- a low ^{222}Rn release due to a high groundwater level in large parts of the country;
- a common building practice with well-ventilated crawl spaces; and
- a legal maximum air permeability of the ground floor.

Country	^{222}Rn (Bq m^{-3})
The Netherlands	14[a]
United Kingdom	20
Belgium	48
Germany	50
Denmark	59
France	62
Spain	90
Sweden	108
Finland	120

[a] Preliminary value (Blaauboer *et al*., 2007).

Table 5.1
Average ^{222}Rn concentrations in dwellings in some European countries (UNSCEAR, 2009).

Therefore, unlike most other countries, the soil beneath the houses only plays a minor role as a source for indoor ^{222}Rn. Consequently, building materials play a more prominent one and are estimated to be responsible for 70% of the indoor ^{222}Rn concentration. The contribution of building materials to the external exposure in houses is calculated at 55% (Table 1.8), leading to an average total exposure due to building materials of 0.6 mSv per year. This corresponds to about 40% of the average radiation burden due to natural radiation sources in the Netherlands (Van Bruggen *et al*., 2004). In summary it may be stated that the situation in the Netherlands with respect to ^{222}Rn and external radiation in dwellings is reasonably well understood.

Things are different for ^{220}Rn. Thus far, ^{220}Rn or its short-lived decay products have not been investigated for dwellings and building materials in the Netherlands. Therefore the number of potential fatalities due to exposure to ^{220}Rn progeny, calculated as 60 per year,

is based on model calculations as reported by De With and De Jong (2009). In that study it was assumed that building materials were not covered with a plaster layer or paint coating. As suggested in section 3.2 and confirmed by model calculations, application of plasters high in ^{228}Ra can seriously enhance the inhabitants' radiation burden and consequently the number of fatalities.

As indicated in section 1.8.2 the average ^{222}Rn concentration as found in the third national survey is more than a factor of two lower than expected on the basis of the results of the second survey. As reported by Vargas and Ortega (2007) the ^{222}Rn measuring devices applied in the second survey show an unintended high sensitivity for ^{220}Rn of about 50%. As the difference between the results of both surveys is of the order of 15 Bq m^{-3}, the average ^{220}Rn concentration near the measuring devices would be about 30 Bq m^{-3}. It is, however, not really possible to reconstruct an (average) source term for ^{220}Rn from this finding. Due to the short half-life of ^{220}Rn, there is a steep concentration gradient of the ^{220}Rn concentration from the surface of construction elements to the centre of a room. The shape of this curve is seriously affected by the so-called turbulent diffusion coefficient (De With and De Jong, 2009), an indicator for mixing of indoor air. This parameter is mainly influenced by time-dependent temperature-driven airflows and is not well known. Conducting a survey on ^{220}Rn concentrations in Dutch dwellings to obtain a better insight in the ^{220}Rn source term in the radiation burden is therefore only meaningful if such a study is combined with explicit attention for this parameter.

Another way to get knowledge on the ^{220}Rn source term, and with that on the exposure of the Dutch population to short-lived decay products of ^{220}Rn is to survey ^{220}Rn exhalation rates of Dutch building materials, comparable with that on ^{222}Rn as reported in section 3.1. Since practically all ^{220}Rn originates from building materials, the source term can be obtained by combination of exhalation rate data with results on the distribution of the various building materials in Dutch dwellings. The exhalation rate of plaster should be considered in this survey, since, as indicated above this material may have high exhalation rates. Determination of retarding effects by coatings and wallpapers regularly applied in Dutch households, will be part of such a study. Although reported in section 4.1 that these materials have no effect with regard to the exhalation of ^{222}Rn, due to the factor 75 lower ^{220}Rn diffusion length, there might be a significant reduction of ^{220}Rn exhalation.

Aim of the suggested studies is to attain a similar knowledge base for ^{220}Rn as for ^{222}Rn, but is experimentally a great challenge.

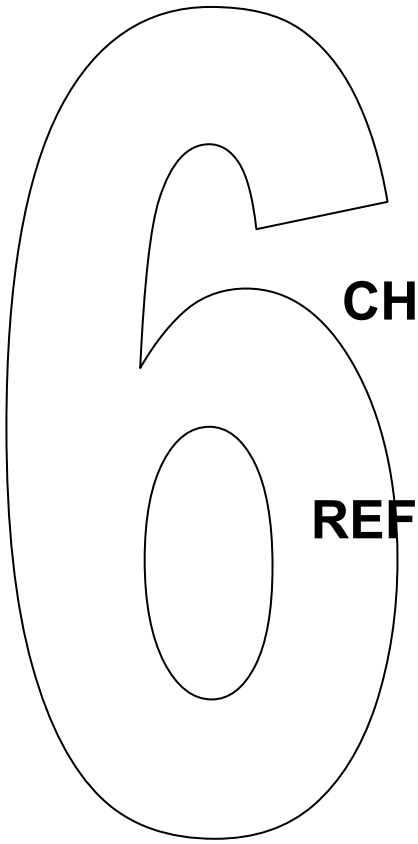

CHAPTER 6

REFERENCES

Abu-Jarad, F. and Fremlin, J. H. (1983)
Effect of internal wall covers on radon emanation inside houses. Health Phys. 44:243-248.

Ackers, J.G. (1985)
Concentratie van radionucliden in bouwmaterialen. Stralenbeschermingsreeks 8. Ministerie van Volkshuisvesting, Ruimtelijke Ordening en Milieubeheer, Den Haag, the Netherlands (in Dutch).

Ackers, J.G. (1990)
Methodiek ter bepaling van toegevoegde stralingsdoses als gevolg van het toepassen in woningen van bouwmaterialen met een verhoogd gehalte aan natuurlijke radioactiviteit. Stralenbeschermingsreeks 42. Ministerie van Volkshuisvesting, Ruimtelijke Ordening en Milieubeheer, Den Haag, the Netherlands (in Dutch).

Ackers, J.G., Den Boer, J.F., De Jong, P. and Wolschrijn, R.A. (1985)
Radioactivity and radon exhalation rates of building materials in the Netherlands. Sci. Total Environm. 45:151-156.

Ademola, J.A. and Farai, I.P. (2005)
Annual effective dose due to natural radionuclides in building blocks in eight cities of south-western Nigeria. Radiat. Prot. Dosim. 114:524-526.

Ahmad, N., Hussein A.J.A. and Aslam. (1998)
Radiation doses in Jordanian dwellings due to natural radioactivity in construction materials and soil. J. Environ. Radioact. 41:127-136.

Aligizaki, K.K. (2006)
Pore structure of cement-based materials. Testing, interpretation and requirements. Modern concrete technology series 12. Taylor & Francis, London.

Al-Zoughool, M. and Krewski, D. (2009)
Health effects of radon: a review of the literature. Int. J. Radiat. Biol. 85:57-69.

Arvela, H. (1995)
Seasonal variation in radon concentrations of 3000 dwellings with model comparisons. Radiat. Prot. Dosim. 59:33-42.

Auxier, J.A., Shinpaugh, W. H., Kerr, G. D. and Christian, D. J. (1974)
Preliminary studies of the effects of sealants on radon emanation from concrete. Health Phys. 27:390-392.

Bader, S., Dekkers, S.A.J. and Blaauboer, R.O. (2009)
Ventilatie en de samenhang met radon in nieuwbouwwoningen in Nederland. Resultaten en analyses van tracermetingen in het project VERA. Rapport 610790006/2009. Rijksinstituut voor Volksgezondheid en Milieu. Bilthoven, the Netherlands (in Dutch).

Bale (1951)
Hazards associated with radon and thoron. Unpublished memorandum to the U.S. Atomic Energy Commission. Reprinted in Health Phys. 38:1061-1066 (1980).

Bannink, D.W., Keen, A., Köster, H.W., Pennders, R.M.J. and De Winkel, J.H. (1986)
De natuurlijke radioactiviteit van Nederlandse gronden. Stralenbeschermingsreeks 13. Ministerie van Volkshuisvesting, Ruimtelijke Ordening en Milieubeheer, Den Haag, the Netherlands (in Dutch).

Barton, T.P. and Ziemer, P.L. (1986)
The effects of particle size and moisture content on the emanation of Rn from coal ash. Health Phys. 50:581-588.

Berkvens, P., Kerkhove, E. and Vanmarcke, H. (1988)
Three-dimensional treatment of steady-state ^{222}Rn diffusion in building materials: introducing a practical modified one-dimensional approach. Health Phys. 55:793-799.

Bosmans, G. (1996)
Stralingsaspecten van gangbare bouwmaterialen: samenvattend rapport. Report R95373. INTRON, Sittard, the Netherlands (in Dutch).

Blaauboer, R.O., Dekkers, S.A.J., Slaper, H. and Bader S. (2007)
Stralingsbelasting in nieuwbouwwoningen – voorlopige resultaten. VERA survey 2006. Report 610790004/2007. Rijksinstituut voor Volksgezondheid en Milieu, Bilthoven, the Netherlands (in Dutch).

Blaauw, M., Bode, P. and Glass, H.J. (2000)
Het bepalen van de prestatiekenmerken van NEN 5697. Report 133-00-01. Interfacultair Reactorinstituut, Delft, the Netherlands (in Dutch).

Blaauw, M., Glass, H.J., De Jong, P. and Van Dijk, W. (2001)
The Dutch norm for the determination of natural radioactivity levels in construction materials applied to concrete samples. J. Radioanal. Nucl. Chem. 249:177-180.

Brenner, D.J. and Sachs, R.K. (2002)
Do low dose-rate bystander effects influence domestic radon risks? Int. J. Radiat. Biol. 78:593-604.

Briesmeister, J.F. (Ed.) (2000)
MCNP - A general Monte Carlo n-particle transport code, version 4C. Report LA-13709-M. Los Alamos National Laboratory, Los Alamos.

Buchli, R. and Burkart, W. (1989)
Influence of subsoil geology and construction technique on indoor air ^{222}Rn levels in 80 houses of the central Swiss alps. Health Phys. 56:423-429.

CBS (2009)
Centraal Bureau voor de Statistiek. Available at http://www.cbs.nl. Accessed October 25, 2009.

Cohen, B.L. (1995)
Test of the linear no-threshold theory of radiation carcinogenesis for inhaled radon decay products. Health Phys. 68:157-174.

Cornelissen, H.J.M. and De Gids, W.F. (1997)
Overzicht luchtdoorlatendheidsgegevens eengezinswoningen. Report 97-BBI-R1295. TNO, Rijswijk, the Netherlands (in Dutch).

Cox, M.G. and Harris, P.M. (2006)
Software specifications for uncertainty evaluation. Technical report DEM-ES 010. National Physics Laboratory, Teddington.

Cozmuta, I. (2001)
Radon generation and transport – A journey through matter. PhD thesis. Rijksuniversiteit Groningen, Groningen, the Netherlands.

Cozmuta, I., Van der Graaf, E.R. and De Meijer, R.J. (2003)
Moisture dependence of radon transport in concrete: measurements and modeling. Health Phys. 85:438-456.

Culot, M.V.J., Schiager, K.J. and Olson, H.G. (1978)
Development of a radon barrier. Health Phys. 35:375-380.

Currie, L.A. (1968)
Limits for qualitative detection and quantitative determination. Application to radiochemistry. Anal. Chem. 40:586-593.

Daoud, W.Z. and Renken, K.J. (2001)
Laboratory assessment of flexible thin-film membranes as a passive barrier to radon gas diffusion. Sci. Total Environm. 272:127-135.

Darby, S.C. and Doll, R. (1990)
Radiation and exposure. Nature 344:824.

Darby, S., Hill, D., Auvinen, A., Barros-Dios, J.M., Baysson, F. *et al*. (2004)
Radon in homes and risk of lung cancer: collaborative analysis of individual data from 13 European case-control studies. BMJ. doi:10.1136/bmj.38308.477650.63.

Darrall, K.G., Richardson, P.J. and Tyler, J.F.C. (1973)
An emanation method for determining radium using liquid scintillation counting. Analyst 98:610-615.

DB (1991)
Besluit van 16 december 1991, houdende technische voorschriften omtrent het bouwen van bouwwerken en de staat van bestaande bouwwerken (Bouwbesluit). Staatsblad 680:1-469 (in Dutch).

De Jong, P. and Van Dijk, W. (1994)
Reduction of the radon entry rate from building materials by industrial surface coatings. Radiat. Prot. Dosim. 56:179-183.

De Jong, P. and Van Dijk, W. (1995)
Laboratoriumwoning: het effect van ventilatie en luchtdoorlatendheid op de radonconcentratie. Report RD-I/9506-354. RD-TNO, Arnhem, the Netherlands (in Dutch).

De Jong, P. and van Dijk, W. (1999)
Factors affecting the radiation dose to inhabitants in a small new housing-estate in the Netherlands. Proc. Int. Symp. on Radon in the Living Environment, 19-23 April, 1999, Athens, Greece. pp 911-919.

De Jong, P. and Van Dijk, W. (2001)
Factors affecting the radiation dose to inhabitants in a small new housing-estate in the Netherlands. Sci. Total Environm. 272:141-142

De Jong, P. and Van Dijk, W. (2005)
Testing of radon-reducing measures under strictly controlled conditions in a laboratory house. Seventh Int. Symp. on the natural Radiation environment (NRE-VII), Rhodes, Greece 20-24 May 2002. Eds. McLaughlin, J.P., Simopoulos, S.E. and Steinhäusler, F. Radioactivity in the Environment 7:276-283. Elsevier.

De Jong, P. and Van Dijk, W. (2008a)
Modeling gamma radiation dose in dwellings due to building materials. Health Phys. 94:33-42.

De Jong, P. and Van Dijk, J.W.E. (2008b)
Calculation of the indoor gamma dose rate distribution due to building materials in the Netherlands. Radiat. Prot. Dosim. 132:381-389.

De Jong, P. and Van Dijk, J.W.E. (2009)
Analyse van het externe dosistempo in woningen. VERA survey 2006. Report NRG-K5098/09.97299. Nuclear Research and consultancy Group, Arnhem, the Netherlands (in Dutch).

De Jong, P., Van Dijk, W., Van Hulst, J.G.A. and Van Heijningen, R.J.J. (1996)
The effect of the composition and production process of concrete on the ^{222}Rn exhalation rate. Environm. Int. 22(Suppl.1):S287-S293.

De Jong, P., Van Dijk, W. and Burger, H.P. (1998a)
^{226}Ra and ^{228}Ra concentrations in gypsum plasters and mortars used in the Netherlands. Proc. Second Int. Symp. on Naturally Occurring Radioactive Materials (NORM II), Nov. 10-13, 1998, Krefeld, Germany. pp 58-61.

De Jong, P., Van Dijk, W. and Brouwer, D.H. (1998b)
Onderzoek naar de stofbelasting van stukadoors. Report 98 CSD 343 PJ/VL. TNO Centrum voor Stralingsbescherming en Dosimetrie, Arnhem, the Netherlands (in Dutch).

De Jong, P., Van Gellecum, J.F.B., Van Dijk, W., Dijkstra, J.B., Van der Graaf, E.R. *et al*. (2001)
Bepaling van de stralingseigenschappen van bouwmaterialen. Report K5002/01.IM260. Nuclear Research and consultancy Group, Arnhem, the Netherlands (in Dutch).

De Jong, P., Van Dijk, W., De Vries, W., Van der Graaf, E.R. and Roelofs, L.M.M. (2005)
Interlaboratory comparison of three methods for the determination of the radon exhalation rate of building materials. Health Phys. 88:59-64.

De Jong, P., Van Dijk, W., Van der Graaf, E.R. and De Groot, T.J.H. (2006)
National survey on the natural radioactivity and ^{222}Rn exhalation rate of building materials in the Netherlands. Health Phys. 91:200-210.

De Meijer, R.J. (1992)
Infiltratie van radon in woningen. Stralenbeschermingsreeks 50A. Ministerie van Volkshuisvesting en Ruimtelijke Ordening en Milieubeheer, Den Haag, the Netherlands (in Dutch).

De Meijer, R.J., Put, L.W. and Veldhuizen, A. (1986)
Radonconcentraties in Nederland. Stralenbeschermingsreeks 14. Ministerie van Volkshuisvesting, Ruimtelijke Ordening en Milieubeheer, Den Haag, the Netherlands (in Dutch).

De Wit, M.S. and Nijland, T.G. (2009)
Monitoring stralingsbelasting door beton: toetsing 2008. Report TNO-034-DTM-2009-03365. TNO Bouw en Ondergrond, Delft, the Netherlands (in Dutch).

De With, G. and De Jong, P. (2009)
Modellering van de thoron- en thorondochterconcentraties in het binnenmilieu. Report NRG-912089/09.93696. Nuclear Research and consultancy Group, Arnhem, the Netherlands (in Dutch).

EC (1988)
Council Directive 89/106/EEC of 21 December 1988 on the approximation of laws, regulations and administrative provisions of the Member States relating to construction products. Off. J. Eur. Commun. L40. European Communities, Luxembourg.

EC (1990)
Commission recommendation 90/143/Euratom of 21 February 1990 on the protection of the public against indoor exposure to radon. Off. J. Eur. Commun. L80. European Communities, Luxembourg.

EC (1996)
Council directive 96/29/Euratom of 13 May 1996 laying down basic safety standards for the protection of the health of workers and the general public against the dangers arising from ionizing radiation. Off. J. Eur. Commun. L159. European Communities, Luxembourg.

EC (1999a)
Enhanced radioactivity of building materials. Radiation Protection 96. European Commission, Luxembourg.

EC (1999b)
Radiological protection principles concerning the natural radioactivity of building materials. Radiation Protection 112. European Commission, Luxembourg.

EC (2009)
European Commission Services considerations with regard to natural radiation sources in BSS Directive. 16 January 2009. Available at: http://ec.europe.eu/energy/nuclear/consultations/doc/2009_04_20_natural_radiation_sources.pdf. Accessed May 2009.

Eichholz. G.G., Matheny, M.D. and Kahn, B. (1980)
Control of radon emanation from building materials by surface coating. Health Phys. 39:301-304.

Emsley, J. (2003)
Nature's building blocks. An A-Z guide to the elements. Oxford University Press, Oxford.

EPA (2003)
EPA assessment of risks from radon in homes. Report EPA 402-R-03-003. U. S. Environmental Protection Agency, Washington.

Fleischer, R.L. (1987)
Moisture and ^{222}Rn emanation. Health Phys. 52:797-799.

Fleischer, R. L. (1992)
Permeability of caulking compounds to ^{222}Rn. Health Phys. 62:91-95.

Folkerts, K.H., Keller, G. and Muth, H. (1984)
Experimental investigations on diffusion and exhalation of ^{222}Rn and ^{220}Rn from building materials. Radiat. Prot. Dosim. 7:41-44.

Gan, T.H., Mason, G.C., Wise, K.N., Whittlestone, S. and Wyllie, H.A. (1986)
Desorption of ^{222}Rn by moisture and heat. Health Phys. 50:407-410.

Gartner, E.M., Young, J.F., Damidot, D.A. and Jawed, I. (2002)
Hydration of Portland cement. In: Bensted, J. and Barnes, P. eds. Structure and performance of cements. 2nd ed., pp 57-113. Spon Press, London.

Gezondheidsraad (2000)
Radon: toetsing rapport 'BEIR VI'. Publication 2000/05. Gezondheidsraad, Den Haag, the Netherlands (in Dutch).

Grove (1999)
MicroShield, version 5.05; user's manual. Grove Engineering, Rockville.

Gualdrini G. and Ferrari P. (2004)
Intercomparison on the usage of computational codes in radiation dosimetry. Proceedings of the Bologna QUADOS International workshop, July 14-16, 2003, Bologna, Italy. ENEA, Bologna.

Gunby, J.A., Darby, S.C., Miles, J.C.H., Green, B.M.R. and Cox, D.R. (1993)
Factors affecting indoor radon concentrations in the United Kingdom. Health Phys. 64:2-12.

Hafez, A.-F. and Somogyi, G. (1986)
Determination of radon and thoron permeability through some plastics by track technique. Nucl. Tracks 12:697-700.

Hart, K.P. and Levins, D.M. (1986)
Steady-state Rn diffusion through tailings and multiple layers of covering materials. Health Phys. 50:369-379.

Hogeweg, B. (1986a)
Activiteitsmetingen in een groep van twintig woningen in de gemeente Bernisse en in een proefkamer. Stralenbeschermingsreeks 16. Ministerie van Volkshuisvesting, Ruimtelijke Ordening en Milieubeheer, Den Haag, the Netherlands (in Dutch).

Hogeweg, B (1986b)
Eindrapportage en evaluatie van het SAWORA-onderzoekprogramma naar het achtergrondniveau van de natuurlijke straling in Nederland. Stralenbeschermingsreeks 23. Ministerie van Volkshuisvesting, Ruimtelijke Ordening en Milieubeheer, Den Haag, the Netherlands (in Dutch).

Hol, G.H.P., Van Hulst, J.G.A., Van Heijningen, R.J.J. and De Jong, P. (1991)
Stralingsaspecten van geïmporteerde gebroken natuursteen. Report F 0205-01-001. DHV Bouw, Amersfoort, the Netherlands (in Dutch).

Hopke, P.K., Jensen, B., Li, C.-S., Montassier, N., Wasiolek, P. *et al*. (1995)
Assessment of the exposure to and dose from radon decay products in normally occupied houses. Environ. Sci. Technol. 29:1359-1364.

Hornung, R.W. and Meinhardt, T.J. (1987)
Quantitative risk assessment of lung cancer in U.S. uranium miners. Health Phys. 52:417-430.

Hubbell, J.H and Seltzer, S.M. (1995)
Tables of X-ray mass attenuation coefficients and mass energy-absorption coefficients 1 keV to 20 MeV for elements Z=1 to 92 and 48 additional substances of dosimetric interest. Report PB95-220539. National Institute of Standards and Technology, Gaithersburg.

Hutter, A.R. and Knutson, E.O. (1998)
An international intercomparison of soil gas radon and radon exhalation measurements. Health Phys. 74:108-114.

ICRP (1991)
1990 Recommendations of the International Commission on Radiological Protection. ICRP publication 60. International Commission on Radiological Protecton. Pergamon Press, Oxford.

ICRP (1993)
Protection against radon-222 at home and at work. ICRP publication 65. International Commission on Radiological Protection. Pergamon Press, Oxford.

ICRP (1994)
Human respiratory tract model for radiological protection. ICRP publication 66. International Commission on Radiological Protecton. Pergamon Press, Oxford.

ICRP (1996)
Conversion coefficients for use in radiological protection against external radiation. ICRP publication 74. International Commission on Radiological Protection. Pergamon Press, Oxford.

ICRP (2005)
Low-dose extrapolation of radiation-related cancer risk. ICRP publication 99. International Commission on Radiological Protecton. Elsevier.

ICRP (2007)
The 2007 recommendations of the International Commission on Radiological Protection. ICRP publication 103. International Commission on Radiological Protecton. Elsevier.

ICRP (2009)
Statement on radon. ICRP Ref 00/902/09. International Commission on Radiological Protection. Available at http://www.icrp.org/icrp_radon.asp. Accessed November, 2009.

ICRU (1992)
Measurement of dose equivalents from external photon and electron radiations. ICRU report 47. International Commission on Radiation Units and measurements, Bethesda.

ICRU (1998)
Conversion coefficients for use in radiological protection against external radiation. ICRU report 57. International Commission on Radiation Units and Measurements, Bethesda.

Ingersoll, J.G. (1983)
A survey of radionuclide contents and radon emanation rates in building materials used in the U.S. Health Phys. 45:363-368.

ISO (1995)
Guide to the expression of uncertainty in measurement. ISO/IEC Guide 98. International Organization for Standardization, Geneva.

ISO/AFNOR (2009)
WG 17 "Radioactivity measurement" report presented at plenary meeting of SC2 in Vienna on 2009-04-09. Doc. number N0994. International Organization for Standardization and Association Française de Normalisation, La Plaine Saint-Denis, France.

Isobe, T., Feigelson, E.D., Akritas, M.G. and Babu, G.J. (1990)
Linear regression in astronomy. I. Astrophys. J. 364:104-113.

Jacobi, W. (1993)
The history of the radon problem in mines and homes. In: Protection against radon-222 at home and at work. ICRP publication 65, pp 39-45. International Commission on Radiological Protecton. Pergamon Press, Oxford.

JCGM (2008)
Evaluation of measurement data - Supplement 1 to the "Guide to the expression of uncertainty in measurement" - Propagation of distributions using a Monte Carlo method. JCGM report 101. Joint Committee for Guides in Metrology. Bureau International des Poids et Mesures, Paris.

Jha, G., Raghavayya, M. and Padmanabhan, N. (1982)
Radon permeability of some membranes. Health Phys. 42:723-725.

Jiránek, M. and Hůlka, J. (2001)
Applicability of various insulating materials for radon barriers. Sci. Total Environm. 272:79-84.

Jonassen, N. (1983)
The determination of radon exhalation rates. Health Phys. 45:369-376.

Jonassen, N. and McLaughlin, J.P. (1980)
Exhalation of radon-222 from building materials and walls. In: Gesell, T.F. and Lowder, W.M. eds. Natural Radiation Environment III. Vol. 2, 1211-1224. US DOE, Oak Ridge.

Julius, H.W. and Van Dongen, R. (1985a)
Radiation doses to the population in the Netherlands, due to external natural sources. Sci. Total Environm. 45:449-458.

Julius, H.W. and Van Dongen, R. (1985b)
Stralingsbelasting van de bevolking en stralingsniveaus in het binnenmilieu in Nederland t.g.v. natuurlijke gammabronnen. Stralenbeschermingsreeks 10. Ministerie van Volkshuisvesting, Ruimtelijke Ordening en Milieubeheer, Den Haag, the Netherlands (in Dutch).

Keller, G. and Schmier, H. (1988)
Measurements and investigations in radioactivity of gypsum from installations for flue-gas desulfurization in comparison with natural gypsum. Wissenschaft u Umwelt 4:199-201 (in German).

Keller, G., Kappel, R.J.A., Gerken, M., Wellmann, J., Kreuzer, M. *et al*. (1996)
Initial results of indoor radon measurements within the German radon studies. Environm Int 22, suppl 1:S665-S670.

Keller, G., Hoffmann, B. and Feigenspan, T. (2001)
Radon permeability and radon exhalation of building materials. Sci. Total Environm. 272:85-89.

Kloosterman, J.L. (1990)
MARMER: a flexible point-kernel shielding code; user manual version 2.0. Report IRI-131-89-03/2. Interfacultair Reactorinstituut, Delft, the Netherlands.

Koblinger, L. (1978)
Calculation of exposure rates from gamma sources in walls of dwelling rooms. Health Phys. 34:459-463.

Koblinger, L. (1984)
Mathematical models of external gamma radiation and congruence of measurements. Radiat. Prot. Dosim. 7:227-234.

Köster, H.W., Keen, A., Pennders, R.M.J., Bannink, D.W. and De Winkel, J.H. (1988)
Linear regression models for the natural radioactivity (^{238}U, ^{232}Th and ^{40}K) in Dutch soils: a key to anomalies. Radiat. Prot. Dosim. 24:63-68.

Kovler, K., Perevalov, A., Steiner, V. and Rabkin, E. (2004)
Determination of the radon diffusion length in building materials using electrets and activated carbon. Health Phys. 86:505-516.

Kovler, K., Perevalov, A., Levit, A., Steiner, V. and Metzger, L.A. (2005)
Radon exhalation of cementious materials made with coal fly ash: Part 2 – testing hardened cement-fly ash pastes. J. Environ. Radioact. 82:335-350.

Krewski, D., Lubin, J.H., Zielinski, J.M., Alavanja, M., Catalan, V.S. *et al*. (2005)
Residential radon and risk of lung cancer: a combined analysis of 7 North American case-control studies. Epidemiology 16:137-145.

Kunsch, B. and Hartl, G. (1989)
Radon exhalation of various concretes. Zem. Beton (Vienna) 34:28-31 (in German).

Lau, B.M.F., Balendran, R.V. and Yu, K.N. (2003)
Metakaolin as a radon retardant from concrete. Radiat. Prot. Dosim. 103:273-276.

Lembechts, J. (2002)
Straling in het binnenmilieu: bronnen en maatregelen. Brochure. Rijksinstituut voor Volksgezondheid en Milieu, Bilthoven, the Netherlands (in Dutch).

Lembrechts, J., Janssen, M. and Stoop, P. (2001)
Ventilation and radon transport in Dutch dwellings: computer modelling and field measurements. Sci. Total Environm. 272:73-78.

Leung, J.K.C., Tso, M.Y.W. and Ho, C.W. (1998)
Behavior of ^{222}Rn and its progeny in high-rise buildings. Health Phys. 75:303-312.

Lévesque, B., Gauvin, D., McGregor, R.G., Martel, R., Gingras, S. *et al*. (1997)
Radon in residences: influences of geological and housing characteristics. Health Phys. 72:907-914.

Li, Y., Schery, S.D. and Turk, B. (1992)
Soil as a source of indoor ^{220}Rn. Health Phys. 62:453-457.

Lide, D.R. and Haynes, W.M. (2010)
CRC Handbook of chemistry and physics. 90th ed., internet version 2010. CRC Press.

Lomas, P.R. and Green B.M.R. (1994)
Temporal variations of radon levels in dwellings. Radiat. Prot. Dosim. 56:323-325.

Lubin, J.H. (2003)
Studies of radon and lung cancer in North America and China. Radiat. Prot. Dosim. 104:315-319.

Lubin, J.H., Boice, J.D., Endling, C., Hornung, R.W., Howe, G. *et al*. (1995)
Radon-exposed underground miners and inverse dose-rate (protraction enhancement) effects. Health Phys. 69:494-500.

Lubin, J.H., Tomášek, L., Edling, C., Hornung, R.W., Howe, G. *et al*. (1997)
Estimating lung cancer mortality from residential radon using data for low exposures of miners. Radiat. Res. 147:126-134.

Máduar, M.F. and Hiromoto, G. (2004)
Evaluation of indoor gamma radiation dose in dwellings. Radiat. Prot. Dosim. 111:221-228.

Majborn, B. (1992)
Seasonal variations of radon concentrations in single-family houses with different sub-structures. Radiat. Prot. Dosim. 45:443-447.

Malanca, A., Pessina, V. and Dallara, G. (1993)
Radionuclide content of building materials and gamma ray dose rates in dwellings of Rio Grande do Norte, Brazil. Radiat. Prot. Dosim. 48:199-203.

Markkanen, M. (2001)
Challenges in harmonising controls on the radioactivity of building materials within the European Union. Sci. Total Environm. 272:3-7.

Marshall, J.L. and Marshall, V.R. (2003)
Ernest Rutherford, the “true discoverer” of radon. Bull. Hist. Chem. 28:76-83.

Mikhail, R.Sh. and Selim, S.A. (1966)
Adsorption of organic vapors in relation to the pore structure of hardened Portland cement pastes. In: Special Report 90:123-134. Symposium on Structure of Portland Cement Paste and Concrete. Highway Research Board. National Research Council, Washington.

Miller, K.M. and Beck, H.L. (1984)
Indoor gamma and cosmic ray exposure rate measurements using a Ge spectrometer and pressurised ionisation chamber. Radiat. Prot. Dosim. 7:185-189.

Mirza, N.M., Ali, B., Mirza, S.M., Tufail, M. and Ahmad, N. (1991)
A shape and mesh adaptive computational methodology for gamma ray dose from volumetric sources. Radiat. Prot. Dosim. 38, 307-314.

Moeller, D.W. and Fujimoto, K. (1984)
Cost evaluation of control measures for indoor radon progeny. Health Phys. 46:1181-1193.

Morawska, L. (1983)
Influence of sealants on ^{222}radon emanation rate from building materials. Health Phys. 44:416-418).

Mustonen, R. (1984)
Methods for evaluation of radiation from building materials. Radiat. Prot. Dosim. 7:235-238.

NAS (1999)
Health effects of exposure to radon. 6th Committee on Biological Effects of Ionizing Radiations (BEIR VI). National Academy of Sciences. National Academy Press, Washington.

NAS (2006)
Health risks from exposure to low levels of ionizing radiation. 7th Committee on Biological Effects of Ionizing Radiations (BEIR VII). National Academy of Science. National Academies Press, Washington.

NEA (2004)
NEA-1307: MARMER, point-kernel shielding calculation with nuclide concentrations from ORIGEN-S. Nuclear Energy Agency. Available at: http://www.nea.fr/abs/html/nea-1307.html. Accessed 23 December 2004.

NEN (1989)
Voorschriften beton uitvoering (VBU 1988). NEN 6722. Nederlands Normalisatie-instituut, Delft, the Netherlands (in Dutch).

NEN (1999)
Beton – Gestorte proefstukken – vervaardiging, bewaring en conditionering. NEN 5965. Nederlands Normalisatie-instituut, Delft, the Netherlands (in Dutch).

NEN (2000)
Cement – Part 1: Composition, specification and conformity criteria for common cements. NEN-EN 197-1(en). Nederlands Normalisatie-instituut, Delft, the Netherlands (in Dutch).

NEN (2001a)
Radioactivity measurements – Determination of the natural radioactivity in stony building materials by means of semiconductor gamma ray spectrometry. NEN 5697(en). Nederlands Normalisatie-instituut, Delft, the Netherlands.

NEN (2001b)
Radioactivity measurements – Determination method of the rate of the radon exhalation of dense building materials. NEN 5699(en). Nederlands Normalisatie-instituut, Delft, the Netherlands.

NEN (2001c)
Concrete – Part 1: Specification, performance, production and conformity. NEN-EN 206-1(en). Nederlands Normalisatie-instituut, Delft, the Netherlands.

NEN (2002)
Radiation performance of a living function – Method of determination. NEN 7181(en). Nederlands Normalisatie-instituut, Delft, the Netherlands.

Neville, A.M. (1978)
Properties of concrete. Pitman Publ., London.

Neville, A.M. (1995)
Properties of concrete. 4th ed. Education Limited, Harlow, England.

Noguchi, M., Takeda, K. and Higuchi, H. (1981)
Semi-emperical γ-ray peak efficiency determination including self-absorption correction based on numerical integration. Int. J. Appl. Radiat. Isotopes 32:17-22.

NOVEM (1992)
Achtergrondstraling op de voorgrond. Eindrapport van het onderzoekprogramma "Reguleerbare vormen van natuurlijke achtergrondstraling" (RENA). Nederlandse Maatschappij voor Energie en Milieu, Utrecht, the Netherlands (in Dutch).

O'Brien, R.S. (1997)
Gamma doses from phospho-gypsum plaster-board. Health Phys. 72:92-96.

O'Brien, R.S., Peggie, J.R. and Leith, I.S. (1995)
Estimates of inhalation doses resulting from the possible use of phospho-gypsum plaster-board in Australian homes. Health Phys. 68:561-570.

Othman, I. and Mahrouka, M. (1994)
Radionuclide content in some building materials in Syria and their indoor gamma dose rate. Radiat. Prot. Dosim. 55:299-304.

PEO (1986)
Straling in het leefmilieu. Resultaten van het onderzoekprogramma Stralingsaspecten van woonhygiëne en verwante radio-ecologische problemen (SAWORA). De Boer en Van Teylingen/Stichting Projectbeheerbureau Energie Onderzoek, Utrecht, the Netherlands (in Dutch).

Petropoulos, N.P., Anagnostakis, M.J. and Simopoulos, S.E. (2001)
Building materials radon exhalation rate: ERRICCA intercomparison exercise results. Sci. Total Environm. 272:109-118.

Pinel, J., Fearn, T., Darby, S.C. and Miles, J.C.H. (1995)
Seasonal correction factors for indoor radon measurements in the United Kingdom. Radiat. Prot. Dosim. 58:127-132.

Poffijn, A., Bourgoignie, R., Marijns, R., Uyttenhove, J., Janssens, A. and Jacobs, R. (1984)
Laboratory measurements of radon exhalation and diffusion. Radiat. Prot. Dosim. 7:77-79.

Pohl-Rühling, J., Steinhäusler, F. and Pohl, E. (1980)
Investigation on the suitability of various materials as ^{222}Rn diffusion barriers. Health Phys. 39:299-301.

Preston, D.L., Pierce, D.A., Shimizu, Y., Cullings, H.M. *et al*. (2004)
Effect of recent changes in atomic bomb survivor dosimetry on cancer mortality risk estimates. Radiat. Res. 162:377-389.

Puskin, J.S. (2003)
Smoking as a confounder in ecologic correlations of cancer mortality rates with average county radon levels. Health Phys. 84:526-532.

Put, L.W., De Meijer, R.J. and Hogeweg, B. (1985)
Survey of radon concentrations in Dutch dwellings. Sci. Total Environm. 45:441-448.

Reinhardt, H.W. (1985)
Beton als constructiemateriaal: eigenschappen en duurzaamheid. Delft University Press, Delft, The Netherlands (in Dutch).

Risica, S., Bolzan, C. and Nuccetelli, C. (2001)
Radioactivity in building materials: room model analysis and experimental methods. Sci Total Environm 272:119-126.

Roelofs, L.M.M. and Scholten, L.C. (1994)
The effect of aging, humidity, and fly-ash additive on the radon exhalation from concrete. Health Phys. 67:266-271.

Roelofs L.M.M. and Wiegers R.B. (1995)
Eenvoudige vertaalslag van stralingseigenschappen van bouwmaterialen naar stralingsdosis. Report 40799-NUC 95-5358. KEMA, Arnhem, the Netherlands (in Dutch).

Rogers, V.C. and Nielson, K.K. (1991)
Multiphase radon generation and transport in porous materials. Health Phys. 60:807-815.

Rogers, V.C., Nielson, K.K., Holt, R.B. and Snoddy, R. (1994)
Radon diffusion coefficients for residential concretes. Health Phys. 67:261-265.

Rutherford, P.M, Dudas, M.J. and Arocena, J.M. (1995)
Radon emanation coefficients for phosphogypsum. Health Phys. 69:513-520.

Samuelsson, C. (1987)
A critical assessment of radon-222 exhalation measurements using the closed-can method. ACS Symp. Ser. 331:203-218.

Schaap, L.E.J.J. (1996)
Effecten van maatregelen ter beperking van de natuurlijke achtergrondstraling in woningen. Report R43029A3.LS. Lichtveld Buis & Partners, Utrecht, the Netherlands (in Dutch).

Schaap, L.E.J.J., Van der Graaf, E.R. and Bosmans, G. (1998)
Stralingsprestatienorm: vooronderzoek. Report R43 111AO.LS. Lichtveld Buis & Partners, Utrecht, the Netherlands (in Dutch).

SenterNovem (2006)
Referentiewoningen. SenterNovem. Available at: http://www.senternovem.nl/epn/referentiewoningen. Accessed June 2006 (in Dutch).

Stoop, P., Glastra, P., Hiemstra, Y., De Vries, L. and Lembrechts, J. (1998)
Results of the second Dutch national survey on radon in dwellings. Report 610058006. Rijksinstituut voor Volksgezondheid en Milieu, Bilthoven, the Netherlands.

Stranden, E. (1979)
Radioactivity of building materials and the gamma radiation in dwellings. Phys. Med. Biol. 24:921-930.

Stranden, E. (1983)
Assessment of the radiological impact of using fly ash in cement. Health Phys 44:145-153.

Stranden, E., Kolstad, A.K. and Lind, B. (1984)
The influence of moisture and temperature on radon exhalation. Radiat. Prot. Dosim. 7:55-58.

Strong, K.P. and Levins, D.M. (1982)
Effects of moisture content on radon emanation from uranium ore and tailings. Health Phys. 42:27-32.

Swedjemark, G.A. (2004)
The history of radon from a Swedish perpective. Radiat. Prot. Dosim. 109:421-426.

SZW (1997)
Nationale MAC-lijst 1997-1998. Ministerie van Sociale Zaken en Werkgelegenheid. SdU, Den Haag, the Netherlands (in Dutch).

Tammes, E. and Vos, B.H. (1980)
Warmte- en vochttransport in bouwconstructies. Kluwer, Deventer, the Netherlands (in Dutch).

Tanner, A.B. (1980)
Radon migration in the ground: a supplementary review. In: Gesell, T.F., Lowder, W.M. eds. Natural Radiation Environment III. Vol. 1, 5-56. US DOE, Oak Ridge.

Thompson, R.E., Nelson, D.F., Popkin, J.H. and Popkin, Z. (2008)
Case-control study of lung cancer risk from residential radon exposure in Worcester county, Massachusetts. Health Phys. 94:228-241.

Tommel (1997)
Brief van staaatssecretaris Tommel aan de Voorzitter van de Tweede Kamer der Staten-Generaal. Tweede Kamer, vergaderjaar 1997, 21483, nr.21 (in Dutch).

Ulbak, K., Jonassen, N. and Bækmark, K. (1984)
Radon exhalation from samples of concrete with different porosities and fly ash additives. Radiat. Prot. Dosim. 7:45-48.

UNSCEAR (1988)
Sources, effects and risks of ionizing radiation. 1988 Report to the General Assembly, with annexes. United Nations Scientific Committee on the Effects of Atomic Radiation. United Nations, New York.

UNSCEAR (1993)
Sources and effects of ionizing radiation. 1993 Report to the General Assembly, with scientific annexes. United Nations Scientific Committee on the Effects of Atomic Radiation. United Nations, New York.

UNSCEAR (2000)
Sources and effects of ionizing radiation. UNSCEAR 2000 report to the General Assembly, with scientific annexes. Volume 1: Sources. United Nations Scientific Committee on the Effects of Atomic Radiation. United Nations, New York.

UNSCEAR (2008)
Sources-to-effects assessment for radon in homes and workplaces. UNCEAR 2006 report. Effects of ionizing radiation. Annex E. United Nations Scientific Committee on the effects of Atomic Radiation. United Nations, New York.

Urban, M. and Piesch, E. (1981)
Low level environmental radon dosimetry with a passive track etch detector device. Radiat. Prot. Dosim. 1:97-109.

Vaas, L.H., Kal, H.B., De Jong, P. and Slooff, W. (eds.) (1993)
Integrated criteria document radon. Report No. 710401021. Rijksinstituut voor Volksgezondheid en Milieu. Bilthoven, the Netherlands.

Valckenborg, R.M.E., Pel, L., Hazrati, K., Kopinga, K. and Marchand, J. (2001)
Pore water distribution in mortar during drying as determined by NMR. Mater. Struct. 34:599-604.

Van Bruggen, M., Van Aernsbergen, L.M., Blaauboer, R.O., Fast, T., Van der Graaf, E.R. *et al*. (2004)
Stralingsbelasting in het binnenmilieu. In: Beoordelingskader Gezondheid en Milieu: GSM-basisstations, Legionella, radon, fijn stof en geluid door wegverkeer. Fast, T. and Van Bruggen, M. Report 609031001/2004, pp 45-62. Rijksinstituut voor Volksgezondheid en Milieu, Bilthoven, the Netherlands (in Dutch).

Van Deynse, A., Poffijn, A. and Buysse, J. (1997)
Radon research among plaster workers and in the phosphate industry. Proc. Int. Symp. on Radiological problems with natural radioactivity in the non-nuclear industry, Sept. 8-10, 1997, Amsterdam, the Netherlands. Paper 2.5.

Van der Ham, E.R., Winder, C. and Ackers, J.G. (1991)
Verkennend onderzoek naar de kosten-effectiviteit van maatregelen ter beperking van natuurlijke achtergrondstraling in de woning. Stralenbeschermingsreeks 49. Ministerie van Volkshuisvesting, Ruimtelijke Ordening en Milieubeheer, Den Haag, the Netherlands (in Dutch).

Van der Pal, M. (2003)
Radon transport in autoclaved aerated concrete. PhD thesis. Bouwstenen series no. 75. Technische Universiteit Eindhoven, Eindhoven, the Netherlands.

Van der Spoel, W.H. (1998)
Radon transport in sand. A laboratory study. PhD thesis. Technische Universiteit Eindhoven, Eindhoven, the Netherlands.

Van Dijk, W. and De Jong, P. (1989)
Exhalatiesnelheid van radon-222 van Nederlandse bouwmaterialen en de invloed van verfsystemen. Stralenbeschermingsreeks 37. Ministerie van Volkshuisvesting, Ruimtelijke Ordening en Milieubeheer, Den Haag, the Netherlands (in Dutch).

Van Dijk, W. and De Jong, P. (1991)
Determining the ^{222}Rn exhalation rate of building materials using liquid scintillation counting. Health Phys. 61:501-509.

Van Dijk, J.W.E. and Julius, H.W. (1993)
Glow curve analysis for constant temperature hot gas TLD readers. Radiat. Prot. Dosim. 47:479-482.

Van Geel, P.L.B.A. (2004)
Bevestiging nadere afspraken met betrekking tot standstill straling in de woning. Letter dated 6 July 2004, reference SAS/2004056843, to the chairman of VNO/NCW. Ministerie van Volkshuisvesting, Ruimtelijke Ordening en Milieubeheer, Den Haag, the Netherlands (in Dutch).

Van Heijningen, R.J.J. and Ackers, J.G. (1990)
Normstelling ioniserende straling voor bouwprodukten. Stralenbeschermingsreeks 47. Ministerie van Volkshuisvesting, Ruimtelijke Ordening en Milieubeheer, Den Haag, the Netherlands (in Dutch).

Van Hulst, J.G.A., Beusen, G.J.H. and De Jong, P. (1993)
Verandering van stralingseigenschappen van beton(producten). Een verkenning van de beïnvloedingsmogelijkheden. Report F0633.01.001. DHV Bouw, Amersfoort, the Netherlands (in Dutch).

Vanmarcke, H. (1994)
Lack of consistency in the ICRP approach on protection against ^{222}Rn at home and at work. Health Phys. 67:668.

Vargas, A. and Ortega, X. (2007)
Influence of environmental changes on integrating radon detectors: results of an intercomparison exercise. Radiat. Prot. Dosim. 123: 529-536.

Verger, P., Hubert, Ph., Cheron, S., Bonnefous, S., Bottard, S. and Brenot, J. (1994)
Use of field measurements in radon mapping in France. Radiat. Prot. Dosim. 56:225-229.

VROM (1989)
Omgaan met risico's. De risicobenadering in het milieubeleid. Tweede Kamer, vergaderjaar 1988-1989, 21137, nr. 5. Ministerie van Volkshuisvesting, Ruimtelijke Ordening en Milieubeheer, Den Haag, the Netherlands (in Dutch).

VROM (1990a)
Omgaan met risico's van straling. Normstelling ioniserende straling voor arbeid en milieu. Tweede Kamer, vergaderjaar 1989-1990, 21483, nr. 1-2. Ministerie van Volkshuisvesting, Ruimtelijke Ordening en Milieubeheer and Ministerie van Sociale Zaken en Werkgelegenheid, Den Haag, the Netherlands (in Dutch).

VROM (1990b)
Straling vanuit bouwmaterialen; normen voor beton. Stralenbeschermingsreeks 43. Ministerie van Volkshuisvesting, Ruimtelijke Ordening en Milieubeheer, Den Haag, the Netherlands (in Dutch).

VROM (1994)
Beleidsstandpunt Radon. Tweede Kamer, vergaderjaar 1993-1994, 21483, nr. 18. Ministerie van Volkshuisvesting, Ruimtelijke Ordening en Milieubeheer, Den Haag, the Netherlands (in Dutch).

VROM (2004)
Nuchter omgaan met risico's. Beslissen met gevoel voor onzekerheden. Hoofddocument. Ministerie van Volkshuisvesting, Ruimtelijke Ordening en Milieubeheer, Den Haag, the Netherlands (in Dutch).

WHO (2006)
Health effects of the Chernobyl accident and special health care programmes. Report of the UN Chernobyl Forum Expert Group "Health". Eds. Bennett, B., Repacholi, M. and Carr, Z. World Health Organization, Geneva.

Winder, C., Van Heijningen, R.J.J., De Jong, P. and Ackers, J.G. (1990)
Positieve en negatieve effecten op de stralingsbelasting door het toenemend gebruik van secundaire grondstoffen in bouwmaterialen. Stralenbeschermingsreeks 48. Ministerie van Volkshuisvesting, Ruimtelijke Ordening en Milieubeheer, Den Haag, the Netherlands (in Dutch).

Yu, K.N., Chan, T.F. and Young, E.C.M. (1995)
The variation of radon exhalation rates from building surfaces of different ages. Health Phys. 68: 716-718.

Yu, K.N., Balendran, R.V., Koo, S.Y. and Cheung, T. (2000)
Silica fume as a radon retardant from concrete. Environ. Sci. Technol. 34:2284-2287.

Nederlandse samenvatting

Inleiding

Een belangrijk deel van de natuurlijke stralingsbelasting die de Nederlander ontvangt, is het gevolg van verblijf in gebouwen, zoals kantoren en woningen. Daarbij zijn drie componenten te onderscheiden, te weten:

- externe blootstelling aan gammastraling;
- inademing van kortlevende dochternucliden van radon;
- inademing van kortlevende dochternucliden van thoron.

Deze blootstelling wordt veroorzaakt door de aanwezigheid van de radionucliden ^{238}U, ^{232}Th en ^{40}K in grond en bouwmaterialen. ^{238}U en ^{232}Th staan aan het begin van vervalreeksen die op hoofdlijnen zijn weergegeven in de Figuren 1.1 en 1.2. Ieder lid van de reeks is zelf ook instabiel en vervalt verder totdat uiteindelijk een stabiel isotoop van het element lood (Pb) is gevormd. Dit betekent dat naast de moedernucliden nog tientallen dochternucliden aanwezig zijn. Een aantal van deze radionucliden vervalt onder uitzending van gammastraling. Daarnaast komt ook bij verval van ^{40}K gammastraling vrij. Gammastraling kenmerkt zich door een hoog doordringend vermogen, waardoor slechts een gedeelte hiervan door het materiaal zelf zal worden geabsorbeerd. Het gevolg hiervan is dat in een woning een zeker stralingsveld heerst en de bewoner een externe stralingsdosis ontvangt.

In elk van genoemde vervalreeksen komt een gasvormig dochternuclide voor; in de ^{238}U-reeks is dit ^{222}Rn (radon) en in de ^{232}Th-reeks ^{220}Rn (thoron). Vanwege het gasvormige karakter kunnen radon en thoron uit bouwmateriaal diffunderen en zich vermengen met lucht in de woning. Daarnaast kan het in de bodem gevormde radon via de kruipruimte eveneens in het woongedeelte terechtkomen. Bij verval van radon en thoron ontstaat een aantal kortlevende dochternucliden die bij inademing in de longen achterblijven en aldus lokaal een stralingsdosis aan het longweefsel afgeven.

Het aantal sterfgevallen in Nederland door externe bestraling en inademing van radon- en thorondochternucliden wordt geschat op 650 per jaar, met een 95% betrouwbaarheidsinterval van 250 tot 1300. Voor de uitgangpunten en kanttekeningen bij deze schattingen, wordt verwezen naar §1.8.

Het doel van dit proefschrift was de rol van bouwmaterialen in kaart te brengen met betrekking tot de natuurlijke stralingsbelasting in Nederland. De meeste van de studies in dit proefschrift zijn uitgevoerd in opdracht van de overheid met een directe relatie met vigerend of toekomstig radonbeleid. De studies zijn gegroepeerd in de onderwerpen

(a) Ontwikkeling van methoden; (b) Concentraties en blootstelling; en (c) Transportmechanismen en tegenmaatregelen. Onderstaand wordt per onderwerp een korte beschrijving van de resultaten gegeven.

Ontwikkelde methoden

De als eerste beschreven methode betreft de bepaling van de radonexhalatiesnelheid van bouwmaterialen, de snelheid waarmee deze materialen radon aan de omgeving afgeven. Het te onderzoeken analysemonster wordt daartoe opgesloten in een vat, dat continu met stikstofgas wordt doorspoeld. Het met de stikstofstroom meegevoerde radon wordt gevangen op silicagel. Dit silicagel wordt in een vloeistofscintillatieteller geanalyseerd op de hoeveelheid radon. Op basis hiervan wordt de exhalatiesnelheid van het analysemonster berekend (§ 2.1.).

Als prestatiekenmerken van de methode zijn onderzocht de herhaalbaarheid, de reproduceerbaarheid binnen het laboratorium en de overeenstemming van de meetresultaten met die van andere laboratoria. De waarden van deze kenmerken variëren van 3% tot 6% (§2.2). Mede gezien de grote spreiding in exhalatiesnelheid tussen monsters van hetzelfde type bouwmateriaal, is de door de analysemethode geïntroduceerde onzekerheid alleszins acceptabel. De beschreven methode is in 2001 als hoofdmethode opgenomen in de NEN-norm 5699. Momenteel ligt een voorstel voor om deze methode op te nemen in een ISO-norm.

De tweede methode, zie §2.3, beschrijft een rekenmethodiek voor de bepaling van de externe stralingsdosis ten gevolge van bouwmateriaal. Als uitgangspunt heeft gediend het in lucht geabsorbeerde dosistempo in het centrum van een bepaalde standaardgeometrie. In genoemde paragraaf zijn correctiefactoren afgeleid voor omstandigheden die van deze standaardgeometrie afwijken, zowel qua woningspecifieke parameters als materiaaleigenschappen. Ter verificatie van de methode is deze toegepast op een drietal Nederlandse standaardwoningen. De resultaten hiervan zijn vergeleken met de berekeningen die zijn uitgevoerd met MCNP, een veel toegepaste Monte Carlo code. De verschillen bedragen 3% tot 7%, afhankelijk van het woningtype. Het voordeel van onze methode is dat de tijd waarin de dosisevaluatie kan worden uitgevoerd veel korter is, waardoor deze de voorkeur boven MCNP verdient wanneer de evaluatie veel woningen omvat.

Concentraties en blootstelling

In hoofdstuk 3 zijn vier studies beschreven die nader ingaan op de concentraties en blootstellingsniveaus in Nederland. In §3.1 wordt verslag gedaan van een studie naar de activiteitsconcentraties aan natuurlijke radionucliden en de radonexhalatiesnelheid van de in Nederland gebruikte steenachtige bouwmaterialen. Naar de activiteitsconcentraties in

gipspleisters en stucmortels is een aparte studie verricht (§3.2). Op basis van de resultaten kunnen drie klassen worden onderscheiden, t.w. (I) materialen met lage activiteitsconcentraties, overeenkomend met die in natuurgips; (II) materialen met intermediaire gehalten van rond 100 tot 150 Bq kg^{-1} aan zowel ^{226}Ra en ^{228}Ra; en (III) materialen met gehalten van 200 tot 250 Bq kg^{-1} per radionuclide. Toepassing van materialen uit de bovengenoemde klasse II en III kunnen aanleiding geven tot een verhoging van zowel het externe dosistempo als de radonconcentratie in een woning. Gezien de geringe dikte van de pleisterlagen in vergelijking tot de totale bouwmassa van een woning, zal deze verhoging echter verwaarloosbaar zijn. Hoge ^{228}Ra activiteitsconcentraties kunnen daarentegen wel aanleiding geven tot een verhoogde thoronconcentratie in de woning.

De derde studie (§3.3) bevat de resultaten van een onderzoek naar de blootstelling aan radon en externe straling in een kleine woonwijk in Alphen a/d Rijn. In deze woonwijk zijn ongeveer gelijktijdig 101 woningen gebouwd naar negen ontwerpen. Afhankelijk van het ontwerp liep het effectieve dosistempo voor de bewoners uiteen van 0,4 tot 1,4 mSv per jaar. De woningen met lage dosistempi kenmerkten zich door een houtskeletbouw met een begane grondvloer van beton, overige vloeren van hout en binnenmuren van rookgasontzwavelingsgips. De ontwerpen die waren gebouwd volgens een meer conventionele bouwwijze (betonvloeren, spouwmuren van baksteen en kalkzandsteen) gaven overeenkomstige radonconcentraties en dosistempi te zien. Een van de belangrijkste conclusies van het onderzoek was dat het ontwerp van meer invloed is op het dosistempo dan de gewoonten en voorkeuren van de bewoners.

In §3.4 is een berekening uitgevoerd naar de verdeling van het gammadosistempo in Nederland ten gevolge van de bouwmaterialen. Hierbij is gebruik gemaakt van het in §2.3 beschreven rekenmodel. Dit model is toegepast op een set woningen waarvan het materiaalgebruik in de woonkamer goed was gedocumenteerd. Met behulp van een Monte Carlo code zijn deze gegevens gecombineerd met de activiteitsconcentraties en dichtheden van 90 monsters bouwmateriaal uit §3.1. Op basis van 100.000 simulaties is een verdeling van het geabsorbeerde dosistempo in lucht verkregen met als resultaat een vrijwel Gaussvormige verdeling. Na correctie voor de bijdrage van kosmische en terrestrische straling binnenshuis beperkt het verschil met metingen zich tot 5%.

Transportmechanismen en tegenmaatregelen

Op verscheidene manieren is nagegaan of de radonafgifte van bouwmaterialen kan worden beperkt. Het aanbrengen van een verfcoating biedt een relatief eenvoudige en goedkope oplossing om een vermindering van de radonexhalatiesnelheid te bewerkstelligen. In §4.1 wordt verslag gedaan van een studie naar het effect van een twintigtal verfsystemen, dat in Nederland wordt toegepast ter afwerking van wanden en plafonds. Uit het onderzoek bleek dat deze verfsystemen in het geheel geen effect hadden op de radonexhalatiesnelheid.

Reducties tot 95% zijn wel te verkrijgen met industriële verven op basis van epoxy of polyurethaan. Een belangrijk nadeel van deze tegenmaatregel is dat beschadigingen en eventuele door veroudering ontstane haarscheurtjes een groot deel van de effectiviteit teniet doen.

Beton levert in Nederland een belangrijke bijdrage aan de radonconcentratie in de woning. In de woningbouw worden uiteenlopende betonmengsels toegepast en het effect van diverse parameters op de radonexhalatiesnelheid is onderzocht. In §4.2 betrof dit parameters die samenhangen met het productieproces en de samenstelling. Uit dit oriënterende onderzoek is een sterke positieve correlatie naar voren gekomen tussen de vochtafgifte en de radonexhalatiesnelheid.

In een serie van 23 betonmengsels is de samenstelling gevarieerd met betrekking tot de hoeveelheid cement, het type cement (Portland- of hoogovencement), de hoeveelheid water bij een vaste hoeveelheid cement, het gebruik van een luchtbelvormer of de hoeveelheid gerecycled granulaat. De porositeit van de betonmengsels in dit onderzoek liep uiteen van 1% tot 16% (§4.3). De radonexhalatiesnelheid is genormeerd op de activiteitsconcentratie van ^{226}Ra in het beton en uitgedrukt in een zogenoemde radonafgiftefactor. Doordat radon vooral afkomstig is uit het cement is een tweede afgiftefactor gebaseerd op de ^{226}Ra-bijdrage vanuit de cementfractie. Hoewel de methoden om de porositeit in de diverse betonmengsels te verkrijgen sterk van elkaar verschillen, correleert deze tweede afgiftefactor goed met de capillaire porositeit van de mengsels. Doordat de water-cementfactor een goede indicator vormt van de capillaire porositeit, is dit de aangewezen parameter om beton te maken met een lage radonexhalatiesnelheid. Hoe lager de water-cementfactor, des te minder capillair porieoppervlak er beschikbaar zal zijn van waaruit het radon vanuit de vaste matrix naar de porie kan emaneren. De goede correlatie tussen de op de cement gebaseerde afgiftefactor en literatuurgegevens betreffende het interne capillaire porieoppervlak staven de resulaten van deze studie.

Conclusies en vooruitblik

Bouwmaterialen zijn verantwoordelijk voor ongeveer 70% van de radon in Nederlandse woningen en 55% van de externe stralingsdosis. Dit betreft ongeveer 40% van de gemiddelde stralingsbelasting in Nederland veroorzaakt door natuurlijke bronnen. Samenvattend kan worden gesteld dat de situatie in Nederland met betrekking tot radon en externe straling redelijk goed wordt begrepen.

Dit ligt anders voor thoron. Tot op heden is in Nederland geen aandacht besteed aan de blootstelling aan thorondochterproducten. De bron voor thoron ligt vrijwel geheel bij bouwmateriaal. Via modelberekeningen is het aandeel van thoron aan de totale stralings-

belasting in de woning geschat op ca. 10%. Bij deze berekeningen is er van uitgegaan dat het bouwmaterial niet is afgewerkt met een pleister- of een verflaag (§1.9.3) omdat gegevens over de invloed hiervan op de exhalatiesnelheid ontbreken.

Uit de resultaten van de laatste landelijke inventarisatie van de radonconcentraties in woningen kan worden afgeleid dat de gemiddelde thoronconcentratie ter plekke van de detectoren gemiddeld ongeveer 30 Bq m^{-3} heeft bedragen. Het is echter niet goed mogelijk om op basis hiervan een gemiddelde bronterm voor thoron te bepalen. Vanwege de korte halveringstijd van thoron is er sprake van een sterke concentratiegradiënt vanaf de bron, i.e. het oppervlak van het bouwmateriaal, tot het midden van de kamer. De vorm van deze curve wordt sterk beïnvloed door de mate waarin menging van lucht plaatsvindt. Onderzoek naar de thoronconcentratie in woningen, met het doel een uitspraak te kunnen doen over de stralingsbelasting ten gevolge van inademing van kortlevende thorondochterproducten is alleen zinvol wanneer aan dit aspect expliciet aandacht wordt besteed.

Een schatting van de thoronbronterm kan ook worden verkregen op basis van gemeten thoronexhalatiesnelheden van bouwmaterialen. Combinatie van deze gegevens met die betreffende het gebruik van deze materialen in Nederlandse woningen resulteert in een verdeling van de thoronbronterm. In een dergelijk onderzoek dient eveneens de exhalatiesnelheid van pleistermateriaal te worden betrokken vanwege de mogelijke bijdrage hiervan. Daarnaast dient aandacht te worden besteed aan het mogelijke effect van afwerklagen zoals verf en behang. Hoewel dergelijke materialen geen effect hebben op de radonexhalatiesnelheid, kan dit mogelijk wel het geval zijn voor de thoronexhalatiesnelheid vanwege de aanzienlijk kortere halveringstijd van thoron in vergelijking met die van radon. Op basis van modelberekeningen kan uit de verdeling van de thoronbronterm een dosisverdeling worden gereconstrueerd. Nader experimenteel onderzoek naar de inputvariabelen van de modelberekening zal de onzekerheid in de schatting op termijn kunnen verminderen.

Het doel van bovengenoemde onderzoeken is een vergelijkbaar kennisniveau voor thoron als voor radon te verkrijgen. Dit vormt experimenteel gezien nog een grote uitdaging.

Curriculum vitae

Peter de Jong is geboren op 20 december 1953 te Delft. Hij heeft in 1971 het diploma H.B.S.-B behaald aan de stedelijke scholengemeenschap Hugo Grotius te Delft. Hierna is hij Scheikundige Technologie gaan studeren aan de Technische Universiteit Delft. Het afstuderen vond plaats bij de vakgroep Biochemie en Biofysica. De studie is afgerond op 15 september 1977.

Tijdens en kort na zijn studie is hij studentassistent geweest bij NUFFIC te Delft en heeft vervolgens tijdelijke arbeidsplaatsen vervuld bij TNO en bij de Erasmus Universiteit. In 1980 is hij opnieuw bij TNO in dienst getreden bij het toenmalige Instituut Maatschappelijke Technologie in Delft als hoofd van de radionuclidenlaboratoria op B- en C-niveau van de afdeling Analytische Chemie. In deze tijd begon juist de natuurlijke radioactiviteit aandacht te krijgen. In Nederland resulteerde dat onder meer in het zogenoemde SAWORA-programma, waarin een brede inventarisatie werd gemaakt van de natuurlijke achtergrondstraling in Nederland.

Binnen TNO zijn diverse functies vervuld bij nog meer Instituten. De werkzaamheden ten aanzien van de natuurlijke stralingsbronnen gingen echter telkens mee. Op 1 januari 2000 is het toenmalige Centrum voor Stralingsbescherming en Dosimetrie TNO te Arnhem door Nuclear Research and consultacy Group (NRG) overgenomen. Momenteel vervult hij daar de functie van teammanager bij de teams Individual Monitoring en Consultancy & Operational Support in Arnhem en is tevens plaatsvervangend hoofd van de produktgroep Radiation & Environment waartoe beide teams behoren.

Nawoord

Het onderzoek naar de natuurlijke stralingsbelasting in Nederland startte in 1982 met het SAWORA-programma waar vrijwel geheel stralend Nederland bij was betrokken, aangevuld met onderzoekers op het gebied van bouwkundige constructies en ventilatie. Een grootschalig, multidisciplinair onderzoeksprogramma, met enerverende discussies tijdens de overlegvergaderingen bij het toenmalige PEO. Bijna dertig jaar later is het aantal onderzoekers op het gebied van de stralingsbelasting in woningen gemakkelijk op de vingers van een hand te tellen. En juist nu ligt er weer een belangrijke nieuwe uitdaging voor.

De aandacht voor radon heeft in Nederland nooit het enthousiaste niveau kunnen halen als in vele andere landen. Wellicht terecht, gezien de relatief lage concentraties in ons land. In dat kader had ik een stelling bedacht (die het overigens niet gehaald heeft), dat het grootste probleem met betrekking tot het radonprobleem in Nederland het gebrek aan radon is. Al pleitend voor meer aandacht voor radon (en thoron) en de schouderophalende reactie daarop van de gesprekspartner, voelde ik me vaak als iemand van een andere planeet. De cartoon van Al Goodwyn op de cover symboliseert dit gevoel.

Het is gebruikelijk een dankwoord van een proefschrift te beginnen met de opmerking dat het proefschrift niet tot stand had kunnen komen zonder de medewerking van vele anderen. Ik sluit me graag bij deze traditie aan en dank een ieder die aan het proefschrift een bijdrage heeft geleverd. In het bijzonder dank ik Rob de Meijer die mij in de gelegenheid heeft gesteld om bij hem te promoveren. Samen met Emiel van der Graaf heeft Rob vele uren besteed aan het kritisch beschouwen en corrigeren van het concept; zonder jullie inbreng zou het proefschrift er heel anders hebben uitgezien. Mijn dank voor jullie inzet!

Dank ben ik zeker ook verschuldigd aan Willem van Dijk met wie ik rond de 25 jaar niet alleen de kamer, maar ook het onderzoek heb gedeeld. Zijn degelijke analytische aanpak en aandacht voor details hebben de basis gelegd voor onze publicaties en daarmee dit proefschrift. Naast Willem wil ik ook de andere coauteurs danken voor hun waardevolle en vaak essentiële inbreng.

De meeste in dit proefschrift opgenomen studies zijn uitgevoerd in opdracht van het ministerie van VROM. Ik wil dit ministerie graag dankzeggen voor de financiering van het onderzoek en Branko Bošnjakovic, Coen Bootsma, Lieneke van Brederode, Dick Jung en Lodewijk van Aernsbergen voor de begeleiding en de prettige samenwerking.

Dank ook aan NRG voor de geboden mogelijkheid om het onderzoek uit te voeren en er een proefschrift over te schrijven.

Als laatste wil ik het thuisfront bedanken; ik realiseer me dat de aandacht, met name in de laatste fase, wel erg scheef is komen te liggen. Mijn dank voor jullie begrip en morele ondersteuning.

Cover:
Cartoon by Al Goodwyn published in the August 1994 issue of the HPS *Newsletter* and used with permission of the Health Physics Society

Printed by VDA, Arnhem

Exposure to natural radiation in the Netherlands: the impact of building materials
by Peter de Jong
Thesis Groningen, with summary in Dutch
ISBN 978-90-367-4326-6
Subject headings: radon, gamma radiation, indoor exposure, building materials